INFORMATION TO USERS

This material was produced from a microfilm copy of the original document. While the most advanced technological means to photograph and reproduce this document have been used, the quality is heavily dependent upon the quality of the original submitted.

The following explanation of techniques is provided to help you understand markings or patterns which may appear on this reproduction.

1. The sign or "target" for pages apparently lacking from the document photographed is "Missing Page(s)". If it was possible to obtain the missing page(s) or section, they are spliced into the film along with adjacent pages. This may have necessitated cutting thru an image and duplicating adjacent pages to insure you complete continuity.

2. When an image on the film is obliterated with a large round black mark, it is an indication that the photographer suspected that the copy may have moved during exposure and thus cause a blurred image. You will find a good image of the page in the adjacent frame.

3. When a map, drawing or chart, etc., was part of the material being photographed the photographer followed a definite method in "sectioning" the material. It is customary to begin photoing at the upper left hand corner of a large sheet and to continue photoing from left to right in equal sections with a small overlap. If necessary, sectioning is continued again — beginning below the first row and continuing on until complete.

4. The majority of users indicate that the textual content is of greatest value, however, a somewhat higher quality reproduction could be made from "photographs" if essential to the understanding of the dissertation. Silver prints of "photographs" may be ordered at additional charge by writing the Order Department, giving the catalog number, title, author and specific pages you wish reproduced.

5. PLEASE NOTE: Some pages may have indistinct print. Filmed as received.

University Microfilms International
300 North Zeeb Road
Ann Arbor, Michigan 48106 USA
St. John's Road, Tyler's Green
High Wycombe, Bucks, England HP10 8HR

77-21,367

CAFKY, James Wright, 1937-
TRANSPORT COEFFICIENTS OF DENSE FLUID SYSTEMS.

The University of Oklahoma, Ph.D., 1977
Physics, general

Xerox University Microfilms, Ann Arbor, Michigan 48106

THE UNIVERSITY OF OKLAHOMA

GRADUATE COLLEGE

TRANSPORT COEFFICIENTS OF DENSE FLUID SYSTEMS

A DISSERTATION

SUBMITTED TO THE GRADUATE FACULTY

in partial fulfillment of the requirements for the

degree of

DOCTOR OF PHILOSOPHY

By

JAMES WRIGHT CAFKY

Norman, Oklahoma

1976

TRANSPORT COEFFICIENTS OF DENSE FLUID SYSTEMS

APPROVED BY:

Stanley E. Babb, Jr.

D. Cook

Robert M. St. John

S. B. Eliason

Stephen C. Whitmore

DISSERTATION COMMITTEE

ACKNOWLEDGEMENT

I cannot in detail adequately acknowledge the contribution of Professor Stanley E. Babb, Jr. to this work or to my education. There were too many penetrating insights and too many long nights of hard work given freely and generously by this man. I count myself priviledged to have been his student.

To my parents, George W. and Dovie B. Cafky, I offer a melancholy acknowledgement. It saddens me that neither lived to see this point, for both took keen interest in my efforts and aided me in every possible way. Again, in this regard, I was priviledged.

Without the cooperation of agencies and individuals associated with data processing at the University of Oklahoma, the work could not have been completed. To all that helped: thank you!

TABLE OF CONTENTS

TABLE OF CONTENTS (Cont'd.)

LIST OF TABLES

List of Tables (Continued)

LIST OF ILLUSTRATIONS

APOLOGIA

The nature of this work seems sufficiently out of the ordinary to warrant an explanatory note.

No theory is developed herein and neither is an experiment performed. What is attempted is the extension of a rather formidable theoretical development purporting to represent the phenomena of transport at high density into tables of predicted results, through numerical methods, and thus the establishment of a coherent, critical link between equation and laboratory observation. Most properly this effort might be called computational physics; it is left to the reader to judge the merit of the name.

Being neither fish nor fowl, theory nor experiment, the reader may not find, in the discussion which follows, the emphasis in either area which he may desire. Theory is only sketched as is necessary with little if any rigor. Experimental results from other sources are merely quoted. The emphasis is elsewhere, in an area which may excite little interest in either the pure theorist or the pure experimentalist: in the discussion of the programming effort. But this is the bridge between theory and experiment (perhaps the only viable link in this case) and it is part and parcel of this endeavor.

Concerning the organization: a particular equation will be encountered repeatedly in varying ways depending on the business at hand; for instance, as a theoretical entity, as the basis for a numerical algorithm, and as a topic for examination in the context of the numerical

results it produces. Additionally, there may be many asides into the details of the programming effort devoted to it. The partition of the narrative along these topical lines is an attempt to preserve the simple flow of the discussion and the logical continuity of the ideas developed, and hopefully to make more palatable the presentation.

ABSTRACT

The predictions of the Rice-Allnatt Theory for shear viscosity and thermal conductivity are evaluated by numerical techniques and compared to experimental results for Argon and Nitrogen over a density range of approximately 30 to 700 amagats and a temperature range from 273°K to 600°K. The Kirkwood, Born and Green, Myer, and Yvon radial distribution function was primarily used, and results using Percus-Yevick and convoluted hypernetted chain formalism are also reported. Lennard-Jones, Modified Buckingham and Barker-Boebetic potentials were used.

All calculations led to substantial disagreement with observation. The nature of the disagreement is discussed.

CHAPTER I

INTRODUCTION

It is well known that many thermodynamic parameters may be expressed in terms of a statistical-mechanical quantity called the *radial distribution function*, g(r). This quantity is related to the probability that in a system of N particles a particle is located at a scalar radial distance r from another particle. A formal route to the definition of g(r) is as follows:[1]

Beginning with the N-particle distribution function

$$f_N(Z_1, Z_2, \cdots Z_N;\ t) \tag{1-1}$$

where $Z_i = (q_i, p_i)$, we define

$$f_N(Z_1, \cdots, Z_N;\ t)\ dZ_1 \cdots dZ_N \tag{1-2}$$

as the probability that a system of N particles is in a state dZ_1, $\ldots, dZ_N$ about a phase point $Z_1, \ldots, Z_N$ at a time t. Next, define the *reduced distribution function*

$$f_\ell(Z_1, \cdots, Z_\ell;\ t) \equiv \int f_N dZ_{\ell+1} \cdots dZ_N \ . \tag{1-3}$$

f_ℓ is the probability that a system is in the state $dZ_1,\cdots,dZ_\ell$ about $Z_1,\cdots,Z_\ell$ without regard to the values $Z_{\ell+1},\cdots,Z_N$.

Order is implied in the definitions of f_N and f_ℓ. $f(Z_1,Z_2,\cdots Z_j;\ t)$ is distinct from $f(Z_2,Z_1,\cdots,Z_j;\ t)$ in the sense that in the former expression, it is "molecule number one" which has the position and momentum Z_1, while in the latter expression, it is "molecule number two" which has Z_1. The probability that a system has the set of positions momenta $\{Z_i\}$ irrespective of the specific permutation of this set among the molecules is obtained by summing over the permutations. This summation gives the *ℓ-tuple distribution function*, F_ℓ. For a homogeneous system, the result is simply:

$$F_\ell = 1!\binom{N}{1} f_\ell = \frac{N!}{(N-\ell)!} f_\ell \tag{1-4}$$

Finally, the *radial distribution function* (or two-particle distribution function) is:

$$g(r) = \frac{V^2}{N(N-1)} \int F_2 dp_1 dp_2, \qquad r = |\vec{x}_1 - \vec{x}_2| \ . \tag{1-5}$$

$g(r)$ is proportional to the probability that a particle of the system (any particle) is located at a radial distance r from some other particle. By virtue of the term multiplying the integral, the absence of any information as to the location of a second particle is given by $g(r) = 1$.

In a system of high density, we envision molecules closely packed together with little opportunity for large displacement. We expect molecules to be arrayed in close proximity to their neighbors. It should be that there exists a relatively large probability of encountering a molecule at slightly greater than one molecular radius, σ, and at approximately even integral multiples thereafter. This is reflected by $g(r)>1$ at these values of r. Additionally, the likelihood of a molecule at r implies molecules will tend to be excluded from that immediate vicinity $\Delta r < \sigma$. In this region, $g(r) < 1$. As r is increased (and hence, as the volume of the spherical shell of thickness Δr increases) the certainty of our anticipation blurs, and g(r) tends toward the value unity for large r. We call this situation "short range ordering". The word correlation is also used to characterize the situation where one molecule influences the behavior (here, the position) of another.

In the opposite case, that of extreme low density, we would expect little definitive knowledge as to the location of particles, except perhaps at small values of r. In such systems where no significant correlation exists, $g(r) = 1$ except for values of r only slightly larger than $r_{\cdot}$.

Typical g-curves are shown in Figures 1 and 2.

Figure 1. A typical family of radical distribution functions. The curves showing most pronounced variation are for highest density (here, approximately 900 amagats).

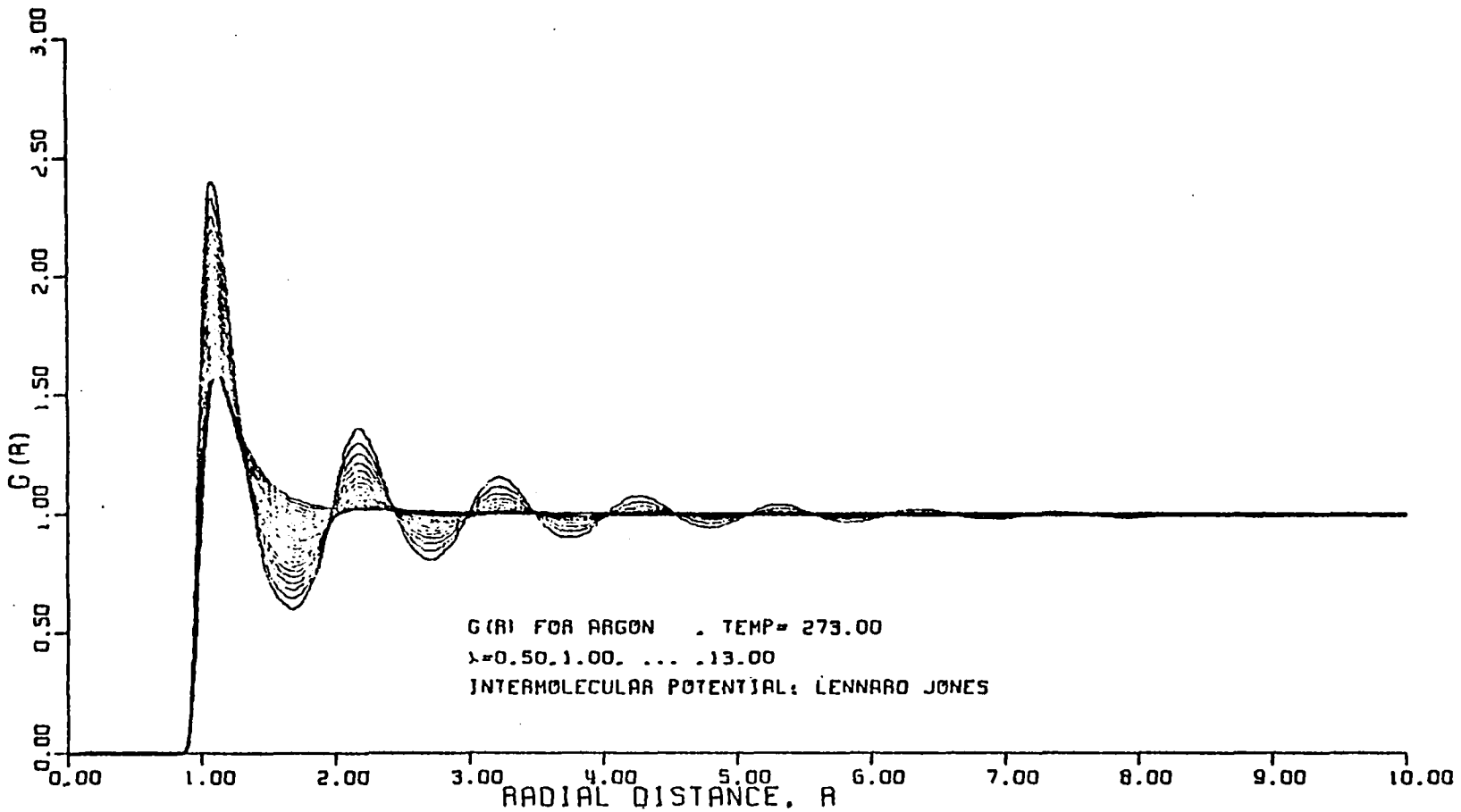
G(R)
3.00
2.50
2.00
1.50
1.00
0.50
0.00
0.00
1.00
2.00
3.00
4.00
5.00
6.00
7.00
8.00
9.00
10.00
RADIAL DISTANCE, R
G(R) FOR ARGON . TEMP= 273.00
λ=0.50,1.00, ... ,13.00
INTERMOLECULAR POTENTIAL: LENNARD JONES

Figure 2a. A perspective view of the data of Figure 1.

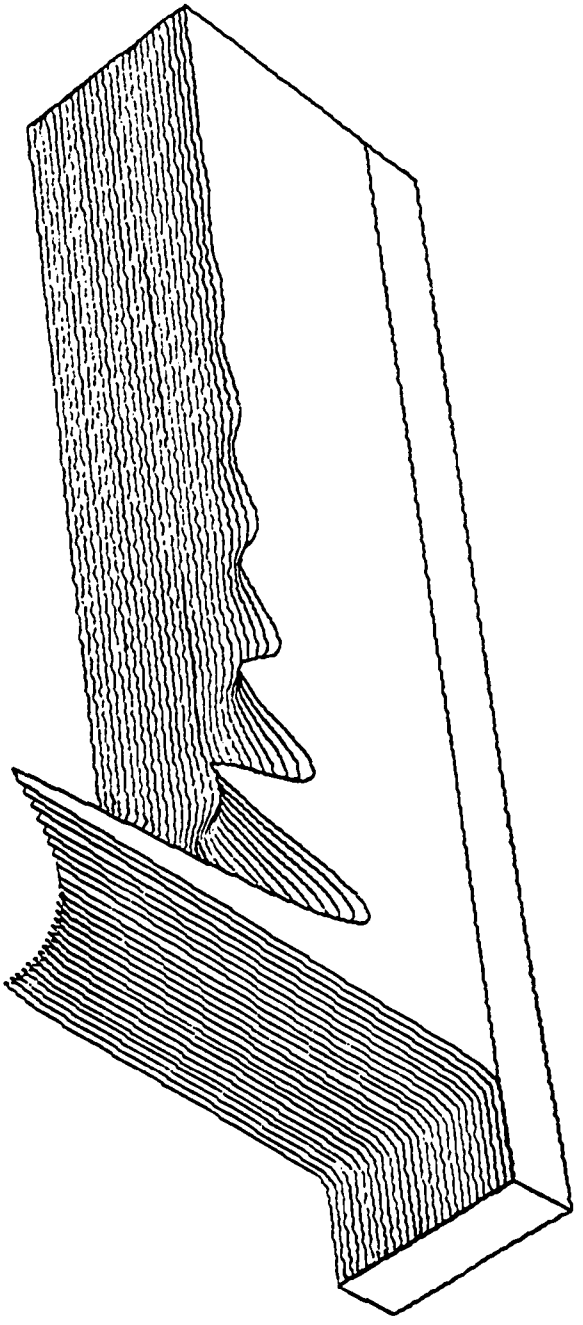

Figure 2b. A perspective view of the data of Figure 2a, rotated 180° about a vertical axis. The short period irregularly in the data lines is an artifact of the plotting device.

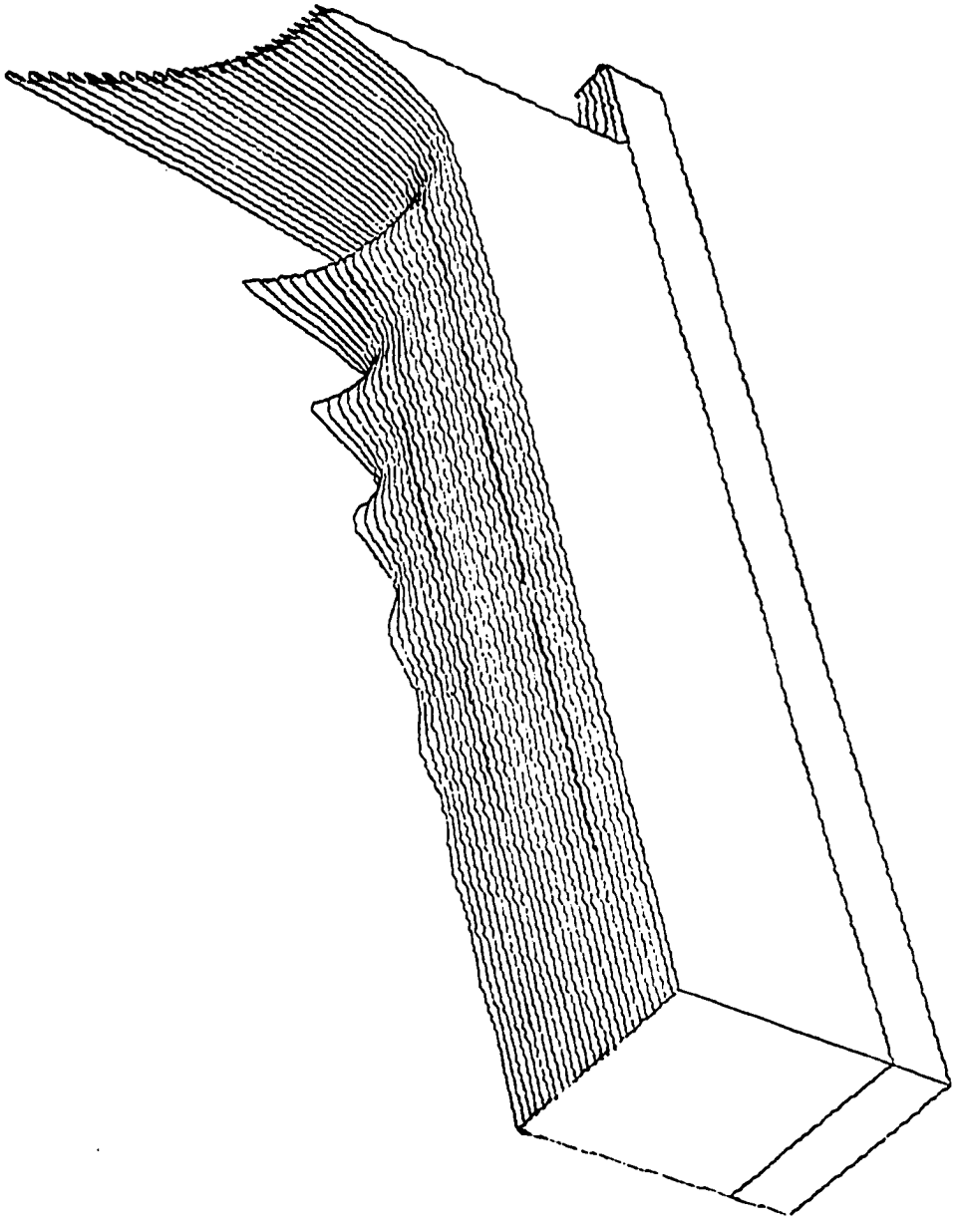

The value of the radial distribution function rests in the fact that many thermodynamic properties of the system may be written in terms of it.[2] The representation of the equilibrium properties in this fashion is well known. For instance, the equation of state of a system in terms of g(r) and the intermolecular potential V(r) (assumed to be a 2-body potential, i.e. neglecting any non-additivity) is:

$$\frac{pv}{NkT} = 1 - \frac{2\pi N}{3vkT} \int_0^\infty r^3 \frac{dV}{dr} g(r) dr \quad . \tag{1-6}$$

Recently, Rice and Allnatt (RA) developed a theory whereby the transport properties of a non-equilibrium system might as well be represented in terms of g(r).[3] It was hoped that their theory might provide an accurate description of the behavior of the diffusion, viscosity and thermal conductivity of a dense fluid system, but the lack of knowledge of the functional form of g(r) or of accurate tables of its values hindered a thorough analysis of the RA equations.

It is the purpose of this present work to develop (within a given theoretical framework) accurate tables of g(r), to apply them to the RA equations, and hopefully, to take some measure of the effectiveness of the RA equations by comparing their predictions with experimental results.

CHAPTER II

THE RADIAL DISTRIBUTION FUNCTION

General Remarks

The "derivation" of g(r) of the preceding chapter is a formalism; while it aids in our understanding of the nature of the function, it furnishes no information as to the functional form of g(r). Kirkwood,[4] Born and Green,[5] Mayer[6] and Yvon[7] developed an integral expression involving g(r) which can be written:

$$\ell n[g(r)] = -\beta\varepsilon\xi\gamma(x) + \frac{\lambda_o}{4x}\int_{-\infty}^{\infty} K(x-s,\xi)s[g(s)-1]ds \qquad (2\text{-}1)$$

where

$$K(t,\xi) = \beta\varepsilon\xi\int_{|t|}^{\infty}(s^2-t^2)g(s,\xi)[\frac{d\gamma(s)}{ds}]ds \quad . \qquad (2\text{-}2)$$

a and ε are respectively the length and energy characteristic of a reduced intermolecular potential γ defined by the equation

$$V(r) = \varepsilon\gamma(x); \quad x = \frac{r}{a} \quad . \qquad (2\text{-}3)$$

The parameter λ_o is proportional to density:

$$\lambda_o = \frac{4\pi N a^3}{v} \tag{2-4}$$

where N is Avogadro's number and v is the molar volume. $\beta = (kT)^{-1}$ and ξ is a coupling constant relating to the intermolecular potential:

$$V_N(r,\xi) = V_{N-1} + \xi \sum_{\substack{k=1 \\ \neq i}}^{N} V(r_{ik}) \quad . \tag{2-5}$$

In what follows, it is assumed $\xi = 1$. We call the integral equation involving g(r) simply "the g-equation".

The g-equation has never been solved analytically for the functional form of g(r). However, it was used by Kirkwood, Maun and Alder[8] (KMA) and later by Kirkwood, Lewinson and Alder[9] (KLA) as the basis of a numerical solution. Although their results were obtained subject to certain restrictive approximations and were of limited accuracy (because of the limitations of data processing devices available to them), their efforts and success in this endeavor are truly impressive.

The KMA-KLA Solution of the g-equation

Because we aim in part to create improved tables of the radial distribution function, it is appropriate to review the KMA-KLA development:

KMA-KLA chose the Lennard-Jones 12-6 intermolecular potential:

$$V_{LJ}(r) = \varepsilon\gamma_{LJ}(x) = \varepsilon\left\{\frac{4}{x^{12}} - \frac{4}{x^6}\right\} , \quad x = \frac{r}{a} \tag{2-6}$$

and modified it as $\gamma_m = \gamma_o + \gamma_1$;

$$\begin{aligned} \exp\{-\beta\varepsilon\gamma_o(x)\} &= 0 , \quad 0 \le x < 1 \\ &= 1 , \quad x \ge 1 \\ \gamma(x) &= 0 , \quad 0 \le x < 1 \\ &= \gamma_{LJ}(x) , \quad x \ge 1 \end{aligned} \tag{2-7}$$

By then defining:

$$\ell n\ g(x) = -\beta\varepsilon\gamma_o(x) + \frac{\psi(x)}{x} \tag{2-8}$$

and expanding the functions $\psi(x)$, $g(x)$, and $K(t)$:

$$\psi(x) = \psi_o(x) + \beta\varepsilon\psi_1(x) + (\beta\varepsilon)^2\psi_2(x) + \cdots$$

$$g(x) = g_o(x)\left\{1 + \beta\varepsilon\frac{\psi_1(x)}{x} + (\beta\varepsilon)^2\left[\frac{\psi_1^2(x)}{2x^2} + \frac{\psi_2(x)}{x}\right] + \cdots\right\} \tag{2-10}$$

and

$$K(t) = k_o(t)K_o(t) + \beta\varepsilon K_1(t) + (\beta\varepsilon)^2 K_2(t) + \cdots , \tag{2-11}$$

where

$$g_o(x) = \exp\left\{-\beta\varepsilon\gamma_o(x) + \frac{\psi_o(x)}{x}\right\} \tag{2-12}$$

and

$$k_o(t) = \langle g_o \rangle = \frac{\int_{|t|}^{1} s \exp\{\frac{\psi(s)}{s}\} ds}{\int_{|t|}^{1} s \, ds} \tag{2-13}$$

they created from the original g-equation a family of integral equations involving these power series, and from which g, in terms of its expansion, could be obtained.

The radial distribution function of a fluid composed of hard spheres, which we denote by $g_o(r)$, is found in the first member of this family. This equation, simplest of the group, is:

$$\psi_o(x) = \frac{\lambda}{4} \int_{-\infty}^{\infty} K_o(x-s)s[g_o(s)-1]ds \quad , \tag{2-14}$$

where

$$K_o(t) = t^2 - 1 \quad , \qquad |t| \leq 1 \quad ,$$
$$= 0 \quad , \qquad |t| > 1 \quad ,$$

and λ is a parameter related to density:

$$\frac{1}{[g_o(1,\lambda)]^{\frac{1}{2}}} \int_o^{\lambda} \frac{d\lambda'}{[g_o(1,\lambda')]^{\frac{1}{2}}} = \frac{4\sqrt{2}\,\pi v_o}{v} \quad . \tag{2-15}$$

Here, v_o is the close packed volume of a system of spheres, and $g(1,\lambda)$ is the g at density λ and x = 1.

By expressing the resolvent kernel of $K_o(t)$ as

$$K_o(t) = -\frac{\lambda}{\pi} \int_o^{\infty} \frac{G(u) \cos ut \, du}{1-\lambda G(u)} \tag{2-16}$$

where

$$G(u) = \frac{1}{4}\int_{-\infty}^{\infty} K_o(t)e^{iut}du = \frac{ucosu-sinu}{u^3} \tag{2-17}$$

KMA replaced the g_o-equation with the following pair:

$$f_o(x) = - x + \int_{-1}^{1} K_o(x-s)f_o(s)ds \quad , \tag{2-18}$$

$$\psi_o(x) = - \int_{-1}^{1} K_o(x-s)f_o(s)ds \quad . \tag{2-19}$$

This pair of equations was more appropriate as the basis for the generation of an algorithm for the data processing equipment at their disposal.

Other ancillary analyses were incorporated into their treatment, but for our purpose their pattern is clear; the resolvent kernel $K_o(t)$ is evaluated, the $f_o(x)$ equation is solved iteratively (see Appendix I), and tables of $K_o(t)$ and $f_o(x)$ are used to evaluate ψ_o . $g_o(x)$ is then known.

The solutions may then be used in succeeding members of the family of equations. These equations are of the form:

$$\psi_n(x) = m_n(x) + \frac{\lambda}{4}\int_{-\infty}^{\infty} K_o(x-s)g_o(s)\psi_n(s)ds, \quad n = 1,2,3,\cdots. \tag{2-20}$$

In principle, sufficient information is generated at each step to proceed to the next family member; however, working one's way

through these equations becomes progressively more difficult because of the ballooning complexity of the $m_n(x)$ terms. For example,

$$m_1(x) = -x\gamma_1(x) + \psi_1(1)\psi_0(x) + \frac{\lambda_0}{4}\int_{-\infty}^{\infty} K_1(x-s)s[g_0(s)-1]ds \qquad (2\text{-}21)$$

but

$$m_2(x) = \psi_2(1)\psi_0(x) + \frac{1}{2}\psi_1^2(1)\psi_0(x) + \frac{\lambda_0}{4}\int_{-\infty}^{\infty} K_2(x-s)s[g_0(s)-1]ds$$

$$+ \frac{\lambda_0}{4}\int_{-\infty}^{\infty} K_1(x-s)g_0(s)\psi_1(s)ds + \frac{\lambda}{4}\int_{-\infty}^{\infty} K_0(x-s)g_0(s)\cdot$$

$$\cdot\left[\frac{\psi_1^2(s)}{2s}\right]ds + \lambda\frac{\psi_1(1)}{4}\int_{-\infty}^{\infty} K_0(x-s)g_0(s)\psi_1(s)ds \quad . \qquad (2\text{-}22)$$

One need only realize that the solutions are obtained by iteration (with each iteration demanding a number of numerical integrations of some considerable intricacy) to appreciate the magnitude of the practical problem involved in the calculation. Quite rapidly in one's progress through the family, there will be reached a point at which further solutions become prohibitively costly of time and effort. Indeed, even at the g_0 stage, certain theoretical considerations led KMA to perform extensive preliminary analysis and numerical manipulations to insure convergence of the $f_0(x)$ equation. KLA obtained solutions through the $g_2(x)$ term at a number of densities, and reported their results to three significant figures.

The Extension of the Solutions

Originally this work was intended to extend the numerical results of KMA (for g_o) and KLA (for the higher order terms) by following their general development while also taking advantage of improvements in data processing hardware and software. This line of attack led to several alterations in the equations on which the computational algorithms they used are based, and, finally, to a radical departure from their technique altogether.

A. The g_o-equation: In the repetitive numerical evaluation of any quantity, time spent in calculation becomes an important consideration. It is advisable to make mathematical modifications in the functional form of an equation on which the calculational algorithm is based in order to reduce the number of individual arithmetic operations involved and to transform more complicated, time consuming operations into simpler, quicker ones. (It is quicker on a computer, for example, to add the quantity A to itself rather than multiply it by 2.)

In the evaluation (which must be done numerically) of the resolvent kernal KMA found that a single partial integration yielding

$$K_o(t) = -\frac{\lambda}{\pi}\int_o^\infty \frac{[3uG(u)+\sin u]}{u^2[1-\lambda G(u)]^2}\sin ut\, du \qquad (2\text{-}23)$$

produced results faster than the original form. The effective

upper limit u_m which replaces the ∞ in the evaluation of the above integral could be set lower than would be in the case in the kernal's original form because the integrand becomes negligible at smaller arguments in comparison to the accumulating sum which approximates the integral. Fewer evaluations of the integrand were necessary and less time was consumed.

But an even more tractable modification can be made: beginning with the original form of $K_o(t)$, add and subtract the quantity

$$\int_o^\infty G(u)\cos ut\,du \quad ,$$

simplify, and obtain:

$$K_o(t) = -\frac{\lambda^2}{\pi}\int_o^\infty \frac{G^2(u)\cos ut\,du}{1-\lambda\, G(u)} - \frac{\lambda}{\pi}\int_o^\infty G(u)\cos ut\,du \quad . \tag{2-24}$$

Since G(u) is a function decreasing as u^{-2}, it is seen that the value of the first integrand of the above modified form is smaller for a given argument u than in the original form. The second integral is analytic . The technique can be repeated any number of times to obtain;

$$K_o(t) = -\frac{\lambda^N}{\pi}\int_o^\infty \frac{G^N(u)\cos ut\,du}{1-\lambda\, G(u)} + \sum_{n=1}^{N-1}\left\{-\frac{\lambda^n}{\pi}\int_o^\infty G^n(u)\cos ut\,du\right\} . \tag{2-25}$$

The improvement in the evaluation of the first integral is dramatic. In its original form the integrand required $u_m \simeq 400$; with N = 5 in Eq. (2-25), $U_m \simeq 20$ was required to achieve the same degree of accuracy.

The series of integrals

$$I_n = \int_0^\infty G^n(u)\cos ut\, du$$

are evaluated by first writing the trigonometric function in terms of Bessel functions:

$$G(u) = -\frac{1}{u}\left\{\frac{\sin u}{u^2} - \frac{\cos u}{u}\right\} = -\frac{j_1(u)}{u} \quad , \tag{2-26}$$

where $j_n(u)$ is the spherical Bessel function defined by:

$$j_n(u) = \left(\frac{\pi}{2u}\right)^{\frac{1}{2}} J_{n+\frac{1}{2}}(u) \quad . \tag{2-27}$$

Similary,

$$\cos ut = -(ut)\eta_o(ut) = \frac{\pi ut}{2} J_{-\frac{1}{2}}(ut) \quad . \tag{2-28}$$

Then, for example,

$$I_1 = -\frac{\pi t}{2}\int_0^\infty \frac{J_{3/2}(u)\, J_{-\frac{1}{2}}(ut)du}{u} \quad . \tag{2-29}$$

For $n > 1$, the powers of trigonometric functions are first reduced by identities to products of first power functions prior to conversion to Bessel functions.

These resulting integrals are of Weber-Schafheitlen type[10] whose solutions are given by

$$\int_0^\infty \frac{J_\mu(at)J_\nu(bt)dt}{t^\lambda} = \frac{a^\mu \Gamma(\frac{\mu+\nu-\lambda+1}{2})}{2^\lambda b^{\mu-\lambda+1}\Gamma(\mu+1)\Gamma(\frac{\nu-\mu+\lambda+1}{2})} \times {}_2F_1(\frac{\mu+\nu-\lambda+1}{2},$$

$$\frac{\mu-\nu-\lambda+1}{2};\ \nu+1,\ \frac{b^2}{a^2}), \qquad 0<a<b\ , \tag{2-30}$$

and

$$\int_0^\infty \frac{J_\mu(at)j_\nu(bt)dt}{t^\lambda} = \frac{b^\nu \Gamma(\frac{\mu+\nu-\lambda+1}{2})}{2^\lambda a^{\nu-\lambda+1}\Gamma(\nu+1)\Gamma(\frac{\mu-\nu+\lambda+1}{2})} \times {}_2F_1(\frac{\mu+\nu-\lambda+1}{2},$$

$$\frac{\nu-\mu-\lambda+1}{2}\ ;\ \mu+1,\ \frac{b^2}{a^2}), \qquad 0<b<a\ , \tag{2-31}$$

where ${}_2F_1$ is the hypergeometric function:

$${}_2F_1(a,b;c,z) = \frac{\Gamma(c)}{\Gamma(a)\Gamma(b)} \sum_{n=0}^{\infty} \frac{\Gamma(a+n)\Gamma(b+n)}{\Gamma(c+n)} \frac{z^n}{n!}\ . \tag{2-32}$$

For our case, the series truncates and yields a polynomial in t. There is an added windfall: it can be shown that the integrals I_n have the property

$$I_n = 0, \quad t > n$$

For sufficiently large t, the polynomial vanishes in the evaluation. Returning to the example, we obtain:

$$I_1 = -\frac{\pi\sqrt{t}}{2}\left\{\frac{t^{-\frac{1}{2}}\Gamma(\frac{1}{2})}{2\Gamma(\frac{1}{2})\Gamma(2)}\,{}_2F_1(\tfrac{1}{2},-1;\tfrac{1}{2},t^2)\right\}$$

$$-\frac{\pi}{4}(1-t^2), \qquad 0<t<1$$

$$= 0, \quad t\geq 1 \tag{2-33}$$

The analytic integrals, I_n, were evaluated for n = 1,2, $\cdots$,5. A more detailed example of the procedure and the results for all the integrals are given in Appendix II. These analytic results were checked by an alternate derivation involving Laplace transforms. The results were confirmed numerically by comparing $k_o(t)$ evaluated from its original integral expression with $k_o(t)$ evaluated from the modified form.

The numerical integration involving $G^6(u)$ converged quite rapidly. The table of $k_o(t)$ required for succeeding steps was generated at an estimated accuracy of $\pm$ 1 x 10^{-8}.

As mentioned earlier, KMA took great care to insure the convergence of the f_o's in the iterative solution of its equation. Certain arguments were offered that a solution could not be directly obtained from the equation and KMA made elaborate analyses to secure the f_o values. However, when a direct iterative solution of the equation

$$f_o(x) = -x + \int_{-1}^{1} k_o(x-s) f_o(s)\,ds$$

was attempted, no difficulty at all was encountered. The subsequent

application of tabular $f_o(x)$ values in the ψ_o equation led to values of $g_o(x)$ in excellent agreement with those given by KMA.

This was mildly surprising; quite possibly the improved accuracy of $k_o(t)$ values brought about by the modification of the equation on which the computational algorithm was based and the greater precision inherent to modern data processing equipment made the f_o-equation more tractable to a direct approach. But for whatever reason, this modest success in spite of the arguments that no direct numerical solution was possible generated an intriguing question: could it be that the entire manipulation of the $g_o(x)$ equation to form f_o- and ψ_o-equations was unnecessary?

The g_o-equation was altered slightly by the change of variable $s' = x-s$ to obtain

$$\ell n\{g_o(x)\} = \frac{\lambda_o}{3} + \frac{\lambda_o}{4x}\int_{-1}^{1}[(s')^2-1](x-s')g_o(x-s')ds' \quad . \tag{2-34}$$

This form was used as the basis of the computational algorthm. The table of $g_o(x)$ obtained was in agreement with the one obtained by use of the f_o- and ψ_o-equations. Almost as important, the time spent in calculation of the tables was reduced by an order of magnitude.

B. The g-equation: The surprising and quite pleasing discovery that dramatic simplifications of the g_o calculation were possible suggested--no, demanded--further investigation along these lines. Perhaps the g-equation itself was a viable basis for an algorithm. The entire tortuous process involving the expansions of ψ, g, and

K could be avoided. Inaccuracies introduced by omission of higher order terms of the expansions would be eliminated. Certainly the programming effort required to construct the algorithms would be reduced. Constraints and approximations placed on the functional form of the intermolecular potential (modifications necessary in the earlier developments facilitate manipulation of intermediate equations) could be disregarded. The machine time devoted to the calculation would be reduced.

Only a small modification in the g-equation is necessary to obtain a form suitable for the generation of the algorthm. Recall that:

$$\ell n\{g(x)\} = -\beta\varepsilon\gamma(x) + \frac{\lambda_o}{4x}\int_{-\infty}^{\infty} K(x-s)s[g(s)-1]ds \quad ,$$

where

$$K(t) = \beta\varepsilon\int_{|t|}^{\infty}(s^2-t^2)g(s)\frac{d\gamma}{ds}ds \quad .$$

With the assumption that g and γ are even functions in x, a change in variables $s' = x-s$ allows us to write the integral portion of the above equation as

$$I = \int_{-\infty}^{0} Zds' + \int_{0}^{\infty} Zds', \quad Z = K(s')(x-s')[g(x-s')-1] \quad . \tag{2-35}$$

The change in variables $s = -s'$ in the first integral, and $s = s'$ in the second yields

$$I = \int_0^\infty K(s)[(x-s)g(x-s)+(x+s)g(x+s)-2s]ds \quad , \tag{2-36}$$

and this form is used to create the algorithm.

The initial calculation gave results which were in good agreement with those of KLA.

This opened the door to a broader line of investigation, for the new algorithm permitted a far more convenient and straightforward interchange of intermolecular potentials in the calculation than was possible using the KLA technique. Radial distribution functions free from the limitations of the earlier procedures could be generated at will for a variety of potentials, rendering the potential itself a parameter of the calculation. The RA theory could be examined in a broader sense, more flexibly than might otherwise have been the case.

C. The Intermolecular Potential: The calculations were performed for three different intermolecular potentials.

The Lennard-Jones (LJ) 12-6 potential is of the form:

$$V_{LJ}(R) = \varepsilon\gamma(x) = 4\varepsilon\{x^{-12} - x^{-6}\}, \quad x = \frac{R}{a} \tag{2-37}$$

in which a is the value for which $V(a) = 0$, and ε is the depth of the potential well.

The Modified Buckingham (MB) potential is of the form

$$V_{MB}(x) = \left(\frac{\varepsilon}{1-\ 6/\alpha}\right)\left(\frac{6}{\alpha}\ \exp[\alpha(1-x)]-x^{-6}\right)\ ,\quad x > \frac{r_{max}}{r_m}$$

$$= \infty\ ,\quad x \le \frac{r_{max}}{r_m}\ ;\quad x = \frac{r}{r_m} \tag{2-38}$$

r_{max} is the value of R for which V(R) as given by the upper relation has a (spurious) maximum; α is the steepness of the exponential repulsion, r_m is the location of the potential minimum.

The Barker-Bobetic[11] (BB) potential is of the form

$$V_{BB}(x) = \varepsilon\left\{\exp[\alpha(1-x)]\ \sum_{i=0}^{L} A_i(x-1)^i - \sum_{i=0}^{2} \frac{C_{2i+6}}{(\delta+x^{2i+6})}\right\}, \tag{2-39}$$

where L = 5, $x = \frac{R}{r_m}$, ε = well depth, α is the steepness of the exponential repulsion, r_m the location of the energy minimum, and the A, C. and δ are substance dependent constants. Argon and nitrogen were analyzed with LJ and MB potentials, argon alone with the BB potential (nitrogen values being unavailable for the BB potential).

CHAPTER III

THE RICE-ALLNATT EQUATIONS

General Remarks

This discussion makes no presumption of rigor; for a detailed treatment of the theory, the reader is referred to the papers and subsequent summary discussions of the original authors. What follows is a treatment of the cardinal points of the Rice-Allnatt development.

In a monatomic dense system, interactions between constituent particles may be conceptually divided into two broad categories: "hard core" collisions at close range, associated with the steep, repulsive portion of the intermolecular potential, and "soft" interactions at longer ranges, associated with the attractive tail of the intermolecular potential. For the present, we exclude consideration of hard core encounters between more than two particles. We might imagine a typical molecule of the fluid moving about in an environment which is the aggregate of the soft, attractive potentials of its neighbors and this motion being occasionally punctuated by close range encounters with particular neighbors. Because of the constantly changing configuration of the neighboring particles, the aggregate soft potential itself exhibits a stochastic character, and this motion between sharp encounters is of a quasi-Brownian nature.

The assumption that there are two categories of interactions allows us to make an inference regarding the nature of a particle's motion: the random character of the soft interactions tend to dissociate one hard core interaction from another. Contrast this to the situation encountered in a fluid of hard spheres, where in principle at least we may expect first a definite knowledge of a particle's trajectory (in a two-body encounter) and, secondly, the ability to extend the trajectory and anticipate subsequent collisions. With the introduction of soft interactions, however, we find the path between sharp collisions to be some what of the nature of a random walk (this is the consequence of the varying soft field) and the knowledge of the details of one collision imply only a statistical subsequent behavior. Similarly, the knowledge of the details of one collision cannot be used to trace back along the path to the preceeding one. The quasi-Brownian motion between collisions has masked what otherwise would have been, in the hard core fluid, the deterministic flow of events. Pursuing this line of reasoning, Rice-Allnatt assume the existence of a time interval τ such that "...the dynamical events occurring in one interval are independent of those in the preceding interval.",[12] and it is in this fashion that they introduce the concept of irreversibility into their equations.

Derivation of the Kinetic Equations

The starting point of the RA derivation, as with many other developments, is the Liouville Equation:

$$\left[\frac{\partial}{\partial t}+\sum_{i=1}^{N}\left\{\frac{1}{m}\vec{p}_i\cdot\nabla_i+\sum_{j(\neq i)=1}^{N}\vec{F}_{ij}\cdot\nabla_{p_i}\right\}\right]f_N(Z_1,\ldots,Z_N;t)=0 \quad . \tag{3-1}$$

Assuming forces are functions of position only, integrations over the variables $Z_{n+1}, \cdots, Z_N$ coupled with multiplication by the factor $(N!)/(N-n)!$ casts the above in terms of an n-tuple distribution function:

$$\left[\frac{\partial}{\partial t} + \sum_{i=1}^{n} \left\{\frac{1}{m} \vec{P}_i \cdot \nabla_i + \sum_{j(\neq i)=1}^{n} \vec{F}_{ij} \cdot \nabla_{p_i}\right\}\right] F_n(Z_1, \ldots, Z_n; t)$$

$$= - \sum_{i=1}^{n} \int \cdots \int \vec{F}_{i,n+1} \cdot \nabla_{p_i} F_{n+1} dz_{n+1} , \quad 1 \leq n \leq N-1 \tag{3-2}$$

Observe that this is a hierarchy of equations, linking the n-tuple reduced distribution function to the (n+1)-tuple reduced distribution function.

Next, the time interval τ is incorporated by defining time coarse graining as the time averaging of F_n at each point in phase space:

Coarse Graining

$$\bar{f}_n(\{Z\}; t) = \frac{1}{\tau} \int_0^{\tau} F_n(\{Z\}; t+s) ds \quad . \tag{3-3}$$

Our equation for the lowest member of the hierarchy, coupling f_1 to f_2 in terms of the coarse grained distribution function, becomes

$$\left[\frac{\partial}{\partial t} + \frac{1}{m} \vec{P}_1 \cdot \nabla\right] \bar{f}_1 = - \frac{1}{\tau} \int_0^{\tau} \int \vec{F}_{12} \cdot \nabla_{p_1} F_2 \, dz_2 ds \ , \tag{3-4}$$

and at this point we may divide the $\vec{F}_{12}$, the force on molecule one

by molecule 2, into its hard and soft componants:

$$[\frac{\partial}{\partial t} + \frac{1}{m}\vec{p}_1 \cdot \nabla_1]\bar{f}_1 = \Omega_H + \Omega_s \quad , \tag{3-5}$$

where

$$\Omega_H = -\frac{1}{\tau}\int_o^\tau\int \vec{F}_{12}^{(H)} \cdot \nabla_{p_1} \bar{F}_2 dz_2 ds \quad , \tag{3-6}$$

and

$$\Omega_s = -\frac{1}{\tau}\int_o^\tau\int \vec{F}_{12}^{(s)} \cdot \nabla_{p_1} \bar{F}_2 dz_2 ds \quad . \tag{3-7}$$

It is required to cast Ω_H and Ω_s in a form suited for the solution of the Liouville equation as modified. We happily omit the details of this process from the discussion, citing only the assumptions made and functions introduced along the way. We will return to these points for additional comments later, in our discussion of the results of our work.

We assume that the soft force $\vec{F}^{(s)}$ does not influence significantly the process or details of a hard core encounter. This assumption is plausible since the time of a hard core encounter τ_1 can be expected to be much shorter than τ and because the interaction forces at play during the hard core collision process are significantly greater than the aggregate soft force. Therefore, it is possible to treat the Ω_s and Ω_H expressions separately, and in fact to disregard $F^{(s)}$ altogether during our manipulation of Ω_H.

The development of a viable functional form for Ω_H stems from several intermediate definitions, assumptions and manipulations.

A <u>phase space transition probability</u>, $K_n(\{Z_n\}|\{Z_n'\};s)$ is defined as the probability density that a subsystem of n molecules will undergo a transition of coordinates from $\{Z_n'\}$ to $\{Z_n\}$ in the time s. If the distribution function (of any type) for this subsystem is $f_n(\{Z_n\};t)$ then

$$f_n(\{Z_n\};t+s) = \int K_n(\{Z_n\}|\{Z_n'\};s) f_n(\{Z_n'\};t) dz_1' \ldots dz_n' \quad . \tag{3-8}$$

The functional form of K_n is deduced, and the integration of Ω_H accomplished.

Then the pair distribution function is expressed as

$$\bar{f}_2(Z_1,Z_2;t) = \bar{f}_1(Z_1;t)\ \bar{f}_1(Z_2;t)\ G_2(Z_1,Z_2;t) \ , \tag{3-9}$$

where G_2 is called the pair phase correlation function (a quantity generally unknown). Next, RA assume it is possible to express as:

$$G_2(Z_1,Z_2;t) = g^{(2)}(r_1,r_2) \tag{3-10}$$

i.e., the pair phase correlation function is independent of momenta and, because of coarse time graining, and the restrictions placed on gradients, approximately independent of time as well. Introduction

of $g^{(2)}$ into the Ω_H expression truncates the hierarchy of equations relating f_n to f_{n+1}. A change of variables and a power series expansion results in the following expression:

$$\Omega_H = \frac{g_o^{(2)}(\vec{r}_1,\sigma)}{m}\int[\bar{f}_1(\vec{r}_1,\vec{p}_1{}^*)\bar{f}_1(\vec{r}_1,\vec{p}_2^*)-\bar{f}_1(\vec{r}_1,\vec{p}_1)\bar{f}_1(\vec{r}_1,\vec{p}_2)]$$

$$\times p_{12}bdbd\varepsilon d\vec{p}_2 + \sigma g_o^{(2)}(\vec{r}_1,\sigma)\int[\bar{f}_1(\vec{r}_1,\vec{p}_1^*)\vec{k}_o\cdot\nabla_1\bar{f}_1(\vec{r}_1,\vec{p}_2^*)$$

$$+ \bar{f}_1(\vec{r}_1,\vec{p}_1)\vec{k}\cdot\nabla_1\bar{f}_1(\vec{r}_1,\vec{p}_2)]p_{12}bdbd\varepsilon d\vec{p}_2 + \frac{\sigma\nabla_1 g_o^{(2)}(\vec{r}_1,\sigma)}{2m}$$

$$\cdot\int\vec{k}[\bar{f}_1(\vec{r}_1,\vec{p}_1^*)\bar{f}_1(\vec{r}_1,\vec{p}_2) + \bar{f}_1(\vec{r}_1,\vec{p}_1)\bar{f}_1(\vec{r}_1,\vec{p}_2)]p_{12}bdbd\varepsilon d\vec{p}_2 \qquad (3\text{-}11)$$

$$\Omega_H = J_1^{(1)} + J_2^{(1)} + J_3^{(1)} \qquad (3\text{-}12)$$

Here, $\vec{k}$ is a unit vector pointing from the center of molecule 1 to the center of molecule 2, and the incremental volume into which molecule 2 can be scattered is $P_{12}\tau\,\frac{bdbd\varepsilon}{m}$. The asterisk denotes pre-collision value of quantities, and σ is the hard core radius of the molecules.

By applying the phase space transition probability to Ω_s, RA obtain

$$\Omega_s = -\frac{N(N-1)}{\tau}\int_o^\tau\int\vec{F}_{12}^{(s)}\cdot\nabla_{p_1}K_N(\{Z_N\}|\{Z_n'\};s)\times \qquad (3\text{-}13)$$

$$\cdot f^{(N-2/2)}(\{Z_{N-2}'\}|\{Z_2'\};t)f_2(Z_1,Z_2;t)\{dz_{N-2}'\}dz_2ds$$

where $f^{(N-n/n)}$ is called the specific phase space probability density and is defined by the equation

$$f_N(\{Z_N\};t) = f_n(\{Z_n\};t)f^{(N-n/n)}(\{Z_{N-n}\}|\{Z_n\};t) \quad . \qquad (3\text{-}14)$$

Again, as with Ω_H, a solution for K_N is deduced; this time, however, the soft force $\vec{F}^{(s)}$ is of the nature of a weak interaction, and the solution to K_N is in the form of a power series

$$K_N = \sum_{i=0}^{\infty} \lambda^i (K_N)^{(i)} \tag{3-15}$$

with λ an ordering parameter, to subsequently be set to one. There results a series expression for Ω_s, which when truncated becomes

$$\Omega_s = \Omega_s^{(0)} + \Omega_s^{(1)} \tag{3-16}$$

where

$$\Omega_s^{(0)} = -\frac{N(N-1)}{\tau} \nabla_{p_1} \cdot \left[\int_o^{\tau}\int \vec{F}_{12}^{(s)} f^{(n)}(\Gamma_N;t)d\Gamma_{N-1}ds\right] \tag{3-17}$$

and

$$\Omega_s^{(1)} = \frac{N(N-1)}{\tau} \nabla_{p_1} \cdot \int_o^{\tau}\int_{\tau_1}^{s} \vec{F}_{12}^{(s)} \sum_{i=1}^{N} \left[\nabla_{p_i} + \frac{s-s'}{m} \nabla_i\right]$$

$$\cdot \left[\vec{F}_i^{(s)} \left[\vec{R}^{(N)} + (s'-s) \frac{\vec{P}^{(N)}}{m}\right)\right] f^{(N)}(\Gamma_{N,o};t)d\Gamma_{N-1}ds'ds \ . \tag{3-18}$$

Additional manipulation of the $\vec{F}^{(s)}$ terms in $\Omega_s^{(1)}$ permits the identification of the $\Omega_s^{(1)}$ expression as "...a Fokker-Planck operator with momentum dependent friction coefficients." RA replaces this equation with a simpler one, involving a constant friction coefficient. The final equation obtained, the singlet equation, is

$$\mathcal{D}^{(1)}\bar{f}^{(1)} = \sum_{i=1}^{3} J_i^{(1)} + \zeta_s A^{(1)}\bar{f}^{(1)} \tag{3-19}$$

where

$$\mathcal{D}^{(1)}\bar{f}^{(1)} = \left(\frac{\partial}{\partial t} + \frac{1}{m}\vec{p}_1\cdot\nabla_1 + F_1^*\cdot\nabla_{p_1}\right)\bar{f}^{(1)} \quad , \tag{3-20}$$

$$A^{(1)}\bar{f}^{(1)} = \nabla_{p_1}\cdot\left(\frac{\vec{p}_1}{m}\vec{u}\bar{f}^{(1)} + kT\nabla_{p_1}\bar{f}^{(1)}\right) \tag{3-21}$$

and

$$\begin{aligned} F_1^* &= \rho\int \vec{F}_{12}^{(s)}(\vec{R}_{12})g_o^{(2)}(\vec{R}_{12})d\vec{R}_{12} \\ &\quad + \rho\int \vec{F}_{12}^{(s)}(\vec{R}_{12})g_1^{(2)}(\vec{R}_1\vec{R}_2)d\vec{R}_{12}, \\ \rho &= \frac{N-1}{V} \quad , \end{aligned} \tag{3-22}$$

and ζ_s is the soft friction coefficient.

The doublet equation, ie, the integro-differential equation deduced from the Liouville equation involving the doublet distribution function $\bar{f}^{(2)}$, is found in a similar manner to that used to obtain the singlet $[\bar{f}^{(1)}]$ equation.

These equations, the singlet and doublet equation, RA call the kinetic equations. The task is now to solve them, and RA do so by techniques similar to that of Enskog and Chapman,[13] finding:

$$\bar{f}^{(1)}(1) = \bar{f}_o^{(1)}\{1+\sqrt{\frac{2kT}{m}}\frac{15}{4}\frac{[\frac{1}{\rho g(\sigma)}+\frac{2\pi\sigma^3}{5}]}{[4\Omega^{(2,2)}+\frac{45\zeta_s}{4\rho m g(\sigma)}]}\times(\frac{5}{2}-W_1^2)\vec{W}_1\cdot\nabla\ell nT$$

$$-\frac{5[\frac{1}{\rho g(\sigma)}+\frac{4\pi\sigma^3}{15}]}{[4\Omega^{(2,2)}+\frac{5\zeta_s}{\rho m g(\sigma)}]}\times(\vec{W}_1\vec{W}_1-\frac{W_1^2}{3}\underline{\underline{I}}):\nabla\vec{u})\quad , \tag{3-23}$$

$$\bar{f}_o^{(1)} = \frac{\rho}{(2\pi mkT)^{3/2}}\exp\{-\frac{(\vec{p}_1-m\vec{u})^2}{2mkT}\} \tag{3-24}$$

$$\Omega^{(2,2)} = (\frac{4\pi kT}{m})^{\frac{1}{2}}\sigma^2 \quad ,$$

$$\vec{W}_1 = \frac{\vec{p}_1-m\vec{u}}{(2mkT)^{\frac{1}{2}}}, \quad \text{and} \quad g(\sigma) = g_o^{(2)}(R_{12}=\sigma) \quad . \tag{3-25}$$

A similar but more complicated solution for $\bar{f}^{(2)}$ is found:

$$\bar{f}^{(2)}(1,2) = \bar{f}_o^{(2)}(1,2)[1-\sum_{i=1,2}\{A_1(\frac{5}{2}-W_i^2)\vec{W}_i\cdot\nabla_i\ell nT_i$$

$$+ B_o^{(1)}\underline{\underline{b}}_i:\nabla_i\vec{u}_i + C_o\vec{W}_i\cdot{}^{(2)}\vec{F}_i\}] \tag{3-26}$$

where

$$\bar{f}_o^{(2)} = g_o^{(2)}(R_1R_2)\prod_{i=1,2}\frac{\rho_i}{(2\pi mkT_i)^{3/2}}\exp\{-\frac{(\vec{p}_i-m\vec{u}_i)^2}{2mkT_i}\} \tag{3-27}$$

$$A_1 = -\frac{15}{4}\left(\frac{2kT}{m}\right)^{1/2} \frac{\left[\frac{1}{\rho g(\sigma)} + \frac{2\pi\sigma^3}{5}\right]}{\left[8\Omega^{(2,2)} + \frac{45\zeta_s}{4\rho m g(\sigma)}\right]} \left\{1 + \frac{4\Omega^{(2,2)}}{4\Omega^{(2,2)} + \frac{45\zeta_s}{4\rho m g(\sigma)}}\right\} \tag{3-28}$$

$$B_1 = \frac{5\left[\frac{1}{\rho g(\sigma)} + \frac{4\pi\sigma^3}{15}\right]}{\left[8\Omega^{(2,2)} + \frac{4\zeta_s}{\rho m g(\sigma)}\right]} \left\{1 + \frac{4\Omega^{(2,2)}}{4\Omega^{(2,2)} + \frac{5\zeta_s}{\rho m g(\sigma)}}\right\} \tag{3-29}$$

$$C_o = -\sqrt{2m/(kT)}\ \zeta_s^{-1} \tag{3-30}$$

$$\underline{\underline{b}}_i = \vec{W}_i \vec{W}_i - \frac{1}{3} W_i^2 \underline{\underline{1}} \tag{3-31}$$

and $\overset{(2)}{\vec{G}}{}_i^F$ is the net mean force on molecule i when another molecule is located at $\vec{R}_j$

$$\overset{(2)}{\vec{G}}{}_i^F = \vec{F}_i^{(2)} - \vec{F}_i^* - kT_i \ell n g^{(2)}(\vec{R}_1 \vec{R}_2) \quad . \tag{3-32}$$

Having obtained these expressions for singlet and doublet equations, RA then proceed to utilize them in the molecular expressions for transport of momentum and energy.

The Transport Equations

Phenomenologically we may define the transport coefficients in terms of the respective fluxes of number, momentum and energy:

if j_{iz} is the flux of particles of the i^{th} species in the z direction and n_i the number density of this species, then the coefficient of diffusion, $\mathcal{D}$, is defined by the equation

$$j_{iz} = - \mathcal{D} \frac{dn_i}{dz} \tag{3-33}$$

Similarly, if P_{yz} is the flux of the y-component of momentum in the z-direction, v_y the y-component of velocity, and η the coefficient of viscosity, then

$$P_{yz} = - \eta \frac{dv_y}{dz} \quad . \tag{3-34}$$

Finally, with q_z the energy flux and T the temperature, the thermal conductivity, χ, is defined by

$$q_z = - \chi \frac{dT}{dz} \quad . \tag{3-35}$$

In this context we see the transport coefficients in their gross, macroscopic nature as nothing more than proportionality constants between flux and gradient. This representation forms the basis for the direct experimental measurements of these quantities.

These definitions, however, provide no insight into the functional nature of the coefficients. In order to gain this understanding, a more precise set of macroscopic equations must be formulated and linked to an analogous set constructed from a microscopic point of view. The transport coefficients so formulated in terms of

the distribution function, may be numerically evaluated and compared to the corresponding experimentally determined quantities. Hopefully, a critical test of the theory upon which the microscopic equations are based may then be made.

It is interesting to note at this point that, originally, the more precise macroscopic equations concerning viscosity did not agree with experiment and that modifications in the theory involving the introduction of a second viscosity coefficient were required in order to account for certain anamolies observed in the coefficients of absorption of sound in fluids.[14] This additional coefficient (called the second visocity coefficient, μ') leads to the further definition of a bulk viscosity coefficient, K, defined as

$$K = \frac{2\eta+3\mu'}{3} \quad . \tag{3-36}$$

The bulk viscosity term relates to the viscous forces at play in the pure compression of a fluid. Several mechanisms have been proposed to explain the origin of K, all relating lag between application of a compressive stress and re-establishment of equilibrium. The one of Hertzfeld and F.O. Rice[15] relates to the exchange of energy between translational motion and internal degrees of freedom; that of Hall,[16] the rearrangement of molecules.

Although the calculation of the bulk viscosity is not a direct object of this present work, a discussion of K is included in what follows in the interest of completeness. Babb has extended this present work to bulk viscosity, basing the calculations on the architecture of the shear viscosity algorithm.

A. The Macroscopic Equations. If ρ_m is the mass density of a fluid and $\vec{u}$ is the fluid velocity, then the equation of continuity of the fluid is

$$\frac{\partial \rho_m}{\partial t} + \nabla\cdot(\rho_m \vec{u}) = 0 \quad . \tag{3-37}$$

If $\vec{f}$ is the external force density and $\underline{\underline{\sigma}}$ is the stress tensor, we may obtain the fluid's equation of motion as

$$\frac{\partial}{\partial t}(\rho_m \vec{u}) + \nabla\cdot(\rho_m \vec{u}\vec{u}) = \vec{f} + \nabla\cdot\underline{\underline{\sigma}} \quad . \tag{3-38}$$

By additionally defining e as the enternal energy per unit mass of the fluid, and $\vec{q}$ as the energy conduction current, an energy transport equation may be written as

$$\vec{u}\cdot\vec{f} + \nabla\cdot(\underline{\underline{\sigma}}\cdot\vec{u}) - \nabla\cdot\vec{q} =$$

$$\frac{\partial}{\partial t}\left\{\left[e + \frac{u^2}{2}\right]\rho_m\right\} + \nabla\cdot\left\{\left[e + \frac{u^2}{2}\right]\rho_m\right\} \quad . \tag{3-39}$$

It is through the Newtonian law defining the stress tensor that the coefficient of shear and bulk (relaxation) viscosity are introduced:

$$\underline{\underline{\sigma}} = -\left(p + \left[\frac{2}{3}\eta + \phi\right]\nabla\cdot\vec{u}\right)\underline{\underline{I}} + 2\eta\underline{\underline{\varepsilon}} \quad , \tag{3-40}$$

where $\underline{\underline{\varepsilon}} = \frac{1}{2}(\nabla\vec{u} + \tilde{\nabla}\vec{u})$, $\quad (\tilde{\nabla}\vec{u})_{ij} = \nabla\vec{u}_{ji}$.

p is the equilibrium pressure and ϕ is the coefficient of bulk viscosity. The equation of motion becomes

$$\rho_m \frac{D\vec{u}}{Dt} = - \nabla p + (\frac{\eta}{3} + \phi)\nabla(\nabla\cdot\vec{u}) + \eta\nabla^2\vec{u} + \vec{f} \quad . \tag{3-41}$$

Using the definition of energy transport in phenomenological terms as

$$\vec{q} = - \chi\nabla T \quad , \tag{3-42}$$

the continuity equation, and some approximations, we may write the energy equation as

$$\frac{\partial T}{\partial t} = \frac{\chi\nabla^2 T}{C_v \rho_m} \quad , \tag{3-43}$$

where C_v is the specific heat at constant volume of the fluid.

Another form of the energy equation, in terms of the internal energy density $E = \rho_m e$, is

$$\frac{\partial E}{\partial t} + \nabla\cdot(E\vec{u}) = \underline{\sigma}:\nabla\vec{u} - \nabla\cdot\vec{q} \quad . \tag{3-44}$$

These are the macroscopic equations used by RA in the formulation of expressions for the transport coefficients.

B. The Microscopic Equations. To obtain the expressions for the transport coefficients in terms of the statistical mechanical variables, RA use. "...the procedure of Irving and Kirkwood; this is quite general and consists simply in defining molecular equivalents of, for instance, mass, momentum, and energy densities, and establishing their equations of motion by suitable contractions of the Liouville equation...".

$$\text{Defining} \quad \langle \alpha; f^{(N)} \rangle = \int \alpha(\Gamma_N) f^{(N)}(\Gamma_N; t) d\Gamma_N \ , \tag{3-45}$$

RA first use the Liouville Equation in the form

$$\frac{\partial f^{(N)}}{\partial t} = [H, f^{(N)}] \tag{3-46}$$

to obtain

$$\frac{\partial}{\partial t} \langle \alpha, f^{(N)} \rangle = \sum_{k=1}^{N} \langle \frac{1}{m} \vec{p}_k \cdot \nabla_k \alpha + \vec{F}_k \cdot \nabla_{p_k} \alpha; f^{(N)} \rangle \ . \tag{3-47}$$

Applying this expression to the conservation of mass, by defining

$$\alpha_m = \sum_{j=1}^{N} m \delta(\vec{R}_j - \vec{r}) \tag{3-48}$$

they show that

$$\frac{\partial \rho_m}{\partial t} (\vec{r}; t) = - \nabla \cdot [\rho_m(\vec{r}; t) \vec{u}(\vec{r}; t)] \ , \tag{3-49}$$

which is the continuity equation. If instead there is defined

$$\vec{\alpha}_j = \sum_{j=1}^{N} \vec{p}_j \delta(\vec{R}_j - \vec{r}) \tag{3-50}$$

and this is applied to the expression for $\frac{\partial}{\partial t} \langle \alpha; f^{(N)} \rangle = \cdots$ it is found that the equation of motion is:

$$\frac{\partial}{\partial t}(\rho_m \vec{u}) + \nabla \cdot (\rho_m \vec{u}\vec{u}) = \vec{f} + \nabla \cdot \left[- \sum_{k=1}^{N} m \left\langle \left(\frac{\vec{p}_k}{m} - \vec{u} \right) \left(\frac{\vec{p}_k}{m} - \vec{u} \right) \delta(\vec{R}_K - \vec{r}); f^{(N)} \right\rangle \right.$$

$$\left. + \tfrac{1}{2} \sum_{j \neq k=1}^{N} \sum \left\langle (\nabla_K u_{jk}) \vec{R}_{jk} \delta(\vec{R}_j - \vec{r}) : f^{(N)} \right\rangle \right] . \tag{3-51}$$

Comparison of this with the macroscopic equation shows that the stress tensor must be

$$\underline{\underline{\sigma}} = \underline{\underline{\sigma}}_k + \underline{\underline{\sigma}}_v \quad , \tag{3-52}$$

where

$$\sigma_k = - \sum_{k=1}^{N} m \left\langle \left(\frac{\vec{p}_k}{m} - \vec{u} \right) \left(\frac{\vec{p}_k}{m} - \vec{u} \right) \cdot \delta(\vec{R}_k - \vec{r}); \quad f^{(N)} \right\rangle \quad , \tag{3-53}$$

$$\sigma_v = \tfrac{1}{2} \sum_{j \neq k=1}^{N} \sum \left\langle \frac{\vec{R}_{jk} \vec{R}_{jk}}{R_{jk}} u_{jk} \cdot \delta(\vec{R}_j - \vec{r}); \quad f^{(N)} \right\rangle \quad , \tag{3-54}$$

at least to the curl of an arbitrary function of $\vec{r}$. The above proves to be the correct form for $\underline{\underline{\sigma}}$, and the two expressions may be reduced to:

$$\underline{\underline{\sigma}}_k = - m\int (\frac{\vec{p}_1}{m} - \vec{u})(\frac{\vec{p}_1}{m} - \vec{u})\bar{f}^{(1)} d\vec{p}_1 \qquad (3\text{-}55)$$

and

$$\underline{\underline{\sigma}}_v = \frac{1}{2\tau}\int_0^\tau \int \vec{R}_{12}\nabla_{12}u\ f^{(2)} d\vec{R}_{12} d\vec{p}_1 d\vec{p}_2 ds \quad . \qquad (3\text{-}56)$$

Since the stress tensor is already known as

$$\underline{\underline{\sigma}} = - (p + [\frac{2}{3}\eta + \phi]\nabla\cdot\vec{u})\underline{\underline{I}} + 2\eta\underline{\underline{\varepsilon}}$$

the evaluation of the integral expressions for $\underline{\underline{\sigma}}_k$ and $\underline{\underline{\sigma}}_v$, using the singlet and doublet distribution functions already obtained will, by comparison, permit η and ϕ to be expressed in terms of the RA theory.

The evaluation of energy transport in microscopic terms is done in two parts, first defining the internal kinetic energy density

$$E_k = \langle \alpha_k ; f^{(N)} \rangle \quad , \qquad (3\text{-}57)$$

where

$$\alpha_k = \sum_{j=1}^{N} \frac{m}{2} (\frac{\vec{p}_j}{m} - \vec{u})^2 \delta(\vec{R}_j - \vec{r}) \quad , \qquad (3\text{-}58)$$

and then the potential energy density, E_v, using

$$\alpha_v = \tfrac{1}{2} \sum_{j\neq k=1}^{N}\sum u_{jk}\delta(\vec{R}_j-\vec{r}) \quad . \tag{3-59}$$

There is obtained

$$\frac{\partial E}{\partial t} + \nabla\cdot(\vec{u}E) = \underline{\underline{\sigma}}:\nabla\vec{u} - \nabla\cdot[<\sum_{k=1}^{N}\frac{m}{2}(\frac{\vec{p}_k}{m}-\vec{u})^2(\frac{\vec{p}_k}{m}-\vec{u})\delta(\vec{R}_k-\vec{r});f^{(N)}>$$

$$+ \tfrac{1}{2}<\sum_{j\neq k=1}^{N}\sum (u_{kj}\underline{\underline{I}} - \frac{\vec{R}_{kj}\vec{R}_{kj}}{R_{kj}}u'_{kj})\cdot(\frac{\vec{p}_k}{m}-\vec{u})\delta(\vec{R}_K-\vec{r});f^{(N)}>] \tag{3-60}$$

which may be compared with

$$\frac{\partial E}{\partial t} + \nabla\cdot(E\vec{u}) = \underline{\underline{\sigma}}:\nabla\vec{u} - \nabla\cdot\vec{q} \quad .$$

By separating the conduction current (or heat flux) $\vec{q}$ into kinetic and potential portions,

$$\vec{q} = \vec{q}_k + \vec{q}_v \quad , \tag{3-61}$$

$$\vec{q}_k = <\sum_{k=1}\frac{m}{2}(\frac{\vec{p}_k}{m}-\vec{u})^2(\frac{\vec{p}_k}{m}-\vec{u})\delta(\vec{R}_k-\vec{r});f^{(N)}> \tag{3-62}$$

$$\vec{q}_v = \tfrac{1}{2}<\sum_{j\neq k=1}^{N}\sum (u_{kj}\underline{\underline{I}} - \frac{\vec{R}_{kj}\vec{R}_{kj}}{R_{kj}}u'_{kj})\cdot(\frac{\vec{p}_k}{m}-\vec{u})\delta(\vec{R}_k-\vec{r});f^{(N)}> \tag{3-63}$$

C. The Coefficients of Viscosity Equations.

Rice and Allnatt assume a potential which is truncated at $v(r) = 0$; i.e., at $r = \sigma$, with $v(r) = \infty$ at $r<\sigma$. This assumption gives a well-defined radius. Further, the departure from equilibrium of $g(r)$ is expanded in a series of spherical harmonics,

$\Delta g = \psi_0 P_0 + \psi_2 P_2 + \ldots$, and then the derivation is carried through as outlined below. The original papers must be consulted for the intricate details.

Rice and Allnatt represent the coefficients of viscosity as

$$\theta = \theta_k + \theta_v(\sigma) + \theta_v(R_{12}>\sigma); \quad \theta = \eta, \phi \quad , \tag{3-64}$$

where η is the coefficient of shear viscosity and ϕ is the coefficient of bulk viscosity.

θ_k, the kinetic term, expresses the effect of hard-core interactions. Substituting the expression for the singlet distribution $\bar{f}^{(1)}$ into

$$\underline{\underline{\sigma}}_k = -m\int(\frac{\vec{p}_1}{m} - \vec{u})(\frac{\vec{p}_1}{m} - \vec{u})\bar{f}^{(1)}d\vec{p}_1 \quad , \tag{3-65}$$

by performing the necessary manipulations and integration, and by then comparing the result to the Newtonian expression for the stress tensor, they obtain

$$\eta_k = \frac{5kT}{8g(\sigma)}\left\{\frac{1+\frac{4\pi\rho\sigma^3 g(\sigma)}{15}}{\Omega^{(2,2)}+\frac{5\zeta_s}{4\rho m g(\sigma)}}\right\} \quad , \tag{3-66}$$

where σ is the hard-core radius, ρ is the density, ζ_s is the soft drag or friction coefficient, and $\Omega^{(2,2)}$ is a collision integral term:

$$\Omega^{(2,2)} = \left\{\frac{4\pi kT}{m}\right\}^{\frac{1}{2}}\sigma^2 \quad .$$

As is to be expected, $\phi_k = 0$.

θ_v results from the attractive short-range potential interaction among molecules of the fluid. The identification of η_v and ϕ_v begins with

$$\underline{\underline{\sigma}}_v = \frac{1}{2\tau} \int_o^\tau \int \vec{R}_{12} \nabla_{12} u f^{(12)} d\vec{R}_{12} d\vec{p}_1 d\vec{p}_2 ds \tag{3-67}$$

and the insertion of the doublet expression previously determined. The subsequent reduction of the expression which results is a much longer process than that with $\underline{\underline{\sigma}}_k$ and divides along mathematical lines into three terms, $\sigma_v^{(1)}$, $\sigma_v^{(2)}$, and $\sigma_v^{(3)}$

$$\eta_v^{(1)} = \frac{5kT}{8g(\sigma)} \cdot \frac{2\pi\rho\sigma^3}{15} \left\{1 + \frac{4\pi\rho\sigma^3 g(\sigma)}{15}\right\} D \ , \tag{3-68}$$

where

$$D = \left\{\Omega^{(2,2)} + \frac{5\zeta_s}{8\rho m g(\sigma)}\right\}^{-1} \left\{1 \div \frac{4\Omega^{(2,2)}}{4\Omega^{(2,2)} + \frac{5\zeta_s}{\rho m g(\sigma)}}\right\} \ , \tag{3-69}$$

$$\phi_v^{(1)} = 0 \ ,$$

$$\eta_v^{(2)} = \frac{8\pi\rho^2\sigma^6 g(\sigma) kT}{15\Omega^{(2,2)}} \ , \quad \phi_v^{(2)} = \frac{5}{3} \eta_v^{(2)} \ , \tag{3-70), (3-71}$$

$$\eta_v^{(3)} = -\frac{37}{70} \cdot \frac{2\pi\rho\sigma^3}{15} \rho g(\sigma) \zeta_s \psi_2(\sigma) \ , \tag{3-72}$$

$$\phi_v^{(3)} = \frac{2\pi\rho\sigma^3}{15} \cdot \rho g(\sigma) \zeta_s \left[\frac{4\psi_2(\sigma) - 35\psi_o(\sigma)}{42}\right] \ , \tag{3-73}$$

where

$$\psi_o = a(x)[Q - 3b(x)] + 3c(x) + d(x) + 3f(x) \ , \tag{3-74}$$

$$\psi_2(x) = d(x) - 3[a(x)b(x)-c(x)] + 6\int_x^\infty [a(x)-a(s)] \cdot g(s)\psi_2(s)ds, \tag{3-75}$$

$$a(x) = \int_x^\infty \frac{ds}{s^2 g(s)} , \qquad b(x) = \int_x^\infty s^2[g(s)-1]ds ,$$

$$c(x) = \int_x^\infty s^2[g(s)-1]a(s)ds, \quad d(x) = \int_x^\infty s[\frac{1}{g(s)} -1]ds ,$$

$$f(x) = \int_x^\infty [a(s)-a(x)] \frac{dg(s)}{d\ell n\rho} s^2 ds , \tag{3-76}$$

$$Q = \sigma^3\int_1^\infty (3s^2 \frac{dg(s)}{d\ell n\rho} - s^3 \frac{dg(s)}{ds})ds . \tag{3-77}$$

$\theta_v(R>r)$ results from long-range potential interactions among molecules of the fluid: its functional form, like that of θ_V, stems from $\underline{\underline{\sigma}}_v$:

$$\eta_v(R>\sigma) = \frac{\pi\zeta_s\rho^2}{15kT}\int_\sigma^\infty v'(s)g_o(s)\psi_2(s)s^3ds \tag{3-78}$$

and

$$\phi_v(R>\sigma) = \frac{\Pi\zeta_s\rho^2}{9kT}\int_\sigma^\infty v'(s)g\psi_o s^3ds . \tag{3-79}$$

D. The Coefficient of Thermal Conductivity Equation.

A similar procedure to that used to develop the coefficients of viscosity beginning with

$$\vec{q}_K = \frac{m}{2}\int(\frac{\vec{p}_1}{m} - \vec{u})^2(\frac{\vec{p}_1}{m} - \vec{u})\bar{f}^{(1)}d\vec{p}_1 \tag{3-80}$$

and

$$\vec{q}_v = -\frac{\sigma}{2m} \int_{(\hat{k}\cdot\vec{p}_{12}<0)} \hat{k}(\hat{k}\cdot\vec{p}_{12})[\hat{k}(\frac{\vec{p}_1}{m} - \vec{u})] \bar{f}^{(2)} d\vec{p}_1 d\vec{p}_2 b db d\varepsilon \tag{3-81}$$

[expressions stemming from analysis of Equations (3-62) and (3-63)] produces the following results for the coefficient of thermal conductivity:

$$\chi = \chi_k + \chi_v^{(1)} + \chi_v^{(2)} + \chi_v^{(3)} + \chi_v(R>\sigma) \tag{3-82}$$

$$\chi_k = \frac{75k^2T}{32mg(\sigma)} \left\{ \frac{1 + \frac{2\pi\rho\sigma^3 g(\sigma)}{5}}{\Omega^{(2,2)} + \frac{45\zeta_s}{16\rho m g(\sigma)}} \right\} , \tag{3-83}$$

$$\chi_v^{(1)} = \frac{75k^2T}{32mg(\sigma)} (\frac{2\pi\rho\sigma^3}{5}) \left\{ \frac{1 + \frac{2\pi\rho\sigma^3 g(\sigma)}{5}}{2\Omega^{(2,2)} + \frac{45\zeta_s}{16\rho m g(\sigma)}} \right\} \times$$

$$\times \left\{ 1 + \frac{\Omega^{(2,2)}}{\Omega^{(2,2)} + \frac{45\zeta_s}{16\rho m g(\sigma)}} \right\} , \tag{3-84}$$

$$\chi_v^{(2)} = \frac{75k^2Tg(\sigma)}{32m\Omega^{(2,2)}} (\frac{2\pi\rho\sigma^3}{5})^2 (\frac{32}{9}\pi^{-3/2}) , \tag{3-85}$$

$$\chi_v^{(3)} = 0 , \tag{3-86}$$

$$\chi_v(R_{12}>\sigma) = \frac{\pi kT\rho^2}{3\zeta_s}\int_\sigma^\infty (R_{12}u'-u)\left\{\frac{d}{dR_{12}}\left[\frac{\partial \ell n g_o^{(2)}}{\partial T}\right]_p\right\} g_o^{(2)} R_{12}^3 dR_{12}$$

$$+ \frac{\pi kT}{\zeta_s}\int_\sigma^\infty (u - \frac{1}{3}R_{12}u')\left[\frac{\partial g_o^{(2)}}{\partial T}\right] R_{12}^2 dR_{12} \qquad (3\text{-}87)$$

In the integral

$$\int_\sigma^\infty (Ru'-u) g R^3 \frac{\partial}{\partial R}\left[\frac{\partial \ell n g}{\partial T}\right]_p dR \quad ,$$

the partial integration yielding

$$\left[\frac{\partial \ell n g}{\partial T}\right]_p g R^3 (Ru'-u)\Big|_\sigma^\infty - \int_\sigma^\infty \left[\frac{\partial \ell n g}{\partial T}\right]_p \{R^3(Ru'-u)\frac{\partial g}{\partial R}$$

$$+ g(R^4u''+3R^3u'-3R^2u\}dR$$

permits one differentiation to be avoided. The LJ potential calculation was made both with and without the partial integration to cross check the programming and to assess the accuracy of the results. The differences were on the order of one per cent. This gives a measure of the numerical precision which can be attached to these procedures.

Lennard Jones data appearing later was obtained using the partial integration form of Eq. (3-87) while all others, the multiple derivative form.

E. The Soft-Drag Coefficient Equations.

The soft-drag coefficient ζ_s appears as a factor of the Rice-Allnatt transport coefficients. Two representations of this quantity are

$$\zeta_s^{RG} = \left\{\frac{4\pi m\rho}{3}\int_0^\infty \nabla^2\, v(s)g(s)s^2 ds\right\}^{\frac{1}{2}} \tag{3-88}$$

given by Rice and Grey, and

$$\zeta_s^{H} = \frac{8n\sigma^2}{3}\sqrt{\pi m\beta}\;\varepsilon\int_0^\infty [g(s)-1][11f_{12}(s)-5f_6(s)]ds \tag{3-89}$$

where

$$f_n(x) = 2\sum_{\ell=1}^{n/2}\frac{x^{2\ell-n}}{2\ell-1} - \frac{1}{x^{n-1}}\,\ell n\left|\frac{x+1}{x-1}\right| \tag{3-90}$$

given by Helfand.[17]

This latter expression for ζ_s is the result of the explicit incorporation of a modified LJ 12-6 potential (Eq. 2-7) in a simplified linear approximation for ζ_s. The soft-drag coefficient represents the molecular analogue to the Stokes drag coefficient for a sphere falling in a viscous fluid.

Rice and Grey also propose an alternate formulation of ζ_s in which a the molecular fluid is replaced by an acoustic (inhomogeneous) continuum with a distributed force field.[18] This was employed as a third attempt to obtain a viable ζ_s late in this work, by Babb, and as a comparison to other formulations. Their result, referred to here (somewhat loosely) as "the speed of sound ζ_s", is

$$\zeta_s = \frac{4\pi\rho_m}{9m^2C^3}\left[\int_\sigma^\infty \nabla_{12}^2 u^{(s)}(R_{12}) g_o(R_{12}) R_{12}^2 dR_{12}\right]^2 \quad . \qquad (3\text{-}91)$$

CHAPTER IV

ALGORITHMS AND PROGRAMMING CONSIDERATIONS

General Comments

The design of the algorithms by which the various quantities were calculated was influenced by a number of sometimes competing considerations. The programs which finally emerged represented a compromise among such factors as accuracy, speed, and the capabilities of the hardware and software available.

Central to theme of this work is the accuracy of the radial distribution function generated and the transport coefficients which follow. These tabular values must be as free from errors originating from computational technique or machine round off as possible. Propagation of such unavoidable errors as exist must be minimized. In almost direct opposition to accuracy is the need for speed in accomplishment of the calculation. The generation of one tabular entry requires tens of thousands of individual arithmetic operations; the tables are themselves voluminous. And, finally, the capabilities of the data processing facilities available must be taken into account. A program which can generate millions of accurate entries efficiently is useless on a machine whose storage permits retention of only thousands of entries for future use.

The first compromise was on speed in favor of accuracy; all calculations were made to 16 digits. This guaranteed a precision of

14 digits in all individual arithmetic operations and compiler-supplied subprograms. But the consequence of this decision was an increase of the computational time. It then became necessary to seek out every possible technique to reduce the time devoted to computation. Techniques employed are given below in the description of specific algorithms.

From the theoretical outline of the preceeding chapters, it should be clear that the pivotal effort of this work centers on the efficient generation of the radial distribution function tables. Having defined the standard of accuracy and fixed upon the basic equations to be utilized, one must then proceed with almost maniacal attention to detail to optimize the algorithm, trimming from it every wasted, repetitious, or inefficient operation or manipulation. The FORTRAN IV programming language used was screened line by line to avoid unnecessarily slow commands. Program architecture avoided subroutines to save time devoted to calls. Constants were defined in DATA statements to create these values during compiling rather than run time. It was a matter of bearing constantly in mind that the unnecessary expenditure of 10 microseconds in the heart of the integration routine could cost 10 minutes in total run time, and only a few such wasted commands could render the entire effort unfeasible.

First, an IBM 360 mod 50 and, later, an IBM 370 mod 158 was used for these calculations. g-equation run times (through 20 densities, at given substance, intermolecular potential, and temperature) on the mod 50 averaged 15 hours and were generally accomplished in block times of between five and eight hours. Run times on the mod 158 averaged three hours.

Having once created the radial distribution function data files, the remainder of the calculation is straightforward and much faster.

For the reader unfamiliar with numerical techniques, a general discussion of the major points of the programming used here is provided in an appendix.

The g_0-equation Algorithm

The hard sphere radial distribution function algorithm is of interest pedagogically; many typical programming considerations and techniques applicable throughout this work are used in its construction.

The KMA equation for $g_0(x)$ was modified by a change in variables and one integration to:

$$\ell n\{g_0(x)\} = \frac{\lambda}{3} + \frac{\lambda}{4x}\int_{-1}^{1}(S^2-1)(x-s)g_0(x-s)ds \qquad (4\text{-}1)$$

and this formed the basis for the computational algorithm.

Tables of singly subscripted variables equivalent to the factors (S^2-1) and $(x-s)$ were initially generated, along with the initial guess of $g_0(x-s)$ (also a singly subscripted variable):

$$g_0(s) = 0, \quad s<1; \quad g_0(s) = 1, \quad s\geq 1 \ .$$

Formulation of the integrand at the arguments became a manipulation in integer arithmetic of indices accompanied by two floating point multiplications; repetitive calculations were thus avoided. It was required to have values of $g_0(s)$ for arguments beyond the

range for which the solution is desired. In the limit of large argument or low density, $g_o(s) = 1$, so the values of $g_o(s)$ beyond the maximum calculational argument, s_m, were set and fixed:

$$g_o(s) = 1, \quad s_m > s \ .$$

In practice it was found that $s_m = 10$ was an effective upper limit, for

$$|g_o(s_m)-1| \approx 1 \times 10^{-7}$$

even for high densities.

The hard core distribution function, by virtue of its potential, possesses a discontinuity at $x-s = 1$; in the calculation, the evaluation of the integral always commenced with a lower limit s_1 such that $x-s_1 = 1$. Otherwise, by the nature of the numerical scheme, an integration across this value of $x-s_1 = 1$ would be an integration over a smoothed continuous function and an error would be introduced.

A combination Simpson's and Trapezoidal rule was used.

It proved wasteful of computational time to initially evaluate $g_0(x)$ at all values of the argument. The initial argument values and mesh size of integration h_1 first chosen were much larger than that finally desired. $g_0(x)$ was evaluated at this mesh over the entire range and an approximate table of values was created. Next, the mesh size was halved, $h_2 = h_1/2$, and the evaluation repeated. The approximate solution $g_0(x)$ at h_1, together with intermediate values determined by Lagrangian interpolation, constituted the initial guess at this new mesh size. The process of halving continued until the desired mesh size was reached.

The algorithm provided for an arbitrarily large range of arguments over which $g_0(x)$ was evaluated. In practice, an upper limit $x_m = 10$ was used.

An additional cyclic feature of the algorithm provided for "stepping up" through the densities. Following the completion of the calculation at some λ, λ was incremented and the calculation reinitiated using the final set of $g_0(x)$ obtained for the old density as the initial guess at the new density. This process provided "reasonable" first guesses to $g_0(x)$ at each density except the lowest, and far less time was spent in calculation.

Here, as in later g(x) calculations, it was found that as the density increased and the variation in $g_0(x)$ became more pronounced, the number of iterations required to produce a specified accuracy increased.

The g-equation Algorithm

The algorithm for the evaluation of the g(x)-equation is based on the expression:

$$\ell n\{g(x)\} = -\beta\varepsilon\gamma(x) + \frac{\lambda_o}{4x}\int_o^\infty K(s)[(x-s)g(x-s)+(x+s)g(x+s)-2s]ds,$$

$$K(t) = \beta\varepsilon\int_{|t|}^\infty (s^2-t^2)g(s)(\frac{d\gamma}{ds})ds$$

and γ is the reduced form of the intermolecular potential.

As in the programming for $g_o(x)$, tables of singly subscripted variables equivalent to the constituent factors of the integrand were initially constructed to minimize time devoted to repetitious calculations. These tables, together with the tabular g(s) values to be used in the integrand, permitted the integrands to be formed and integrals to be evaluated by relatively simple and speedy fixed point indices manipulations and a minimum number of floating point additions and multiplications.

Although the evaluation procedure was essentially the same as with $g_o(x)$, certain troublesome complications appeared.

In what follows, where it becomes necessary to distinguish among g values, those used to construct the integrands will be designated g^{IN} and those obtained by evaluation of the integrals will be designated g^{OUT}.

An initial concern in assessing the possibilities for the success of the algorithm centered on the multiple appearance of g(x) explicitly and implicitly [through K(t)] in the integral. It

was feared that in initial iterations the error in g(x) would be of sufficient compound magnitude to produce a divergent series of g^{OUT} values. Indeed, some difficulties were encountered; convergence was not so quickly obtained as had been the case with $g_o(x)$, and the tendency to diverge at all but the lowest densities was very pronounced.

Again, solutions through the range of densities λ_o were stepped to provide good initial guesses of g^{IN}. But at higher densities, the $\Delta g = g^{OUT}-g^{IN}$ tended to be too large, and the matter of securing convergent solutions at these large values of λ_o became a delicately balanced proposition. Consequently, a mixing parameter α was introduced to reduce the size of Δg and proportion the value of g^{IN} at the n+1 iteration between the g^{IN} and g^{OUT} values of the n^{th} iteration.

$$(g^{IN})_{n+1} = \alpha(g^{OUT})_n+(1-\alpha)(g^{IN})_n \quad . \tag{4-2}$$

Trial and error led to setting

$$\alpha = (\lambda_m-\lambda_o)/\lambda_m \tag{4-3}$$

where λ_m is some maximum value of density slightly above the highest density to be calculated, and λ_o the density at which the current calculation is to be made. Although the effect of the use of α was to increase the number of iterations required (and thus lengthen run times) it permitted the extension of calculations to much higher densities than was otherwise possible.

But particularly at the higher densities came the marked increase in the number of iterations required and a drastic lengthening of run times. While convergence of the g(x) values might be obtained for as few as twenty iterations at low densities, as many as 10,000 or more might be required for high densities. Even with the speed inherent to modern data processing equipment, the situation was discouraging.

Fortunately, Δg exhibited a systematic behavior which enabled the number of iterations to be significantly reduced. It was observed that after an initially erratic fluctuation in the early iterative steps, the trend of differences between successive g^{IN} values could be represented to good approximation as

$$\ell n\{\Delta g\} = mn+b \quad , \tag{4-4}$$

n being the number of iterations, m and b, constants, and $\Delta g = g^{IN}_{n+1}(x_o) - g^{IN}_{n}(x_o)$, where x_o is an arbitrary but particular argument. (See Fig. 3) An approximate cumulative correction, C_T, could be determined and applied, thus bypassing many iterations.

If i, j, k are three specific numbers of iterations, i j k, and g_i, g_j and g_k, the respective g values calculated at these stages then

$$m = \ell n\left\{\left(\frac{\Delta g_{ij}}{\Delta g_{ik}}\right)^{1/(k-j)}\right\} \tag{4-5}$$

Figure 3. Correction-per-iteration of g as a function of iteration. $\Delta g(1.8)$ changes sign.

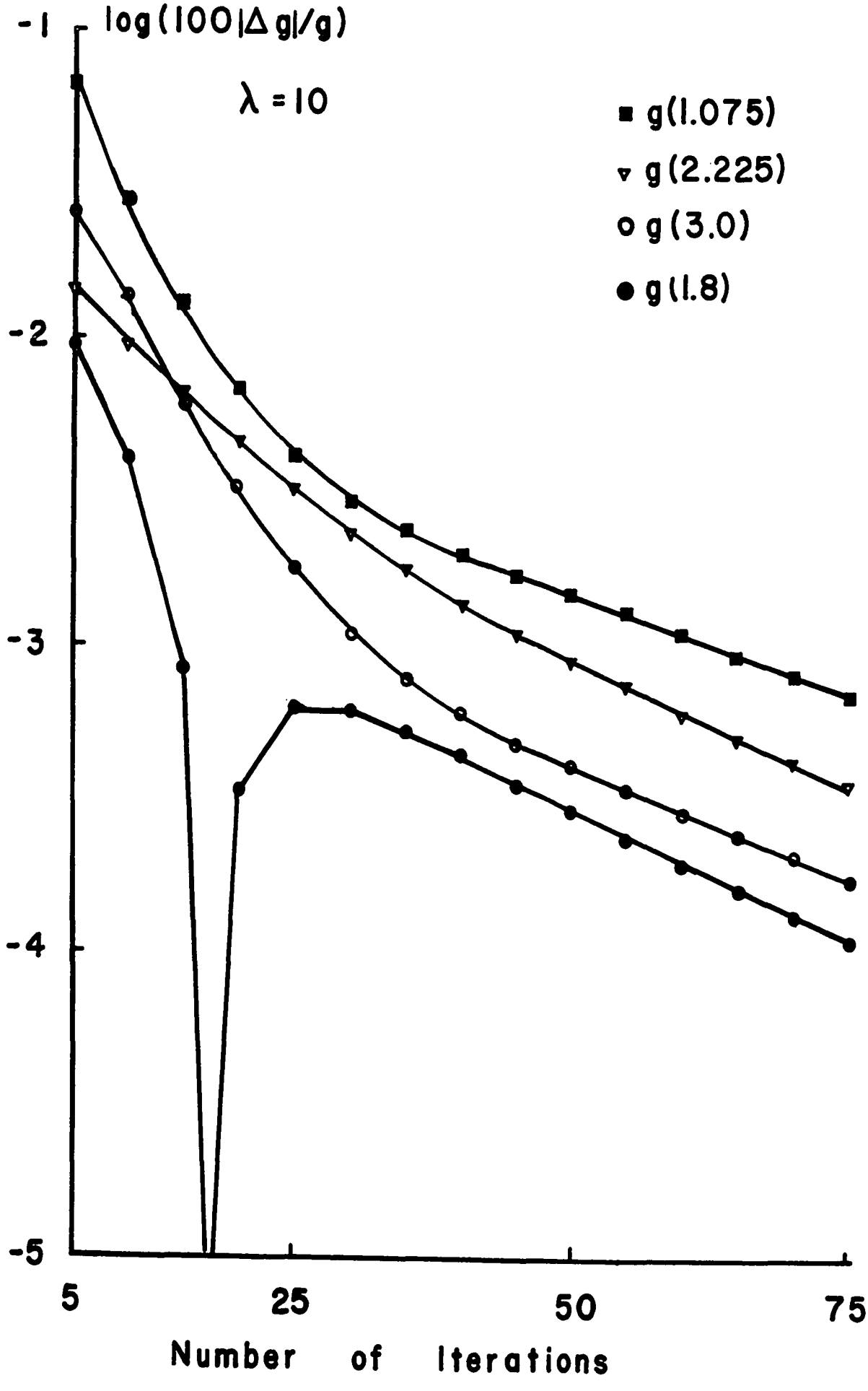
log(100|Δg|/g)
λ = 10
g(1.075)
g(2.225)
g(3.0)
g(1.8)
-1
-2
-3
-4
-5
5
25
50
75
Number of Iterations

and

$$b = \left\{ \frac{(\Delta g_{ij})^k}{(\Delta g_{ik})^j} \right\}^{1/(j-k)} , \qquad (4\text{-}6)$$

where

$$\Delta g_{ij} = g_i - g_j \quad .$$

The cumulative correction becomes

$$C_T = be^{-km}(1+e^{-m}+e^{-2m}+\cdots) = \frac{be^{-km}}{1-e^{-m}} \quad . \qquad (4\text{-}7)$$

The rate of convergence of the g's was not found to be sufficiently uniform over the range of arguments to permit the application of a single blanket, averaged correction. A C_T was determined for the g corresponding to each argument.

In practice, the application of the full C_T value proved too traumatic to the delicately balanced family of g's, for it resulted in a wild, erratic fluctuation of the g values in succeeding iterations and ultimately, little progress toward a final result. However, the application of $C_T/2$ to those same g's resulted in a far less pronounced fluctuation and the reduction of the Δg's by as much as one order of magnitude (equivalent to 200 or more iterations). The correction could be applied repeatedly as deemed necessary.

The criterion determining a final solution set of g values was that

$$\frac{g^{OUT}(x_o)-g^{IN}(x_o)}{g^{IN}(x_o)} < \varepsilon \qquad (4\text{-}8)$$

over the entire range of arguments x_o, where

$$\varepsilon = h^6 \quad , \qquad (4\text{-}9)$$

h being the mesh size. It can be shown that the error E associated with a Simpson's rule integration

$$\int_{x_o}^{x_{2n}} f(x)dx$$

is

$$|E| = \frac{nh^5 f^{(4)}(\xi)}{90} \quad , \qquad x_o<\xi<x_{2n} \quad . \qquad (4\text{-}10)$$

(19)

$f^{(4)}(\xi)$ was not analytically available by virtue of the unknown g; however, from the smoothly varying nature of the integrand, and its lack of precipitous change over the range of integration, it could safely be assumed that

$$f^{(4)}(\xi) \sim 0(1) \quad ,$$

and was in fact probably much less. Linking the error criterion to this power of the mesh scaled ε to the accuracy possible at that h and placed its value well within the order of magnitude range of the maximum possible accuracy. Convergence criterion scans were conducted only periodically, at intervals based on experience.

The evaluation of K(t) was itself a time consuming calculation preliminary to that of g; in order to take advantage of any smoothing effect which this integration might possibly have on g errors as they influenced K(t) values, the option to hold K(t) as a fixed set through a number of iterations in which the g's appearing explicitly in the g-equation integral were improved was included in the program. Although some limited use was made of this feature, experience showed that in general the calculation proceeded most swiftly to completion when K(t) was also calculated at each interation.

It was found that the largest absolute change in Δg occurred at smaller argument values; the g's at larger arguments could be left unadjusted over several interations. Although this mixed the sets of g's, the saving in computational time outweighed any diminuition of accuracy and hastened convergence. Any scan of $g^{IN}(x)$ and $g^{OUT}(x)$ along ascending argument values (in the process of checking for

convergence) halted at the first argument value, say x_f, at which the convergence test failed and the maximum value x_m to which g(x) was recalculated on succeeding iterations was set somewhat larger than x_f. At intervals, x_m was reset to insure that g(x) was calculated throughout the range of the arguments.

At the successful completion of a calculation at some particular density, the solution set was read to (stored on) a magnetic disk, and became a portion of the reference library to be used in later calculations. Disk was chosen as the working library receptacle because of its capability for rapid access to any segment of the volume. Back-up magnetic tapes were also maintained.

The Equation of State Algorithm

The first use of the radial distribution functions was in the equation of state:

$$\frac{pv}{NkT} = 1 - \frac{2\pi N}{3kTv}\int_0^\infty r^3 v'(r) g(r) dr \quad .$$

Being a simple, straightforward calculation, it acted as a convenient introductory exercise in the manipulation of data files as well as a routine cross check against earlier published results.

The above integral and all similar integrals of the transport coefficient calculations separate at the upper limit of argument to which g(x) is known (in this work, $x_m = 10$); the range from 0 to x_m being evaluated numerically, and the range from x_m to infinity, by virtue of the assumption that in this region g = 1, being evaluated analytically.

The Soft-Drag Coefficient

The soft drag coefficient as given by Rice:

$$\zeta_s^{RG} = \left\{\frac{4\pi m\rho}{3}\int_\sigma^\infty \nabla^2 v(s)g(s)s^2 ds\right\}^{\frac{1}{2}}$$

formed the basis for one of the computational algorithms for this quantity. It possessed the obvious advantage of the use of any of a number of intermolecular potentials; the Helfand formulation,

$$\zeta_s^H = \frac{8n\sigma^2}{3}(\pi m\beta)^{\frac{1}{2}}\varepsilon\int_0^\infty [g(s)-1][11f_{12}(s)-5f_6(s)]ds$$

where

$$f_n(x) = 2\sum_{\ell=1}^{n/2}\left\{\frac{x^{2\ell-n}}{2\ell-1}\right\} - x^{1-n}\ell n\left|\frac{x+1}{x-1}\right|$$

directly incorporated the modified LJ 12-6 potential, (Eq. 2-7).

To say the least, the use of ζ_s^H required an extensive programming effort. This was seen at the outset, and in light of the limited applicability of ζ_s^H, a forceful, if only pragmatic, argument was at hand to abandon this formulation altogether. But such arguments carry their appropriate weight only in hind sight.

Helfand's use of the modified LJ 12-6 made the resulting radial distribution function $g(1) = 1$ and permitted him to avoid the problem of the singularity of the logarithmic term at $x = 1$. The aim here, however, was to relax as many such restrictions as possible. The unmodified LJ potential used here caused g to take on a different value. The problem of the singularity could not be avoided.

After verifying that the ratio test, Raabe's test and Gauss' test for convergence all failed to give any hope that an analytic path around the problem might exist, it was decided to formulate an approximation which would pragmatically, if not esthetically, skirt the problem.

The singularity at $x_o = 1$ of the logarithmic term is essentially a numerical problem brought on by the absence of an analytical expression for g. Since it can easily be shown that $\int x^m \ell n|x-1|dx$ exists, it was decided to approximate the factor g(x)-1 of the integrand as

$$g_1(x)-1 = Ax+B$$

for a number of mesh sizes on either side of x = 1. The problem producing portion of the Helfand integral,

$$\int [g(x)-1]\ell n|x-1|dx \quad ,$$

may then be handled as follows: add and subtract $\int [g_1(x)-1]\ell n|x-1|dx$ from the above expression, obtaining

$$\int \{[g(x)-1]-[g_1(x)-1]\}\ell n|x-1|dx + \int [g_1(x)-1]\ell n|x-1|dx \quad .$$

The first of these two integrals,

$$\int [g(x)-g_1(x)]\ell n|x-1|dx \quad ,$$

vanishes at the singularity for in the approximation $g_1(x) = Ax+B+1$, A and B are determined such that $g_1(1) = g(1)$ and $g_1(1+h) = g(1+h)$,

and the evaluation in this region (an interval of three mesh sizes on either side of x = 1) proceeds analytically. The second integration is numerical. The linear approximation also assured that the numerical contribution to this divided integral was small compared to that contribution from the analytic portion. This enhanced the precision of the result in this region.

The evaluation of ζ_s^H then naturally separated into four segments:

i) $0 \leq x \leq d$, where $d \simeq 0.65$: In this region, experience showed $g(x)=0$ and the integral portion of the Helfand formulation reduces to the expression.

$$\int_0^d \{11f_{12}(x)-5f_6(x)\}dx = 24\, d^3 \sum_{\ell=1}^{\infty} \frac{\ell\, d^{2\ell-2}}{(2\ell+1)(2\ell+5)(2\ell+11)} \quad .$$

The infinite series could be straightforwardly evaluated to a specified accuracy. Difference equations were used in evaluating the polynomial appearing here and in later summations.

ii) $d \leq x \leq 1-3h$: In this range, a direct numerical integration was performed.

iii) $1-3h \leq x \leq 1+3h$: In this range, the singularity at $x = 1$ is dealt with as described above.

iv) $1+3h \leq x \leq x_m$: where x_m is the numerical upper limit of integration. In this region, the form of the integral stands unaltered, and a Simpson's rule evaluation is performed. Above x_m it is assumed $g = 1$, so that the integrand vanishes.

But the application of the Helfand formulation encounters an immediate problem: if the portions of g for $x \leq 1$ are included in the evaluation of ζ_s^H, the value of this function becomes negative, and this is physically absurd. A cursory examination of the original Helfand derivation indicates that the truncation of the potential is crucial in the development which results in the final form of ζ_s^H, and no obvious extension of the Helfand result is apparent wherein this constraint is relaxed,

Pragmatically, it was decided to neglect all the contribution of g for values of $x<1$ and to rely on special functions which are the solution of the truncated potential for a critical test of this Helfand formulation.

But it remains a fact that the application of the Helfand formulation in conjunction with radial distribution functions calculated with the full potential to the evaluation of the transport coefficients is flawed to an extent that such a procedure is not theoretically defensible; the Helfand formulation was used sparingly, and then only from curiosity rather than need. This "flaw" is in the same spirit as the use of RA theory with g's from a full potential. Ironically, it still gave better results than other formulations. See Chapter V.

The ψ_2 Equation Algorithm

The ψ_2 equation (Eq. 3-75) is an integral equation solved by the same general techniques as those applied in connection with the solution of any integral equation, but with the added boundary condition that

$$\lim_{x\to\infty} \psi_2(x) = \frac{P}{x^3}, \quad P = \text{const.} \tag{4-12}$$

The proper solution is obtained by selecting two values of P, solving Eq. 3-75 for those two values by demanding $\psi_2(x)$ obey Eq. (3-75) in the region where $g(x) = 1$; i.e., for $x>x_m$. The results are compared with a known condition on ψ_2, namely

$$\int_1^\infty g(s)\psi_2(s)ds = \frac{1}{6}\,[g(1)-1] + \frac{b(1)}{2} \tag{4-13}$$

and extrapolating P to the proper value, so that this equation is satisfied. With P so determined, the correct ψ_2 data is determined.

Although ψ_2 is explicitly a function of g, and therefore implicitly a function of λ, T, and the intermolecular potential, the algorithm for its calculation was incorporated into the architecture for the calculation of the transport coefficients. This

was done in almost flagrent disregard for the principle of conservation of machine time; certainly the calculation of a particular table of ψ_2 values could have been calculated once, stored as were the radial distribution functions, and called and used as needed in subsequent calculations. However, the transport calculations were themselves relatively brief, and the ψ_2 calculation converged rapidly; certain job control considerations--limitations on number of perepheral job control commands--made advisable the inclusion of this calculation in the larger algorithms.

The Viscosity and Thermal Conductivity Calculation

Inspection of Eqs. 3-66, 3-68 through 3-77, 3-83 through 3-87 makes apparent that the calculation of the coefficients of viscosity and thermal conductivity are so straightforward after the effort devoted to g as to be almost anticlimatical. Apart from the preliminary determination of ψ_2-through the numerical solution of a integral equation--the operations are routine and quick.

Their directness, however, does not mean they do not possess their own unique difficulties.

First of all, beyond a general qualitative idea regarding the behavior of these calculated coefficients, one has little guidance as to what to expect. If the theory is correct, the agreement with experiment should be good; however, earlier calculations give only approximate agreement and no indication of whether or not a more precise data base (the g-values) will produce better or poorer agreement. In short, the entire train of calculations is sufficiently complex, and the results enough in question as to permit a programming

error to pass completely unrecognized. The nature of the calculation does not lend itself to any automatic confirmation.

Babb has created a set of hypothetical, analytical g functions which, when inserted in the equation for the viscosities and thermal conductivities, permitted an analytic solution of the equations. A numerical solution of the equations was made with the hypothetical g-function and the results of both analytic and numerical techniques agree within better than 1 per cent. This is reassuring and builds confidence in the validity of the algorithms (Appendix III).

The thermal conductivity and bulk viscosity calculations presented a problem not encountered in earlier programs in that derivatives of the radial distribution function occur in integrands of $\chi_v(R>\sigma)$ and $\phi_v(R>\sigma)$. The lack of knowledge of the functional form of g meant that these derivatives must ultimately be determined numerically.

In principle, this presented no difficulty since the aggregate tables form a three-dimensional matrix $g(x,T,\lambda)$. Differentiation over length, temperature and density could be performed a number of ways; here, an IBM supplied scientific subroutine (DDGT3) calculating the derivative of a Lagrangian interpolation polynomial of second degree was used.

Nevertheless, there were awkward aspects to this calculation. $(\partial g/\partial T)_p$ appears in the thermal conductivity term $\chi_v(R>\sigma)$; the g-matrix was not formulated so as to permit a direct calculation of this quantity. But

$$\left(\frac{\partial g}{\partial T}\right)_p = \left(\frac{\partial g}{\partial T}\right)_\rho - \alpha p \left(\frac{\partial g}{\partial \rho}\right)_T \tag{4-14}$$

where

$$\alpha = -\frac{1}{\rho}\left(\frac{\partial \rho}{\partial T}\right)_p \tag{4-15}$$

and the difficulty shifts from the evaluation of $(\partial g/\partial T)_p$ to that of $(\partial \rho/\partial T)_p$. α could be evaluated from experimental data or from a gas law. For example, we might write

$$\rho = P/(kT)$$

and obtain

$$\left(\frac{\partial \rho}{\partial T}\right)_p = -P^2/(kT^2)$$

although at the high densities we consider here, this would be a most inappropriate choice.

The equation of state expression (1-6) may be written in terms of density and it might first appear that this equation could be used to form $(\partial \rho/\partial T)_p$; however, the g appearing in the integrand is itself a function of T and we are back where we started.

The method finally settled upon, after considerable experimentation with a variety of techniques was that of employing an equation of state particularly suited to high densities. The Becker equation of state[20]

$$PV = RT[1+k'\rho\exp(k'\rho)]-a\rho + x\rho^6 \qquad (4\text{-}16)$$

was derived to fit Amagat's high pressure data. Here, k', a and x are disposable constants.

Sets of three calculated pressures were used to evaluate the values of k, a, and x at the temperatures of this present work's calculation. The resulting equations were interpolated to find the density corresponding to a given pressure. Numerical techniques were then used to obtain the derivatives at constant pressure from the densities so obtained.

The results of this process were in some respects flawed. It would have been possible, perhaps, to obtain the values of the quantities needed by reference to the variety of experimental results available in the literature. But the shifting ranges of densities and temperatures adopted, the variety of experimental techniques used, and the mere presence of experimental error occurring in this data would have introduced a haphazard variation undesirable in this present effort. The mixing of the experimental results of various authors would tend to obscure the effort at hand: that of attempting to evaluate various theoretical expressions on their own merit.

Since the Becker equation is not an exact fit for the data, the constants vary slowly over the range for which they were evaluated. However, the functional form is close and the derivatives were evaluated at the central of the three points selected whereever possible.

A Newton-Raphson iterative technique involving the derivatives was used to evaluate the densities and in some cases, because of the small value of these derivatives, convergence was slow. Where this problem appeared, the technique was modified to increase the rate of convergence.

Other troublesome problems were more specific. Certain isotherms of Nitrogen, particularly at 323°K and 328°K, misbehaved when used in the derivative calculations. The problem appears to relate to the proximity of these two curves and the inevitable errors of numerical differentiation compound as a result--a nightmare of the programmer's existence. The solution, however, was relatively simple: the two offending isotherms were not used jointly in the same calculations. Thus the derivatives for 308°K incorporate the 273°K, 308°K, and 373°K isotherms rather than 273°K, 308°K and 328°K. The solution is not elegant but suffices although the first differences at higher densities are not as smooth as one would prefer. It is not clear why the problem does not appear elsewhere.

CHAPTER V

NUMERICAL RESULTS AND DISCUSSION

The Radial Distribution Function

The tables of the radial distribution function are quite voluminous, amounting to over 220,000 individual 16-digit entries arranged in sets of 401 values spanning a number of densities, temperatures, substances and intermolecular potentials as listed in Table 1. Obviously they cannot be individually listed, nor would such a listing be of any particular benefit to the reader. A reference data set can be obtained by coordinating with the High Pressure Laboratory, Department of Physics and Astronomy, University of Oklahoma, Norman, Oklahoma 73071 Here, we have contented ourselves with graphical representations of the typical data sets, Figures 4 through 7.

Table 1. Precis of g Data

°K POTENTIAL	LJ	MB	BB
		Argon Densities	
180	1,2,...,11		
273	0.5,1,...,13	0.5,1,...,16.5	0.5,1,...,9
308	0 5,1,...,13.5	0.5,1,...,6.5	0.5,1,...,9
323		0.5,1,...,7.0	0.5,1,...,9
328	0.5,1,...,11.5	0.5,1,...,7.0	0.5,1,...,9
373	0.5,1,...,10	0.5,1,...,7	0.5,1,...,9
500	0.5,1,...,12.5		
600	0.5,1,...,14		
		Nitrogen Densities	
180	1,2,...,13		
273	0.5,1,...,13.5	0.5,1,...,8	
308	0.5,1,...,13.5	0.5,1,...,8	
323		0.5,1,...,8	
328	0.5,1,...,14	0.5,1,...,8	
373	0.5,1,...,14	0.5,1,...,8	
500	0.5,1,...,14.5		
600	0.5,1,...,14		

The correlation between density in terms of λ and other common systems is provided in Table 2 through 6.

Figure 4. g(r) isotherm (308°K) for Argon, Lennard-Jones potential.

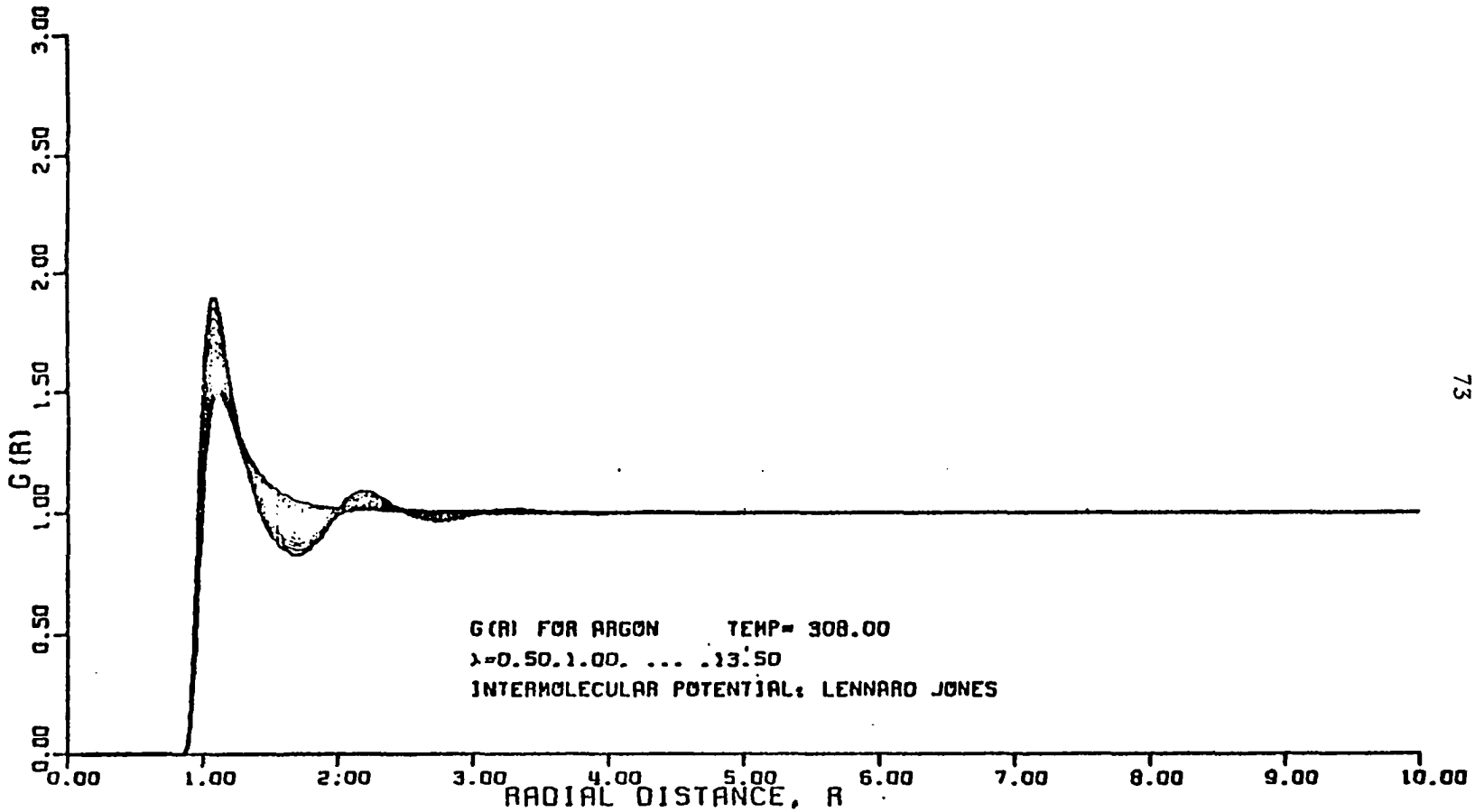
G(R)
0.00
0.50
1.00
1.50
2.00
2.50
3.00
0.00
1.00
2.00
3.00
4.00
5.00
6.00
7.00
8.00
9.00
10.00
RADIAL DISTANCE, R
G(R) FOR ARGON TEMP= 308.00
λ=0.50,1.00, ... ,13.50
INTERMOLECULAR POTENTIAL: LENNARD JONES

Figure 5. Figure 4 data in perspective view.

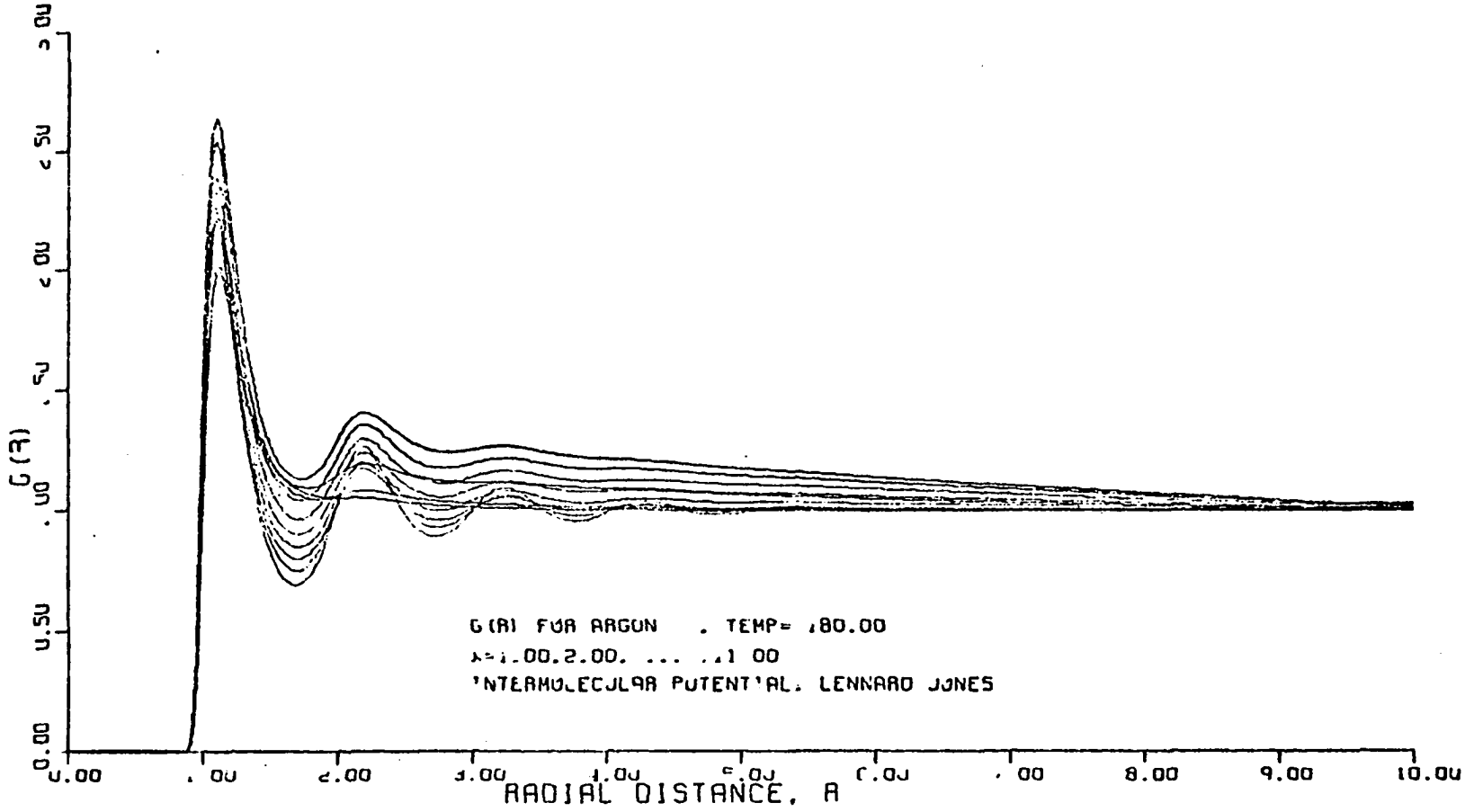
G(R)
RADIAL DISTANCE, R
G(R) FOR ARGON . TEMP= 180.00
INTERMOLECULAR POTENTIAL: LENNARD JONES

Figure 6. g(r) isotherm (328°K) for Nitrogen, Lennard-Jones potential.

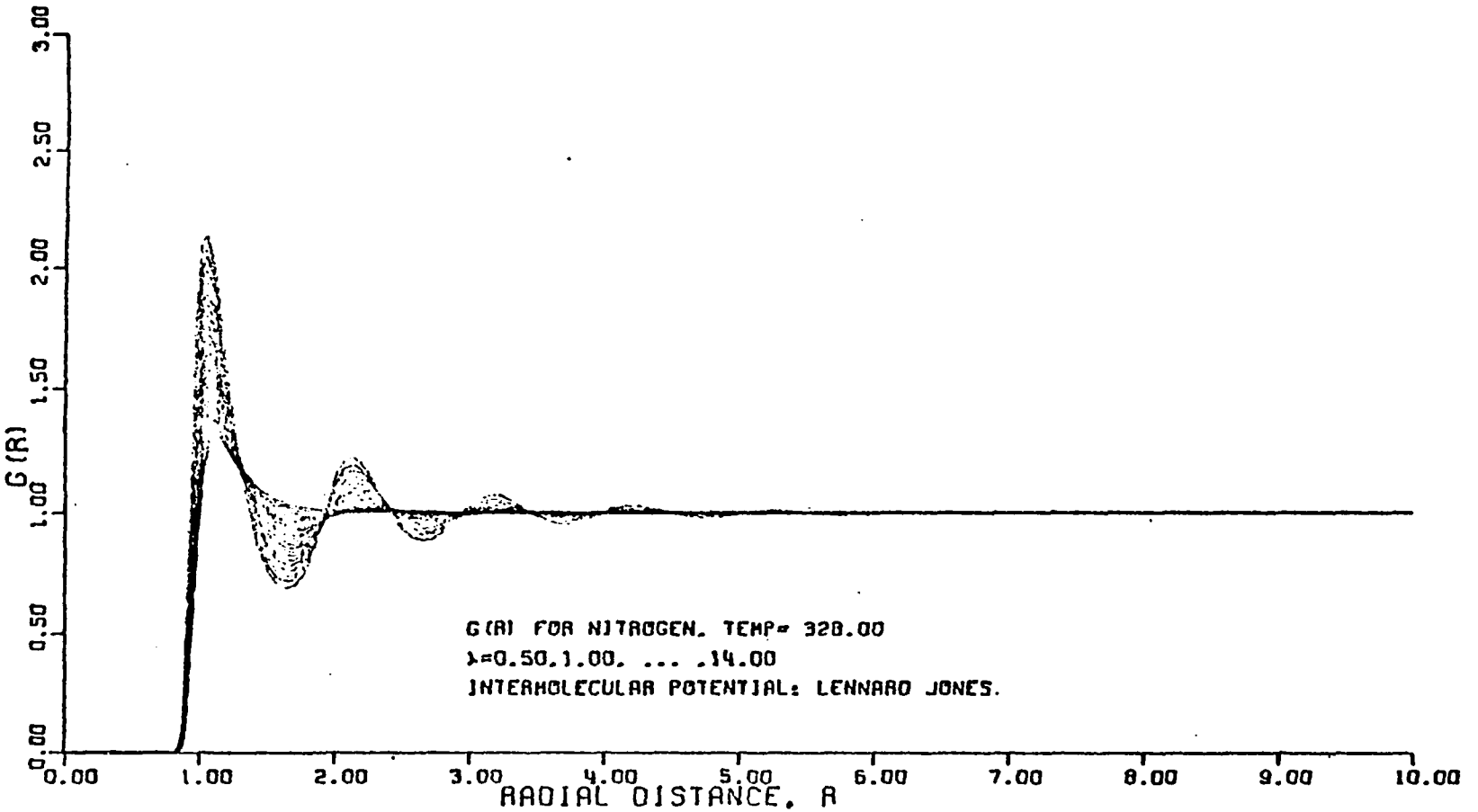
G(R)
3.00
2.50
2.00
1.50
1.00
0.50
0.00
0.00
1.00
2.00
3.00
4.00
5.00
6.00
7.00
8.00
9.00
10.00
RADIAL DISTANCE, R
G(R) FOR NITROGEN. TEMP= 328.00
λ=0.50,1.00, ... ,14.00
INTERMOLECULAR POTENTIAL: LENNARD JONES.

Figure 7. g(r) isotherm (180°K) for Argon, Lennard-Jones potential.

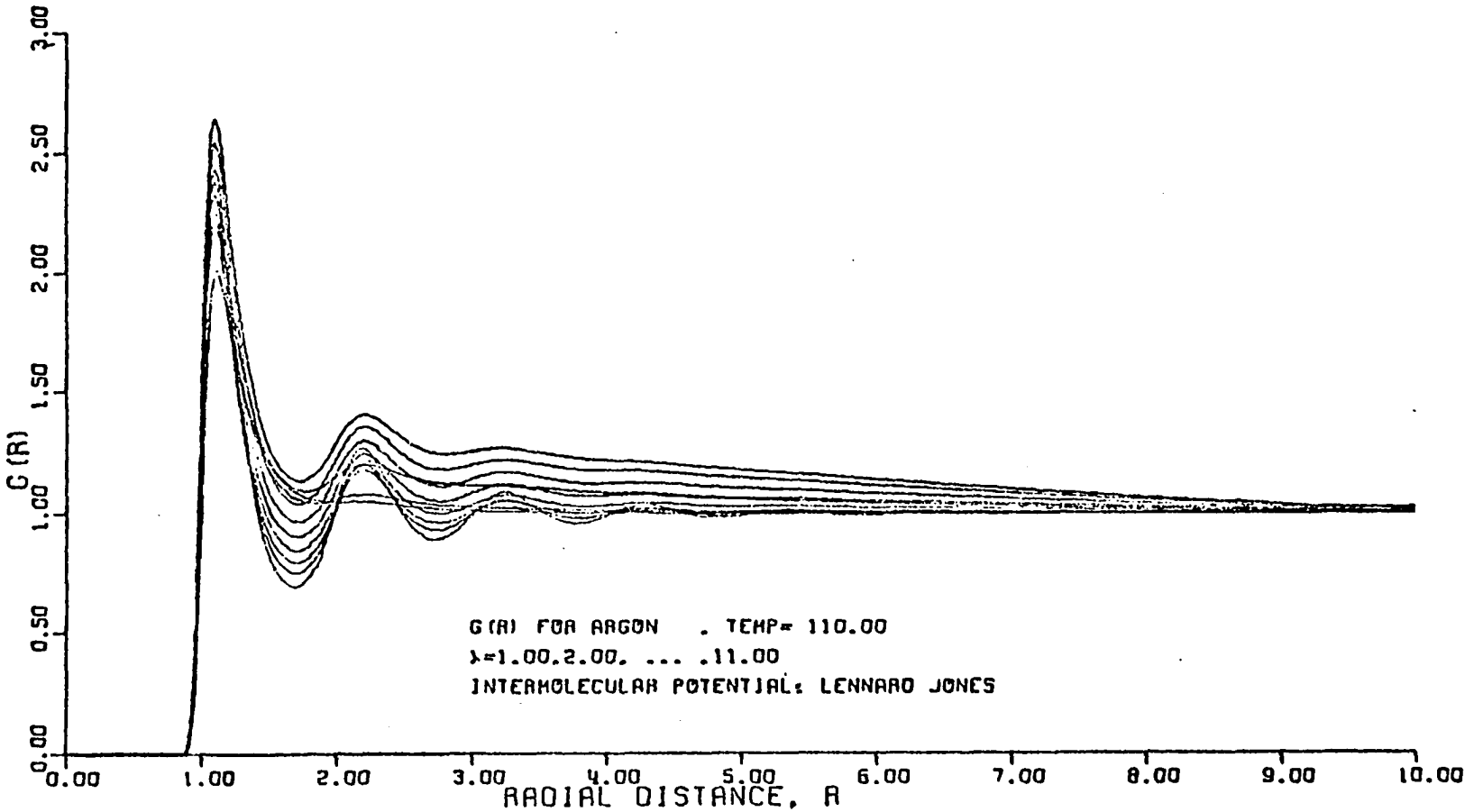
G(R)
3.00
2.50
2.00
1.50
1.00
0.50
0.00
0.00
1.00
2.00
3.00
4.00
5.00
6.00
7.00
8.00
9.00
10.00
RADIAL DISTANCE, A
G(R) FOR ARGON . TEMP= 110.00
λ=1.00,2.00, ... ,11.00
INTERMOLECULAR POTENTIAL: LENNARD JONES

Figure 8a. Figure 7 data in perspective, showing the anamolous behavior of g(r) at mid-range densities.

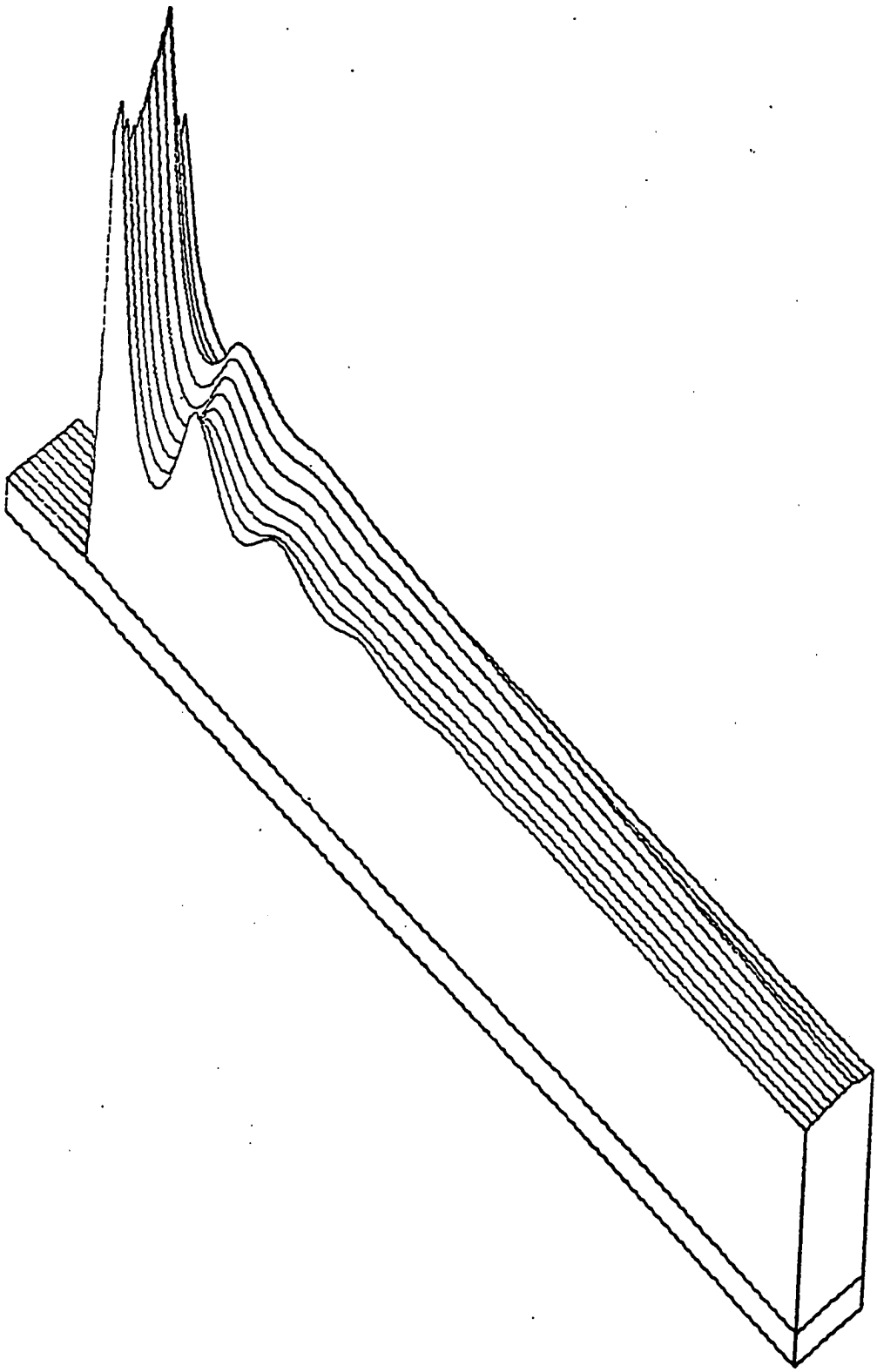

Figure 8b. The same graph as Figure 8a, but here the lines indicating the surface are drawn at constant r, instead of constant λ, making the anomolous ridge even more obvious.

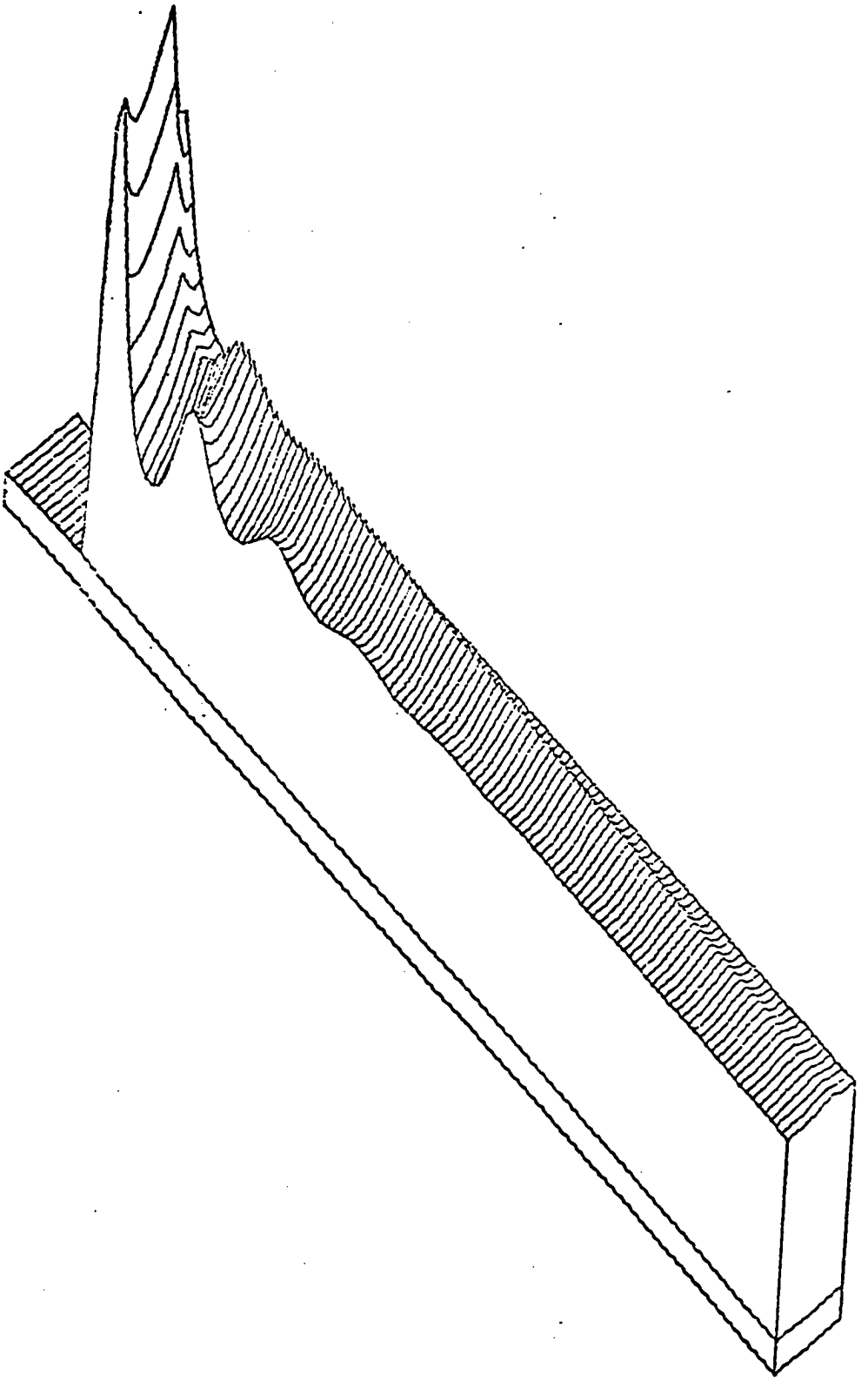

Table 2. Correlation of Density in λ_o with other Common Units.

ARGON, Lennard-Jones

λ_o	ρ_1 $\frac{\text{particles}}{m^3} \times 10^{27}$	ρ_2 $\frac{\text{moles}}{cm^3} \times 10^{-3}$	ρ_3 amagats $\times 10^2$
0.5	0.9964	1.6545	0.3706
1.0	1.9928	3.3090	0.7411
1.5	2.9893	4.9635	1.1117
2.0	3.9857	6.6180	1.4823
2.5	4.9821	8.2725	1.8529
3.0	5.9785	9.9270	2.2234
3.5	6.9750	11.5815	2.5940
4.0	7.9714	13.2360	2.9646
4.5	8.9678	14.8905	3.3352
5.0	9.9642	16.5450	3.7057
5.5	10.9607	18.1995	4.0763
6.0	11.9571	19.8540	4.4469
6.5	12.9535	21.5084	4.8174
7.0	13.9500	23.1629	5.1880
7.5	14.9464	24.4817	5.5586
8.0	15.9428	26.4719	5.9292
8.5	16.9392	28.1264	6.2997
9.0	17.9356	29.7809	6.6703
9.5	18.9320	31.4354	7.0409
10.0	19.9285	33.0899	7.4115
10.5	20.9249	34.7444	7.7820
11.0	21.9213	36.3989	8.1526
11.5	22.9177	38.0534	8.5232
12.0	23.9142	39.7079	8.8937
12.5	24.9106	41.3624	9.2643
13.0	25.9070	43.0169	9.6349
13.5	26.9034	44.6714	10.0055
14.0	27.8999	46.3259	10.3760

Table 3. Correlation of Density in λ_o with other Common Units.
ARGON, Modified Buckingham

λ_o	ρ_1 $\frac{\text{particles}}{m^3} \times 10^{27}$	ρ_2 $\frac{\text{moles}}{cm^3} \times 10^{-3}$	ρ_3 amagats $\times 10^2$
0.5	0.9798	1.6268	0.3644
1.0	1.9595	3.2536	0.7287
1.5	2.9393	4.8805	1.0931
2.0	3.9190	6.5073	1.4575
2.5	4.8988	8.1341	1.8219
3.0	5.8785	9.7609	2.1862
3.5	6.8583	11.3877	2.5506
4.0	7.8380	13.0145	2.9150
4.5	8.8178	14.6414	3.2794
5.0	9.7975	16.2682	3.6437
5.5	10.7773	17.8950	4.0081
6.0	11.7570	19.5218	4.3725
6.5	12.7368	21.1486	4.7369
7.0	13.7166	22.7754	5.1012

Table 4. Correlation of Density in λ_o with Other Common Units.

ARGON, Barker-Bobetic

λ_o	ρ_1 $\frac{\text{particles}}{m^3} \times 10^{27}$	ρ_2 $\frac{\text{moles}}{cm^3} \times 10^{-3}$	ρ_3 amagats $\times 10^2$
0.5	1.0428	1.7307	0.3876
1.0	2.0855	3.4614	0.7753
1.5	3.1283	5.1921	1.1629
2.0	4.1711	6.9228	1.5506
2.5	5.2138	8.6535	1.9382
3.0	6.2566	10.3842	2.3259
3.5	7.2994	12.1149	2.7135
4.0	8.3421	13.8456	3.1011
4.5	9.3849	15.5764	3.4888
5.0	10.4277	17.3071	3.8764
5.5	11.4704	19.0378	4.2641
6.0	12.5132	20.7685	4.6517
6.5	13.5560	22.4992	5.0393
7.0	14.5987	24.2299	5.4270
7.5	15.6415	25.9606	5.8146
8.0	16.6843	27.6913	6.2023
8.5	17.7270	29.4300	6.5899
9.0	18.7698	31.1527	6.9776

Table 5. Correlation of Density in λ_o with other Common Units.
NITROGEN, Lennard-Jones

λ_o	ρ_1 $\frac{\text{particles}}{m^3} \times 10^{27}$	ρ_2 $\frac{\text{moles}}{cm^3} \times 10^{-3}$	ρ_3 amagats $\times 10^2$
0.5	0.7751	1.2538	0.2809
1.0	1.5102	2.5076	0.5618
1.5	2.2654	3.7615	0.8427
2.0	3.0205	5.0153	1.1236
2.5	3.7756	6.2691	1.4045
3.0	4.5307	7.5229	1.6854
3.5	5.2858	8.7768	9.9663
4.0	6.0409	10.0306	2.2472
4.5	6.7961	11.2844	2.5281
5.0	7.5512	12.5382	2.8090
5.5	8.3063	13.7920	3.0899
6.0	9.0614	15.0459	3.3708
6.5	9.8165	16.2997	3.6517
7.0	10.5716	17.5535	3.9326
7.5	11.3267	18.8073	4.2135
8.0	12.0819	20.0611	4.4944
8.5	12.8370	21.3150	4.7753
9.0	13.5921	22.5688	5.0562
9.5	14.3472	23.8226	5.3371
10.0	15.1023	25.0764	5.6180
10.5	15.9574	26.3302	5.8989
11.0	16.6126	27.5841	6.1798
11.5	17.3677	28.8379	6.4607
12.0	18.1228	30.0917	6.7416
12.5	18.8779	31.3455	7.0225
13.0	19.6330	32.5993	7.3034
13.5	20.3881	33.8532	7.5843
14.0	21.1433	35.1070	7.8652

Table 6. Correlation of Density in λ_o with other Common Units.
NITROGEN, Modified Buckingham

λ_o	ρ_1 $\frac{\text{particles}}{m^3} \times 10^{27}$	ρ_2 $\frac{\text{moles}}{cm^3} \times 10^{-3}$	ρ_3 amagats $\times 10^2$
0.5	0.8293	1.3770	0.3085
1.0	1.6586	2.7540	0.6170
1.5	2.4879	4.1310	0.9255
2.0	3.3172	5.5080	1.2340
2.5	4.1465	6.8850	1.5425
3.0	4.9758	8.2620	1.8510
3.5	5.8051	9.6390	2.1595
4.0	6.6344	11.0160	2.4680
4.5	7.4637	12.3930	2.7765
5.0	8.2930	13.7700	3.0849
5.5	9.1223	15.1470	3.3934
6.0	9.9516	16.5240	3.7019
6.5	10.7809	17.9010	4.0104
7.0	11.6102	19.2780	4.3189
7.5	12.4395	20.6550	4.6274
8.0	13.2688	22.0320	4.9359

Lists of the numerical values of constants and parameters used in the generation of the tables of radial distribution functions are provided in Tables 7 and 8.

The anomalous results for argon at 180 °K using the LJ 12-6 potential are of some tangential interest. While all other families of radial distribution functions at given T showed a predictable consistency over the range of densities, this set exhibited a peculiar variation from anticipated results in the mid-range densities, $4 \leq \lambda \leq 9$. It is quite possible that these are spurious solutions similar to those reported by Watts,[21] but a definitive statement is not possible now.

These "solutions"converge very slowly and were obtained after extremely long run times. Neither financial or hardware resources were sufficient to support the detailed examination necessary to identify the nature of these anomalous results; for the moment they are merely a curiosity, a puzzle for future exploration.

It is also ruefully noted that this data set caused a good deal of consternation and wasted debugging effort at the time of its generation, because quite by accident it was the first family of g's to be generated. Its nature as an anomaly was not originally recognized, and it was thought to be the result of a programming error. Later, the fear arose that it was the product of some basic inadequacy in the algorithm, or, worse yet, the theory.

Table 7 Constants and Parameters for Argon

Name	Symbol	Value		Source [bibliography]
		Lennard-Jones		
Char. Length	a	= 3.4180×10^{-10}m		(2)
Char Energy	ϵ	= 1.7120×10^{-21}j	=	124°K•k
		Modified Buckingham		
Char. Length	r_m	= 3.866×10^{-10}m		(2)
Char. Energy	ϵ	= 1.7009×10^{-21}j	=	123.2°K•K
Slope	α	= 14		
		Barker-Bobetic		
Char. Length	r_m	= 3.7630×10^{-10}m		(11)
Char. Energy	ϵ	= 1.9360×10^{-21}j	=	140.23°K•K
Slope	α	= 12.5		
Constant	A_0	= 0.29214		
Constant	A_1	= -4.41458		
Constant	A_2	= -7.70182		
Constant	A_3	= -31.9293		
Constant	A_4	= -136.026		
Constant	A_5	= -151.000		
Constant	C_6	= 1.11976		
Constant	C_8	= 0.171551		
Constant	C_{10}	= 0.013748		
Constant	δ	= 0.01		

Table 8 Constants and Parameters for Nitrogen

Name	Symbol	Value	Source [bibliography]
		Lennard-Jones	
Char. Length	a	= 3.749×10^{-10}m	(2)
Char. Energy	ε	= 1.1017×10^{-21}j = 79.8°K·k	
		Modified Buckingham	
Char. Length	r_m	= 4.040×10^{-10}m	(2)
Char. Energy	ε	= 1.5670×10^{-21}j = 113.5°K·k	
Slope	α	= 16.2	

Throughout this examination of the program, algorithm and theory, there loomed the possibility (really, the spectre) that the entire scheme was inoperable and, after so much effort, would have to be abandoned. Such paranoia must afflict all graduate students.

Viscosity and Thermal Conductivity Results

Beginning with the Kirkwood formulation of the radial distribution function, the aim of this work has been the critical examination of the Rice-Allnatt theory of transport. It may be argued that this effort, based as it is on this single formulation of g, and branching only on the choice of intermolecular potential, is too narrow and falls short of the critical test envisioned. But this perhaps represents only the beginning of a more broadly based effort. As an accompanying portion of this total program Babb has already extended its scope by calculating the RA coefficient of bulk viscosity using the Kirkwood g, has generated other distribution functions using Pervis-Yevick and Convoluted Hypernetted Chain theory and has used the molecular dynamics results of Verlet[22] to further test Rice-Allnatt. Because this additional work extends as well as reinforces the Kirkwood based results, it appears in tabular form here and in the accompanying discussion.

Discrepancies and Their Sources

A cursory examination of the computed and observed values for the transport coefficients shows a very serious disagreement at all densities. The calculated values fall far below the observed values, to so great an extent in the case of the coefficient of shear viscosity, for example, as to predict the wrong sign. In this regard, even the gross quantitative nature of the results is at variance with the observations.

This is disturbing, particularly in light of the tentative good agreement seen in earlier work.

The problem would now seem to be the isolation and identification of the source or sources of the disagreement. We may examine and choose among such possibilities as the accuracy of the programming effort, the suitability of the radial distribution function formalism, that of the intermolecular potential, and finally, the accuracy of the Rice-Allnatt theory itself.

A. Accuracy of the Programming Effort.

The accuracy of these results is very difficult to assess. Normal procedures whereby accuracy of numerical calculations are estimated rapidly lose their viability in extended chains of operations such as those associated with the calculation of g, η and χ. However, the following comments are in order:

The decision to perform all calculations to sixteen significant figures rendered machine round-off error completely negligible. Sufficient care was taken in the design of the algorithms,

the selection of commands and the order of execution to make finite word length problems minimal if not altogether nonexistent. Additionally, iterative solutions possess the saving feature that errors do not propagate beyond one cycle.

The integration techniques used throughout do not produce inherently significant errors; the relatively small mesh size guarantees errors no larger than 1×10^{-8}, even when extravagantly estimated.

Of far more significance in the g calculation is the approximation that, beyond some upper limit x_m, g=1. This is "tieing the tail" of the radial distribution function, forcing on it a restriction warranted only by virtue of the practical limits of the computing devices at hand. Still, choosing $x_m = 10$ extends the value of g beyond that of earlier work, and a trial calculation with $x_m = 20$ resulted in variations in g only in the seventh or eighth place. (It should also be noted that this more than doubled the calculational time.) There are no other significant errors in the radial distribution function algorithm.

But there are other errors. The least well-known portion of the viscosity calculation involves the calculation of ψ_2, which is developed as a solution to an integral equation. The integrands involve differences between the g's and 1, and then the integrals themselves are differenced. This double differencing increases errors markedly and these errors extend through each iterative cycle. Comparison between numerical and analytic solutions of ψ_2, using artifical distribution functions, indicate this error to

be less than one per cent. This could be improved through more stringent demands placed on the accuracy of the match of boundary conditions, and on the value of the convergence criterion.

For thermal conductivity or bulk viscosity, errors are introduced through the operation of numerical differentiation. Comparison of results using three-term differentiation and five-term differentiation indicates the errors introduced are again small. Differentiations with respect to range (r) or reduced range (x) are essentially error free, because of the small mesh size, and those across density (λ or ρ) are also probably negligible. Errors in differentiation across temperature are also small but of a less certain nature. Here, it is simply a matter of not having available all the isotherms of g desired; one can realistically calculate only so much and so long.

But conservatively, each transport coefficient should be known to an accuracy of the order of one per cent, and most results, particularly for the shear viscosity, would be better than this figure by at least one order of magnitude. The results listed in the tables are given to four figures, through conceivably not every entry is good to the full four figures.

In view of the generally poor agreement between calculation and observation, a more precise statement of the error seems superfluous.

B. Radial Distribution Function Formalism.

The Kirkwood formulation of g is to some extent flawed; it is known to possess weaknesses from the standpoint of prediction of thermodynamic properties[23]. However, the RA work relied on this form through the KMA and KLA results. They were after all essentially the only radial distribution function data base available and some agreement had been achieved with their use. Precedent dictated the Kirkwood formulation of g to be the first used.

The original KMA-KLA results, however, are weak in that at relatively high densities they predict *negative* pressures. But this data is given to a precision of only ±0.002 in the exponential form, or about ±0.02 in g itself. It was anticipated that a data base (i.e., g-tables) of higher precision would yield better agreement.

The results are in poor agreement with observation. It is possible that the Kirkwood g is at the bottom of the disagreement between calculation and observation. Recently Babb applied radial distribution functions derived from Percus-Yevick and Convoluted Hypernetted Chain formalisms, and g's obtained by Verlet from molecular dynamics calculations as well to the RA equations. These results are essentially in agreement with those deriving from Kirkwood but exhibit the negative sign at even lower densities. It does not appear likely, in light of this work, that the form of the radial distribution function is the root of the difficulty.

C. Intermolecular Potential Formulation.

The Lennard-Jones intermolecular potential as modified (Eq. 2-7) formed the basis of earlier calculations. It was envisioned

that easing the restrictions on the absolute hard core,

$$V(r) = \infty \quad r < a \ ,$$

would render the calculation more realistic and the results more accurate. With regard to the results, such was obviously not the case. Replacement of the LJ potential with the Modified Buckingham and the Barker Bobetic potentials did not result in any particular improvement. Although not determined with reference to transport phenomena, and formulated without the Axilrod-Teller three body term, the Barker-Bobetic potential could be expected, by virtue of its many substance dependant constants, to accurately reflect the geometry of the potential curve. In this regard the BB potential merely confirmed that the conventional potentials such as the LJ and MB produced consistent results and that the calculation was not sensitive to the potential used. This conclusion is reinforced by other independant results.[24] Although one may wonder what undetected dependancy on density may exist in any of these expressions (and this is a point for future examination) it does not appear that the functional form of the intermolecular potential, as conventionally formulated, is the source of the discrepancies encountered.

D. The Rice-Allnatt Theory.

Thus we come, by the process of elimination, to the Rice-Allnatt theory itself, and ask if some oversight or inadvertent error in the development might produce the divergence from observation. But the main features of the development, while intricate,

follow standard, well-defined techniques (for instance, the singlet and doublet distribution functions are obtained by techniques developed by Enskog and Chapman), and we may conclude that this possibility is highly unlikely.

But certain basic concepts of the theory are of note even from the brief descriptions presented here. In particular, the analysis of the reduced Liouville equation, where interactions of a "hard" and "soft" nature are cleanly separated and treated independently seems, at least at high densities, to be suspect. The related distinction between times, where it is assumed that the quasi-Brownian motion between two collisions is of a duration orders of magnitude longer than the collision time, seems questionable. Independent calculations based on molecular dynamics would seem to indicate that the distinction in these times blurs at high density.[25] Certainly it is possible at these densities, given a realistic core for the potential, to envision that no constituent molecule is ever effectively free of a strong repulsive influence of its neighbors. But never in the calculation does it appear that the proper balance between η_v and η_k, for example, is achieved.

But the problem does not end with the preceding qualitative remarks. A more detailed examination of the theory, cast against experimental results, contrasts the shortcomings of the theory even more vividly.

Production of Comparison Experimental Results

The results of these calculations employing the Rice-Allnatt theory are so poor in some cases as to be at complete variance with physical reality and on that basis alone can be rejected out of hand. So stated, there seems little point in comparing them with experimental results. But there is some merit, for example, in comparing the pressures calculated from the various radial distribution functions generated as a measure of the accuracy of these g's. Additionally, an effort should be made to quantitatively assess the disagreement at the lower ranges of pressure or density (where disagreement is generally smallest) to determine how badly and in what manner the theory fails.

Babb has surveyed the experimental results and compiled comparison data sets from them. The collection of equation of state, shear viscosity, thermal conductivity and bulk viscosity data for both argon and nitrogen over so broad a range of temperatures and densities quite naturally required bridging gaps and smoothing disagreements between various sets of results as well as extending the ranges of others. In this process of blending and extending, precision was not the primary aim, but, rather, the accumulation of a viable body of reference data against which a measure of the RA-theory and other incidental comparisons could be made. Efforts directed toward refinement of the experimental data proceeded only so far as was needed for the purpose at hand.

A. The Equation of State.

Jacobsons' work[26] in nitrogen is very extensive and the equation of state which results reproduces the experimental values over a wide range of pressures and temperatures. This equation was programmed and calculations were made for densities and temperatures of interest. These and other results all appear tabulated in the tables for shear viscosity

The same comprehensive work is apparently not available for argon and the results of a number of workers[27-33] were extrapolated by a variety of techniques, as appropriate to cover the ranges of pressures required. Virial expansions, Lagrangian interpolations, least squares fits of a variety of functions [including those specifically developed for high pressure representation of PVT data[34]] were all used. The sources are not all entirely consistent with each other and so on the boundaries between the various investigations, some smoothing was done. Some irregularities in first differences may still be present; however, these differences are less than the disagreement between calculated and observed pressures in practically all cases.

B. The Shear Viscosity.

Trappenier, *et al.*[35] performed a searching corresponding states examination of the noble gases, including argon, which resulted in a double expansion in reduced temperature and reduced density with evaluated coefficients. This result was extrapolated by Mr. Jerome Kaiser, to whom the author is indebted for his work, over the range of temperatures and densities encountered here.

No similar study seems to have been performed on nitrogen so one was improvised when polynomial fits attempted across isotherms resulted in non-smooth behavior. The concept of corresponding states was employed to improve the validity of the expansion. The expansion is

$$\eta = \eta_o \sum_{ij} a_{ij} \rho^{*i} (\log_{10} T^*)^j ,$$

where the parameters which reduce the observed viscosities, densities and temperatures to those which are a best fit must be determined. The a_{ij} are those for argon from Trappeniers *et al.* A least-squares analysis of combined data runs of Michels and Gibson[36] and Vermesse[37] was used for the evaluation of other constants. The inconsistencies produced by this technique were small in comparison to the divergence of the RA predictions.

Obviously, the concept of corresponding states is not strictly applicable to nitrogen, for the reducing parameters found for the high and low density expansions which were made are not the same. But the technique uses the 'best' values of reducing parameters which map the nitrogen behavior onto the noble gas behavior, and in so doing, achieve predicted experimental values approximately in as good agreement as was obtained for argon. For the high density expansion, the error in fit was approximately 9.1 per cent. The expansion based on low density data was not sufficiently more accurate and therefore was not used. Because the range of values of ρ were so large, it was the sum of the

squares of the percentage errors which was minimized in this treatment of nitrogen.

C. The Thermal Conductivity.

Polynomial expansions of the van der Waals Laboratory data data[38,39] was exclusively used. The fit proved good and the rapidly diminishing size of the coefficients of the higher order density terms supported the possibility of extensive extrapolations. Four isotherms for argon and three for nitrogen were available.

Although the extrapolations were extensive, confidence in their merit was gained by noting that these results agreed quite well with the atmospheric values for thermal conductivity for nitrogen and were only somewhat high for argon[40].

D. The Bulk Viscosity.

There is no extensive experimental data for bulk viscosity; for a survey, the reader is referred to Cowan and Ball[41]. The only data directly applicable to this investigation was that of Madigosky[42], but this is an isotherm at -38.6°C. Since the temperature dependence of bulk viscosity appears weak (at least for small temperature ranges), these results are used without any temperature correction for a comparison at 0°C and are so listed as "observed" at that temperature in the tables.

Comparisons

From the experimentally based data we may draw a reasonably concise picture of the actual behavior of the specific quantities of interest here, and a comparison of this behavior with the RA predictions can then afford the viable test we desire. It would also be

possible to compare in detail the various RA predictions as they are influenced by the variety of intermolecular potentials and other quantities used in these calculations. For instance, Babb has already extended this work by certain calculations of the RA transport coefficients using other radial distribution functions. But this sort of detailed comparison will be made only sparingly in light of the very serious disagreement of the data generated by nearly all the calculational paths to the experimental results. Rather, we take here the view that the discrepancies between the individual calculational paths are minor compared to the serious disagreement with RA, so minor, in fact, to be of almost parenthetical comment. Much more relevant to the examination at hand is the bleak fact that no matter what path was followed, it was not possible to achieve good agreement.

It surely must be possible to detect, in what follows, some of the disappointment of the author for the disagreement found. The RA formulation represents an imposing intellectual effort. It seemed at the outset of this work that agreement would be obtained. But as the work progressed and the prospects for agreement were diminished, it began to appear that the theory as formulated was in trouble. The comparisons below only too clearly bear this out.

A. The Equation of State.

The results of these calculations, using the virial equation of state and the Kirkwood formulation for g is in good agreement with other similar calculations appearing in the literature.

It is to be noted that the calculations using the truncated potential, equation (2-7), are in slightly worse agreement than those obtained here, using the full LJ potential. This could be expected, for the parameters of the potential were obtained by fitting calculations using the full potential to experimental data. The introduction of these parameters so obtained into the truncated potential function would alter the results slightly.

At low densities, the results are in good agreement with experiment.

B. The Shear Viscosity.

This calculation was, perhaps, the major undertaking of this work. Certainly it was the most thoroughly examined because it was the first transport coefficient calculated and as discrepancies between its predictions and experimental results began to appear, all aspects of its formulation were intensely examined.

Furthermore, it is 'simpler' than either thermal conductivity or bulk viscosity in that it incorporates none of the numerical differentiations across density or temperature and can therefore be assumed free of the entanglements of numerical error associated with these operations.

The characteristics of all the calculations were similar: the results have very low values of viscosity at low density, increase too rapidly and at high densities pass through a maximum and then fall to negative values.

The failure at low densities, while surprising, could be understood from the fundamental equations. The theory was designed to approach the Enskog limit when the potential is taken to be that of a hard sphere for which the soft drag coefficient vanishes. For a more realistic potential, however, the soft drag coefficient vanishes as density (in the normal calculation). It appears in the Enskog terms in the denominator, itself divided by ρ^2, so that the terms which are supposed to predict the correct low density limit in fact vanish.

But since in the low density range the behavior of ζ_s is critical, this function was further examined. It might be that the particular formulation used in the majority of these calculations was at fault. This was checked by using other formulations.

The speed of sound ζ_s, Equation (3-91), also makes the viscosity prediction go negative, but at a different density. The low density value for this ζ_s gives even poorer results for η. But perhaps most discouraging of all is that the ζ_s so formulated drops with increasing density. Since ζ_s is supposedly related inversely to the diffusion coefficient this is a most unphysical behavior. The previous assertion "We wish to suggest that Eq. (12) [the speed of sound formulation of ζ] be recognized as the best available estimate of the molecular friction constant"[43] is apparently no longer tenable.

The Helfand formulation gives the best low density result, being off by a factor of 2; but as seen from the extensive tables, it also gives negative results at high densities.

For these reasons, it was only in the case of shear viscosities that the Helfand and sound speed ζ_s's were used, for other than a truncated LJ potential.

As a final attempt to secure a workable ζ_s and to examine the viscosity formulation, Babb considered it an unknown in the viscosity formulation and evaluated it by force fitting to experimental data. So obtained, ζ_s becomes negative at high density, and this in turn caused the total friction coefficient to fall. If correct, this would imply, for instance, that the diffusion coefficient would at some point commence increasing with increasing density. This is contrary to expectation.

This work is not the first to point out the difficulties involving the friction constant formulation. Collings[44,45] has stated that the conclusions of the correctness of the RA formalism is premature and that serious problems still exist.

The fall to negative viscosities at high density is related to the calculation of ψ_2; at these densities the dominant terms are $\eta_v^{(3)}$ and $\eta_v(R>\sigma)$, equations (3-72) and (3-78). Both terms become strongly negative here in consequence of the value of ψ_2.

It was then natural to suspect that the iterative solution of ψ_2 contains some programming error. But when original KLA radial distribution function values were substituted for those generated here, the ψ_2 calculation performed, and the results compared with those of Rice *et al.*, the results were in good agreement. But most encouraging was Babb's creation of artifical

functions which permitted the solution of the ψ_2 equation analytically. It was possible to then check programming by comparing an analytic solution with the numerical solution. The results were quite good, giving an rms deviation between the two functions of 0.8 per cent, and this could have been improved by making the convergence criterion of the numerical solution more stringent.

As a last resort, the formulation of ψ_2 was checked for some mathematical error trivial or otherwise, but none was found. The result using artifical functions, the lack of consistency (the failure of the ζ_s obtained from force fitting the shear viscosity expression to predict a consistent diffusion behavior) and the accumulated other analyses all pointed to the same conclusion: nothing seems to help and the theory with regard to shear viscosity is not viable as presently formulated. The numerical results supporting this conclusion are contained in Tables

Davis *et al.*[46] considered a square well fluid in connection with the RA theory. The results are often cited as supportive. The original paper must be consulted for the details of their rather complex calculation; however, they avoid much of the RA formalism, in fact obtaining the values of $g(\sigma)$ by force fitting one of the viscosity equations to the experimental value. They avoid the entire ψ_2 and ζ_s formalism, discussing ζ_s by showing their formulation is in reasonable agreement with diffusion constants which have been measured. This calculation has very little impact on the present work.

C. The Bulk Viscosity.

An effective comparison of theory and experiment here is difficult since experimental results are so few, and in some ways contradictory. For example, some low-temperature work indicates a dramatic rise in bulk viscosity with decreasing density while the work (at higher temperature) of Madigosky shows a smooth rise; however, this could indeed be a bonafide temperature effect. In any event, the theory predicts a lowering of bulk viscosity with decrease in density at all temperatures and must therefore be considered not in agreement with observations at low temperature.

Additionally, bulk viscosity calculations exhibit the same behavior as determined for shear viscosity, the prediction of negative values at sufficiently high density. Here, the calculations of ψ_0 and ψ_2 are the cause. Again, the programming was checked by artificial functions and found correct.

That problems would arise could be seen from the Rice and Grey discussion of earlier work[3]. The function Q, Equation (3-77), relates to the limiting behavior of ψ_0, and it can be shown from (3-77) that

$$Q = -\frac{3kT}{4\pi}\rho^2\kappa_T^2\left(\frac{\partial p^2}{\partial \rho^2}\right)_T + \sigma^3[g(\sigma)-1] \quad . \tag{5-1}$$

The former expression (3-77) is amenable to evaluation by calculation (Q_{CAL}) and the latter, by use of experimental data (Q_{EXP}). But Rice and Grey point out that while $Q_{EXP} \leq 0$, $Q_{CAL} > 0$. Their somewhat drastic compromise was simply to set $Q = 0$, and thus ignore a portion of the theory.

This discrepancy has been partially resolved by the present work. While the KLA $g(\sigma)$ used earlier was generally $g(\sigma)<1$, we find generally, that $g(\sigma)>1$. Additionally, in this work, the experimental values used here were obtained from two sources: real argon[28] and from virial expansions to the pressures calculated for the truncated LJ potential. These results are shown in Table 4-87, page 227, and there the signs agree at higher densities. The further discrepancy results from the failure of argon to conform to the truncated LJ potential and from inconsistencies in the Percus-Yevik approximation used in this particular calculation: the viral pressures do not agree with those obtained from the compressibility equation used in deriving Equation (5-1).

The signs now agree, and undoubtedly could be made even if better agreement by closer attention to the details of calculations in Equation (5-1). It is to be noted that a sufficiently positive Q guarantees negative values of ϕ.

Even the artifice of setting $Q = 0$ does not suffice. In the special table (p. 227) comparing ζ_s formulations, one entry was with the normal ζ_s but with $Q = 0$. The predictions still become negative at sufficiently high density. It is assumed that this would happen as well for other ζ_s formulations, but this has not been directly checked.

One of the early encouraging aspects of the RA theory came from the apparent agreement obtained with experimental results after the publication of the theoretical calculations, But the calculations were obtained at the expense of neglecting Q and, hence, using an inaccurate ψ_0. Further, the variation in g and ψ_0 with increasing density was neglected; the results at one temperature were thus scaled by their coefficients without proper regard to the major effects of increasing density.

Changing the method by which ζ_s is found does not materially improve the agreement; however, the Helfand formulation is somewhat better than the other expressions. Once again the basic theory fails.

D. The Thermal Conductivity.

Since the calculation of this transport coefficient does not depend on either ψ_0 or ψ_2, it does not become negative as the viscosities; however, the results are still at wide variance with observation. For example, the RA thermal conductivity at the lowest density, using the truncated LJ potential (which corresponds to the theory's basic assumptions) rises 18 per cent in value from 0°C to 100°C and the experimental values climb some 24 per cent; however, the RA values are low by a factor of eight. The increase with density is at variance with experiment: from a factor of .81 too low at the lowest density to a factor of 3.3 too low at the highest. Variation with both parameters are poorly represented.

Again, changing the ζ_s used in this calculation; the Helfand formulation remains the best as an order of magnitude estimation, but gives results low by a factor of ½ at low densities and (surprisingly) increasing to a factor of 2 at the highest density.

Considering the change in thermal conductivity as a function of density, and examining the influence of the drag coefficient ζ_s as it influences this variation, the Helfand formulation gives too small an increase while the speed of sound and normal calculations give to great an increase. All fail to give a sufficiently high increase with temperature although here, in comparison with other results, the agreement, off by only a factor of two, is better.

Thermal conductivity presents the best of all the calculational agreement, but still the results fall far wide of the mark. Thus, one must regard the statement.[47]

> "It is our opinion that the available equilibrium distribution functions for this themodynamic state are unreliable and that the discrepancy between theoretical and experimental thermal conductivity arises from this discrepancy"

as being half true. The radial distribution functions were weak, but increasing their accuracy worsens rather than improves the agreement. It is the tentative conclusion of the author that the discrepancies in the earlier functions made the theory appear better than it is.

Final Conclusions

This work was above all else a pragmatic inquiry. The RA theory purported to represent the transport behavior of a simple, dense fluid. The philosophy was to take this theory as it exists and to inquire: do the equations in fact give a reasonably accurate description of what has been observed?

The results are particularly disappointing.

Based on earlier work it was presumed that the results would be reasonably close, and this presumption dictated the quest for precision which permeated the formulation of the algorithms used.

But not only do the results not accord very closely to physical reality, they defy even qualitative physical intuition. This most fundamental disagreement seems independent of the source of the radial distribution functions used, even those which are presumably exact solutions of the appropriate (in this case Lennard-Jones) intermolecular potential. What ever might be the relevancy of the Lennard-Jones potential to the representation of a real gas, it is quite certain that even a Lennard-Jones gas cannot possess a negative shear or bulk viscosity.

From the variety of problems, checks, manipulations and alternate attempts taken, one is led to the final conclusion that there must be a fault either in the mathematical procedure used for the derivation of these equations, or in the basic assumptions under which the equations were derived. The mathematics is straightforward enough to seem to preclude the former possibility,

and one is left with the depressing conclusion that the basic assumptions of the RA approach, and, hence, their equations, are flawed, and not in any sort of accord with reality.

Figure 9. A typical shear visociety isotherm for Argon.

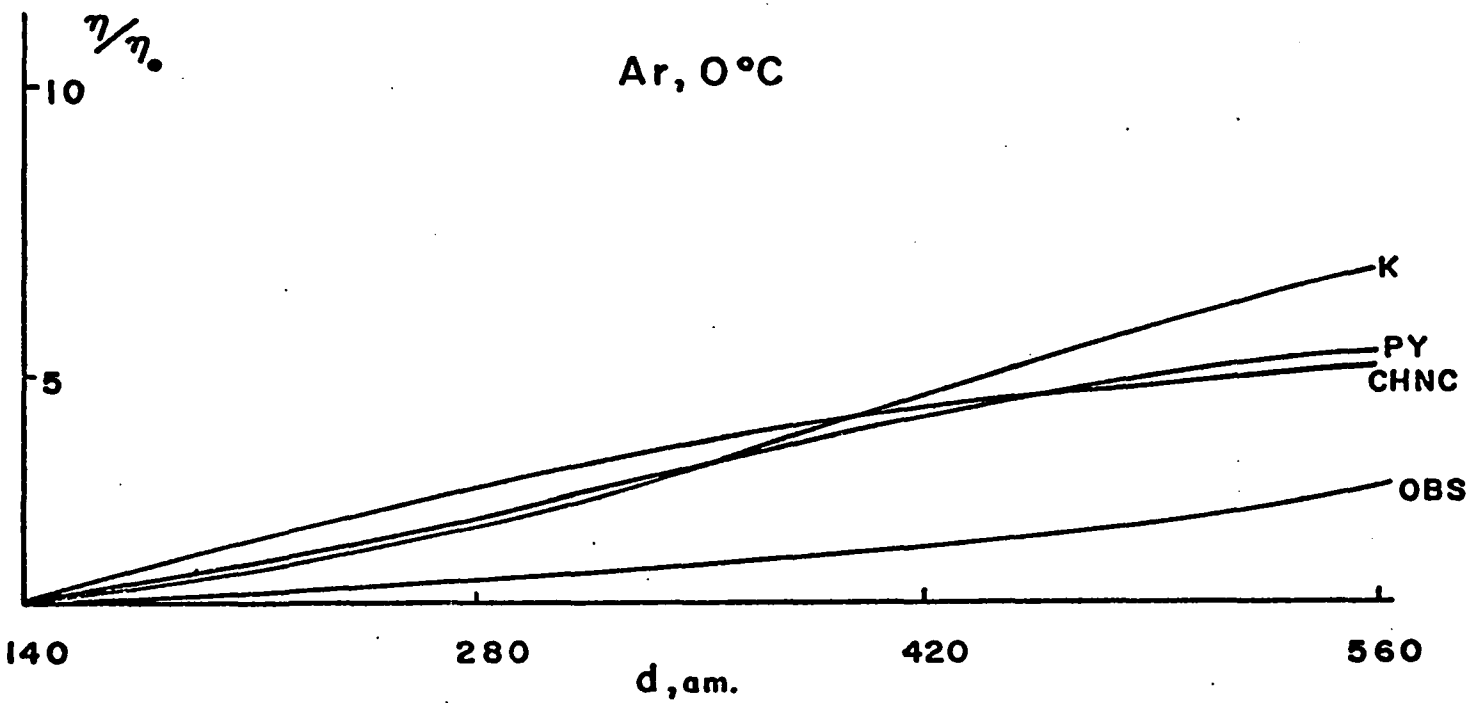
η/η₀
10
5
Ar, 0°C
K
PY
CHNC
OBS
140
280
420
560
d, am.

Figure 10. A typical set of shear viscosity isochores for Argon. Density is in amagats.

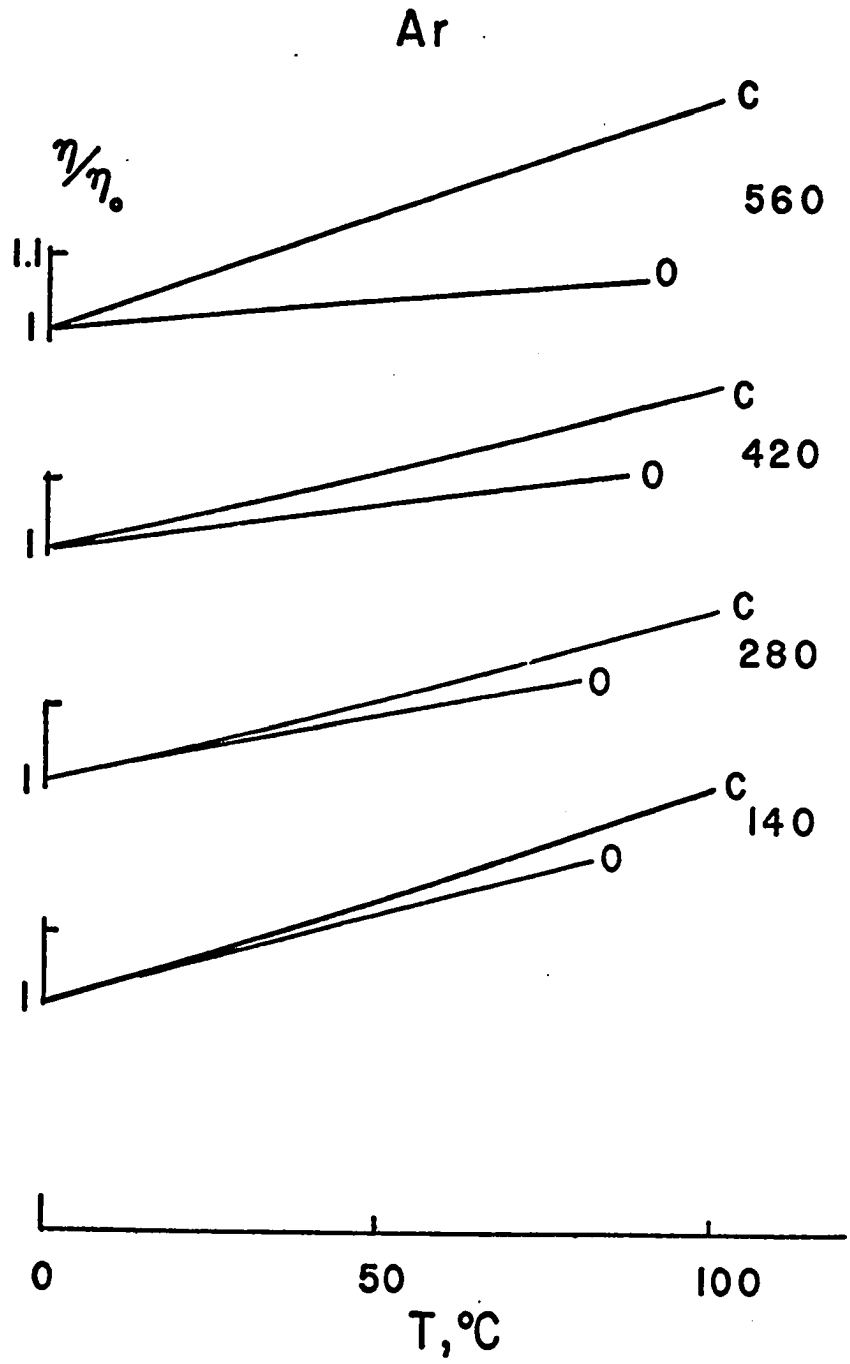
Ar
η/η₀
1.1
1
C
560
0
C
420
0
C
280
0
C
140
0
0
50
100
T, °C

Figure 11. A typical bulk viscosity isotherm for Argon.

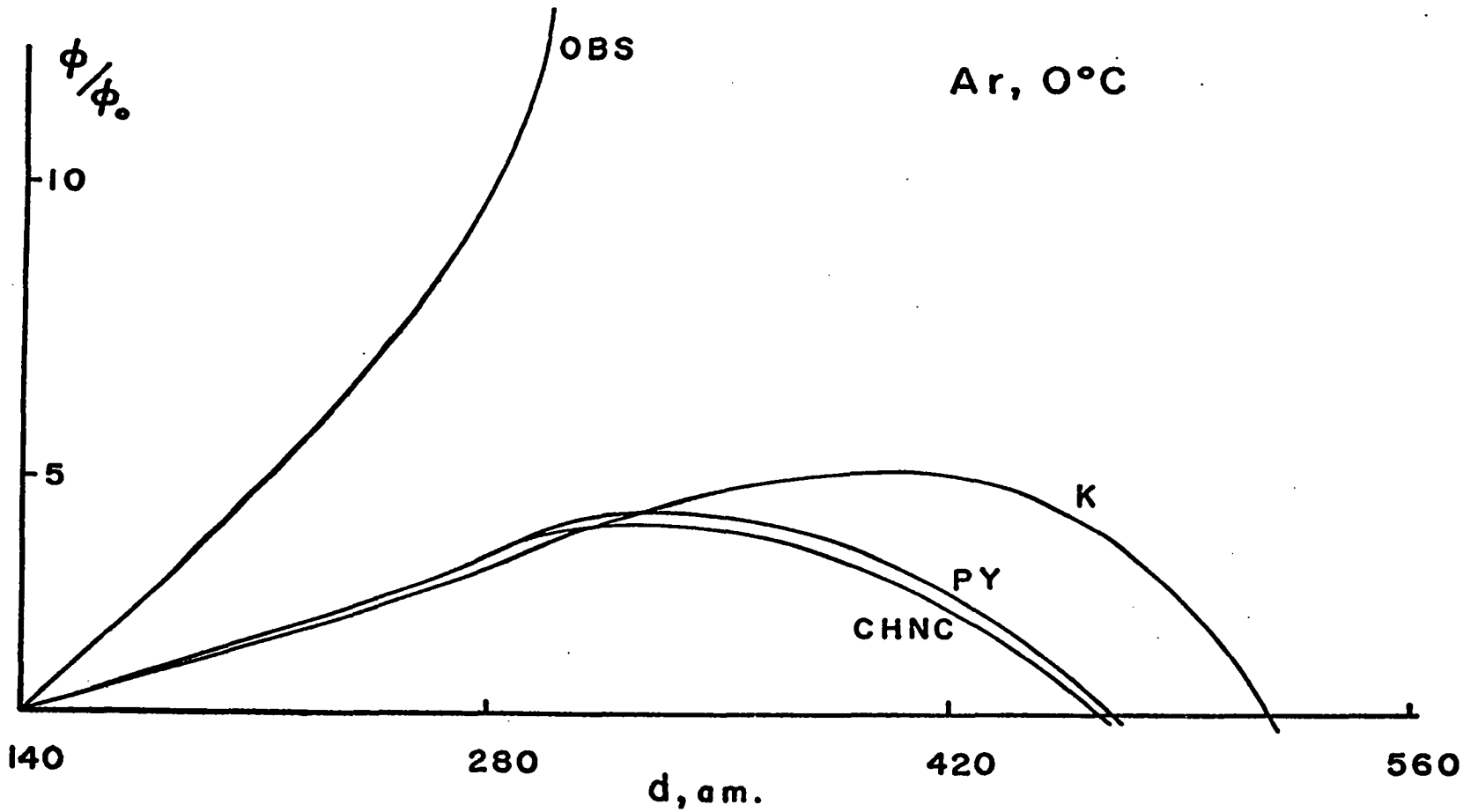
ϕ/ϕ_∞
10
5
OBS
Ar, 0°C
K
PY
CHNC
140
280
420
560
d, a.m.

Figure 12. A typical thermal conductivity isotherm for Argon.

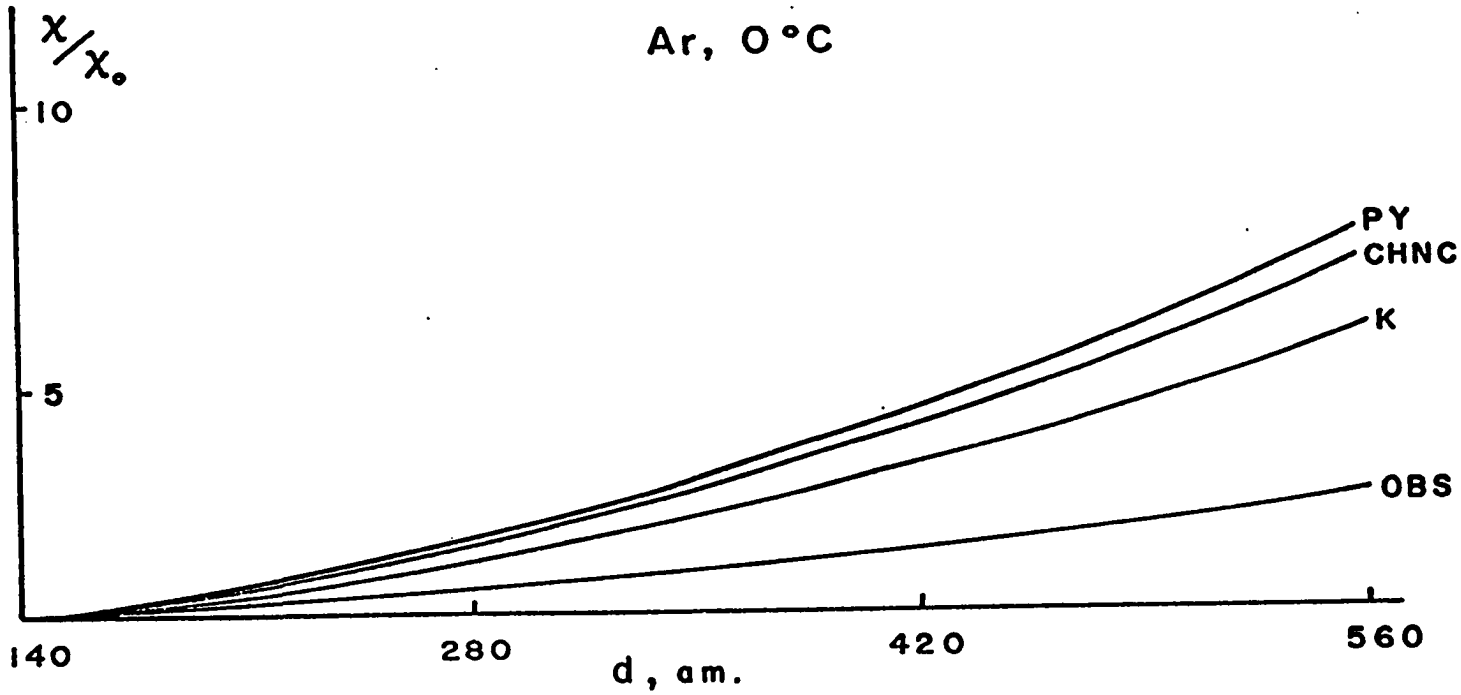
Ar, 0 °C
χ/χ₀
10
5
PY
CHNC
K
OBS
140
280
420
560
d, am.

Figure 13. A typical set of thermal conductivity isochores for Argon. Density is in amagats.

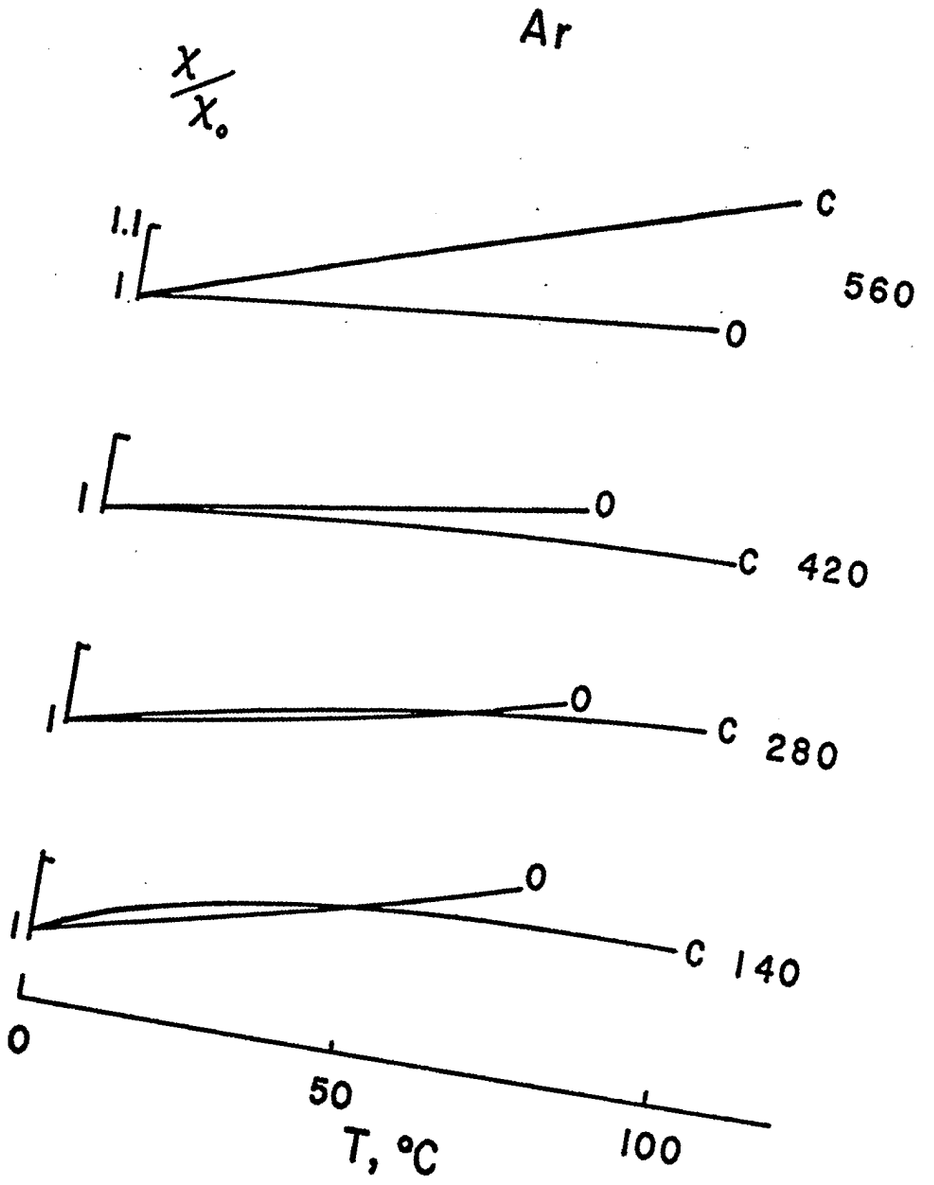
Ar
χ/χ₀
1.1
1
C
560
0
1
0
C 420
1
0
C 280
1
0
C 140
0
50
T, °C
100

BIBLIOGRAPHY

1. Richard L. Liboff, "Introduction to the Theory of Kinetic Equations", John Wiley and Sons, Inc., New York 1969, p. 81 ff.

2. J. O. Hirschfelder, C. F. Curtis and R. B. Bird. "Molecular Theory of Gases and Liquids". John Wiley and Sons, Inc., New York 1954, p. 134 ff.

3. S. A. Rice and P. Gray. "The Statistical Mechanics of Simple Liquids". John Wiley and Sons, Inc., New York 1965, p. 275 ff., and many original papers referenced in this monograph.

4. J. G. Kirkwood. *J. Chem. Phys. 3,* 300 (1935).

5. M. Born and H. S. Green. *Proc. Roy. Soc. (London) A188,* 10 (1946).

6. J. E. Meyer. *J. Chem. Phys. 15,* 187 (1947).

7. J. Yvon. Actualities Scientifiques et Industrielles (Hermann et Cie, Paris, 1935), p. 203.

8. J. G. Kirkwood, E. K. Maun, and B. J. Alder. *J. Chem. Phys. 18,* 1040 (1950).

9. J. G. Kirkwood, V. A. Lewinson and B. J. Alder, *J. Chem. Phys. 20,* 929 (1952).

10. "Handbook of Mathematical Functions:, M. Abramowitz and I. A. Stegun eds. U.S. Government Printing Office, Washington 1965, p. 487.

11. J. A. Barker, M. V. Bobetic and A. Pompe. *Mol. Phys.20,* 349 (1971).

12. S. A. Rice and S. Gray, *op.cit.*, p. 276.

13. J. O. Hirschfelder, C. F. Curtiss and R. B. Bird, *op. cit.*, p. 464 ff.

14. S. M. Karim and L. Rosenhead. *Rev. Mod. Phys. 24,* 108 (1952).

15. K. Herzfeld and F. O. Rice. *Phys. Rev. 31,* 691 (1928).

16. L. Hall. *Phys. Rev. 71,* 318 (1947); *73,* 775 (1948).

17. E. Helfand. *Physics Fluids 4,* 681 (1961).

18. Peter Grey and Stuart A. Rice. *J. Chem. Phys. 40,* 3671 (1964).

19. "Handbook of Mathematical Functions", M. Abromowitz and I. A. Stegun eds. U. S. Government Pringing Office, Washington 1965, p. 886.

20. R. Becker. *Z. für Physik 4,* 393 (1921).

21. R. O. Watts. *Chem. Phys. 48,* 50 (1968).

22. L. Verlet. *Phys. Rev. 165,* 201 (1968).

23. J. S. Rowlinson. "Reports on Progress in Physics", Vol. 28, p. 191 (1965).

24. M. Klien and H.J.M. Hanley. *Trans. Far. Soc. 64II,* 2927 (1968).

25. R. A. Fisher and R. O. Watts. *Aust. J. Phys. 25,* 21 (1972).

26. R. T. Jacobson, Thesis, Washington State University, Pullman, Washington, 1972.

27. S. L. Robertson, Thesis, University of Oklahoma, Norman, Oklahoma, 1969.

28. E. V. Polyakov and D. S. Tsiklis. *Zh. Fiz. Khim. 41,* 2370 (1967).

29. A. Michels, H.U.B. Wijker and H. K. Wijker. *Physics 15,* 627 (1949).

30. J.M.H. Levelt (Sengers), Thesis, University of Amsterdam, Amsterdam, 1958.

31. A. Lecocq, J. Rech. *du C.N.R.S. 11,* 55 (1960).

32. R. K. Crawford, Thesis, Princeton University, Princeton, New Jersey, 1968.

33. V. M. Cheng, Thesis, Princeton University, Princeton, New Jersey, 1972.

34. S. E. Babb, Jr. *J. Chem. Phys. 54,* 4200 (1971).

35. N. J. Trappeniers, A. Botzen, C. A. TenSeldam, H. R. Van den Berg and J. Van Oosten, *Physica 31,* 1681 (1965).

36. A. Michels and R. O. Gibson. *Proc. Roy. Soc. 134A,* 288 (1931).

37. J. Vermesse, University of Paris, Paris, 1969.

38. A. Michels, J. V. Sengers and L.J.M. Van de Klundert. *Physica 29,* 149 (1963) (for Argon).

39. A. Michels and A. Botzen. *Physica 19,* 585 (1953) (for Nitrogen).

40. P. Johannin, Proc. Conf. on Thermo and Transport Properties of Fluids, London, 1957; Institution of Mech. Engineers, London, 1958; p. 193. The disagreemwnt is at 75°C and Johannin's result indicates a lesser density dependance of the thermal conductivity than do the earlier results.

41. J. A. Cowan and R. N. Ball. *Can. J. Phys. 50,* 1881 (1972).

42. W. M. Madigosky. *J. Chem. Phys. 46,* 4441 (1967).

43. J. Naghizadeh and S. A. Rice. *J. Chem. Phys. 36,* 2710 (1962).

44. A. F. Collings. *J. Chem. Phys. 47,* 1265 (1967).

45. A. F. Collings and L. A. Woolf. *Aust. J. Chem. 24,* 225 (1971).

46. H. T. Davis. S. A. Rice, and J. V. Sengers. *J. Chem. Phys. 35,* 2210 (1961).

47. L. D. Ikenberry and S. A. Rice. *J. Chem. Phys. 41,* 4002 (1964).

APPENDIX I

NUMERICAL TECHNIQUES

A. Iteration

Iteration is a standard technique for the location of the roots of an equation $f(x) = 0$. In its simplest form, the technique involves the following steps:

The original equation is transformed by appropriate manipulation into the form $x = g(x)$. A trial value, say x_o is selected and $g(x_o)$ evaluated to yield $x_1 = g(x_o)$. The process is repeated, $x_{n+1} = g(x_n)$, in hopes that the series $x_o, x_1, \ldots, x_{n+1}$ possesses successive differences such that

$$|x_o - x_1| > |x_1 - x_2| > \ldots > |x_i - x_{i+1}| > \ldots$$

and that at some stage:

$$x_n \simeq x_{n+1}$$

to the limits of the precision of our calculating device or our needs for accuracy. Then by definition x_{n+1} is a root of the equation $f(x) = 0$.

There is no guarantee that our method will succeed. Many forms of $x = g(x)$ are possible from any specific $f(x) = 0$. Some

forms may give roots while others fail. For example, two possible forms of the equation

$$5x^2 - 2x\ell n|x| - 8 = 0$$

are

$$x = \frac{5x^2 - 8}{2\ell n|x|}$$

and

$$x = \left\{\frac{2x\ell n|x| + 8}{5}\right\}^{\frac{1}{2}} .$$

Using a trial solution $x_0 = 2$, it is found the first form fails and the second form succeeds in giving a root.

Many improvements in the technique are possible, but the point is made: iteration is a cyclic process performed in hopes that a modified form of the function being examined will refine our guess and ultimately deliver a solution.

The problem at hand is of this basic cyclic nature. The values of a function h(x) at certain specified arguments are required. The functional form of h(x) is unknown, but it is known that h(x) satisfies the integral equation:

$$h(x) = A(x) + \int_a^b K(x-s)B(s)h(s)ds$$

where A, K, and B are of known form. Although analytically this can be a difficult if not impossible task, numerically the procedure is straightforward: a set of values $\{h_0(s_i)\}$ at appropriate values of the argument are chosen, the function evaluated for a designated x, say x_1, and $h_1(x_1)$ is obtained. The process is

repeated at $x_2, x_3, \ldots$, until a new set $\{h_1(x_i)\}$ is obtained. The iterate set $\{h_1(x_i)\}$ replaces $\{h_0\}$ and the process repeated to form $\{h_2(x_i)\}$.

Again, we hope for a diminishing set of successive differences $\Delta h_n(x_i) = |h_n(x_i) - h_{n+1}(x_i)|$ such that each member of the set is less than some prescribed accuracy criterion; we then have our answer.

B. Numerical Integrations.

It was desired to obtain values of the radial distribution function at regularly spaced intervals of its argument. The length of the interval over which the integrals were to be evaluated varied. The first requirement narrowed the choice of basic integration schemes, and the second further limited the choice within viable categories by requiring a great deal of flexibility.

Ultimately, a simple combination of Simpson's and trapezoidal-rules was chosen. The integrands encountered, being smoothly varying functions, were compatible to such a simple choice, and the interval between argument values

$$h = x_{i+1} - x_i$$

could be adjusted to sufficiently small size to insure retention of accuracy.

Simpson's rule gives the evaluation of an integral as

$$I = \int_a^b f(x)dx \simeq \frac{h}{3}\left\{f(a)+4f\left(\frac{a+b}{2}\right)+f(b)\right\}$$

where

$$h = \frac{b-a}{2} \quad .$$

This can be extended to

$$I \simeq \frac{h}{3} \{f(x_1)+4f(x_2)+2f(x_3)+4f(x_4)+2f(x_5)$$

$$+\ldots+4f(x_{n-1})+f(x_n)\} \ ,$$

where $x_1 = a$, $x_n = b$, and $h = \frac{b-a}{n}$; by the scheme, n must be odd.

The trapezoidal rule gives:

$$I \simeq \frac{h}{2} \{f(x_1)+2f(x_2)+2f(x_3)+\ldots+2f(_{n-1}x_{n-1})+f(x_n)\} \quad .$$

Here, n may be odd or even.

A definite upper limit was chosen in the integrals to replace the ∞ normally appearing there. This cut off value in some cases implied the number of points at which the integrand was to be evaluated could be either odd or even. When even numbers of arguments were encountered, a trapizoidal rule segment was appended to the basic Simpson's rule to account for the final points. The fineness of the mesh, $h = 0.025$ in units of the reduced radial distance x, insured that accuracy was maintained.

C. Difference Equations.

Consider the quadratic function

$$f(x) = ax^2 + bx + c$$

and assume that it is required to evaluate f(x) at regularly spaced

intervals x, $x+\Delta x$, $x+2\Delta x,\ldots$. Direct substitution of any argument requires three multiplications and two additions.

An alternate technique for evaluation of the function at regularly spaced intervals exists, one which reduces the number and complexity of the operations to be performed:

$$
\begin{aligned}
f(x) &= ax^2 + bx + c,\\
f(x+\Delta x) &= a(x+\Delta x)^2 + b(x+\Delta x) + c,\\
&= ax^2 + 2ax\Delta x + \Delta x^2 + bx + b\Delta x + c,\\
f(x+2\Delta x) &= ax^2 + 4ax\Delta x + 4\Delta x^2 + bx + 2b\Delta x + c,\\
f(x+3\Delta x) &= ax^2 + 6ax\Delta x + 9\Delta x^2 + bx + 3b\Delta x + c.
\end{aligned}
$$

We note:

$$
\begin{aligned}
\Delta_{11} &= f(x+\Delta x) - f(x) = 2ax\Delta x + \Delta x^2 + b\Delta x,\\
\Delta_{12} &= f(x+2\Delta x) - f(x+\Delta x) = 2ax\Delta x + 3\Delta x^2 + b\Delta x,\\
\Delta_{13} &= f(x+3\Delta x) - f(x+2\Delta x) = 2ax\Delta x + 5\Delta x^2 + b\Delta x,
\end{aligned}
$$

and

$$
\begin{aligned}
\Delta_{21} &= \Delta_{12} - \Delta_{11} = -2\Delta x^2\\
\Delta_{22} &= \Delta_{13} - \Delta_{12} = -2\Delta x^2 .
\end{aligned}
$$

Thus, if the value of $f(x)$ is known, $f(x+\Delta x)$ may be obtained by adding $2\Delta x^2$ to $(2ax\Delta x - \Delta x^2 + b\Delta x^2)$ and then adding the result to $f(x)$. Now $f(x+\Delta x)$ is known. To find $f(x+2\Delta x)$, add $2\Delta x^2$ to $(2ax\Delta x + \Delta x^2 + b\Delta x)$ and that to $f(x+\Delta x)$. Note that the differences $\Delta_{21}, \Delta_{22}, \ldots, \Delta_{2i}$ are the same, and hence Δ_{12} is obtained by adding Δ_{2i} to Δ_{11}, Δ_{13} by adding Δ_{2i} to Δ_{12}, and so on. At every stage, the function and first difference is ready to form the evaluation

of the function at the next argument with only two additions.

The time spent in this latter technique is far less than the former on IBM computers because multiplications on such data processing equipment require between five to seven times more time than additions.

Where ever practical in the design of programs, difference equations were used to evaluate polynomials.

APPENDIX II

DERIVATION OF THE $K_o(t)$ POLYNOMIALS

As an example of the $K_o(t)$ polynomials, write

$$K_o(t) = -\frac{\lambda}{\pi}\int_o^\infty \frac{G(u)\cos ut\,du}{1-\lambda\, G(u)}, \quad \text{where} \quad G(u) = \frac{u\cos u - \sin u}{u^3}$$

By adding and substracting $\int_o^\infty G(u)\cos ut\,du$ twice, we obtain

$$K_o(t) = -\frac{\lambda^3}{\pi}\int_o^\infty \frac{G^3(u)\cos ut\,du}{1-\lambda\, G(u)} - \frac{\lambda^2}{\pi} I_2 - \frac{\lambda}{\pi} I_1 ,$$

where

$$I_2 = \int_o^\infty G^2(u)\cos ut\,du ,$$

and

$$I_1 = \int_o^\infty G(u)\cos ut\,du .$$

By substituting for G(u), expanding and using trigonometric identities, the second integral becomes

$$I_2 = \int_o^\infty \left[\left(\frac{1}{2u^4} + \frac{1}{2u^6}\right) + \frac{\cos 2u}{2u^4} - \frac{\sin 2u}{u^5} - \frac{\cos 2u}{2u^6}\right]\cos ut\,du .$$

It is further modified by use of the identities

$$\sin\rho = \sqrt{\frac{\pi\rho}{2}}\, J_{\frac{1}{2}}(\rho) \text{ and } \cos\rho = \sqrt{\frac{\pi\rho}{2}}\, J_{-\frac{1}{2}}(\rho):$$

$$I_2 = \int_0^\infty \left(\frac{1}{2u^4} + \frac{1}{2u^6}\right)\sqrt{\frac{\pi ut}{2}}\, J_{-\frac{1}{2}}(ut)\,du + \frac{\pi\sqrt{t}}{2^{3/2}} \int_0^\infty \frac{J_{-\frac{1}{2}}(2u)J_{-\frac{1}{2}}(ut)\,du}{u^3}$$

$$- \frac{\pi\sqrt{t}}{2^{\frac{1}{2}}} \int_0^\infty \frac{J_{\frac{1}{2}}(2u)J_{-\frac{1}{2}}(ut)\,du}{u^4} - \frac{\pi\sqrt{t}}{2^{3/2}} \int_0^\infty \frac{J_{-\frac{1}{2}}(2u)J_{-\frac{1}{2}}(ut)\,du}{u^5} \quad .$$

Each of these integrals may now be treated according to the Weber-Schafheitlen result:

$$\int_0^\infty \frac{J_\mu(at)J_\nu(bt)\,dt}{t^\lambda} = \frac{a^\mu\, \Gamma\left(\frac{\mu+\nu-\lambda+1}{2}\right)}{2^\lambda b^{\mu-\lambda+1}\Gamma(\mu+1)\Gamma\left(\frac{\nu-\mu+\lambda+1}{2}\right)}\, {}_2F_1\left(\frac{\mu+\nu-\lambda+1}{2},\right.$$

$$\left.\frac{\mu-\nu-\lambda+1}{2};\ \nu+1,\ \frac{b^2}{a^2}\right), \quad 0<a<b \quad ,$$

or

$$= \frac{b^2\Gamma\left(\frac{\mu+\nu-\lambda+1}{2}\right)}{2^\lambda a^{\nu-\lambda+1}\Gamma(\nu+1)\Gamma\left(\frac{\mu-\nu+\lambda+1}{2}\right)}\, {}_2F_1\left(\frac{\mu+\nu-\lambda+1}{2},\ \frac{\nu-\mu-\lambda+1}{2};\ \mu+1,\ \frac{b^2}{a^2}\right) ,$$

$$0<b<a \quad .$$

where

$${}_2F_1(a,b;c,z) = \frac{\Gamma(c)}{\Gamma(a)\Gamma(b)} \sum_{n=0}^{\infty} \frac{\Gamma(a+n)\Gamma(b+n)}{\Gamma(c+n)} \frac{z^n}{n!} \quad .$$

Consider the second integral of I_2, for example; if $0<t<2$

$$\frac{\pi\sqrt{t}}{2^{3/2}} \int_0^\infty \frac{J_{-\frac{1}{2}}(2u)J_{-\frac{1}{2}}(ut)du}{u^3}$$

$$= \frac{\pi\sqrt{t}}{2^{3/2}} \left\{ \frac{t^{-\frac{1}{2}}\Gamma(-\frac{3}{2})}{2^3 2^{-5/2}\Gamma(\frac{1}{2})\Gamma(2)} \, {}_2F_1(-\frac{3}{2}, -\frac{1}{2}, \frac{1}{2}, \frac{t^2}{2}) \right\}$$

$$= \frac{\pi}{3}\left(1+\frac{3t^2}{2^2}\right) \quad .$$

If, for this same integral $t>2$, we have

$$\frac{\pi\sqrt{t}}{2^{3/2}} \int_0^\infty \frac{J_{-\frac{1}{2}}(2u)J_{-\frac{1}{2}}(ut)du}{u^3} = \frac{\pi t^3}{2^3 \cdot 3}\left(1+\frac{3.2^2}{t^2}\right)$$

$$= \pi\left(\frac{t^3}{2^3 3} + \frac{t}{2}\right) \quad .$$

The third and fourth integrals of I_2 are treated in a similar fashion.

For $a = 0$, $J_0(au) = 1$. Multiply the first integral of I_2 by $J_0(au)$ and obtain for the first term of this integral

$$\tfrac{1}{2}\sqrt{\frac{\pi t}{2}} \int_0^\infty \frac{J_0(au)J_{-\frac{1}{2}}(ut)du}{u^{7/2}} = A \quad .$$

By applying the Weber-Schafheitlen result, and setting $a = 0$,

$$A = \frac{\pi t^2}{2^3 3} \quad , \qquad 0<t<2 \quad .$$

The second term of this integral is treated in a similar fashion.

When all integrals of I_2 are evaluated and the results collected in powers of t, we find

$$I_2 = \frac{\pi}{2}\left\{\frac{2}{15} - \frac{t^2}{6} + \frac{t^3}{12} - \frac{t^5}{240}\right\} \quad 0<t<2$$

$$= 0, \quad t>2 \quad .$$

This technique was applied to $I_1,\ldots,I_5$ so that the algorithm on which the evaluation of the resolvent kernal $k_o(t)$ was based was

$$K_o(t) = -\frac{\lambda^6}{\pi}\int_o^\infty \frac{G^6(u)\cos ut\,du}{1-\lambda\, G(u)} + \sum_{n=1}^{5}\left(-\frac{\lambda^n}{\pi} I_n\right) ,$$

where

$$I_n = \int_o^\infty G^n(u)\cos ut\,du \quad .$$

The results of the evaluation of the I_n are as follows

$$I_1 = -\frac{\pi}{4}(1-t^2), \qquad 0<t<1$$

$$= 0, \quad t>1$$

$$I_2 = \frac{\pi}{6}\left(\frac{2}{5} - \frac{t^2}{2} + \frac{t^3}{4} - \frac{t^5}{80}\right) \qquad 0\leq t\leq 2$$

$$= 0, \quad t>2$$

$$I_3 = -\frac{\pi}{2^6}\left(\frac{141}{120} - \frac{5t^2}{6} + \frac{t^4}{4} - \frac{t^6}{30} + \frac{t^8}{2520}\right), \qquad 0\le t\le 1$$

$$= -\frac{\pi}{2^6}\left(\frac{81}{80} + \frac{27t}{35} - \frac{9t^2}{4} + \frac{6t^3}{5} - \frac{t^4}{8} - \frac{t^5}{15} + \frac{t^6}{60} - \frac{t^8}{5040}\right), \quad 1<t\le 3$$

$$= 0, \quad t>3$$

$$I_4 = \frac{\pi}{15}\left(\frac{167}{2079} - \frac{17t^2}{378} + \frac{t^4}{84} - \frac{7t^6}{2880} + \frac{t^7}{1792} + \frac{t^8}{32256} - \frac{t^9}{64512} + \frac{t^{11}}{14192640}\right),$$

$$0\le t\le 2$$

$$= \frac{\pi}{45}\left(\frac{64}{693} + \frac{16t}{35} - \frac{44t^2}{63} + \frac{t^3}{3} - \frac{t^4}{28} - \frac{t^5}{48} + \frac{7t^6}{960} - \frac{t^7}{1792} - \frac{t^8}{10752}\right.$$

$$\left. + \frac{t^9}{64512} - \frac{t^{11}}{14192640}\right), \quad 2<t\le 4$$

$$= 0; \quad t>4$$

$$I_5 = \frac{\pi}{2^{15}3^4}\left(-\frac{6891623}{3\cdot 7^2\cdot 11} + \frac{40949t^2}{3\cdot 7} - \frac{14697t^4}{35} + \frac{281t^6}{5} - 5t^8 + \frac{9t^{10}}{35}\right.$$

$$\left. - \frac{t^{12}}{385} + \frac{t^{14}}{175175}\right), \qquad 0\le t\le 1$$

$$= \frac{\pi}{2^{12}\cdot 3\cdot 7}\left(-\frac{97\cdot 35507}{2^2\cdot 3^4\cdot 7\cdot 11} - \frac{3727t}{3^2\cdot 5\cdot 11\cdot 13} + \frac{127\cdot 167t^2}{2^2 3^4} - \frac{23\cdot 199t^3}{3^4\cdot 11} - \frac{373t^4}{60}\right.$$

$$- \frac{562t^5}{81} + \frac{7\cdot 461t^6}{2^2 3^3 5} - \frac{10t^7}{7} + \frac{t^8}{108} + \frac{19t^9}{405} - \frac{t^{10}}{180} - \frac{t^{11}}{4455}$$

$$\left. + \frac{t^{12}}{2^2\cdot 3^4\cdot 5\cdot 11} - \frac{t^{14}}{2^2 3^4 5^2 7\cdot 11\cdot 13}\right) \qquad 1<t\le 3$$

$$I = \frac{\pi}{2^{16}3^{5}7}\left(\frac{7421845}{77} - \frac{95625000t}{143} + \frac{734375t^2}{1} - \frac{3275000t^3}{11}\right.$$

$$+ 16875t^4 + 26000t^5 - 8925t^6 + \frac{6480t^7}{7} + 93t^8 - \frac{152t^9}{5} + \frac{9}{5}t^{10}$$

$$\left. + \frac{8}{55}t^{11} - \frac{t^{12}}{55} + \frac{t^{14}}{25025}\right), \qquad 3<t\leq 5$$

$$= 0, \quad t>5$$

APPENDIX III

ARTIFICIAL FUNCTIONS

The complexity associated with certain particular programs of this calculation and the uncertainty as to just what might constitute "correct" answers for some of the more abstract functions [ψ_2, Eq. (3-75), for example] made desirable the existence of an alternate check specifically designed to examine the correctness of the programming effort. This was accomplished by the creation of artificial functions, by Babb.

These artifical functions are useful because they permit the analytic solution of the equation which, in the actual program and using 'real' functions, must be solved numerically. The results of the analytic solution may be compared to those of the numerical solution (where, of course, the artifical function has replaced the 'real' function). Added confidence is thus gained in the correctness of the programming effort by agreement of these two values. Obviously, this procedure does not supplant other analysis, but rather enlarges the library of precautionary procedures.

The ψ_2 Function

In reduced units $x = r/\sigma$, if g is defined as

$$g(x) = x, \quad 0 \leq x \leq 5$$

$$g(x) = 15-2x \qquad 5\leq x\leq 7$$

$$g(x) = 1, \qquad x\geq 7 \ ,$$

it becomes possible to solve the ψ_2 equation analytically:

$$\psi_2 = C_1 x^{\sqrt{7}-1} + C_2 x^{-\sqrt{7}-1} + \frac{x^2}{2} \ , \qquad 0\leq x\leq 5 \ ,$$

$$\psi_2 = \frac{A_1}{x^3} F_A + A_2 x^2 F_B + \frac{x^2}{2} \ , \qquad 5\leq x\leq 7 \ ,$$

where the F's are hypergeometric functions

$$F_A = {}_2F_1(-2+\sqrt{7}, \ -2-\sqrt{7}; \ 1, \ 1-\frac{2x}{15}) \ ,$$

$$F_B = {}_2F_1(3-\sqrt{7}, \ 3+\sqrt{7}; \ 6, \ \frac{2x}{15}) \ ,$$

and $$\psi_2 = \frac{P}{x^3} \ , \qquad x\geq 7 \ .$$

Here C_1, C_2, A_1, A_2, and P must be evaluated from boundary conditions, at 1, 5 and 7. Their values were obtained by numerical techniques (as opposed to the use of the algebraic solutions which involve transcendental hypergeometric functions) as

$$C_1 = - 0.419555 \ , \qquad C_2 = 0.0848981$$

$$A_1 = 476.984 \ , \qquad A_2 = - 0.0125097 \ ,$$

and $$P = 3266.72.$$

The ψ_0 Function

In addition to defining g for the analytic solution, one must have an expression for $\partial \ell n g/\partial \rho$ as well and it was taken quite

arbitrarily to be

$$\frac{\partial \ell ng}{\partial \rho} = \frac{1}{x}, \quad 0 \leq x \leq 7$$

$$= 0, \quad x \geq 7 \quad .$$

It can then be easily shown that:

$$\psi_o = -\frac{5}{8x^2} + \frac{x^2}{8} - \frac{3}{2}\ell nx + C_2, \qquad 0 \leq x \leq 5$$

$$\psi_o = \frac{1}{16}\left\{\frac{(15-2x)^2}{2} - 30(15-2x) + 225\ell n(15-2x)\right\} + \frac{3}{4}\ell n(15-2x)$$

$$+ A_1\left\{\frac{1}{x} + \frac{2}{15}\ell n\left(\frac{15-2x}{x}\right)\right\} + A_2; \qquad 5 \leq x \leq 7$$

$$\psi_o = \frac{Q}{x}, \quad x \geq 7$$

The various constants may be evaluated numerically or analytically. From matching boundary conditions and evaluating the logs, the results are

$$Q = 804$$

$$A_1 = -\frac{94}{3}$$

$$A_2 = 113.047$$

$$C_2 = 121.340$$

The Thermal Conductivity

The ψ functions are not required for the evaluation of the thermal conductivity and a different set of g's were chosen

$$g(x) = (1+\frac{\rho}{x^3})\exp(-\frac{T\ \phi(x)}{273.15})$$

where $\phi(x)$ was either the Lennard-Jones $(x^{-12}-x^{-6})$ or x^{-3}. This latter form of permitted full, simple analytic integrations of the integrals appearing in the expressions for $x_V(R>\sigma)$ and thus was very useful in the checking process.

APPENDIX IV

DATA TABLES for η, ϕ, χ

Table 4.1 Coefficient of Shear Viscosity.

Substance: Argon
Radial Distribution Function: Kirkwood
Remarks: ζ_s^{RG}

Intermolecular Potential: Lennard-Jones
Temperature: 180°K

λ	ρ Amagat	P_{CAL} bar	P_{OBS} bar	ζ_s^{RG} $\times 10^{13}$ kg/sec	η_k	η_v	$\eta_v(R>\sigma)$	η_{CAL}	η_{OBS}
					←		$\times 10^6$ kgm/m sec		→
1.00	74.11	39.70	40.68	1.144	1.426	.414	.1641	2.003	16.9
2.00	148.2	62.71	67.76	1.638	2.063	1.536	.9353	4.535	20.4
3.00	222.3	73.24	87.37	2.124	2.515	3.292	3.924	9.731	25.4
4.00	296.5	95.02	105.3	2.704	2.860	4.819	13.40	21.08	31.3
5.00	370.6	114.3	128.5	2.978	3.389	6.939	18.59	28.91	38.4
6.00	444.7	132.1	169.3	3.195	3.928	9.460	22.09	35.48	47.7
7.00	518.8	149.4	250.2	3.382	4.469	12.51	23.76	40.74	60.7
8.00	592.9	168.1	411.5	3.553	5.006	15.95	23.60	44.56	79.3
9.00	667.0	201.1	715.6	3.743	5.526	19.03	23.25	47.81	106
10.00	741.1	279.7	125.6	4.003	6.005	19.27	26.57	51.88	144
11.00	815.3	401.8	21.61	4.308	6.460	14.06	33.27	53.78	197

Table 4.2 Coefficient of Shear Viscosity.

Substance: Argon
Radial Distribution Function: Kirkwood
Remarks: ζ_s^{RG}

Intermolecular Potential: Lennard-Jones
Temperature: 273°K

λ	ρ Amagat	P_{CAL} bar	P_{OBS} bar	ζ_s^{RG} $\times 10^{13}$ kg/sec	η_k	η_v	$\eta_v(R>\sigma)$	η_{CAL}	η_{OBS}
					← $\times 10^6$ kgm/m sec →				
0.5	37.06	36.16	36.38	.7378	1.629	.1553	.0106	1.795	21.6
1.0	74.11	69.95	70.84	1.048	2.305	.5583	.0573	2.921	22.9
1.5	111.2	102.0	104.1	1.289	2.843	1.197	.1510	4.190	24.9
2.0	148.2	133.1	137.1	1.495	3.313	2.066	.2967	5.676	26.4
2.5	185.3	163.9	170.6	1.681	3.744	3.164	.4971	7.405	28.5
3.0	222.3	195.1	205.7	1.852	4.149	4.484	.7536	9.389	30.9
3.5	259.4	227.7	243.4	2.013	4.536	6.026	1.067	11.63	33.6
4.0	296.5	262.6	285.4	2.167	4.909	7.773	1.440	14.12	36.7
4.5	333.6	300.9	333.1	2.317	5.271	9.715	1.873	16.86	40.3
5.0	370.06	343.8	389.0	2.464	5.626	11.83	2.369	19.82	44.4
5.5	407.06	392.6	455.6	2.608	5.976	14.09	2.928	22.99	49.1
6.0	444.7	449.0	536.5	2.752	6.321	16.44	3.552	26.32	54.6
6.5	481.7	514.5	635.8	2.895	6.663	18.85	4.238	29.75	60.9
7.0	518.8	591.0	758.8	3.039	7.004	21.22	4.980	33.21	68.3
7.5	555.9	680.3	912.0	3.184	7.344	23.48	5.766	36.59	77.0
8.0	592.9	784.2	1102	3.330	7.686	25.50	6.579	39.76	87.4
8.5	630.0	904.4	1338	3.477	8.028	27.13	7.393	42.55	99.8
9.0	667.0	1042	1630	3.627	8.374	28.19	8.179	44.75	114
9.5	704.1	1199	1991	3.778	8.722	28.49	8.901	46.11	144

Table to be continued

Table4-2 continued

λ	ρ Amagat	P_{CAL} bar	P_{OBS} bar	ζ_s^{RG} $\times 10^{13}$ kg/sec	η_k	η_v	$\eta_v(R>\sigma)$ $\times 10^6$ kgm/m sec	η_{CAL}	η_{OBS}
10.0	741.1	1375	1991	3.930	9.073	27.78	9.526	46.37	165
10.5	778.2	1571	2433	4.085	9.426	25.75	10.03	45.20	189
11.0	815.3	1783	2971	4.241	9.781	22.07	10.40	42.25	216
11.5	852.3	2011	3622	4.399	10.14	16.35	10.69	37.18	247
12.0	889.4	2248	4406	4.560	10.49	8.069	11.03	29.58	282
12.5	926.4	2488	5341	4.722	10.83	-3.471	11.73	19.09	321
13.0	963.5	2720	6451	4.888	11.17	-19.32	13.53	5.381	366

Table 4-3. Coefficient of Shear Viscosity.

Substance: Argon
Radial Distribution Function: Kirkwood
Remarks: ζ_s^{RG}

Intermolecular Potential: Lennard-Jones
Temperature: 308°

λ	ρ Amagat	P_{CAL} bar	P_{OBS} bar	ζ_s^{RG} $\times 10^{13}$ kg/sec	η_k	η_v	$\eta_v(R>\sigma)$ $\times 10^6$ kgm/m sec	η_{CAL}	η_{OBS}
0.5	37.06	41.35	41.56	.7245	1.861	.1697	.0081	2.039	24.1
1.0	74.11	81.13	81.96	1.030	2.626	.6078	.0436	3.278	25.4
1.5	111.2	120.0	122.0	1.268	3.230	1.301	.1154	4.646	26.9
2.0	148.2	158.8	162.5	1.473	3.757	2.245	.2277	6.230	28.6
2.5	185.3	198.3	204.5	1.657	4.237	3.439	.3836	8.060	30.6
3.0	222.3	239.4	249.1	1.828	4.687	4.878	.5852	10.15	33.0
3.5	259.4	283.2	297.7	1.990	5.115	6.557	.8348	12.51	35.6
4.0	296.5	330.6	351.8	2.145	5.578	8.465	1.134	15.13	38.6
4.5	333.6	383.0	413.5	2.296	5.929	10.59	1.486	18.01	42.1
5.0	370.6	441.9	485.1	2.444	6.321	12.90	1.892	21.11	46.1
5.5	407.6	508.7	569.6	2.590	6.706	15.37	2.351	24.43	50.8
6.0	444.7	585.2	670.8	2.735	7.087	17.96	2.862	27.90	56.2
6.5	481.7	673.3	793.1	2.880	7.466	20.59	3.420	31.48	62.6
7.0	518.8	775.0	941.9	3.025	7.844	23.21	4.016	35.07	69.9
7.5	555.9	892.3	1124	3.170	8.222	25.70	4.634	38.56	78.5
8.0	592.9	1027	1347	3.317	8.601	27.95	5.255	41.81	88.4
8.5	630.0	1182	1619	3.465	8.982	29.80	5.850	44.64	99.9
9.0	667.0	1357	1951	3.614	9.367	31.07	6.387	46.83	111.
9.5	704.1	1555	2356	3.765	9.756	31.55	6.826	48.13	128.

Table . To be continued.

Table 4-3. Continued

λ	ρ	P_{CAL}	P_{OBS}	ζ_s^{RG}	η_k	η_v	$\eta_v(R>\sigma)$	η_{CAL}	η_{OBS}
	Amagat	bar	bar	$\times 10^{13}$ kg/sec	←	$\times 10^{6}$	kgm/m sec		→
10.0	741.1	1775	2848	3.917	10.15	30.98	7.128	48.25	146
10.5	778.2	2019	3433	4.071	10.54	29.07	7.256	46.86	165
11.0	815.3	2284	4137	4.226	10.94	25.47	7.185	43.59	188
11.5	852.3	2567	4973	4.384	11.34	19.77	6.919	38.03	213
12.0	889.4	2865	5959	4.543	11.74	11.48	6.520	29.74	242
12.5	926.4	3169	7115	4.704	12.13	-.011	6.169	18.24	274
13.0	963.5	3470	8466	4.868	12.52	-15.78	6.300	3.037	309
13.5	1001	3753	1004	5.036	12.89	-37.17	7.892	-16.39	349

Table 4-4 Coefficient of Shear Viscosity.

Substance: Argon
Radial Distribution Function: Kirkwood
Remarks: ζ_s^{RG}

Intermolecular Potential: Lennard-Jones
Temperature: 328°K

λ	ρ Amagat	P_{CAL} bar	P_{OBS} bar	ζ_s^{RG} $\times 10^{13}$ kg/sec	η_k	η_v	$\eta_v(R>\sigma)$ $\times 10^6$ kgm/m sec	η_{CAL}	η_{OBS}
0.5	37.06	44.31	44.52	.7183	1.993	1.778	.0070	2.178	25.4
1.0	74.11	87.48	88.27	1.021	2.808	.6352	.0380	3.481	26.7
1.5	111.2	130.2	132.1	1.258	3.449	1.358	.1006	4.808	
2.0	148.2	173.4	176.9	1.463	4.007	2.344	.1994	6.550	29.7
2.5	185.3	217.9	223.8	1.647	4.515	3.590	.3370	8.442	31.7
3.0	222.3	264.6	273.9	1.818	4.989	5.093	.5161	10.60	34.0
3.5	259.4	314.6	328.6	1.980	5.441	6.848	.7389	13.03	36.6
4.0	296.5	369.2	389.6	2.135	5.875	8.844	1.008	15.73	39.7
4.5	333.6	429.6	459.1	2.287	6.297	11.06	1.324	18.69	43.2
5.0	370.6	497.5	539.6	2.435	6.710	13.49	1.690	21.89	47.3
5.5	407.6	574.4	634.3	2.581	7.116	16.08	2.104	25.30	52.1
6.0	444.7	662.3	746.8	2.727	7.517	18.79	2.565	28.87	57.6
6.5	481.7	763.1	881.9	2.872	7.916	21.57	3.065	32.55	64.1
7.0	518.8	878.8	1045	3.017	8.314	24.32	3.594	36.23	71.6
7.5	555.9	1012	1247	3.163	8.713	26.96	4.138	39.81	80.2
8.0	592.9	1164	1483	3.310	9.113	29.35	4.674	43.14	90.2
8.5	630.0	1338	1776	3.458	9.516	31.35	5.174	46.04	102
9.0	667.0	1534	2131	3.607	9.922	32.76	5.605	48.29	115
9.5	704.1	1754	2558	3.757	10.33	33.37	5.927	49.63	130
10.0	741.1	2000	3075	3.909	10.75	32.93	6.099	49.78	146
10.5	778.2	2270	3687	4.062	11.16	31.14	6.079	48.39	166
11.0	815.3	2564	4420	4.217	11.59	27.65	5.836	45.07	187
11.5	852.3	2879	5288	4.374	12.01	22.05	5.359	39.41	212

Table 4-5. Coefficient of Shear Viscosity.

Substance: Argon
Radial Distribution Function: Kirkwood
Remarks: ζ_s^{RG}

Intermolecular Potential: Lennard-Jones
Temperature: 373°K

λ	ρ	P_{CAL}	P_{OBS}	ζ_s^{RG}	η_k	η_v	$\eta_v(R>\sigma)$	η_{CAL}	η_{OBS}
	Amagat	bar	bar	$\times 10^{13}$ kg/sec	←		$\times 10^6$ kgm/m sec		→
0.5	37.06	50.96	51.15	.7071	2.287	.1954	.0053	2.489	27.9
1.0	74.11	101.7	102.4	1.007	3.213	.6947	.0288	3.936	29.2
1.5	111.2	153.1	154.8	1.241	3.936	1.483	.0769	5.496	30.5
2.0	148.2	206.1	209.2	1.444	4.561	2.557	.1533	7.272	32.1
2.5	185.3	261.6	266.8	1.628	5.129	3.917	.2610	9.307	34.0
3.0	222.3	320.8	329.0	1.799	5.658	5.559	.4028	11.62	36.2
3.5	259.4	384.9	397.4	1.961	6.160	7.477	.5809	14.22	38.9
4.0	296.5	455.2	473.8	2.117	6.643	9.662	.7975	17.10	42.0
4.5	333.6	533.4	560.7	2.269	7.111	12.10	1.054	20.26	45.6
5.0	370.7	621.2	660.8	2.418	7.569	14.76	1.351	23.68	49.9
5.5	407.1	720.6	777.5	2.565	8.019	17.61	1.686	27.32	54.9
6.0	444.7	833.5	915.0	2.711	8.465	20.61	2.057	31.13	60.7
6.5	481.7	862.2	1078	2.856	8.908	23.69	2.455	35.05	67.4
7.0	518.8	1109	1273	3.002	9.351	26.76	2.869	38.98	75.1
7.5	555.9	1276	1506	3.148	9.795	29.74	3.283	42.82	83.9
8.0	592.9	1466	1785	3.294	10.24	32.48	3.676	46.40	93.9
8.5	630.0	1681	2121	3.441	10.69	34.84	4.019	49.55	105
9.0	667.0	1923	2525	3.590	11.14	36.63	4.278	52.05	118
9.5	704.1	2193	2992	3.739	11.60	37.62	4.415	53.64	132
10.0	741.1	2493	3563	3.889	12.06	37.57	4.386	54.02	148

Table 4-6 Coefficient of Shear Viscosity.

Substance: Argon
Radial Distribution Function: Kirkwood
Remarks: ζ_s^{RG}

Intermolecular Potential: Lennard-Jones
Temperature: 500°K

λ	ρ	P_{CAL}	P_{OBS}	ζ_s^{RG}	η_k	η_v	$\eta_v(R>\sigma)$	η_{CAL}	η_{OBS}
	Amagat	bar	bar	$\times 10^{13}$kg/sec	←		$\times 10^{6}$ kgm/m sec		→
0.5	37.06	69.64	70.14	.6871	3.108	.2424	.0028	3.353	34.3
1.0	74.11	141.6	142.1	.9800	4.330	.8509	.0157	5.196	35.5
1.5	111.2	212.1	218.2	1.211	5.272	1.807	.0427	7.222	36.7
2.0	148.2	297.2	299.1	1.412	6.080	3.109	.0868	9.275	38.2
2.5	185.3	383.3	386.6	1.594	6.806	4.758	.1504	11.71	39.9
3.0	222.3	476.9	482.0	1.764	7.480	6.753	.2359	14.47	42.2
3.5	259.4	579.6	587.4	1.926	8.117	9.091	.3451	17.55	44.9
4.0	296.5	693.4	704.6	2.082	8.727	11.76	.4794	20.97	48.3
4.5	333.6	820.2	836.2	2.234	9.318	14.75	.6391	24.71	52.3
5.0	370.6	962.4	984.8	2.383	9.895	18.04	.8235	28.76	57.2
5.5	407.6	1122	1154	2.530	10.46	21.59	1.030	33.08	62.7
6.0	444.7	1303	1379	2.675	11.03	25.35	1.254	37.63	69.1
6.5	481.7	1506	1615	2.820	11.50	29.27	1.487	42.35	76.3
7.0	518.8	1736	1893	2.964	12.14	33.26	1.720	47.13	84.4
7.5	555.9	1995	2206	3.108	12.70	37.23	1.937	51.87	93.3
8.0	592.9	2285	2580	3.252	13.27	41.05	2.119	56.44	103
8.5	630.0	2610	3023	3.396	13.84	44.37	2.232	60.44	113
9.0	667.0	2973	3544	3.541	14.41	47.62	2.279	64.31	125
9.5	704.1	3374	4154	3.686	14.99	49.99	2.195	67.17	136
10.0	741.1	3817	4866	3.832	15.57	51.42	1.953	68.94	149
10.5	778.2	4302	5691	3.980	16.16	51.64	1.509	69.31	162
11.0	815.3	4828	6645	4.128	16.76	50.29	.8177	67.86	175
11.5	952.3	5394	7745	4.278	17.36	46.97	-.1693	64.16	189
12.0	889.4	5996	9009	4.429	17.96	41.21	-1.496	57.68	202
12.5	926.4	6630	10460	4.583	18.57	32.41	-3.197	47.78	216

Table 4-7. Coefficient of Shear Viscosity.

Substance: Argon
Radial Distribution Function: Kirkwood
Remarks: ζ_s^{RG}

Intermolecular Potential: Lennard-Jones
Temperature: 600°K

λ	ρ	P_{CAL}	P_{OBS}	ζ_s^{RG}	η_k	η_v	$\eta_v(R>\sigma)$	η_{CAL}	η_{OBS}
	Amagat	bar	bar	$\times 10^{13}$ kg/sec	←		$\times 10^6$ kgm/m sec		→
0.5	37.06	84.29	83.89	.6775	3.742	.2772	.0019	4.021	38.9
1.0	74.11	172.9	172.7	.9673	5.188	.9647	.0109	6.164	40.0
1.5	111.2	267.0	267.0	1.196	6.295	2.040	.0301	8.365	41.1
2.0	148.2	368.1	368.8	1.396	7.237	3.504	.0618	10.80	42.5
2.5	185.3	477.7	479.2	1.577	8.081	5.358	.1083	13.55	44.3
3.0	222.3	597.7	599.8	1.747	8.861	7.603	.1714	16.64	46.5
3.5	259.4	730.0	731.6	1.908	9.597	10.27	.2525	20.09	49.5
4.0	296.5	876.8	876.2	2.063	10.30	13.25	.3526	23.91	53.1
4.5	333.6	1041	1054	2.215	10.98	16.64	.4718	28.09	57.4
5.0	370.6	1224	1237	2.363	11.65	20.38	.6087	32.63	62.6
5.5	407.6	1429	1474	2.509	12.30	24.43	.7610	37.49	68.5
6.0	444.7	1660	1755	2.653	12.95	28.76	.9240	42.63	75.1
6.5	481.7	1919	2026	2.796	13.59	33.30	1.091	47.98	82.4
7.0	518.8	2210	2348	2.938	14.23	37.88	1.248	53.36	90.2
7.5	555.9	2537	2734	3.080	14.88	42.59	1.380	58.85	98.6
8.0	592.9	2901	3176	3.222	15.52	47.27	1.498	64.30	107
8.5	630.0	3307	3694	3.363	16.18	51.76	1.553	69.49	126
9.0	667.0	3758	4298	3.505	16.83	55.84	1.527	74.20	141
9.5	704.1	4256	5000	3.647	17.50	59.28	1.390	78.16	158

Table to be continued.

Table 4-7 continued.

λ	ρ	P_{CAL}	P_{OBS}	ζ_s^{RG}	η_k	η_v	$\eta_v(R>\sigma)$	η_{CAL}	η_{OBS}
	Amagat	bar	bar	$\times 10^{13}$ kg/sec	←		$\times 10^{6}$ kgm/m sec		→
10.0	741.1	4803	5810	3.790	18.17	62.24	1.131	81.54	176
10.5	778.2	5401	6739	3.933	18.84	63.92	.6838	83.44	197
11.0	815.3	6050	7807	4.077	19.52	64.21	.0183	83.75	219
11.5	852.3	6749	9026	4.23	20.21	62.73	-.9110	82.03	244
12.0	889.4	7496	10420	4.370	20.91	59.02	-2.152	77.78	271
12.5	926.4	8285	12010	4.519	21.61	52.53	-3.755	70.38	300
13.0	963.5	9110	13820	4.671	22.30	42.54	-5.760	59.09	332
13.5	1001	9958	15890	4.827	23.00	28.13	-8.191	42.94	367
14.0	1037.6	10810	18240	4.986	23.70	8.03	-11.02	20.71	404

Table 4-8 Coefficient of Shear Viscosity.

Substance: Nitrogen
Intermolecular Potential: Lennard-Jones
Radial Distribution Function: Kirkwood
Temperature: 180°K
Remarks: ζ_s^{RG}

λ	ρ	P_{CAL}	P_{OBS}	ζ_s^{RG}	η_k	η_v	$\eta_v(R>\sigma)$	η_{CAL}	η_{OBS}
	Amagat	bar	bar	$\times 10^{13}$ kg/sec	←		$\times 10^{6}$ kgm/m sec		→
1.0	56.18	35.16	33.60	.6392	1.322	.3173	.0303	1.669	19.0
2.0	112.4	67.33	61.38	.9128	1.898	1.173	.1569	3.228	22.9
3.0	168.5	99.31	86.42	1.131	2.375	2.548	.3994	5.322	27.9
4.0	224.7	134.4	112.2	1.325	2.808	4.416	.7653	7.990	33.8
5.0	280.9	176.8	143.3	1.507	3.217	6.722	1.262	11.20	40.6
6.0	337.1	231.8	186.5	1.683	3.612	9.347	1.897	14.86	49.3
7.0	393.3	305.5	253.1	1.850	4.002	12.07	2.662	18.73	60.7
8.0	449.4	405.3	360.8	2.038	4.391	14.50	3.511	22.40	76.4
9.0	505.6	538.0	535.4	2.220	4.784	16.45	4.347	25.18	98.4
10.0	561.8	708.5	813.5	2.406	5.183	15.84	5.023	26.04	129
11.0	618.0	917.0	1247	2.596	5.587	12.66	5.407	23.66	171
12.0	674.2	1155	1900	2.791	5.992	4.827	5.587	16.41	228
13.0	730.3	1397	2848	2.991	6.385	-10.45	6.627	2.561	303

Table 4-9. Coefficient of Shear Viscosity.

Substance: Nitrogen
Intermolecular Potential: Lennard-Jones
Radial Distribution Function: Kirkwood
Temperature: 273°K
Remarks: ζ_s^{RG}

λ	ρ Amagat	P_{CAL} bar	P_{OBS} bar	ζ_s^{RG} $\times 10^{13}$ kg/sec	η_k	η_v	$\eta_v(R>\sigma)$	η_{CAL}	η_{OBS}
					← $\times 10^6$ kgm/m sec →				
0.5	28.09	28.53	28.16	.4272	1.463	.1200	.0022	1.586	17.5
1.0	56.18	57.48	55.98	.6087	2.048	.4241	.0123	2.484	18.4
1.5	84.27	87.31	83.90	.7515	2.502	.9034	.0330	3.438	19.6
2.0	112.4	118.5	112.4	.8751	2.893	1.557	.0664	4.516	20.9
2.5	140.4	151.7	142.0	.9872	3.247	2.384	.1139	5.744	22.4
3.0	168.5	187.3	173.3	1.092	3.576	3.383	.1771	7.136	24.0
3.5	196.6	226.3	206.9	1.191	3.887	4.553	.2572	8.697	25.8
4.0	224.7	269.2	243.9	1.287	4.186	5.887	.3550	10.43	27.9
4.5	252.8	317.1	285.0	1.380	4.476	7.377	.4713	12.32	30.2
5.0	280.9	370.8	331.7	1.471	4.759	9.008	.6058	14.37	32.7
5.5	309.0	431.3	385.3	1.561	5.038	10.76	.7573	16.55	35.7
6.0	337.1	500.0	447.6	1.651	5.314	12.61	.9234	18.85	39.1
6.5	365.2	577.7	520.7	1.740	5.589	14.52	1.100	21.21	42.9
7.0	393.3	666.0	607.1	1.829	5.863	16.45	1.280	23.59	47.4
7.5	421.3	765.9	709.6	1.918	6.138	18.33	1.454	25.92	52.5
8.0	449.4	878.9	831.9	2.007	6.414	20.10	1.612	28.13	58.5
8.5	477.5	1006	977.7	2.097	6.692	21.67	1.739	30.10	65.4
9.0	505.6	1148	1152	2.187	6.973	22.94	1.815	31.73	73.3
9.5	533.7	1307	1360	2.277	7.257	23.78	1.822	32.86	82.5

Table to be continued.

Table 4-9 Continued.

λ	ρ Amagat	P_{CAL} bar	P_{OBS} bar	ζ_s^{RG} $\times 10^{13}$kg/sec	η_k	η_v	$\eta_v(R>\sigma)$ $\times 10^6$ kgm/m sec	η_{CAL}	η_{OBS}
10.0	561.8	1482	1608	2.368	7.544	24.06	1.734	33.34	93.0
10.5	589.9	1674	1903	2.460	7.834	23.61	1.528	32.97	105
11.0	618.0	1882	2252	2.553	8.126	22.23	1.176	31.53	119
11.5	646.1	2106	2665	2.646	8.421	19.69	.6559	28.76	135
12.0	674.2	2343	3148	2.741	8.717	15.71	-.0485	24.38	152
12.5	702.2	2592	3710	2.838	9.013	9.961	-.9404	18.03	172
13.0	730.3	2845	4361	2.935	9.307	1.981	-1.981	9.308	195
13.5	758.4	3098	5108	3.036	9.598	-8.842	-3.052	-2.296	220

Table 4-10 Coefficient of Shear Viscosity.

Substance: Nitrogen
Radial Distribution Function: Kirkwood
Remarks: ζ_s^{RG}

Intermolecular Potential: Lennard-Jones
Temperature: 308°K

λ	ρ Amagat	P_{CAL} bar	P_{OBS} bar	ζ_s^{RG} $\times 10^{13}$ kg/sec	η_k	η_v	$\eta_v(R>\sigma)$	η_{CAL}	η_{OBS}
					← $\times 10^6$ kgm/m sec →				
0.5	28.09	32.57	32.06	.4202	1.667	.1314	.0016	1.800	17.5
1.0	56.18	66.38	64.29	.5994	2.324	.4621	.0090	2.795	18.3
1.5	84.27	102.0	97.18	.7408	2.831	.9822	.0245	3.838	19.3
2.0	112.4	140.0	131.2	.8636	3.266	1.691	.0498	5.006	20.4
2.5	140.4	181.0	167.1	.9752	3.657	2.589	.0864	6.332	21.7
3.0	168.5	225.8	205.3	1.079	4.020	3.674	.1356	7.830	23.2
3.5	196.6	275.2	246.8	1.179	4.364	4.946	.1985	9.508	24.8
4.0	224.7	330.2	292.4	1.274	4.693	6.399	.2760	11.37	26.6
4.5	252.8	391.7	343.4	1.367	5.012	8.023	.3681	13.40	28.7
5.0	280.9	461.0	401.0	1.458	5.324	9.806	.4744	15.60	31.1
5.5	309.0	539.1	466.9	1.548	5.631	11.73	.5933	17.95	33.9
6.0	337.1	627.4	542.9	1.637	5.936	13.76	.7220	20.42	37.1
6.5	365.2	727.3	631.3	1.726	6.239	15.87	.8562	22.97	40.7
7.0	393.3	840.1	734.7	1.814	6.541	18.01	.9892	25.54	44.9
7.5	421.3	967.5	856.2	1.902	6.845	20.13	1.113	28.09	49.6
8.0	449.4	1111	999.4	1.990	7.150	22.06	1.210	30.42	55.1
8.5	477.5	1271	1168	2.078	7.458	24.01	1.283	32.75	61.4
9.0	505.6	1450	1368	2.167	7.768	25.46	1.292	34.52	68.6
9.5	533.7	1648	1603	2.255	8.082	26.77	1.245	36.09	76.8

Table to be continued

Table 4-10 Continued

λ	ρ	P_{CAL}	P_{OBS}	ζ_s^{RG}	η_k	η_v	$\eta_v(R>\sigma)$	η_{CAL}	η_{OBS}
	Amagat	bar	bar	$\times 10^{13}$ kg/sec	←		$\times 10^{6}$ kgm/m sec		→
10.0	561.8	1867	1882	2.345	8.399	27.42	1.098	36.91	86.1
10.5	589.9	2107	2209	2.435	8.719	27.37	.8322	36.93	96.7
11.0	618.0	2368	2594	2.525	9,043	26.45	.4204	35.91	109
11.5	646.1	2648	3044	2.617	9.369	24.42	-.1656	33.62	122
12.0	674.2	2947	3567	2.709	9.698	21.01	-.9528	29.75	137
12.5	702.2	3055	4172	2.816	9.993	15.74	-.1624	24.11	154
13.0	730.3	3356	4866	2.912	10.32	9.407	-2.774	15.95	173
13.5	758.4	3661	5658	3.011	10.64	-1.657	-4.077	4.909	194

Table 4-L1 Coefficient of Shear Viscosity.

Substance: Nitrogen
Radial Distribution Function: Kirkwood
Remarks: ζ_s^{RG}

Intermolecular Potential: Lennard-Jones
Temperature: 328°K

λ	ρ	P_{CAL}	P_{OBS}	ζ_s^{RG}	η_k	η_v	$\eta_v(R>\sigma)$	η_{CAL}	η_{OBS}
	Amagat	bar	bar	$\times 10^{13}$ kg/sec	←		$\times 10^6$ kgm/m sec		→
0.5	28.09	34.51	34.28	.4224	1.761	.1369	.0016	1.900	17.4
1.0	56.18	69.98	69.03	.6023	2.454	.4803	.0090	2.944	18.2
1.5	84.27	106.9	104.7	.7442	2.989	1.019	.0244	4.032	19.2
2.0	112.4	145.8	142.0	.8675	3.447	1.753	.0484	5.250	20.2
2.5	140.4	187.4	181.3	.9781	3.859	2.683	.0855	6.627	26.4
3.0	168.5	232.4	223.5	1.084	4.241	3.808	.1337	8.182	22.8
3.5	196.6	281.4	269.4	1.183	4.602	5.126	.1953	9.923	24.3
4.0	224.7	335.5	320.0	1.278	4.947	6.634	.2709	11.85	26.1
4.5	252.8	395.5	376.4	1.371	5.282	8.322	.3607	13.97	28.1
5.0	280.9	462.5	440.2	1.463	5.609	10.18	.4645	16.25	30.4
5.5	309.0	537.8	512.9	1.553	5.931	12.19	.5810	18.70	33.1
6.0	337.1	662.4	596.6	1.642	6.249	14.32	.7076	21.27	36.1
6.5	365.2	717.8	693.6	1.731	6.565	16.54	.8403	23.94	39.7
7.0	393.3	825.3	806.5	1.819	6.880	18.81	.9734	26.66	43.7
7.5	421.3	946.2	938.5	1.907	7.197	21.07	1.099	29.36	48.3
8.0	449.4	1082	1093	1.996	7.515	23.25	1.206	31.97	53.6
8.5	477.5	1234	1274	2.085	7.835	25.27	1.283	34.39	59.6
9.0	505.6	1403	1488	2.174	8.158	27.03	1.314	36.50	66.5
9.5	533.7	1591	1739	2.263	8.484	28.42	1.280	38.18	74.3

Table to be continued

Table 4-11 Continued

λ	ρ	P_{CAL}	P_{OBS}	ζ_s^{RG}	η_k	η_v	$\eta_v(R>\sigma)$	η_{CAL}	η_{OBS}
	Amagat	bar	bar	$\times 10^{13}$ kg/sec	←		$\times 10^6$ kgm/m sec		→
10.0	561.8	1797	2034	2.353	8.813	29.29	1.161	39.26	83.0
10.5	589.9	2024	2379	2.444	9.146	29.47	.9340	39.55	92.9
11.0	618.0	2269	2783	2.535	9.482	28.79	.5757	38.85	104
11.5	646.1	2533	3254	2.627	9.820	27.01	.0594	36.88	116
12.0	674.2	2813	3798	2.721	10.16	23.86	-.6359	33.38	130
12.5	702.2	3313	4425	2.803	10.54	19.17	-1.844	27.86	146
13.0	730.3	3641	5143	2.899	10.88	12.26	-3.010	20.13	163
13.5	758.4	3974	5960	2.997	11.22	2.682	-4.368	9.547	182
14.0	786.5	4304	6885	3.087	11.56	-10.37	-5.817	-4.626	202

Table 4-12 Coefficient of Shear Viscosity.

Substance: Nitrogen
Radial Distribution Function: Kirkwood
Remarks: ζ_s^{RG}

Intermolecular Potential: Lennard Jones
Temperature: 373°K

λ	ρ	P_{CAL}	P_{OBS}	ζ_s^{RG}	η_k	η_v	$\eta_v(R>\sigma)$	η_{CAL}	η_{OBS}
	Amagat	bar	bar	$\times 10^{13}$ kg/sec	←		$\times 10^{6}$ kgm/m sec		→
0.5	28.09	39.65	39.27	.4160	2.018	.1509	.0012	2.170	17.4
1.0	56.18	81.20	79.65	.5938	2.800	.5260	.0065	3.333	18.1
1.5	84.27	125.3	121.7	.7344	3.400	1.114	.0179	4.531	18.9
2.0	112.4	172.5	165.9	.8566	3.911	1.913	.0368	5.860	19.8
2.5	140.4	223.6	213.2	.9679	4.369	2.925	.0643	7.359	20.8
3.0	168.5	279.5	264.2	1.072	4.793	4.152	.1016	9.045	22.0
3.5	196.6	341.2	320.0	1.171	5.192	5.590	.1495	10.93	23.4
4.0	224.7	409.5	381.4	1.266	5.575	7.237	.2086	13.02	25.0
4.5	252.8	485.7	450.1	1.359	5.945	9.084	.2790	15.31	26.9
5.0	280.9	571.0	527.5	1.450	6.307	11.12	.3599	17.79	29.1
5.5	309.0	666.8	615.4	1.539	6.663	13.33	.4500	20.44	31.6
6.0	337.1	774.4	715.9	1.627	7.015	15.68	.5467	23.24	34.5
6.5	365.2	895.4	831.6	1.715	7.364	18.15	.6460	26.16	37.8
7.0	393.3	1031	965.1	1.803	7.714	20.69	.7425	29.15	41.7
7.5	421.3	1184	1120	1.890	8.064	23.19	.8268	32.08	46.0
8.0	449.4	1354	1300	1.977	8.416	25.69	.8929	35.00	50.9
8.5	477.5	1545	1509	2.064	8.771	28.08	.9285	37.78	56.4
9.0	505.6	1756	1753	2.151	9.128	30.22	.9184	40.28	62.5
9.5	533.7	1989	2036	2.239	9.489	32.01	.8446	42.34	69.4

Table to be continued.

Table 4-12 Continued

λ	ρ Amagat	P_{CAL} bar	P_{OBS} bar	ζ_s^{RG} $\times 10^{13}$kg/sec	η_k	η_v	$\eta_v(R>\sigma)$ $\times 10^6$ kgm/m sec	η_{CAL}	η_{OBS}
10.0	561.8	2246	2366	2.326	9.854	33.54	.7024	44.10	77.2
10.5	589.9	2527	2750	2.415	10.22	34.31	.4505	44.98	85.7
11.0	618.0	2831	3194	2.503	10.59	34.28	.0732	44.95	95.1
11.5	646.1	3159	3708	2.593	10.97	33.24	-.4554	43.76	106
12.0	674.2	3509	4298	2.683	11.35	30.93	-1.162	41.12	117
12.5	702.2	3879	4974	2.776	11.73	27.03	-2.074	36.69	130
13.0	730.3	4265	5743	2.869	12.10	21.15	-3.212	30.04	143
13.5	758.4	4661	6614	2.965	12.49	12.74	-4.584	20.64	158
14.0	786.5	5059	7594	3.064	12.86	10.99	-6.158	7.804	174

Table 4-13 Coefficient of Shear Viscosity.

Substance: Nitrogen
Radial Distribution Function: Kirkwood
Remarks: ζ_s^{RG}

Intermolecular Potential: Lennard Jones
Temperature: 500°K

λ	ρ	P_{CAL}	P_{OBS}	ζ_s^{RG}	η_k	η_v	$\eta_v(R>\sigma)$	η_{CAL}	η_{OBS}
	Amagat	bar	bar	$\times 10^{-3}$ kg/sec	←		$\times 10^{6}$ kgm/m sec		→
0.5	28.09	53.71	53.31	.4084	2.705	.1873	.0006	2.893	17.3
1.0	56.18	111.1	109.4	.5836	3.725	.6435	.0037	4.372	17.9
1.5	84.27	172.9	169.0	.7225	4.496	1.353	.0103	5.859	18.4
2.0	112.4	240.0	232.9	.8434	5.148	2.315	.0216	7.484	19.1
2.5	140.4	313.4	301.9	.9536	5.728	3.532	.0384	9.299	19.8
3.0	168.5	394.2	377.2	1.057	6.263	5.008	.0614	11.33	20.7
3.5	196.6	483.5	460.0	1.154	6.764	6.741	.0913	13.60	21.9
4.0	224.7	582.7	551.6	1.249	7.244	8.732	.1282	16.10	23.3
4.5	252.8	693.1	653.7	1.340	7.707	10.98	.1721	18.85	24.9
5.0	280.9	816.4	768.0	1.430	8.159	13.46	.2222	21.84	26.8
5.5	309.0	954.2	896.9	1.518	8.602	16.18	.2774	25.06	29.2
6.0	337.1	1108	1043	1.605	9.041	19.07	.3348	28.45	31.8
6.5	365.2	1280	1208	1.690	9.477	22.17	.3926	32.04	34.8
7.0	393.3	1472	1396	1.776	9.911	25.43	.4462	35.79	38.1
7.5	421.3	1686	1611	1.860	10.35	28.83	.4914	39.67	41.7
8.0	449.4	1924	1857	1.944	10.78	32.26	.5197	43.56	45.8
8.5	477.5	2187	2138	2.028	11.22	35.67	.5234	47.41	50.1
9.0	505.6	2478	2459	2.112	11.66	38.96	.4922	51.11	54.8
9.5	533.7	2798	2827	2.196	12.11	42.11	.4169	54.64	59.8

Table to be continued.

Table 4-13. Continued

λ	ρ Amagat	P_{CAL} bar	P_{OBS} bar	ζ_s^{RG} $\times 10^{13}$ kg/sec	η_k ←	η_v → $\times 10^6$	$\eta_v(R>\sigma)$ kgm/m sec	η_{CAL}	η_{OBS}
10.0	561.8	3149	3248	2.280	12.56	44.81	.2762	57.64	65.1
10.5	589.9	3532	3729	2.364	13.01	46.95	.0544	60.02	70.6
11.0	618.0	3946	4278	2.449	13.47	48.87	-.2452	62.10	76.4
11.5	646.1	4394	4902	2.534	13.93	49.86	-.6650	63.12	82.4
12.0	674.2	4872	5609	2.619	14.40	49.86	-1.221	63.04	88.5
12.5	702.2	5382	6409	2.706	14.87	48.58	-1.940	61.51	94.7
13.0	730.3	5919	7310	2.794	15.34	45.70	-2.850	58.19	101
13.5	758.4	6479	8318	2.884	15.81	40.78	-3.980	52.61	107
14.0	786.5	7055	9443	2.977	16.28	33.24	-5.358	44.16	113

Table 4-14 Coefficient of Shear Viscosity.

Substance: Nitrogen
Intermolecular Potential: Lennard Jones
Radial Distribution Function: Kirkwood
Temperature: 600°K
Remarks: ζ_s^{RG}

λ	ρ	P_{CAL}	P_{OBS}	ζ_s^{RG}	η_k	η_v	$\eta_v(R>\sigma)$	η_{CAL}	η_{OBS}
	Amagat	bar	bar	$\times 10^{13}$ kg/sec	←		$\times 10^6$ kgm/m sec		→
0.5	28.09	64.75	64.33	.4047	3.234	.2144	.0004	3.449	17.2
1.0	56.18	134.5	132.7	.5786	4.433	.7294	.0026	5.165	17.7
1.5	84.27	210.1	206.0	.7164	5.332	1.526	.0074	6.865	18.2
2.0	112.4	292.6	285.0	.8366	6.087	2.603	.0157	8.706	18.7
2.5	140.4	383.2	370.9	.9459	6.758	3.966	.0280	10.75	19.3
3.0	168.5	483.0	464.9	1.048	7.373	5.616	.0452	13.03	20.1
3.5	196.6	593.5	568.4	1.145	7.950	7.558	.0675	15.58	21.2
4.0	224.7	716.1	682.9	1.239	8.500	9.789	.0950	18.38	22.5
4.5	252.8	852.5	810.4	1.329	9.031	12.31	.1277	21.47	24.1
5.0	280.9	1004	952.8	1.418	9.548	15.08	.1646	24.80	25.9
5.5	309.0	1174	1112	1.505	10.06	18.15	.2051	28.41	28.1
6.0	337.1	1362	1292	1.590	10.56	21.46	.2471	32.26	30.5
6.5	365.2	1572	1495	1.674	11.05	25.03	.2888	36.37	33.2
7.0	393.3	1806	1724	1.758	11.55	28.85	.3274	40.72	36.1
7.5	421.3	2065	1983	1.841	12.04	32.79	.3570	45.19	39.3
8.0	449.4	2353	2277	1.923	12.54	36.85	.3729	49.77	42.7
8.5	477.5	2670	2610	2.005	13.04	40.83	.3651	54.24	46.1
9.0	505.6	3019	2988	2.086	13.54	44.99	.3344	58.87	49.6
9.5	533.7	3403	3417	2.168	14.05	49.00	.2654	63.31	53.2

Table to be continued.

Table 4-14 Continued

λ	ρ Amagat	P_{CAL} bar	P_{OBS} bar	ζ_s^{RG} $\times 10^{13}$kg/sec	η_k ← $\times 10^6$	η_v	$\eta_v(R>\sigma)$ kgm/m sec	η_{CAL} →	η_{OBS} →
10.0	561.8	3822	3904	2.249	14.56	52.88	.1508	67.59	56.7
10.5	589.9	4279	4455	2.330	15.07	56.26	-.0298	71.30	60.1
11.0	618.0	4773	5078	2.412	15.59	59.05	-.2905	74.35	63.2
11.5	646.1	5307	5781	2.494	16.11	61.68	-.6252	77.17	65.0
12.0	674.2	5879	6574	2.576	16.64	63.34	-1.075	78.91	72.2
12.5	702.2	6490	7463	2.660	17.17	63.98	-1.655	79.49	81.4
13.0	730.3	7135	8458	2.744	17.70	63.29	-2.390	78.60	90
13.5	758.4	7813	9567	2.830	18.24	60.92	-3.308	75.84	100
14.0	786.5	8517	10800	2.918	18.77	56.37	-4.440	70.70	110

Table 4-15 Coefficient of Shear Viscosity.

Substance: Argon
Radial Distribution Function: Percus-Yevick
Remarks: ζ_s^{RG}

Intermolecular Potential: Lennard-Jones
Temperature: 273°

ρ^*	ρ Amagat	P_{CAL} bar	P_{OBS} bar	ζ_s^{RG} $\times 10^{13}$kg/sec	η_k	η_v	$\eta_v(R>\sigma)$	η_{CAL}	η_{OBS}
					←		$\times 10^6$ kgm/m sec		→
0.15	139.7	126.5	142.4	1.444	3.211	1.850	.2479	5.309	26.2
0.30	279.4	258.3	293.9	2.113	4.718	6.960	1.112	12.79	35.3
0.45	419.1	485.1	490.7	2.719	6.016	14.45	2.332	22.80	50.1
0.60	558.8	982.9	853.2	3.355	7.285	19.45	1.990	28.73	76.4
0.75	698.5	2058	1674	4.041	8.674	3.764	-8.658	3.780	124
0.90	838.2	4188	4075	4.770	10.31	-87.38	-57.69	-134.8	205
1.05	977.9	8128	8340	5.510	12.28	-403.7	-221.5	-612.9	338
1.20	1118	14740	16000	6.210	14.66	-1372	-725.2	-2082	543

Table 4-16 Coefficient of Shear Viscosity.

Substance: Argon
Radial Distribution Function: Percus-Yevick
Remarks: ζ_s^{RG}

Intermolecular Potential: Lennard-Jones
Temperature: 328°K

ρ^*	ρ Amagat	P_{CAL} bar	P_{OBS} bar	ζ_s^{RG} $\times 10^{13}$kg/sec	η_k	η_v	$\eta_v(R>\sigma)$	η_{CAL}	η_{OBS}
					←		$\times 10^6$ kgm/m sec		→
0.15	139.7	164.0	166.5	1.418	3.883	2.099	.1680	6.150	29.3
0.30	279.4	355.6	360.6	2.082	5.646	7.931	.7977	14.38	38.2
0.45	419.1	676.0	667.0	2.689	7.158	16.66	1.729	25.55	53.7
0.60	558.8	1315	1261	3.314	8.640	23.63	1.393	33.66	80.9
0.75	698.5	2593	2487	3.977	10.25	12.26	-6.855	15.65	127
0.90	838.2	4999	4945	4.670	12.11	-65.05	-43.09	-96.04	202
1.05	977.9	9260	9492	5.362	14.31	-335.2	-159.5	-480.4	317
1.20	1118	16310	17520	5.997	16.91	-1135	-484.5	-1602	486

Table 4-17 Coefficient of Shear Viscosity.

Substance: Argon
Radial Distribution Function: Percus-Yevick
Remarks: ζ_s^{RG}

Intermolecular Potential: Lennard-Jones
Temperature: 373°

ρ^*	ρ Amagat	P_{CAL} bar	P_{OBS} bar	ζ_s^{RG} $\times 10^{13}$kg/sec	η_k	η_v	$\eta_v(R>\sigma)$ $\times 10^6$ kgm/m sec	η_{CAL}	η_{OBS}
0.15	139.7	194.2	196.4	1.401	4.421	2.290	.1296	6.841	31.7
0.30	279.4	433.4	437.5	2.063	6.386	8.668	.6374	15.69	40.5
0.45	419.1	827.2	817.6	2.668	8.066	18.35	1.403	27.82	56.6
0.60	558.8	1576	1523	2.286	9.712	26.88	1.077	37.67	84.7
0.75	698.5	3009	2914	2.932	11.49	18.86	-5.758	24.60	130
0.90	838.2	5627	5597	4.599	13.52	-48.69	-34.79	-69.96	199
1.05	977.9	10150	10420	5.258	15.88	-286.4	-124.6	-395.1	299
1.20	1118	17610	18780	5.855	18.66	-988.6	-366.9	-1337	439

Table 4-L8 Coefficient of Shear Viscosity.

Substance: Argon
Radial Distribution Function: Verlet
Remarks: $\rho^* = 0.85$

Intermolecular Potential: Lennard-Jones
Density = 791.6 Amagats

T °C	P_{CAL} bar	P_{OBS} bar	ζ_s^{RG} $\times 10^{13}$ kg/sec	η_k ←	η_v	$\eta_v(R>\sigma)$ $\times 10^6$ kgm/m sec	η_{TOTAL} →
157.86	1476	1434	4.582	5.793	-35.79	-35.98	-65.98
273.05	3409	3194	4.432	9.775	-24.68	-24.88	-39.79
358.11	4595	4381	4.313	12.44	-9.541	-17.53	-.4.63

Table 4-19 Coefficient of Shear Viscosity.

Substance: Argon
Radial Distribution Function: Percus-Yevick
Remarks: ζ_s^{RG}

Intermolecular Potential: Truncated Lennard-Jones
Temperature: 273.2°K

ρ^*	ρ Amagat	P_{CAL} bar	P_{OBS} bar	ζ_s^{RG} $\times 10^{13}$ kg/sec	η_k	η_v	$\eta_v(R>\sigma)$	η_{TOTAL}
					← $\times 10^6$ kgm/m sec →			
0.15	139.7	133.1	142.4	1.459	3.193	1.838	.2480	5.279
0.30	279.4	287.1	293.9	2.150	4.658	6.715	1.127	12.50
0.45	419.1	564.1	490.7	2.807	5.900	12.58	2.289	20.77
0.60	558.1	1170	853.2	3.529	7.111	9.047	.6787	16.84
0.75	698.5	2495	1674	4.355	8.446	-47.59	-18.88	-58.02

Table 4-20 Coefficient of Shear Viscosity.

Substance: Argon
Radial Distribution Function: CHNC
Remarks: ζ_s^{RG}

Intermolecular Potential: Lennard-Jones
Temperature: 273.2°K

ρ^*	ρ Amagat	P_{CAL} bar	P_{OBS} bar	ζ_s^{RG} $\times 10^{13}$kg/sec	η_k	η_v	$\eta_v(R>\sigma)$	η_{CAL}	η_{OBS}
					← $\times 10^6$ kgm/m sec →				
0.15	139.7	126.6	142.4	1.450	3.211	1.852	.3498	5.313	26.2
0.30	279.4	260.9	293.9	2.114	4.717	6.994	1.132	12.84	35.3
0.45	419.1	513.5	490.7	2.728	6.018	14.49	2.292	22.80	50.1
0.60	558.8	1134	953.3	3.370	7.329	18.22	1.150	26.70	76.4
0.75	698.5	2604	1674	4.031	8.852	-5.332	-12.50	-8.983	124
0.90	838.2	5717	4075	4.640	10.72	-114.1	-61.13	-164.5	205
1.05	977.9	11590	8340	5.089	12.95	-383.7	-165.5	-536.3	338
1.20	1118	21670	16000	5.264	15.41	-782.0	-297.9	-1064	543

Table 4-21 Coefficient of Shear Viscosity.

Substance: Argon
Radial Distribution Function: CHNC
Remarks: ζ_s^{RG}

Intermolecular Potential: Lennard Jones
Temperature: 328.2°

ρ^*	ρ Amagat	P_{CAL} bar	P_{OBS} bar	ζ_s^{RG} $\times 10^{13}$kg/sec	η_k	η_v	$\eta_v(R>\sigma)$	η_{CAL}	η_{OBS}
					← $\times 10^6$ kgm/m sec →				
0.15	139.7	164.1	166.5	1.419	3.882	2.101	.1690	6.152	29.3
0.30	279.4	360.3	360.6	2.085	5.640	7.959	.8030	14.40	38.2
0.45	419.1	715.8	667.0	2.701	7.151	16.64	1.646	25.43	53.7
0.60	558.8	1502	1261	3.332	8.679	22.16	.5618	31.40	80.9
0.75	698.5	3217	2487	3.963	10.43	3.814	-9.901	4.339	127
0.90	838.2	6655	4945	4.531	12.52	-83.73	-44.38	-115.6	202
1.05	977.9	12960	9492	4.941	14.95	-290.0	-114.1	-389.2	317
1.20	1118	23670	17520	5.093	17.61	-564.2	-195.9	-742.5	486

Table 4-22 Coefficient of Shear Viscosity.

Substance: Argon
Radial Distribution Function: CHNC
Remarks: ζ_s^{RG}

Intermolecular Potential: Lennard Jones
Temperature: 373.2°

ρ^*	ρ Amagat	P_{CAL} bar	P_{OBS} bar	ζ_s^{RG} $\times 10^{13}$kg/sec	η_k	η_v	$\eta_v(R>\sigma)$	η_{CAL}	η_{OBS}
					←		$\times 10^6$ kgm/m sec		→
0.15	139.7	194.4	196.4	1.402	4.419	2.292	.1303	6.841	31.7
0.30	279.4	439.1	437.5	2.068	6.376	8.692	.6379	15.71	40.5
0.45	419.1	874.1	817.6	2.683	8.052	18.32	1.313	27.68	56.6
0.60	558.8	1787	1526	3.304	9.746	25.47	.3231	35.54	84.7
0.75	698.5	3692	2914	3.914	11.66	11.49	-8.272	14.89	130
0.90	838.2	7387	5597	4.455	13.92	-61.17	-35.17	-82.14	199
1.05	977.9	13940	10426	4.842	12.97	-26.13	-118.2	-366.6	299
1.20	1118	25350	18780	4.982	19.33	-43.37	-146.0	-560.3	439

Table 4-23 Coefficient of Shear Viscosity.

Substance: Argon
Radial Distribution Function: Kirkwood
Remarks: ζ_s^{RG}

Intermolecular Potential: Modified Buckingham
Temperature: 273°

λ	ρ Amagat	P_{CAL} bar	P_{OBS} bar	ζ_s^{RG} $\times 10^{13}$ kg/sec	η_k	η_v	$\eta_v(R>\sigma)$	η_{CAL}	η_{OBS}
					←		$\times 10^6$ kgm/m sec		→
0.5	36.44	35.80	35.79	.7184	1.642	.1553	.0096	1.807	22.0
1.0	72.87	69.98	69.71	1.024	2.312	.5598	.0518	2.924	23.3
1.5	109.3	103.6	102.5	1.267	2.137	1.203	.1371	4.177	24.8
2.0	145.7	137.6	134.9	1.479	3.291	2.081	.2723	5.644	26.5
2.5	182.2	173.4	167.8	1.672	3.703	3.189	.4623	7.354	28.5
3.0	218.6	212.2	202.0	1.854	4.087	4.516	.7111	9.314	30.8
3.5	255.1	255.6	238.8	2.028	4.452	6.044	1.0210	11.52	33.4
4.0	291.5	305.3	279.4	2.198	4.804	7.742	1.392	13.94	36.3
4.5	327.9	362.9	325.5	2.365	5.147	9.567	1.821	16.53	39.6
5.0	364.4	430.4	379.0	2.529	5.484	11.46	2.299	19.24	43.4
5.5	400.8	509.8	442.4	2.693	5.819	13.32	2.813	21.96	47.7
6.0	437.2	603.0	518.9	2.857	6.153	15.06	3.341	24.56	52.7
6.5	437.7	711.6	612.4	3.021	6.487	16.53	3.858	26.87	58.6

Table 4-24 Coefficient of Shear Viscosity.

Substance: Argon
Radial Distribution Function: Kirkwood
Remarks: ζ_s^{RG}

Intermolecular Potential: Modified Buckingham
Temperature: 308°

λ	ρ Amagat	P_{CAL} bar	P_{OBS} bar	ζ_s^{RG} $\times 10^{13}$ kg/sec	η_k	η_v	$\eta_v(R>\sigma)$ $\times 10^6$ kgm/m sec	η_{CAL}	η_{OBS}
0.5	36.44	40.90	40.88	.7056	1.875	.1698	.0073	2.052	24.2
1.0	72.87	80.94	80.62	1.008	2.632	.6096	.0400	3.282	25.5
1.5	109.3	121.2	120.0	1.247	3.222	1.308	.1070	4.637	26.8
2.0	145.7	162.9	159.8	1.457	3.729	2.264	.2141	6.207	28.5
2.5	182.2	207.3	200.9	1.649	4.188	3.471	.3662	8.026	30.5
3.0	218.6	256.0	244.5	1.830	4.615	4.922	.5667	10.10	32.7
3.5	255.1	310.6	291.8	2.003	5.021	6.597	.8176	12.43	35.3
4.0	291.5	372.9	344.2	2.172	5.412	8.468	1.118	15.00	38.2
4.5	327.9	444.9	403.6	2.337	5.793	10.49	1.465	17.75	41.5
5.0	364.4	528.7	472.3	2.501	6.168	12.61	1.850	20.63	45.4
5.5	400.8	626.5	553.0	2.663	6.539	14.73	2.258	23.53	49.9
6.0	437.2	740.5	649.0	2.826	6.910	16.76	2.669	26.34	55.1
6.5	437.7	872.5	764.5	2.988	7.282	18.55	3.057	28.88	61.1

Table 4-25 Coefficient of Shear Viscosity.

Substance: Argon
Radial Distribution Function: Kirkwood
Remarks: ζ_s^{RG}

Intermolecular Potential: Modified Buckingham
Temperature: 323°

λ	ρ Amagat	P_{CAL} bar	P_{OBS} bar	ζ_s^{RG} $\times 10^{13}$kg/sec	η_k	η_v	$\eta_v(R>\sigma)$ $\times 10^6$ kgm/m sec	η_{CAL}	η_{OBS}
0.5	36.44	43.08	43.05	.7010	1.975	.1759	.0062	2.157	25.0
1.0	72.87	85.61	85.26	1.002	2.769	.6304	.0362	3.435	26.2
1.5	109.3	128.7	127.4	1.240	3.385	1.352	.0971	4.834	27.7
2.0	145.7	173.7	170.4	1.449	3.915	2.339	.1951	6.449	29.3
2.5	182.2	221.8	215.1	1.640	4.394	3.588	.3345	8.316	31.3
3.0	218.6	274.6	262.6	1.821	4.839	5.088	.5188	10.45	33.5
3.5	255.1	333.9	314.4	1.994	5.262	6.824	.7498	12.84	36.0
4.0	291.5	401.6	371.8	2.162	5.669	8.766	1.027	15.46	39.0
4.5	327.9	479.7	437.0	2.327	6.066	10.87	1.346	18.28	42.4
5.0	364.4	570.4	512.1	2.490	6.456	13.08	1.699	21.24	46.3
5.5	400.8	675.9	600.0	2.652	6.843	15.32	2.072	24.23	50.8
6.0	437.2	798.6	704.2	2.813	7.230	17.46	2.445	27.14	56.1
6.5	473.7	940.4	828.9	2.975	7.617	19.39	2.791	29.79	62.2
7.0	510.1	1103	979.2	3.137	8.006	20.91	3.077	31.99	69.3

Table 4-26 Coefficient of Shear Viscosity.

Substance: Argon
Radial Distribution Function: Kirkwood
Remarks: ζ_s^{RG}

Intermolecular Potential: Modified Buckingham
Temperature: 328°

λ	ρ Amagat	P_{CAL} bar	P_{OBS} bar	ζ_s^{RG} $\times 10^{13}$kg/sec	η_k	η_v	$\eta_v(R>\sigma)$	η_{CAL}	η_{OBS}
					← $\times 10^6$ kgm/m sec →				
0.5	36.44	43.80	43.78	.6996	2.008	1.799	.0064	2.192	25.2
1.0	72.87	87.17	86.82	.9996	2.814	6.372	.0351	3.486	26.5
1.5	109.3	131.2	129.9	1.238	3.439	1.366	.0942	4.900	27.9
2.0	145.7	177.2	173.9	1.447	3.977	2.364	.1893	6.530	29.6
2.5	182.2	226.6	219.8	1.638	4.462	3.626	.3249	8.413	31.5
3.0	218.6	280.8	268.7	1.818	4.914	5.143	.5043	10.56	33.8
3.5	255.1	341.7	321.9	1.991	5.342	6.898	.7292	12.97	36.3
4.0	291.5	411.1	381.1	2.159	5.754	8.864	.9990	15.62	39.2
4.5	327.9	491.3	448.1	2.324	6.156	11.00	1.310	18.46	42.6
5.0	364.4	584.3	525.4	2.487	6.552	13.24	1.653	21.44	46.6
5.5	400.8	692.3	615.7	2.649	6.944	15.51	2.015	24.47	51.1
6.0	437.2	817.8	722.7	2.810	7.336	17.70	2.376	27.41	56.4
6.5	473.7	962.9	850.6	2.971	7.728	19.66	2.710	30.10	62.6
7.0	510.1	1129	1004	3.133	8.122	21.24	2.983	32.35	69.7

Table 4-27 Coefficient of Shear Viscosity.

Substance: Argon
Radial Distribution Function: Kirkwood
Remarks: ζ_s^{RG}

Intermolecular Potential: Modified Buckingham
Temperature: 373°

λ	ρ Amagat	P_{CAL} bar	P_{OBS} bar	ζ_s^{RG} $\times 10^{13}$kg/sec	η_k	η_v	$\eta_v(R>\sigma)$ $\times 10^6$ kgm/m sec	η_{CAL}	η_{OBS}
0.5	36.44	50.33	50.29	.6885	2.305	.1957	.0049	2.506	27.8
1.0	72.87	101.1	100.7	.9848	3.220	.6969	.0269	3.944	29.0
1.5	109.3	753.7	152.1	1.229	3.925	1.492	.0728	5.499	30.4
2.0	145.7	209.3	205.5	1.427	4.528	2.579	.1476	7.255	32.0
2.5	182.2	269.6	262.0	1.617	5.072	3.957	.2552	9.284	33.8
3.0	218.6	336.2	325.5	1.796	5.576	5.618	.3984	11.59	36.0
3.5	255.1	411.0	389.6	1.968	6.054	7.546	.5786	14.18	38.5
4.0	291.5	496.3	463.0	2.134	6.513	9.715	.7949	17.02	41.5
4.5	327.9	594.3	546.7	2.298	6.962	12.09	1.043	20.10	45.0
5.0	364.4	707.4	643.1	2.459	7.402	14.60	1.316	23.32	49.2
5.5	400.8	838.2	754.5	2.619	7.839	17.18	1.599	26.62	53.9
6.0	437.2	989.1	885.3	2.779	8.275	19.72	1.876	29.87	59.5
6.5	473.7	1163	1040	2.938	8.712	22.10	2.121	32.93	65.9
7.0	510.1	1361	1224	3.096	9.152	24.13	2.303	35.59	73.2

Table 4-28 Coefficient of Shear Viscosity.

Substance: Nitrogen
Radial Distribution Function: Kirkwood
Remarks: ζ_s^{RG}

Intermolecular Potential: Modified Buckingham
Temperature: 273°

λ	ρ Amagat	P_{CAL} bar	P_{OBS} bar	ζ_s^{RG} $\times 10^{13}$kg/sec	η_k	η_v	$\eta_v(R>\sigma)$ $\times 10^6$ kgm/m sec	η_{CAL}	η_{OBS}
0.5	30.85	30.89	30.90	.5709	1.226	1.165	.0053	1.348	17.6
1.0	61.69	61.53	61.44	.8153	1.726	.4200	.0292	2.175	18.7
1.5	92.55	92.66	92.21	1.009	2.116	.9029	.0788	3.098	19.9
2.0	123.4	125.1	123.9	1.178	2.453	1.563	.1594	4.175	21.4
2.5	154.2	159.8	157.1	1.333	2.759	2.394	.2756	5.429	23.1
3.0	185.1	197.8	192.8	1.479	3.044	3.390	.4312	6.865	25.1
3.5	215.9	240.2	231.9	1.619	3.315	4.536	.6294	8.480	27.2
4.0	246.8	288.4	275.8	1.756	3.576	5.808	.8722	10.26	29.7
4.5	277.6	343.7	326.0	1.889	3.831	7.175	1.159	12.16	32.4
5.0	308.5	407.8	384.3	2.022	4.081	8.590	1.487	14.16	35.6
5.5	399.3	482.1	453.1	2.153	4.330	9.990	1.850	16.19	39.4
6.0	370.2	568.2	535.1	2.285	4.579	11.29	2.237	18.11	43.7
6.5	401.0	667.8	633.7	2.416	4.827	12.40	2.633	19.86	48.7
7.0	431.9	782.0	753.0	2.548	5.078	13.17	3.018	21.27	54.7
7.5	462.7	911.9	897.8	2.681	5.330	13.46	3.370	22.16	61.6
8.0	493.6	1058	1074	2.814	5.585	13.06	3.669	22.31	69.8

Table 4-29. Coefficient of Shear Viscosity.

Substance: Nitrogen
Radial Distribution Function: Kirkwood
Remarks: ζ_s^{RG}

Intermolecular Potential: Modified Buckingham
Temperature: 308°

λ	ρ Amagat	P_{CAL} bar	P_{OBS} bar	ζ_s^{RG} $\times 10^{13}$kg/sec	η_k	η_v	$\eta_v(R>\sigma)$ $\times 10^6$ kgm/m sec	η_{CAL}	η_{OBS}
0.5	30.85	35.21	35.21	.5617	1.399	.1272	.0041	1.530	17.5
1.0	61.69	70.80	70.69	.8030	1.962	.4570	.0227	2.442	18.5
1.5	92.55	107.6	107.1	.9948	2.399	.9812	.0618	3.442	19.6
2.0	123.4	146.5	145.1	1.163	2.776	1.698	.1262	4.600	20.9
2.5	154.2	188.6	185.5	1.317	3.116	2.604	.2198	5.940	22.3
3.0	185.1	235.0	229.3	1.462	3.433	3.690	.3462	7.470	24.1
3.5	215.9	286.9	277.7	1.602	3.734	4.944	.5079	9.186	26.0
4.0	246.8	346.0	332.0	1.737	4.024	6.344	.7062	11.07	28.3
4.5	277.6	413.6	393.9	1.870	4.307	7.856	.9404	13.10	30.8
5.0	308.5	49.16	465.6	2.002	4.585	9.436	1.207	15.23	33.8
5.5	339.3	581.7	549.5	2.133	4.861	11.02	1.499	17.38	37.3
6.0	370.2	685.6	648.6	2.263	5.136	12.53	1.806	19.47	41.4
6.5	401.0	805.0	766.5	2.394	5.412	13.86	2.112	21.38	46.1
7.0	431.9	941.5	907.3	2.525	5.691	14.88	2.399	22.97	51.6
7.5	462.7	1096	1076	2.656	5.971	15.43	2.642	24.04	58.0
8.0	493.6	1270	1278	2.789	6.254	15.33	2.816	24.40	65.4

Table 4-30 Coefficient of Shear Viscosity.

Substance: Nitrogen
Radial Distribution Function: Kirkwood
Remarks: ζ_s^{RG}

Intermolecular Potential: Modified Buckingham
Temperature: 323°

λ	ρ Amagat	P_{CAL} bar	P_{OBS} bar	ζ_s^{RG} $\times 10^{13}$ kg/sec	η_k	η_v	$\eta_v(R>\sigma)$ $\times 10^6$ kgm/m sec	η_{CAL}	η_{OBS}
0.5	30.85	37.05	37.05	.5584	1.472	.1317	.0037	1.607	17.5
1.0	61.69	74.76	74.64	.7986	2.062	.4724	.0206	2.555	18.4
1.5	92.55	114.0	113.4	.9897	2.520	1.014	.0563	3.590	19.5
2.0	123.4	155.6	154.1	1.157	2.913	1.154	.1153	4.782	20.7
2.5	152.2	200.8	197.6	1.311	3.268	2.690	.2013	6.159	22.1
3.0	185.1	250.8	244.9	1.456	3.598	3.814	.3178	7.730	23.7
3.5	215.9	306.8	297.1	1.596	3.912	5.113	.4671	9.492	25.6
4.0	246.8	370.5	355.8	1.730	4.214	6.565	.6504	11.43	27.8
4.5	277.6	443.3	422.8	1.863	4.508	8.138	.8666	13.51	30.3
5.0	308.5	527.2	500.1	1.915	4.797	9.786	1.112	15.70	33.2
5.5	339.3	623.9	590.4	2.125	5.085	11.45	1.381	17.91	36.6
6.0	370.2	735.2	696.6	2.255	5.371	13.04	1.661	20.08	40.6
6.5	401.0	863.0	822.5	2.385	5.659	14.47	1.938	22.07	45.2
7.0	431.9	1009	972.2	2.516	5.949	15.60	2.192	23.74	50.6
7.5	462.7	1174	1151	2.647	6.241	16.27	2.400	24.91	56.8
8.0	493.6	1360	1364	2.779	6.536	16.30	2.537	25.37	63.9

Table 4-31 Coefficient of Shear Viscosity.

Substance: Nitrogen
Radial Distribution Function:
Remarks: ζ_s^{RG}

Intermolecular Potential: Modified Buckingham
Temperature: 328°

λ	ρ Amagat	P_{CAL} bar	P_{OBS} bar	ζ_s^{RG} $\times 10^{13}$kg/sec	η_k	η_v	$\eta_v(R>\sigma)$ $\times 10^6$ kgm/m sec	η_{CAL}	η_{OBS}
0.5	30.85	37.66	37.66	.5574	1.497	.1332	.0036	1.633	17.5
1.0	61.69	76.08	75.95	.7972	2.096	.4774	.0199	2.593	18.4
1.5	92.55	116.1	115.5	.9881	2.560	1.024	.0546	3.639	19.5
2.0	123.4	158.7	157.1	1.155	2.959	1.772	.1119	4.843	20.7
2.5	154.2	204.9	201.6	1.309	3.319	2.718	.1957	6.232	22.0
3.0	185.1	256.1	250.0	1.454	3.653	3.854	.3092	7.817	23.6
3.5	215.9	313.4	303.6	1.593	3.971	5.168	.4547	9.593	25.5
4.0	246.8	378.6	363.8	1.728	4.276	6.637	.6333	11.55	27.6
4.5	277.6	453.2	432.4	1.861	4.575	8.230	.8441	13.65	30.1
5.0	308.5	539.0	511.6	1.992	4.868	9.901	1.083	15.85	33.0
5.5	339.3	637.9	603.9	2.113	5.159	11.59	1.344	18.09	36.4
6.0	370.2	751.7	712.5	2.253	5.449	13.21	1.616	20.28	40.3
6.5	401.0	882.3	841.0	2.383	5.541	14.67	1.884	22.30	44.9
7.0	431.9	1031	993.7	2.513	6.034	15.83	2.129	24.00	50.2
7.5	462.7	1200	1176	2.644	6.330	16.55	2.327	25.20	56.4
8.0	493.6	1390	1393	2.775	6.629	16.62	2.453	25.70	63.4

Table 4-32 Coefficient of Shear Viscosity.

Substance: Nitrogen
Radial Distribution Function: Kirkwood
Remarks: ζ_s^{RG}

Intermolecular Potential: Modified Buckingham
Temperature: 373°

λ	ρ Amagat	P_{CAL} bar	P_{OBS} bar	ζ_s^{RG} $\times 10^{13}$ kg/sec	η_k	η_v	$\eta_v(R>\sigma)$	η_{CAL}	η_{OBS}
					←		$\times 10^6$ kgm/m sec		→
0.5	30.85	43.19	43.18	.5494	1.716	.1463	.0027	1.865	17.5
1.0	61.69	87.92	87.76	.7865	2.395	.5218	.0154	2.932	18.2
1.5	92.55	135.1	134.5	.9757	2.918	1.117	.0425	4.078	19.2
2.0	123.4	185.9	184.1	1.142	3.365	1.932	.0879	5.385	20.1
2.5	154.2	241.5	237.7	1.294	3.768	2.964	.1549	6.887	21.3
3.0	185.1	303.2	296.4	1.438	4.141	4.207	.2462	8.595	22.8
3.5	215.9	372.6	361.5	1.577	4.495	5.649	.3637	10.51	24.5
4.0	246.8	451.3	434.7	1.711	4.836	7.268	.5081	82.61	26.5
4.5	277.6	541.3	518.0	1.843	5.168	9.036	.6780	14.88	28.8
5.0	308.5	644.4	613.8	1.973	5.494	10.91	.8700	17.27	31.6
5.5	339.3	762.8	724.7	2.102	5.818	1.282	1.077	19.71	34.8
6.0	370.2	898.5	854.1	2.231	6.141	1.470	1.290	22.13	38.5
6.5	401.0	1054	1006	2.360	6.466	1.645	1.494	24.41	42.8
7.0	431.9	1230	1184	2.489	6.792	1.794	1.671	26.40	47.7
7.5	462.7	1429	1395	2.618	7.121	1.901	1.798	27.93	53.4
8.0	493.6	1653	1644	2.748	7.454	1.950	1.850	28.80	59.8

Table 4-33 Coefficient of Shear Viscosity.

Substance: Argon
Radial Distribution Function: Percus Yevick
Remarks: ζ_s^{RG}

Intermolecular Potential: Modified Buckingham
Temperature: 273.15°

ρ^*	ρ Amagat	P_{CAL} bar	P_{OBS} bar	ζ_s^{RG} $\times 10^{13}$kg/sec	η_k	η_v	$\eta_v(R>\sigma)$	η_{CAL}	η_{OBS}
					← $\times 10^6$ kgm/m sec →				
0.25	160.9	150.6	148.4	1.537	3.513	2.490	.3322	6.335	27.23
0.50	321.8	336.9	317.2	2.264	5.199	9.328	1.466	15.99	39.01
0.75	482.7	727.9	638.7	2.296	6.691	18.24	2.622	27.55	61.17
1.00	643.6	1676	1438	3.709	8.241	16.05	-2.592	21.70	101.7
1.25	804.6	3789	3420	4.514	10.06	-48.03	-41.64	-79.62	181.4
1.35	868.9	5153	4757	4.843	10.89	-119.79	-82.71	-191.6	229.5

Table 4-33 Coefficient of Shear Viscosity.

Substance: Argon
Radial Distribution Function: Percus Yevick
Remarks: ζ_s^{RG}

Intermolecular Potential: Modified Buckingham
Temperature: 273.15°

ρ^*	ρ Amagat	P_{CAL} bar	P_{OBS} bar	ζ_s^{RG} $\times 10^{13}$kg/sec	η_k	η_v	$\eta_v(R>\sigma)$ $\times 10^6$ kgm/m sec	η_{CAL}	η_{OBS}
0.25	160.9	150.6	148.4	1.537	3.513	2.490	.3322	6.335	27.23
0.50	321.8	336.9	317.2	2.264	5.199	9.328	1.466	15.99	39.01
0.75	482.7	727.9	638.7	2.296	6.691	18.24	2.622	27.55	61.17
1.00	643.6	1676	1438	3.709	8.241	16.05	-2.592	21.70	101.7
1.25	804.6	3789	3420	4.514	10.06	-48.03	-41.64	-79.62	181.4
1.35	868.9	5153	4757	4.843	10.89	-119.79	-82.71	-191.6	229.5

Table 4-34.

Substance: Argon
Radial Distribution Function: Percus Yevick
Remarks: ζ_s^{RG}

Intermolecular Potential: Modified Buckingham
Temperature: 328.15°

ρ^*	ρ Amagat	P_{CAL} bar	P_{OBS} bar	ζ_s^{RG} $\times 10^3$ kg/sec	η_k	η_v	$\eta_v(R>\sigma)$	η_{CAL}	η_{OBS}
					← $\times 10^6$ kgm/m sec →				
.25	160.9	193.6	192.7	1.506	4.240	2.823	.2272	7.290	30.39
.50	321.8	449.0	436.1	2.232	6.208	10.64	1.062	17.91	41.93
.75	412.7	949.4	885.8	2.922	7.947	21.27	1.894	31.11	64.30
1.00	643.6	2053	1899	3.648	9.750	22.41	-2.196	29.96	106.2
1.25	804.6	4358	4198	4.409	11.82	-30.64	-30.86	-4.968	180.8
1.45	933.3	7661	7752	4.963	13.87	-206.1	-101.9	-294.2	275.1
1.50	965.5	8760	8969	5.166	14.32	-272.2	-142.4	-400.3	304.8
1.55	997.6	9993	10370	5.310	14.87	-371.5	-185.5	-542.1	337.3
1.60	1030	11360	11970	5.450	15.45	-498.3	-239.5	-722.3	322.8
1.65	1062	12890	13780	5.584	16.04	-610.0	-307.0	-901.0	411.4
1.70	1094	15170	15830	5.626	16.81	-903.6	-366.9	-1253	455

Table 4-35 Coefficient of Shear Viscosity.

Substance: Argon
Radial Distribution Function: Percus Yevick
Remarks: ζ_s^{RG}

Intermolecular Potential: Modified Buckingham
Temperature: 373.15°

ρ^*	ρ Amagat	P_{CAL} bar	P_{OBS} bar	ζ_s^{RG} $\times 10^{13}$ kg/sec	η_k	η_v	$\eta_v(R>\sigma)$	η_{CAL}	η_{OBS}
					← $\times 10^6$ kgm/m sec →				
0.25	160.9	228.3	228.5	1.487	4.822	3.077	.1763	8.076	32.72
0.50	321.8	538.9	531.9	2.212	7.013	11.630	.8520	19.50	44.42
0.75	482.7	1125	1083	2.895	8.948	23.59	1.522	34.06	67.64
1.00	643.6	2352	2252	3.603	10.94	27.47	-1.885	36.53	109.8
1.25	804.6	4280	4791	4.336	13.21	-17.12	-24.70	-28.60	180.0
1.35	868.9	6340	6436	4.627	14.23	-69.08	-47.28	-102.1	218.3

Table 4-36 Coefficient of Shear Viscosity

Substance: Argon
Radial Distribution Function: Kirkwood
Remarks: ζ_s^{RG}

Intermolecular Potential: Barker Bobetic
Temperature: 273°

λ	ρ Amagat	P_{CAL} bar	P_{OBS} bar	ζ_s^{RG} $\times 10^{13}$kg/sec	η_k	η_v	$\eta_v(R>\sigma)$ $\times 10^6$ kgm/m sec	η_{CAL}	η_{OBS}
0.50	38.78	38.32	38.01	.9165	1.389	.1501	.0147	1.554	21.7
1.00	77.56	75.23	73.94	1.302	1.975	.5470	.0789	2.601	23.1
1.50	116.3	111.5	108.7	1.603	2.442	1.179	.2073	3.828	24.8
2.00	155.1	148.2	143.2	1.861	2.852	2.041	.4071	5.301	26.8
2.50	193.9	186.0	178.5	2.095	3.229	3.127	.6829	7.039	29.0
3.00	232.7	226.2	215.8	2.312	3.583	4.428	1.038	9.049	31.6
3.50	271.5	270.0	256.4	2.517	3.922	5.929	1.476	11.33	34.5
4.00	310.2	318.6	302.2	2.715	4.249	7.610	1.999	13.86	38.0
4.50	349.0	373.7	355.2	2.909	4.567	9.438	2.610	16.62	41.9
5.00	387.8	437.1	418.2	3.099	4.880	11.37	3.305	19.55	46.5
5.50	426.6	510.8	494.5	3.289	5.188	13.34	4.081	22.61	51.8
6.00	465.3	596.9	588.8	3.478	5.494	15.27	4.922	25.68	58.0
6.50	504.2	697.9	706.2	3.667	5.799	17.04	5.807	28.65	65.2
7.00	542.9	816.0	8535	3.859	6.104	18.52	6.700	31.32	73.8
7.50	581.7	953.5	1039	4.051	6.411	19.52	7.553	33.48	84.1
8.00	620.5	1113	1271	4.247	6.720	19.82	8.304	34.85	96.5
8.50	659.3	1295	1562	4.444	7.031	19.17	8.881	35.08	107
9.00	698.1	1501	1924	4.643	7.346	17.23	9.207	33.78	123

Table 4-37 Coefficient of Shear Viscosity

Substance: Argon
Radial Distribution Function: Kirkwood
Remarks: ζ_s^{RG}

Intermolecular Potential: Barker-Bobetic
Temperature: 308°

λ	ρ Amagat	P_{CAL} bar	P_{OBS} bar	ζ_s^{RG} $\times 10^{13}$ kg/sec	η_k	η_v	$\eta_v(R>\sigma)$	η_{CAL}	η_{OBS}
					←		$\times 10^6$ kgm/m sec		→
0.50	38.78	43.80	43.46	.9012	1.587	.1637	.0112	1.762	24.1
1.00	77.56	87.10	85.68	1.282	2.249	.5948	.0606	2.904	25.5
1.50	116.3	130.8	127.6	1.580	2.775	1.281	.1601	4.216	27.1
2.00	155.1	176.0	170.2	1.837	3.234	2.218	.3165	5.769	29.0
2.50	193.9	223.6	214.6	2.070	3.655	3.400	.5346	7.589	31.2
3.00	232.7	275.0	262.2	2.287	4.049	4.817	.8184	9.684	33.7
3.50	271.5	331.5	314.6	2.494	4.425	6.454	1.171	12.05	36.5
4.00	310.2	394.7	373.8	2.694	4.788	8.289	1.595	14.67	39.8
4.50	349.0	466.6	442.1	2.889	5.142	10.29	2.089	17.52	43.7
5.00	387.8	549.0	522.6	3.081	5.489	12.40	2.651	20.54	48.2
5.50	426.6	644.3	619.1	3.271	5.831	14.56	3.271	23.66	53.5
6.00	465.3	754.9	736.1	3.462	6.172	16.68	3.931	26.79	59.7
6.50	504.2	883.4	879.5	3.653	6.512	18.64	4.606	29.76	66.9
7.00	542.9	1032	1056	3.845	6.852	20.30	5.256	32.41	75.4
7.50	581.7	1204	1274	4.038	7.195	21.46	5.830	34.49	85.3
8.00	620.5	1402	1543	4.233	7.541	21.91	6.262	35.71	96.8
8.50	659.3	1620	1876	4.430	7.891	21.35	6.477	35.72	110
9.00	698.1	1879	2284	4.629	8.244	19.47	6.389	34.11	126

Table 4-38 Coefficient of Shear Viscosity

Substance: Argon
Radial Distribution Function: Kirkwood
Remarks: ζ_s^{RG}

Intermolecular Potential: Barker-Bobetic
Temperature: 323°

λ	ρ Amagat	P_{CAL} bar	P_{OBS} bar	ζ_s^{RG} $\times 10^{13}$ kg/sec	η_k	η_v	$\eta_v(R>\sigma)$	η_{CAL}	η_{OBS}
					← $\times 10^6$ kgm/m sec →				
0.50	38.78	46.13	45.78	.8957	1.671	.1694	.0101	1.850	25.2
1.00	77.56	92.17	90.67	1.275	2.366	.6146	.0547	3.035	26.5
1.50	116.3	139.0	135.6	1.572	2.916	1.323	.1449	4.384	28.1
2.00	155.1	187.8	181.7	1.829	3.396	2.291	.2873	5.975	29.8
2.50	193.9	239.6	230.0	2.062	3.835	3.512	.4867	7.834	31.8
3.00	232.7	295.7	282.0	2.279	4.246	4.977	.7470	9.971	34.3
3.50	271.5	357.6	339.4	2.486	4.638	6.671	1.071	12.38	37.1
4.00	310.2	427.1	404.3	2.686	5.016	8.570	1.461	15.05	40.5
4.50	349.0	506.0	479.0	2.881	5.385	10.64	1.917	17.94	44.6
5.00	387.8	596.5	566.9	3.074	5.746	12.83	2.432	21.01	49.1
5.50	426.6	700.8	671.8	3.265	6.103	15.07	2.999	24.18	54.5
6.00	465.3	821.7	798.4	3.456	6.458	17.28	3.597	27.34	60.8
6.50	504.2	961.7	952.6	3.647	6.813	19.33	4.201	30.34	68.1
7.00	542.9	1124	1141	3.839	7.169	21.07	4.770	33.01	76.6
7.50	581.7	1310	1373	4.032	7.527	22.32	5.253	35.10	86.6
8.00	620.5	1523	1658	4.227	7.888	22.84	5.584	36.32	98.1
8.50	659.3	1765	2007	4.423	8.253	22.37	5.687	36.31	111
9.00	698.1	2037	2435	4.622	8.623	20.56	5.474	34.66	127

Table 4-39. Coefficient of Shear Viscosity

Substance: Argon
Radial Distribution Function: Kirkwood
Remarks: ζ_s^{RG}

Intermolecular Potential: Barker-Bobetic
Temperature: 328°

λ	ρ Amagat	P_{CAL} bar	P_{OBS} bar	ζ_s^{RG} $\times 10^{13}$ kg/sec	η_k	η_v	$\eta_v(R>\sigma)$ $\times 10^6$ kgm/m sec	η_{CAL}	η_{OBS}
0.50	38.78	46.92	46.55	.8940	1.699	.1713	.0098	1.880	25.5
1.00	77.56	93.86	92.32	1.272	2.405	.6211	.0529	3.079	26.8
1.50	116.3	141.8	138.2	1.569	2.963	1.337	.1404	4.441	28.3
2.00	155.1	191.7	185.5	1.826	3.450	2.315	.2786	6.044	30.1
2.50	193.9	244.9	235.1	2.059	3.895	3.549	.4723	7.916	32.1
3.00	232.7	302.6	288.6	2.276	4.312	5.030	.7255	10.07	34.5
3.50	271.5	366.3	347.6	2.483	4.709	6.743	1.041	12.49	37.4
4.00	310.2	437.8	414.4	2.683	5.092	8.663	1.421	15.18	40.8
4.50	349.0	519.1	491.3	2.879	5.465	10.76	1.864	18.09	44.8
5.00	387.8	612.2	581.6	3.072	5.832	12.97	2.366	21.17	49.5
5.50	426.6	719.6	689.3	3.263	6.194	15.24	2.916	24.36	55.0
6.00	465.3	843.9	819.0	3.454	6.553	17.48	3.496	27.53	61.3
6.50	504.2	987.7	976.8	3.645	6.913	19.56	4.078	30.55	68.5
7.00	542.9	1154	1169	3.837	7.273	21.33	4.622	33.23	77.0
7.50	581.7	1345	1406	4.030	7.636	22.61	5.078	35.32	87.0
8.00	620.5	1564	1696	4.225	8.003	23.16	5.379	36.54	102
8.50	659.3	1811	2050	4.421	8.373	22.71	5.449	36.54	112
9.00	698.1	2090	2485	4.619	8.748	20.94	5.200	34.89	127

Table 4-42 Coefficient of Shear Viscosity

Substance: Argon
Radial Distribution Function: Kirkwood
Remarks: ζ_s^{RG}

Intermolecular Potential: Barker-Bobetic
Temperature: 373°

λ	ρ Amagat	P_{CAL} bar	P_{OBS} bar	ζ_s^{RG} $\times 10^{13}$ kg/sec	η_k	η_v	$\eta_v(R>\sigma)$ $\times 10^6$ kgm/m sec	η_{CAL}	η_{OBS}
0.50	38.78	53.92	53.50	.8811	1.951	.1878	.0074	2.146	28.0
1.00	77.56	109.0	107.2	1.255	2.752	.6782	.0404	3.471	29.3
1.50	116.3	166.3	162.2	1.550	3.383	1.458	.1079	4.949	30.8
2.00	155.1	227.0	219.5	1.806	3.931	2.524	.2159	6.671	32.5
2.50	193.9	292.4	280.7	2.038	4.429	3.871	.3688	8.669	34.4
3.00	232.7	364.2	347.2	2.256	4.895	5.489	.5701	10.95	36.8
3.50	271.5	440.0	421.0	2.463	5.339	7.364	.8226	13.53	39.7
4.00	310.2	533.8	504.5	2.664	5.767	9.470	1.127	16.36	43.1
4.50	349.0	635.8	600.4	2.860	6.183	11.77	1.480	19.44	47.2
5.00	387.8	752.4	712.3	3.053	6.592	14.22	1.878	22.69	52.0
5.50	426.6	886.4	844.3	3.245	6.997	16.74	2.306	26.04	57.7
6.00	465.3	1041	1002	3.436	7.400	19.24	2.748	29.38	64.4
6.50	504.2	1218	1190	3.627	7.801	21.60	3.173	32.57	72.0
7.00	542.9	1422	1418	3.818	8.205	23.66	3.543	35.41	80.8
7.50	581.7	1655	1693	4.010	8.612	25.25	3.807	37.66	90.8
8.00	620.5	1919	2027	4.204	9.023	26.11	3.903	39.04	102
8.50	659.3	2218	2431	4.439	9.439	25.99	3.754	39.19	115
9.00	698.1	2552	2910	4.595	9.859	24.55	3.275	37.68	130

Table 4-41 Coefficient of Shear Viscosity.

Substance: Argon
Radial Distribution Function: Percus-Yevick
Remarks: ζ_s^{RG}

Intermolecular Potential: Barker-Bobetic
Temperature: 273.15°K

ρ^*	ρ Amagat	P_{CAL} bar	P_{OBS} bar	ζ_s^{RG} $\times 10^{13}$ kg/sec	η_k	η_v	$\eta_v(R>\sigma)$	η_{CAL}	η_{OBS}
					← $\times 10^6$ kgm/m sec →				
0.15	104.7	97.24	98.35	1.350	2.506	.9264	.1508	3.584	24.50
0.30	209.4	188.0	193.1	1.935	3.575	3.545	.7274	7.847	30.24
0.45	314.1	298.5	307.2	2.424	4.425	7.855	1.717	14.00	38.29
0.60	418.8	468.5	478.2	2.894	5.156	13.70	2.962	21.82	50.08
0.75	523.5	767.6	776.0	3.382	5.821	20.23	3.738	29.79	68.20
0.90	628.2	1301	1325	3.901	6.470	24.66	1.540	32.67	96.47
1.05	732.9	2221	2325	4.456	7.150	19.96	-10.22	16.89	139.9
1.20	837.5	3733	4079	5.042	7.904	-9.884	-46.51	-48.49	204.6
1.35	942.2	6099	6968	5.648	8.764	-98.70	-138.3	-228.3	298.1
1.50	1047	9659	11580	6.257	9.758	-317.9	-348.6	-656.8	429.0

Table 4-42 Coefficient of Shear Viscosity.

Substance: Argon
Radial Distribution Function: Percus-Yevick
Remarks: ζ_s^{RG}

Intermolecular Potential: Barker-Bobetic
Temperature: 328.15°K

ρ^*	ρ Amagat	P_{CAL} bar	P_{OBS} bar	ζ_s^{RG} $\times 10^{13}$kg/sec	η_k	η_v	$\eta_v(R>\sigma)$	η_{CAL}	η_{OBS}
					← $\times 10^6$ kgm/m sec →				
0.15	104.7	123.3	124.4	1.315	3.053	1.044	.1006	4.198	27.76
0.30	209.4	251.0	255.9	1.896	4.312	4.011	.5023	8.825	33.17
0.45	314.1	411.5	421.4	2.387	5.297	8.933	1.232	15.46	41.28
0.60	418.8	650.9	665.8	2.859	6.144	15.67	2.168	23.99	53.67
0.75	523.5	1044	1068	3.343	6.917	23.39	2.695	33.01	72.59
0.90	628.2	1703	1759	3.850	7.675	29.45	.8305	37.96	101.0
1.05	732.9	2783	2947	4.382	8.467	27.36	-8.331	27.50	142.5
1.20	837.5	449.5	4927	4.938	9.334	2.878	-35.51	-23.30	201.6
1.35	942.2	7105	8066	5.504	10.31	-72.96	-101.9	-164.5	283.1
1.50	1047	10970	12890	6.065	11.42	-259.6	-248.7	-496.9	392.9

Table 4-43 Coefficient of Shear Viscosity.

Substance: Argon
Radial Distribution Function: Percus Yevick
Remarks: ζ_s^{RG}

Intermolecular Potential: Barker Bobetic
Temperature: 373.15°

ρ^*	ρ Amagat	P_{CAL} bar	P_{OBS} bar	ζ_s^{RG} $\times 10^{13}$kg/sec	η_k	η_v	$\eta_v(R>\sigma)$	η_{CAL}	η_{OBS}
					← $\times 10^6$ kgm/m sec →				
0.15	104.7	144.5	145.5	1.295	3.493	1.135	.0766	4.705	30.22
0.30	209.4	302.1	306.6	1.872	4.903	4.364	.3922	9.659	35.41
0.45	314.1	503.8	513.6	2.363	5.996	9.744	.9828	16.72	43.65
0.60	418.8	800.0	816.3	2.835	6.933	17.16	1.746	25.84	56.59
0.75	523.5	1270	1299	3.313	7.793	25.82	2.141	35.75	76.20
0.90	628.2	2030	2103	3.810	8.636	33.21	.5163	42.36	104.7
1.05	732.9	3147	3424	4.327	9.514	33.35	-7.078	35.79	144.7
1.20	837.5	5112	5577	4.861	10.47	13.39	-29.00	-5.144	198.9
1.35	942.2	7924	8915	5.400	11.53	-52.06	-89.19	-121.7	270.5
1.50	1047	12030	13970	5.928	12.72	-213.7	-193.7	-394.6	362.9

Table 4-44 Coefficient of Shear Viscosity.

Substance: Argon
Radial Distribution Function: Kirkwood
Remarks: ζ_s^{ss}

Intermolecular Potential: Lennard-Jones
Temperature: 273°K

λ	ζ_s^{ss} $\times 10^{13}$ kg/sec	η_k	η_v	$\eta_v(R>\sigma)$	η_{TOT}
		←		$\times 10^6$ kgm/m sec	→
0.5	2.612	.4832	.1136	.0375	.6344
1.0	5.170	.5043	.4015	.2828	1.189
1.5	7.412	.5444	.8225	.8683	2.235
2.0	9.142	.6066	1.331	1.814	3.752
2.5	10.27	.6952	1.893	3.037	5.625
3.0	10.80	.8158	2.481	4.394	7.692
3.5	10.82	.9761	3.144	5.734	9.854
4.0	10.44	1.185	3.877	6.937	12.00
4.5	9.812	1.453	4.743	7.929	14.12
5.0	9.033	1.792	5.798	8.681	16.27
5.5	8.193	2.214	7.103	9.197	18.51
6.0	7.358	2.734	8.722	9.496	20.95
6.5	6.563	3.363	10.71	9.607	23.68
7.0	5.831	4.112	13.14	9.556	26.80
7.5	5.171	4.988	16.05	9.366	30.41
8.0	4.585	5.996	19.52	9.058	34.57
8.5	4.068	7.134	23.58	8.648	39.36
9.0	3.615	8.394	28.28	8.151	44.83
9.5	3.218	9.765	33.67	7.584	51.02
10.0	2.874	11.23	39.77	6.965	57.97
10.5	2.573	12.77	46.58	6.315	65.66
11.0	2.310	14.35	54.10	5.665	74.11
11.5	2.080	15.96	62.25	5.054	83.28
12.0	1.879	17.58	70.97	4.544	93.10
12.5	1.704	19.19	80.07	4.232	103.5
13.0	1.551	20.76	89.27	4.291	114.3

Table 4-45 Coefficient of Shear Viscosity.

Substance: Argon
Radial Distribution Function: Kirkwood
Remarks: ζ_s^{ss}

Intermolecular Potential: Lennard-Jones
Temperature: 308°K

λ	ζ_s^{ss} $\times 10^{13}$ kg/sec	η_k	η_v	$\eta_v(R>\sigma)$	η_{TOT}
		←	$\times 10^6$ kgm/m sec		→
0.5	2.027	.6975	.1288	.0226	.8489
1.0	4.027	.7251	.4567	.1707	1.353
1.5	5.797	.7796	.9541	.5274	2.261
2.0	7.182	.8646	1.584	1.110	3.559
2.5	8.103	.9859	2.316	1.875	5.178
3.0	8.562	1.151	3.136	2.740	7.027
3.5	8.617	1.369	4.051	3.614	9.035
4.0	8.361	1.651	5.094	4.421	11.17
4.5	7.892	2.012	6.316	5.108	13.44
5.0	7.297	2.464	7.778	5.647	15.89
5.5	6.646	3.023	9.551	6.032	18.61
6.0	5.989	3.703	11.71	6.267	21.68
6.5	5.359	4.517	14.31	6.365	25.19
7.0	4.774	5.474	17.44	6.338	29.25
7.5	4.242	6.578	21.16	6.202	33.94
8.0	3.767	7.826	25.53	5.968	39.33
8.5	3.346	9.211	30.61	5.649	45.47
9.0	2.975	10.72	36.43	5.257	52.40
9.5	2.650	12.32	43.04	4.805	60.17
10.0	2.366	13.99	50.46	4.306	68.76
10.5	2.118	15.72	58.68	3.775	78.17
11.0	1.901	17.46	67.70	3.231	88.39
11.5	1.711	19.19	77.47	2.701	99.36
12.0	1.545	20.90	87.91	2.218	111.0
12.5	1.400	22.57	98.88	1.836	123.3
13.0	1.273	24.19	110.2	1.648	136.0
13.5	1.163	25.75	121.4	1.823	149.0

Table 4-46 Coefficient of Shear Viscosity.

Substance: Argon
Radial Distribution Function: Kirkwood
Remarks: ζ_s^{ss}

Intermolecular Potential: Lennard-Jones
Temperature: 328°K

λ	ζ_s^{ss} $\times 10^{13}$kg/sec	η_k	η_v	$\eta_v(R>\sigma)$	η_{TOT}
		←		$\times 10^6$ kgm/m sec	→
0.5	1.782	.8407	.1378	.0174	.9959
1.0	3.549	.8723	.4863	.1320	1.491
1.5	5.120	.9356	1.021	.4096	2.367
2.0	6.356	1.035	1.711	.8664	3.613
2.5	7.188	1.177	2.527	1.471	5.175
3.0	7.162	1.370	3.456	2.161	6.988
3.5	7.679	1.625	4.509	2.866	9.000
4.0	7.466	1.955	5.718	3.523	11.20
4.5	7.061	2.373	7.136	4.090	13.60
5.0	6.541	2.896	8.827	4.540	16.26
5.5	5.967	3.540	10.86	4.865	19.27
6.0	5.385	4.318	13.32	5.065	22.71
6.5	4.824	5.243	16.28	5.148	26.67
7.0	4.302	6.323	19.81	5.125	31.26
7.5	3.826	7.558	23.98	5.005	36.54
8.0	3.399	8.941	28.85	4.799	42.59
8.5	3.019	10.46	34.47	4.518	49.45
9.0	2.685	12.09	40.90	4.173	57.16
9.5	2.391	13.81	48.15	3.713	65.73
10.0	2.135	15.58	56.26	3.331	75.17
10.5	1.911	17.39	65.21	2.859	85.46
11.0	1.714	19.19	75.00	2.372	96.57
11.5	1.542	20.97	85.59	1.890	108.5

Table 4-47 Coefficient of Shear Viscosity.

Substance: Argon
Radial Distribution Function: Kirkwood
Remarks: ζ_s^{ss}

Intermolecular Potential: Lennard-Jones
Temperature: 373°K

λ	ζ_s^{ss}	η_k	η_v	$\eta_v(R>\sigma)$	η_{TOT}
	$\times 10^{13}$ kg/sec	←		$\times 10^6$ kgm/m sec	→
0.5	1.380	1.220	.1589	.0103	1.389
1.0	2.759	1.261	.5516	.0790	1.891
1.5	3.998	1.346	1.164	.2475	2.757
2.0	4.985	1.482	1.972	.5289	3.983
2.5	5.660	1.677	2.957	.9076	5.542
3.0	6.019	1.942	4.112	1.348	7.402
3.5	6.095	2.289	5.452	1.805	9.547
4.0	5.948	2.736	7.013	2.241	11.99
4.5	5.644	3.299	8.852	2.622	14.77
5.0	5.244	3.996	11.04	2.930	17.97
5.5	4.797	4.843	13.66	3.153	21.65
6.0	4.338	5.855	16.78	3.291	25.93
6.5	3.893	7.038	20.50	3.346	30.89
7.0	3.476	8.395	24.89	3.322	36.60
7.5	3.094	9.916	30.01	3.227	43.15
8.0	2.750	11.58	35.93	3.068	50.58
8.5	2.443	13.37	42.70	2.853	58.92
9.0	2.173	15.25	50.35	2.589	68.19
9.5	1.934	17.18	58.92	2.284	78.38
10.0	1.726	19.12	68.41	1.946	89.48

Table 4-48 Coefficient of Shear Viscosity

Substance: Argon Intermoledular Potential: Lennard-Jones

Radial Distribution Function: Percus-Yevick

Remarks: ζ_s^{ss} Temperature: 273.15°

ρ^*	ζ_s^{ss}	η_k	η_v	$\eta_v(R>\sigma)$	η_{TOT}
	$\times 10^{13}$kg/sec	←	$\times 10^6$ kgm/m sec		→
0.15	8.779	.5919	1.192	1.501	3.285
0.30	10.96	1.059	2.825	5.769	9.653
0.45	8.749	2.201	3.068	7.502	12.77
0.60	6.217	4.473	1.598	3.688	9.759
0.75	4.392	8.185	-2.485	-9.409	-3.709
0.90	3.159	13.13	-12.67	-38.20	-3.773
1.05	2.290	18.57	-36.71	-92.05	-110.2
1.20	1.637	23.77	-94.68	-191.1	-262.1
			328.2°		
0.15	6.115	1.008	1.529	.7243	3.262
0.30	7.846	1.747	4.683	3.006	9.436
0.45	6.351	3.521	8.736	4.085	16.34
0.60	4.498	6.890	15.60	1.890	24.38
0.75	3.129	11.94	27.88	-5.393	34.43
0.90	2.203	17.88	47.50	-20.33	45.04
1.05	1.560	23.63	74.91	-46.39	52.15
1.20	1.081	28.67	108.6	-87.33	49.92

Table 4-4 Coefficient of Shear Viscosity

Substance: Argon Intermoledular Potential: Lennard-Jones

Radial Distribution Function: Percus-Yevick

Remarks: ζ_s^{ss} Temperature: 373.2°K

ρ^*	ζ_s^{ss} $\times 10^{13}$ kg/sec	η_k	η_v	$\eta_v(R>\sigma)$	η_{TOT}
		←		$\times 10^6$ kgm/m sec	→
0.15	5.797	1.444	1.764	.4438	3.651
0.30	6.242	2.452	5.946	1.928	10.33
0.45	5.079	4.827	12.61	2.670	20.11
0.60	3.584	9.137	24.75	1.174	35.06
0.75	2.465	15.13	46.36	-3.611	57.87
0.90	1.709	21.56	81.13	-12.93	89.76
1.05	1.189	27.33	132.8	-28.17	131.9
1.20	.8103	32.15	203.9	-50.77	185.2

Table 4-50 Coefficient of Shear Viscosity

Substance: Argon | Intermoledular Potential: Lennard-Jones, Truncated

Radial Distribution Function: Percus-Yevick

Remarks: ζ_s^{ss} | Temperature: 273.15°

ρ^*	ζ_s^{ss} $\times 10^{13}$ kg/sec	η_k	η_v	$\eta_v(R>\sigma)$	η_{TOT}
		←		$\times 10^6$ kgm/m sec	→
0.15	9.011	.5775	1.044	1.532	3.153
0.30	11.74	.9958	.5437	6.159	7.698
0.45	9.940	1.981	-7.023	8.102	3.060
0.60	7.613	3.849	-29.92	1.464	-24.61
0.75	5.923	6.781	-94.40	-2.568	-113.3

Table 4-51 Coefficient of Shear Viscosity

Substance: Argon Intermoledular Potential: Barker-Bobetic

Radial Distribution function: Kirkwood

Remarks: ζ_s^{ss} Temperature: 273°K

λ	ζ_s^{ss} $\times 10^{13}$ kg/sec	η_k	η_v	$\eta_v(R>\sigma)$	η_{TOT}
		← $\times 10^6$ kgm/m sec →			
0.5	5.941	.2248	.1020	.0952	.4220
1.0	11.74	.2351	.3360	.7113	1.282
1.5	16.75	.2551	.5893	2.167	3.011
2.0	20.53	.2865	.7306	4.491	5.508
2.5	22.89	.3314	.6448	7.461	8.438
3.0	23.87	.3932	.2601	10.72	11.38
3.5	23.72	.4759	-.4401	13.91	13.95
4.0	22.74	.5848	-1.424	16.74	15.90
4.5	21.22	.7261	-2.623	19.04	17.14
5.0	19.43	.9072	-3.956	20.72	17.67
5.5	17.55	1.136	-5.330	21.78	17.58
6.0	15.71	1.423	-6.661	22.23	16.99
6.5	13.98	1.777	-7.864	22.14	16.05
7.0	12.40	2.209	-8.859	21.54	14.89
7.5	10.99	2.728	-9.565	20.49	13.66
8.0	9.743	3.344	-9.908	19.05	12.49
8.5	8.646	4.065	-9.816	17.28	11.53
9.0	7.686	4.896	-9.219	15.24	10.92

Table 4-52 Coefficient of Shear Viscosity

Substance: Argon — Intermoledular Potential: Barker-Bobetic

Radial Distribution function: Kirkwood

Remarks: ζ_s^{ss} — Temperature: 308°K

λ	ζ_s^{ss} $\times 10^{13}$ kg/sec	η_k	η_v	$\eta_v(R>\sigma)$	η_{TOT}
		← $\times 10^6$ kgm/m sec →			
0.5	4.634	.3241	.1155	.0576	.4972
1.0	9.200	.3374	.4002	.4347	1.172
1.5	13.20	.3643	.7618	1.337	2.463
2.0	16.26	.4070	1.083	2.801	4.291
2.5	18.22	.4685	1.252	4.705	6.426
3.0	19.10	.5530	1.195	6.835	8.583
3.5	19.08	.6661	.8910	8.958	10.52
4.0	18.37	.8145	.3699	10.88	12.06
4.5	17.22	1.007	-.2989	12.45	13.16
5.0	15.83	1.252	-1.022	13.62	13.85
5.5	14.34	1.561	-1.695	14.34	14.20
6.0	12.87	1.945	-2.214	14.62	14.35
6.5	11.48	2.418	-2.477	14.48	14.42
7.0	10.20	2.990	-2.388	13.95	14.55
7.5	9.052	3.674	-1.856	13.07	14.89
8.0	8.028	4.477	-.1923	11.88	15.56
8.5	7.126	5.408	.8729	10.42	16.70
9.0	6.334	6.466	3.213	8.742	18.43

Table 4-53 Coefficient of Shear Viscosity

Substance: Argon — Intermoledular Potential: Barker-Bobetic

Radial Distribution function: Kirkwood — Temperature: 323°K

Remarks: ζ_s^{ss}

λ	ζ_s^{ss} $\times 10^{13}$ kg/sec	η_k	η_v	$\eta_v(R>\sigma)$	η_{TOT}
		← $\times 10^6$ kgm/m sec →			
0.5	4.212	.3734	.1209	.0475	.5417
1.0	8.377	.3880	.4237	.3594	1.171
1.5	12.04	.4182	.8234	1.110	2.352
2.0	14.86	.4663	1.208	2.335	4.010
2.5	16.69	.5358	1.471	3.939	5.946
3.0	17.53	.6313	1.540	5.744	7.916
3.5	17.53	.7590	1.393	7.556	9.707
4.0	16.91	.9265	1.061	9.200	11.19
4.5	15.87	1.143	.6158	10.56	12.32
5.0	14.60	1.419	.1544	11.56	13.13
5.5	13.25	1.766	-.2154	12.17	13.72
6.0	11.90	2.197	-.3841	12.39	14.20
6.5	10.62	2.726	-2.453	12.23	14.71
7.0	9.441	3.364	.3010	11.73	15.40
7.5	8.378	4.123	1.352	10.92	16.39
8.0	7.431	5.012	2.993	9.818	17.82
8.5	6.595	6.036	5.303	8.479	19.82
9.0	5.862	7.195	8.348	6.943	22.49

Table 4-54 Coefficient of Shear Viscosity

Substance: Argon Intermoledular Potential: Barker-Bobetic

Radial Distribution function: Kirkwood

Remarks: ζ_s^{ss} Temperature: 328°K

λ	ζ_s^{ss} $\times 10^{13}$ kg/sec	η_k	η_v	$\eta_v(R>\sigma)$	η_{TOT}
		←		$\times 10^6$ kgm/m sec	→
0.5	4.085	.3907	.1227	.0446	.5580
1.0	8.130	.4058	.4312	.3381	1.175
1.5	11.69	.4371	.8428	1.046	2.326
2.0	14.44	.4871	1.248	2.203	3.938
2.5	16.22	.5594	1.541	3.721	5.821
3.0	17.05	.6587	1.649	5.433	7.741
3.5	17.06	.7915	1.553	7.153	9.498
4.0	16.46	.9656	1.283	8.718	10.97
4.5	15.46	1.191	.9117	10.01	12.11
5.0	14.23	1.477	.5369	10.96	12.97
5.5	12.91	1.838	.2676	11.54	13.64
6.0	11.60	2.285	.2148	11.74	14.24
6.5	10.35	2.833	.4862	11.58	14.90
7.0	9.027	3.494	1.183	11.09	15.77
7.5	8.170	4.279	2,404	10.30	16.98
8.0	7.247	5.197	4.234	9.227	18.66
8.5	6.432	6.252	6.754	7.927	20.93
9.0	5.716	7.445	10.03	6.435	23.91

Table 4-55 Coefficient of Shear Viscosity

Substance: Argon — Intermoledular Potential: Barker-Bobetic

Radial Distribution function: Kirkwood

Remarks: ζ_s^{ss} — Temperature: 373°K

λ	ζ_s^{ss} $\times 10^{13}$ kg/sec	η_k	η_v	$\eta_v(R>\sigma)$	η_{TOT}
		← $\times 10^6$ kgm/m sec →			
0.5	3.177	.5683	.1385	.0266	.7334
1.0	6.353	.5874	.4934	.2043	1.285
1.5	9.180	.6299	.9999	.6391	2.269
2.0	11.39	.6988	1.566	1.362	3.626
2.5	12.85	.7988	2.100	2.325	5.223
3.0	13.56	.9365	2.539	3.427	6.903
3.5	13.62	1.120	2.871	4.548	8.540
4.0	13.19	1.361	3.132	5.577	10.07
4.5	12.42	1.670	3.400	6.428	11.50
5.0	11.46	2.063	3.778	7.046	12.89
5.5	10.45	2.554	4.384	7.404	14.34
6.0	9.372	3.159	5.337	7.494	15.99
6.5	8.373	3.894	6.757	7.324	17.98
7.0	7.448	4.772	8.750	6.910	20.43
7.5	6.610	5.803	11.42	6.274	23.49
8.0	5.861	6.991	14.85	5.440	27.28
8.5	5.199	8.334	19.13	4.436	31.90
9.0	4.617	9.826	24.32	3.290	37.43

Table 4-56 Coefficient of Shear Viscosity

Substance: Argon Intermolecular Potential: Lennard-Jones

Radial Distribution Function: Kirkwood

Remarks: ζ_s^H Temperature: 180°K

λ	ζ_s^H $\times 10^{13}$ kg/sec	η_k	η_v	$\eta_v(R>\sigma)$	η_{TOT}
		← $\times 10^6$ kgm/m sec →			
1.0	.1682	6.878	.7933	.0241	7.6955
2.0	.3381	7.239	2.334	.1930	9.7656
3.0	.5591	7.065	4.775	1.032	12.87
4.0	.8853	6.604	8.346	4.386	19.34
5.0	1.060	7.275	12.14	6.612	26.03
6.0	1.209	8.003	16.40	8.355	32.75
7.0	1.345	8.732	21.15	9.441	39.33
8.0	1.476	9.435	26.38	9.800	45.62
9.0	1.631	10.02	31.91	10.13	52.06
10.0	1.865	10.33	36.82	12.38	59.54
11.0	2.177	10.47	38.99	16.81	66.27

Table 4-57 Coefficient of Shear Viscosity

Substance: Argon Intermolecular Potential: Lennard-Jones

Radial Distribution Function: Kirkwood

Remarks: ζ_s^H Temperature: 273°K

λ	ζ_s^H $\times 10^{13}$ kg/sec	η_k	η_v	$\eta_v(R>\sigma)$	η_{TOT}
		←	$\times 10^6$ kgm/m sec		→
0.5	.0501	12.52	.5196	.0001	13.04
1.0	.1001	12.86	1.271	.0055	14.14
1.5	.1502	13.21	2.260	.0176	15.48
2.0	.2008	13.53	3.492	.0398	17.07
2.5	.2519	13.85	4.976	.0745	18.90
3.0	.3040	14.16	6.717	.1237	21.00
3.5	.3572	14.45	8.726	.1893	23.37
4.0	.4118	14.73	11.01	.2735	26.02
4.5	.4682	15.00	13.58	.3783	28.96
5.0	.5266	15.26	16.44	.5061	32.31
5.5	.5874	15.50	19.61	.6593	35.77
6.0	.6510	15.74	23.08	.8402	39.66
6.5	.7175	15.96	26.86	1.050	43.87
7.0	.7874	16.18	30.94	1.290	48.41
7.5	.8610	16.39	35.31	1.559	53.26
8.0	.9384	16.60	39.93	1.854	58.34
8.5	1.020	16.81	44.76	2.169	63.74
9.0	1.106	17.01	49.73	2.495	69.24
9.5	1.198	17.21	54.75	2.822	74.78
10.0	1.295	17.41	59.68	3.138	80.23
10.5	1.398	17.61	64.34	3.432	85.39
11.0	1.509	17.80	68.52	3.700	90.02
11.5	1.628	17.98	71.88	3.955	93.82
12.0	1.757	18.14	74.03	4.250	96.41
12.5	1.900	18.27	74.33	4.720	97.32
13.0	2.060	18.36	71.89	5.700	95.95

Table 4-58 Coefficient of Shear Viscosity

Substance: Argon Intermolecular Potential: Lennard-Jones

Radial Distribution Function: Kirkwood

Remarks: ζ_s^H Temperature: 308°K

λ	ζ_s^H $\times 10^{13}$ kg/sec	η_k	η_v	$\eta_v(R>\sigma)$	η_{TOT}
		← $\times 10^6$ kgm/m sec →			
0.5	.0044	14.52	.5929	.0005	15.12
1.0	.0880	14.89	1.433	.0037	16.32
1.5	.1325	15.24	2.527	.0121	17.78
2.0	.1777	15.58	3.884	.0275	19.49
2.5	.2237	15.90	5.513	.0518	21.47
3.0	.2707	16.21	7.423	.0867	23.72
3.5	.3191	16.51	9.628	.1338	26.27
4.0	.3690	16.80	12.14	.1951	29.13
4.5	.4207	17.07	14.97	.2723	32.31
5.0	.4745	17.33	18.13	.3672	35.83
5.5	.5306	17.59	21.63	.4816	39.70
6.0	.5892	17.83	25.48	.6165	43.93
6.5	.6505	18.07	29.69	.7726	48.53
7.0	.7148	18.31	34.25	.9491	53.51
7.5	.7823	18.54	39.15	1.144	58.84
8.0	.8532	18.78	44.37	1.352	64.50
8.5	.9277	19.01	49.86	1.566	70.44
9.0	1.006	19.25	55.57	1.778	76.60
9.5	1.089	19.49	61.41	1.974	82.87
10.0	1.176	19.73	67.26	2.141	89.13
10.5	1.269	19.98	72.96	2.262	95.19
11.0	1.368	20.21	78.30	2.326	100.8
11.5	1.474	20.45	83.01	2.327	105.8
12.0	1.589	20.66	86.71	2.281	109.6
12.5	1.715	20.86	88.86	2.249	112.0
13.0	1.854	21.02	88.71	2.400	112.1
13.5	2.011	21.13	85.03	3.152	109.3

Table 4-59 Coefficient of Shear Viscosity

Substance: Argon Intermolecular Potential: Lennard-Jones

Radial Distribution Function: Kirkwood

Remarks: ζ_s^H Temperature: 328°K

λ	ζ_s^H $\times 10^{13}$ kg/sec	η_k	η_v	$\eta_v(R>\sigma)$	η_{TOT}
		← $\times 10^6$ kgm/m sec →			
0.5	.0411	15.62	.6329	.0004	16.25
1.0	.0825	15.98	1.521	.0031	17.51
1.5	.1245	16.34	2.672	.0100	19.02
2.0	.1672	16.68	4.097	.0228	20.80
2.5	.2108	17.01	5.804	.0431	22.86
3.0	.2556	17.32	7.807	.0725	25.20
3.5	.3016	17.62	10.11	.1126	27.85
4.0	.3493	17.91	12.75	.1648	30.83
4.5	.3988	18.19	15.72	.2310	34.14
5.0	.4503	18.46	19.04	.3125	37.81
5.5	.5039	18.71	22.73	.4108	41.85
6.0	.5600	18.97	26.78	.5267	46.28
6.5	.6188	19.22	31.22	.6603	51.10
7.0	.6802	19.46	36.04	.8104	56.32
7.5	.7447	19.71	41.23	.9742	61.92
8.0	.8123	19.96	46.77	1.147	67.88
8.5	.8833	20.21	52.63	1.322	74.16
9.0	.9578	20.47	58.74	1.489	80.70
9.5	1.036	20.73	65.02	1.635	87.39
10.0	1.119	21.00	71.37	1.746	94.12
10.5	1.207	21.27	77.64	1.806	100.7
11.0	1.300	21.53	83.63	1.799	107.0
11.5	1.400	21.79	89.08	1.715	112.6

Table 4-60 Coefficient of Shear Viscosity

Substance: Argon Intermolecular Potential: Lennard-Jones

Radial Distribution Function: Kirkwood

Remarks: ζ_s^H Temperature: 373°K

λ	ζ_s^H $\times 10^{13}$ kg/sec	η_k	η_v	$\eta_v(R>\sigma)$	η_{TOT}
		←	$\times 10^6$ kgm/m sec		→
0.5	.0361	17.95	.7182	.0003	18.66
1.0	.0728	18.32	1.709	.0021	20.03
1.5	.1101	18.68	2.982	.0068	21.67
2.0	.1484	19.02	4.550	.0157	23.59
2.5	.1876	19.36	6.425	.0301	25.81
3.0	.2281	19.67	8.623	.0511	28.35
3.5	.2700	19.98	11.16	.0800	31.22
4.0	.3135	20.27	14.05	.1181	34.45
4.5	.3586	20.56	17.32	.1666	38.05
5.0	.4057	20.84	20.98	.2266	42.05
5.5	.4548	21.11	25.05	.2990	46.46
6.0	.5061	21.38	29.54	.3840	51.31
6.5	.5596	21.66	34.47	.4809	56.61
7.0	.6156	21.93	39.84	.5884	62.36
7.5	.6741	22.21	45.64	.7033	68.55
8.0	.7354	22.49	51.86	.8206	75.17
8.5	.7995	22.78	58.47	.9336	82.19
9.0	.8666	23.08	65.44	1.033	89.55
9.5	.9370	23.39	72.68	1.106	97.17
10.0	1.011	23.70	80.10	1.140	104.9

Table 4-61 Coefficient of Shear Viscosity

Substance: Argon Intermolecular Potential: Lennard-Jones

Radial Distribution Function: Kirkwood

Remarks: ζ_s^H Temperature: 500°K

λ	ζ_s^H $\times 10^{13}$ kg/sec	η_k	η_v	$\eta_v(R>\sigma)$	η_{TOT}
		← $\times 10^6$ kgm/m sec →			
0.5	.0276	23.71	.9298	.0001	24.64
1.0	.0559	24.08	2.174	.0009	26.26
1.5	.0851	24.45	3.749	.0030	28.20
2.0	.1154	24.80	5.673	.0071	30.47
2.5	.1467	25.14	7.964	.0138	33.18
3.0	.1793	25.47	10.65	.0240	36.14
3.5	.2131	25.79	13.74	.0382	39.57
4.0	.2484	26.12	17.28	.0572	43.45
4.5	.2851	26.44	21.28	.0816	47.79
5.0	.3234	26.76	25.77	.1117	52.64
5.5	.3632	27.08	30.77	.1479	58.00
6.0	.4047	27.42	36.32	.1897	63.92
6.5	.4480	27.76	42.43	.2363	70.42
7.0	.4929	28.11	49.11	.2860	77.51
7.5	.5396	28.47	56.39	.3363	85.19
8.0	.5882	28.85	64.25	.3832	93.48
8.5	.6387	29.24	72.66	.4197	102.3
9.0	.6911	29.65	81.70	.4448	111.8
9.5	.7457	30.07	91.23	.4441	121.7
10.0	.8027	30.50	101.2	.4090	132.1
10.5	.8622	30.94	111.6	.3270	142.9
11.0	.9247	31.40	122.3	.1832	153.9
11.5	.9907	31.86	133.1	-.0392	164.9
12.0	1.061	32.33	143.9	-.3583	175.8
12.5	1.136	32.79	154.3	-.7923	186.3

Table 4-62 Coefficient of Shear Viscosity

Substance: Argon Intermolecular Potential: Lennard-Jones

Radial Distribution Function: Kirkwood

Remarks: ζ_s^H Temperature: 600°K

λ	ζ_s^H $\times 10^{13}$ kg/sec	η_k	η_v	$\eta_v(R>\sigma)$	η_{TOT}
		←		$\times 10^6$ kgm/m sec	→
0.5	.0236	27.60	1.073	.0001	28.68
1.0	.0480	27.98	2.491	.0005	30.47
1.5	.0734	28.35	4.272	.0019	32.62
2.0	.0998	28.71	6.438	.0044	35.15
2.5	.1272	29.06	9.014	.0087	38.08
3.0	.1557	29.41	12.02	.0153	41.45
3.5	.1855	29.76	15.50	.0245	45.28
4.0	.2165	30.11	19.47	.0370	49.61
4.5	.2488	30.47	23.96	.0530	54.48
5.0	.2824	30.83	29.00	.0727	59.90
5.5	.3173	31.20	34.63	.0963	65.93
6.0	.3536	31.58	40.88	.1232	72.58
6.5	.3913	31.98	47.76	.1527	79.89
7.0	.4304	32.39	55.29	.1829	87.86
7.5	.4709	32.81	63.52	.2125	96.55
8.0	.5128	33.26	72.45	.2385	106.0
8.5	.5562	33.72	82.08	.2568	116.1
9.0	.6011	34.20	92.40	.2619	126.9
9.5	.6476	34.70	103.4	.2469	138.3
10.0	.6958	35.21	115.1	.2077	150.5
10.5	.7460	35.74	127.3	.1297	163.2
11.0	.7984	36.29	140.1	.0036	176.4
11.5	.8532	36.84	153.2	-.1841	190.0
12.0	.9111	37.41	166.7	-.4488	203.7
12.5	.9727	37.97	180.2	-.8080	217.4
13.0	1.039	38.54	193.6	-1.281	230.8
13.5	1.111	39.10	206.3	-1.885	243.5
14.0	1.190	39.64	217.9	-2.629	254.9

Table 4-63 Coefficient of Shear Viscosity

Substance: Nitrogen Intermolecular Potential: Lennard-Jones

Radial Distribution Function: Kirkwood

Remarks: ζ_s^H Temperature: 180°K

λ	ζ_s^H $\times 10^{13}$ kg/sec	η_k	η_v	$\eta_v(R>\sigma)$	η_{TOT}
		← $\times 10^6$ kgm/m sec →			
1.0	.0597	7.407	.7275	.0028	8.137
2.0	.1199	7.783	1.993	.0206	9.796
3.0	.1818	8.133	3.829	.0642	12.03
4.0	.2466	8.456	6.272	.1424	14.87
5.0	.3157	8.750	9.366	.2646	18.38
6.0	.3906	9.019	13.15	.4404	22.61
7.0	.4729	9.269	17.64	.6770	27.58
8.0	.5638	9.508	22.79	.9714	33.27
9.0	.6648	9.744	28.41	1.302	39.46
10.0	.7779	9.978	34.16	1.624	45.75
11.0	.9060	10.20	39.33	1.887	51.42
12.0	1.055	10.41	42.72	2.112	55.24
13.0	1.235	10.54	41.99	2.736	55.27

Table 4-64 Coefficient of Shear Viscosity

Substance: Nitrogen Intermolecular Potential: Lennard-Jones

Radial Distribution Function: Kirkwood

Remarks: ζ_s^H Temperature: 273°K

λ	ζ_s^H $\times 10^{13}$ kg/sec	η_k	η_v	$\eta_v(R>\sigma)$	η_{TOT}
		← $\times 10^6$ kgm/m sec →			
0.5	.0196	11.39	.4513	.0001	11.84
1.0	.0396	11.60	1.065	.0008	12.67
1.5	.0600	11.80	1.847	.0026	13.65
2.0	.0811	12.00	2.807	.0062	14.81
2.5	.1028	12.18	3.953	.0119	16.15
3.0	.1254	12.36	5.296	.0203	17.68
3.5	.1487	12.54	6.845	.0321	19.41
4.0	.1730	12.71	8.614	.0477	21.37
4.5	.1982	12.87	10.61	.0677	23.55
5.0	.2246	13.04	12.85	.0925	25.99
5.5	.2520	13.20	15.35	.1222	28.68
6.0	.2807	13.37	18.11	.1570	31.64
6.5	.3106	13.54	21.65	.1963	34.88
7.0	.3418	13.71	24.46	.2391	38.41
7.5	.3743	13.88	28.06	.2838	42.22
8.0	.4802	14.06	31.93	.3279	46.31
8.5	.4435	14.25	36.06	.3678	50.67
9.0	.4805	14.44	40.44	.3989	55.28
9.5	.5191	14.64	45.04	.4153	60.09
10.0	.5595	14.84	49.81	.4098	65.06
10.5	.6020	15.05	54.69	.3739	70.11
11.0	.6468	15.26	59.61	.2980	75.16
11.5	.6944	15.47	64.44	.1721	80.09
12.0	.7453	15.68	69.07	-.0135	84.74
12.5	.8002	15.89	73.26	-.2652	88.89
13.0	.8602	16.09	76.75	-.5804	92.27
13.5	.9267	16.28	79.13	-.9317	94.47

Table 4-65 Coefficient of Shear Viscosity

Substance: Nitrogen Intermolecular Potential: Lennard-Jones

Radial Distribution Function: Kirkwood

Remarks: ζ_s^H Temperature: 308°K

λ	ζ_s^H $\times 10^{13}$ kg/sec	η_k	η_v	$\eta_v(R>\sigma)$	η_{TOT}
		← $\times 10^6$ kgm/m sec →			
0.5	.0171	12.82	.5035	.0001	13.32
1.0	.0347	13.02	1.179	.0005	14.20
1.5	.0530	13.21	2.034	.0017	15.25
2.0	.0718	13.40	3.080	.0041	16.48
2.5	.0913	13.58	4.328	.0081	17.92
3.0	.1116	13.76	5.788	.0140	19.56
3.5	.1327	13.94	7.475	.0224	21.43
4.0	.1548	14.11	9.401	.0335	23.54
4.5	.1776	14.28	11.58	.0478	25.91
5.0	.2015	14.46	14.03	.0655	28.55
5.5	.2263	14.63	16.76	.0867	31.48
6.0	.2522	14.81	19.78	.1112	34.70
6.5	.2791	15.00	23.10	.1385	38.24
7.0	.3071	15.19	26.74	.1675	42.10
7.5	.3362	15.39	30.70	.1967	46.29
8.0	.3664	15.59	34.95	.2228	50.77
8.5	.3978	15.81	39.56	.2457	55.61
9.0	.4305	16.03	44.42	.2568	60.70
9.5	.4644	16.26	49.61	.2565	66.12
10.0	.4998	16.49	55.01	.2341	71.74
10.5	.5367	16.74	60.62	.1835	77.54
11.0	.5755	16.99	66.37	.0958	83.45
11.5	.6164	17.24	72.18	-.0390	89.37
12.0	.6598	17.49	77.92	-.2321	95.18
12.5	.7221	17.65	82.69	-.4165	99.92
13.0	.7745	17.89	87.57	-.7377	104.7
13.5	.8321	18.12	91.62	-1.127	108.6

Table 4-66 Coefficient of Shear Viscosity

Substance: Nitrogen Intermolecular Potential: Lennard-Jones

Radial Distribution Function: Kirkwood

Remarks: ζ_s^H Temperature: 328°K

λ	ζ_s^H $\times 10^{13}$k g/sec	η_k	η_v	$\eta_v(R>\sigma)$	η_{TOT}
		←	$\times 10^6$ kgm/m sec		→
0.5	.1700	13.38	.5246	.0001	13.90
1.0	.3445	13.60	1.227	.0005	14.83
1.5	.5242	13.81	2.116	.0017	15.93
2.0	.7098	14.01	3.200	.0040	17.22
2.5	.9020	14.21	4.492	.0078	18.71
3.0	1.102	14.40	6.004	.0136	20.42
3.5	1.309	14.59	7.747	.0216	22.36
4.0	1.525	14.78	9.737	.0323	24.55
4.5	1.750	14.96	11.99	.0460	27.00
5.0	1.984	15.14	14.52	.0630	29.72
5.5	2.228	15.33	17.33	.0834	32.74
6.0	2.482	15.51	20.45	.1070	36.08
6.5	2.747	15.70	23.89	.1334	39.73
7.0	3.023	15.90	27.66	.1618	43.72
7.5	3.310	16.10	31.75	.1907	48.05
8.0	8.609	16.32	36.18	.2181	52.72
8.5	3.919	16.53	40.94	.2412	57.72
9.0	4.242	16.76	46.02	.2564	63.04
9.5	4.479	16.99	51.39	.2590	68.65
10.0	4.931	17.24	57.04	.2434	74.52
10.5	5.299	17.48	62.90	.2027	80.59
11.0	5.686	17.74	68.92	.1291	86.79
11.5	6.095	18.00	75.01	.0138	93.02
12.0	6.530	18.26	81.06	-.1526	99.16
12.5	6.845	18.60	87.66	-.4502	105.8
13.0	7.332	18.87	93.27	-.7613	111.4
13.5	7.867	19.12	98.19	-1.147	116.2
14.0	8.463	19.36	102.0	-1.589	119.7

Table 4-67 Coefficient of Shear Viscosity

Substance: Nitrogen Intermolecular Potential: Lennard-Jones

Radial Distribution Function: Kirkwood

Remarks: ζ_s^H Temperature: 373°K

λ	ζ_s^H $\times 10^{13}$ kg/sec	η_k	η_v	$\eta_v(R>\sigma)$	η_{TOT}
		← $\times 10^6$ kgm/m sec →			
0.5	.0149	14.99	.5837	$4\times.5^5$	15.57
1.0	.0303	15.20	1.356	.0003	16.56
1.5	.0462	15.41	2.328	.0011	17.74
2.0	.0628	15.61	3.512	.0027	19.12
2.5	.0800	15.80	4.919	.0053	20.73
3.0	.0979	15.99	6.565	.0092	22.57
3.5	.1166	16.19	8.464	.0149	24.66
4.0	.1361	16.38	10.62	.0224	27.03
4.5	.1563	16.57	13.09	.0321	29.69
5.0	.1774	16.77	15.84	.0441	32.66
5.5	.1994	16.97	18.92	.0583	35.95
6.0	.2222	17.18	22.33	.0746	39.59
6.5	.2459	17.39	26.09	.0926	43.58
7.0	.2704	17.62	30.22	.1114	47.84
7.5	.2959	17.85	34.70	.1295	52.68
8.0	.3223	18.09	39.57	.1456	57.80
8.5	.3497	18.34	44.82	.1573	63.32
9.0	.3780	18.60	50.44	.1614	69.20
9.5	.4074	18.87	56.41	.1537	75.44
10.0	.4379	19.15	62.77	.1322	82.05
10.5	.4696	19.43	69.41	.0876	88.93
11.0	.5028	19.72	76.32	.0147	96.06
11.5	.5376	20.03	83.43	-.0944	103.4
12.0	.5744	20.33	90.66	-.2488	110.7
12.5	.6135	20.63	97.89	-.4584	118.1
13.0	.6556	20.94	105.0	-.7338	125.2
13.5	.7015	21.24	111.6	-1.084	131.8
14.0	.7521	21.53	117.5	-1.512	137.5

Table 4-68 Coefficient of Shear Viscosity

Substance: Nitrogen Intermolecular Potential: Lennard-Jones

Radial Distribution Function: Kirkwood

Remarks: ζ_s^H Temperature: 500°K

λ	ζ_s^H $\times 10^{13}$kg/sec	η_k	η_v	$\eta_v(R>\sigma)$	η_{TOT}
		←	$\times 10^6$ kgm/m sec		→
0.5	.0118	18.74	.7221	2×15^5	19.46
1.0	.0241	18.96	1.663	.0001	20.62
1.5	.0369	19.18	2.835	.0005	22.01
2.0	.0503	19.39	4.255	.0013	23.65
2.5	.0643	19.61	5.939	.0026	25.55
3.0	.0789	19.83	7.904	.0046	27.74
3.5	.0941	20.05	10.17	.0074	30.23
4.0	.1099	20.28	12.75	.0113	33.05
4.5	.1264	20.52	15.68	.0162	36.22
5.0	.1435	20.76	18.97	.0223	39.75
5.5	.1612	21.02	22.63	.0295	43.68
6.0	.1796	21.28	26.70	.0375	48.08
6.5	.1986	21.55	31.19	.0461	52.79
7.0	.2181	21.84	36.12	.0548	58.01
7.5	.2383	22.14	41.50	.0639	63.71
8.0	.2592	22.45	47.36	.0693	69.88
8.5	.2806	22.77	53.69	.0724	76.54
9.0	.3026	23.10	60.51	.0705	83.69
9.5	.3252	23.45	67.83	.0617	91.34
10.0	.3486	23.81	75.61	.0422	99.46
10.5	.3727	24.18	83.85	.0086	108.0
11.0	.3976	24.56	92.61	-.0398	117.1
11.5	.4234	24.95	101.8	-.1111	126.6
12.0	.4504	25.34	111.3	-.2100	136.5
12.5	.4787	25.74	121.3	-.3433	146.7
13.0	.5087	26.15	131.4	-.5188	157.1
13.5	.5408	26.55	141.8	-.7462	167.6
14.0	.5756	26.95	152.0	-1.036	178.0
14.5	.6139	27.34	162.0	-1.399	188.0

Table 4-69 Coefficient of Shear Viscosity

Substance: Nitrogen Intermolecular Potential: Lennard-Jones

Radial Distribution Function: Kirkwood

Remarks: ζ_s^H Temperature: 600°K

λ	ζ_s^H $\times 10^{13}$ kg/sec	η_k	η_v	$\eta_v(R>\sigma)$	η_{TOT}
		← $\times 10^6$ kgm/m sec →			
0.5	.0103	21.27	.8160	1×10^{-5}	22.09
1.0	.0211	21.51	1.871	.0001	23.38
1.5	.0324	21.74	3.181	.0003	24.92
2.0	.0442	21.98	4.763	.0008	26.74
2.5	.0565	22.22	6.636	.0017	28.85
3.0	.0693	22.46	8.820	.0030	31.29
3.5	.0827	22.72	11.33	.0049	34.06
4.0	.0967	22.98	14.20	.0074	37.19
4.5	.1111	23.25	17.44	.0107	40.70
5.0	.1262	23.53	21.08	.0147	44.63
5.5	.1417	23.83	25.14	.0193	48.99
6.0	.1577	24.13	29.64	.0245	53.80
6.5	.1742	23.45	34.61	.0301	59.09
7.0	.1912	24.78	40.07	.0356	64.89
7.5	.2087	25.13	46.03	.0404	71.20
8.0	.2267	25.49	52.51	.0440	78.04
8.5	.2450	25.87	59.51	.0446	85.42
9.0	.2639	26.25	67.09	.0422	93.38
9.5	.2831	26.65	75.21	.0346	101.9
10.0	.3029	27.07	83.92	.0203	111.0
10.5	.3232	27.50	93.17	-.0041	120.7
11.0	.3440	27.93	103.0	-.0414	130.8
11.5	.3655	28.38	113.34	-.0916	141.7
12.0	.3877	28.84	124.3	-.1618	153.0
12.5	.4109	29.30	135.7	-.2557	164.8
13.0	.4352	29.77	147.7	-.3791	177.0
13.5	.4609	30.24	160.0	-.5388	189.7
14.0	.4884	30.70	172.6	-.7431	202.6

Table 4-70 Coefficient of Shear Viscosity

Substance: Argon
Radial Distribution Function: Percus-Yevick
Intermolecular Potential: Lennard-Jones
Temperature: 273.2°K, 328.2°K
Remarks: ζ_s^H

ρ^*	ζ_s^H $\times 10^{13}$ kg/sec	η_k	η_v	$\eta_v(R>\sigma)$	η_{TOT}
		←	$\times 10^6$ kgm/m sec		→
			273.2°		
0.15	.1891	13.44	3.191	.0323	16.66
0.30	.3866	14.49	10.04	.2035	24.73
0.45	.6127	15.25	21.41	.5254	37.18
0.60	.8765	15.99	38.06	.5200	54.57
0.75	1.159	17.04	57.91	-2.484	72.47
0.90	1.407	18.69	70.43	-17.01	72.12
1.05	1.525	21.15	51.44	-61.30	11.39
1.20	1.368	24.66	-19.30	-159.8	-154.4
			328.2°		
0.15	.1577	16.55	3.746	.0186	20.31
0.30	.3293	17.56	11.62	.1262	29.30
0.45	.5282	18.34	24.74	.3397	43.41
0.60	.7522	19.16	44.36	.3182	63.84
0.75	.9976	20.35	69.77	-1.719	88.40
0.90	1.203	22.15	94.56	-11.10	105.6
1.05	1.294	24.76	103.9	-38.50	90.20
1.20	1.166	28.32	86.87	-94.23	20.96

Table 4-71 Coefficient of Shear Viscocity

Substance: Argon
Radial Distribution Function: Percus-Yevick
Intermolecular Potential: Lennard-Jones
Temperature: 373.2°K
Remarks: ζ_s^H

ρ^*	ζ_s^H $\times 10^{13}$kg/sec	η_k	η_v	$\eta_v(R>\sigma)$	η_{TOT}
		←	$\times 10^6$ kgm/m sec		→
			373.2°		
0.15	.1400	18.87	4.163	.0130	23.05
0.30	.2958	19.87	12.79	.0914	32.75
0.45	.4772	20.67	27.20	.2509	48.12
0.60	.6845	21.56	48.95	.2243	70.74
0.75	.8992	22.86	78.12	-1.317	99.66
0.90	1.080	24.77	110.5	-8.172	127.1
1.05	1.160	27.47	135.8	-27.48	135.8
1.20	1.043	31.11	148.3	-65.37	114.1

Table 4-72 Coefficient of Shear Viscosity

Substance: Argon
Radial Distribution Function: Percus-Yevick
Intermolecular Potential: Lennard-Jones, Truncated
Temperature: 273.15°K
Remarks: ζ_s^{II}

ρ^*	ζ_s^{II} $\times 10^{13}$ kg/sec	η_k	η_v	$\eta_v(R>\sigma)$	η_{TOT}
		← $\times 10^6$ kgm/m sec →			
0.15	.1924	13.27	3.183	.0327	16.49
0.30	.4045	14.07	10.03	.2121	24.31
0.45	.6648	14.55	21.29	.5419	36.38
0.60	.9941	15.00	36.18	.1912	51.38
0.75	1.389	15.78	43.60	-6.019	53.36
0.90	1.807	17.12	-9.748	-39.51	-32.14

Table 4-73 Coefficient of Shear Viscosity

Substance: Argon Intermolecular Potential: Lennard-Jones

Radial Distribution Function: Percus-Yevick

Remarks: Comparison of Drag Coefficients Temperature: 273.2°K

ρ^*	ζ $\times 10^{13}$ kg/sec	η $\times 10^{6} \leftrightarrow$ kg/msec	η_{OBS}	ζ_{TOTAL}
		Normal ζ		
0.15	1.459	5.279	26.2	
0.30	2.150	12.50	35.3	
0.45	2.807	20.77	50.1	
0.60	3.529	16.84	76.4	
0.75	4.355	-58.02	124	
		Sound Speed ζ		
0.15	9.011	3.153	26.2	
0.30	11.74	7.698	35.3	
0.45	9.940	3.060	50.1	
0.60	7.613	-24.61	76.4	
0.75	5.923	-113.3	124	
		Helfand ζ		
0.15	.1924	16.49	26.2	
0.30	.4045	24.31	35.3	
0.45	.6648	36.38	50.1	
0.60	.9941	51.37	76.4	
0.75	1.389	53.35	124	
0.90	1.807	-32.14	205	
		Force Fit		
	ζ_S	ζ_H		
0.15	.0342	.0328		.067
0.30	.0726	.0656		.138
0.45	.0966	.0984		.195
0.60	.0319	.1312		.163
0.75	-.116	.1640		.048

Table 4-74 Coefficient of Bulk Viscosity

Substance: Argon
Radial Distribution Function: Kirkwood
Intermolecular Potential: Lennard Jones
- Temperatures: 180°K,
Remarks: ζ_s^{RG}

	T = 180°K			T =		
λ	ϕ_V	$\phi_V(R>\sigma)$	ϕ_{TOT}	ϕ_V	$\phi_V(R>\sigma)$	ϕ_{TOT}
	←×10⁶ kgm/m sec→			←×10⁶ kgm/m sec→		
1	1.269	-1.408	-.1388			
2	-31.23	63.84	32.61			
3	-428.8	751.3	322.4			
4	-1111	1620	509.3			
5	452.3	-562.0	-109.7			
6	1514	-1925	-411.1			
7	2763	-3469	-705.8			
8	3725	-4596	-870.8			
9	3082	-3694	-611.7			
10	1054	-1264	-209.7			
11	-1503	1260	-243.7			

Table 4-75. Coefficient of Bulk Viscosity

Substance: Argon
Radial Distribution Function: Kirkwood
Intermolecular Potential: Lennard Jones
- Temperatures: 273°, 308°
Remarks: ζ_s^{RG}

	T = 273°				T = 308°		
λ	ϕ_V	$\phi_V(R>\sigma)$	ϕ_{TOT}	ϕ_{OBS}	ϕ_V	$\phi_V(R>\sigma)$	ϕ_{TOT}
	←×10⁶ kgm/m sec→				←×10⁶ kgm/m sec→		
0.5	.0977	.0964	.1942	-	.1201	.0711	.1911
1.0	.3015	.4990	.8005	-	.4104	.3626	.7729
1.5	.5720	1.239	1.811	.1	.8407	.8931	1.734
2.0	.9326	2.254	3.187	1.3	1.414	1.629	3.043
2.5	1.434	3.436	4.870	3.2	2.121	2.531	4.652
3.0	2.111	4.676	6.787	5.6	2.903	3.586	6.489
3.5	2.914	5.931	8.846	8.6	3.602	4.840	8.442
4.0	3.641	7.279	10.92	12	3.925	6.412	10.34
4.5	3.867	8.949	12.82	17	3.417	8.493	11.91
5.0	2.926	11.31	14.23	21	1.459	11.32	12.78
5.5	-.0773	14.78	14.70	27	-2.732	15.13	12.40
6.0	-6.215	19.78	13.57	33	-10.08	20.14	10.06
6.5	-16.69	26.63	9.938	39	-21.63	26.50	4.867
7.0	-32.82	35.49	2.670	47	-38.60	34.28	-4.320
7.5	-56.05	46.40	-9.654	55	-62.35	43.47	-18.88
8.0	-88.05	59.29	-28.77	63	-94.49	54.00	-40.49
8.5	-130.8	74.03	-56.80	71	-137.0	65.77	-71.23
9.0	-186.9	90.52	-96.38	82	-192.3	78.66	-113.6
9.5	-259.7	108.8	-150.9	92	-263.6	92.60	-171.0
10.0	-353.9	129.0	-224.9	103	-355.2	107.6	-247.5
10.5	-476.4	151.9	-324.5	-	-473.1	124.0	-349.1
11.0	-638.1	179.1	-459.0	-	-626.7	142.5	-484.2
11.5	-857.2	213.7	-643.5	-	-830.4	164.6	-665.8
12.0	-1167	262.6	-904.4	-	-1110	193.8	-195.8
12.5	-1635	341.6	-1294	-	-1513	237.7	-1275
13.0	-2303	455.2	-1848	-	-2140	314.6	-1826
13.5					-3054	429.5	-2624

Table 4-76 Coefficient of Bulk Viscosity

Substance: Argon
Radial Distribution Function: Kirkwood
Intermolecular Potential: Lennard Jones
- Temperatures: 328°K, 373°K
Remarks: ζ_s^{RG}

	T = 328°			T = 373°		
λ	ϕ_V	$\phi_V(R>\sigma)$	ϕ_{TOT}	ϕ_V	$\phi_V(R>\sigma)$	ϕ_{TOT}
	←×10⁶ kgm/m sec→			←×10⁶ kgm/m sec→		
0.5	.1309	.0610	.1919	.1520	.0451	.1971
1.0	.4607	.3103	.7710	.5549	.2299	.7848
1.5	.9589	.7656	1.725	1.174	.5739	1.748
2.0	1.616	1.408	3.023	1.978	1.079	3.056
2.5	2.399	2.219	4.618	2.895	1.756	4.651
3.0	3.217	3.213	6.429	3.792	2.644	6.436
3.5	3.880	4.451	8.331	4.443	3.814	8.257
4.0	4.077	6.051	10.13	4.517	5.368	9.885
4.5	3.350	8.179	11.53	3.566	7.430	11.00
5.0	1.089	11.03	12.13	1.023	10.13	11.15
5.5	-3.420	14.78	11.36	-3.802	13.58	9.779
6.0	-11.08	19.60	8.516	-11.72	17.88	6.160
6.5	-22.90	25.59	2.686	-23.67	23.08	-.5933
7.0	-40.04	32.79	-7.247	-40.75	29.19	-11.56
7.5	-63.84	41.19	-22.64	-64.22	36.17	-28.06
8.0	-95.87	50.71	-45.16	-95.60	43.94	-51.65
8.5	-138.1	61.25	-76.81	-136.7	52.41	-84.28
9.0	-192.8	72.67	-120.1	-189.8	61.44	-128.3
9.5	-263.1	84.89	-178.2	-257.7	70.90	-186.8
10.0	-353.2	97.89	-255.4	-343.8	80.64	-263.2
10.5	-468.9	111.8	-357.1			
11.0	-618.5	127.1	-491.4			
11.5	-809.5	143.4	-666.1			

Table 4-77 Coefficient of Bulk Viscosity

Substance: Argon
Radial Distribution Function: Kirkwood
Intermolecular Potential: Lennard Jones
- Temperatures: 500°K, 600°K
Remarks: ζ_s^{RG}

	T = 500°K			T = 600°K		
λ	ϕ_V	$\phi_V(R>\sigma)$	ϕ_{TOT}	ϕ_V	$\phi_V(R>\sigma)$	ϕ_{TOT}
	←×10⁶ kgm/m sec→			←×10⁶ kgm/m sec→		
0.5	.1976	.0236	.2212	.2258	.0162	.2420
1.0	.7496	.1243	.8739	.8679	.0876	.9555
1.5	1.611	.3249	1.936	1.877	.2367	2.114
2.0	2.715	.6470	3.363	3.178	.4871	3.665
2.5	3.949	1.122	5.072	4.648	.8697	5.518
3.0	5.140	1.795	6.935	6.111	1.423	7.535
3.5	6.041	2.722	8.763	7.327	2.192	9.519
4.0	6.327	3.967	10.29	7.989	3.223	11.21
4.5	5.587	5.594	11.18	7.717	4.560	12.28
5.0	3.322	7.664	10.99	6.059	6.242	12.30
5.5	-1.061	10.22	9.161	2.482	8.296	10.78
6.0	-8.253	13.30	5.044	-3.633	10.74	7.102
6.5	-19.06	16.90	-2.161	-13.00	13.56	.5595
7.0	-34.41	21.00	-13.40	-26.42	16.74	-9.675
7.5	-55.39	25.58	-29.82	-44.89	20.25	-24.63
8.0	-83.29	30.54	-52.75	-69.52	24.03	-45.48
8.5	-119.6	35.83	-83.79	-101.6	28.01	-73.63
9.0	-166.3	41.29	-125.0	-142.9	32.08	-110.8
9.5	-225.7	46.83	-178.9	-195.2	36.16	-159.0
10.0	-300.8	52.31	-248.5	-261.2	40.11	-221.1
10.5	-395.5	57.58	-337.9	-344.2	43.81	-300.4
11.0	-515.3	62.52	-452.7	-448.5	47.11	-401.4
11.5	-667.7	67.01	-600.7	-580.3	49.87	-530.4
12.0	-863.9	71.04	-792.8	-747.9	51.91	-696.0
12.5	-1113	73.96	-1039	-936.9	53.11	-910.8
13.0				-1247	53.42	-1194
13.5				-1628	53.10	-1575
14.0				-2130	51.01	-2079

Table 4-78. Coefficient of Bulk Viscosity

Substance: Nitrogen
Radial Distribution Function: Kirkwood
Intermolecular Potential: Lennard Jones
- Temperatures: 180°K
Remarks: ζ_s^{RG}

	T = 180°K			T =		
λ	ϕ_V	$\phi_V(R>\sigma)$	ϕ_{TOT}	ϕ_V	$\phi_V(R>\sigma)$	ϕ_{TOT}
	←×10⁶ kgm/m sec→			←×10⁶ kgm/m sec→		
1.0	.1821	.2600	.4421			
2.0	.5797	1.176	1.755			
3.0	1.268	2.475	3.743			
4.0	2.025	3.995	6.021			
5.0	1.375	6.404	7.779			
6.0	-3.987	11.17	7.188			
7.0	-18.96	19.68	.7197			
8.0	-49.79	32.40	-17.39			
9.0	-105.0	49.06	-55.93			
10.0	-198.4	69.60	-128.8			
11.0	-358.2	96.40	-261.8			
12.0	-659.6	142.2	-517.3			
13.0	-1208	219.4	-988.3			

Table 4-79. Coefficient of Bulk Viscosity

Substance: Nitrogen
Radial Distribution Function: Kirkwood
Intermolecular Potential: Lennard Jones
- Temperatures: 273°K, 308°K
Remarks: ζ_s^{RG}

	T = 273°K			T = 308°K		
λ	ϕ_V	$\phi_V(R>\sigma)$	ϕ_{TOT}	ϕ_V	$\phi_V(R>\sigma)$	ϕ_{TOT}
	←×10⁶ kgm/m sec→			←×10⁶ kgm/m sec→		
0.5	.0962	.0188	.1150	.1079	.0135	.1214
1.0	.3587	.0971	.4557	.4090	.0712	.4801
1.5	.7655	.2467	1.012	.8772	.1867	1.064
2.0	1.288	.4756	1.764	1.474	.3732	1.847
2.5	1.874	.7981	2.672	2.135	.6495	2.784
3.0	2.435	1.240	3.674	2.761	1.042	3.803
3.5	2.835	1.838	4.673	3.216	1.583	4.799
4.0	2.889	2.639	5.528	3.317	2.310	5.626
4.5	2.354	3.695	6.049	2.834	3.259	6.093
5.0	.9294	5.056	5.986	1.492	4.464	5.956
5.5	-1.745	6.767	5.022	-1.039	5.952	4.913
6.0	-6.091	8.856	2.765	-5.142	7.738	2.596
6.5	-12.60	11.34	-1.262	-11.26	9.826	-1.436
7.0	-21.85	14.21	-7.637	-19.81	12.20	-7.709
7.5	-34.50	17.45	-17.05	-31.70	14.85	-16.85
8.0	-51.34	21.01	-30.33	-47.31	17.72	-29.59
8.5	-73.33	24.84	-48.49	-67.65	20.76	-46.99
9.0	-101.6	28.86	-72.77	-93.68	23.92	-69.76
9.5	-137.7	33.01	-104.7	-126.8	27.10	-99.66
10.0	-183.5	37.21	-146.3	-168.5	30.25	-138.3
10.5	-241.6	41.40	-200.2	-221.1	33.26	-187.8
11.0	-315.6	45.56	-270.1	-287.5	36.07	-251.4
11.5	-410.7	49.71	-361.0	-371.8	38.60	-333.2
12.0	-534.8	54.06	-480.7	-575.8	47.75	-528.0
12.5	-701.0	59.14	-641.9	-754.1	52.20	-701.9
13.0	-932.7	66.27	-866.4	-848.8	48.75	-800.1
13.5	-124.6	75.15	-1171	-111.7	51.87	-1065

Table 4-80. Coefficient of Bulk Viscosity

Substance: Nitrogen
Radial Distribution Function: Kirkwood
Intermolecular Potential: Lennard Jones
- **Temperatures:** 328°K, 373°K
Remarks: ζ_s^{RG}

	T = 328°			T = 373°		
λ	ϕ_V	$\phi_V(R>\sigma)$	ϕ_{TOT}	ϕ_V	$\phi_V(R>\sigma)$	ϕ_{TOT}
	←×10⁶ kgm/m sec→			←×10⁶ kgm/m sec→		
0.5	.1106	.0136	.1242	.1231	.0097	.1328
1.0	.4193	.0711	.4904	.4720	.0522	.5243
1.5	.9022	.1844	1.087	1.020	.1401	1.160
2.0	1.524	.3642	1.889	1.725	.2867	2.011
2.5	2.226	.6266	2.853	2.519	.5094	3.029
3.0	2.912	.9956	3.908	3.305	.8306	4.135
3.5	3.446	1.502	4.948	3.946	1.276	5.222
4.0	3.646	2.182	5.828	4.269	1.874	6.143
4.5	3.278	3.073	6.351	4.059	2.650	6.709
5.0	2.061	4.210	6.270	3.058	3.629	6.686
5.5	-.3442	5.619	5.275	.9612	4.826	5.787
6.0	-4.332	7.321	2.989	-2.584	6.250	3.667
6.5	-10.36	9.320	-1.041	-7.985	7.902	-.0828
7.0	-18.96	11.61	-7.357	-15.71	9.770	-59.45
7.5	-30.77	14.16	-16.60	-26.31	11.83	-14.48
8.0	-46.50	16.94	-29.56	-40.44	14.05	-26.38
8.5	-67.05	19.91	-47.14	-58.85	16.39	-42.46
9.0	-93.50	22.99	-70.51	-82.49	18.80	-63.69
9.5	-127.2	26.13	-101.1	-112.5	21.21	-91.29
10.0	-169.9	29.25	-140.6	-150.4	23.55	-126.8
10.5	-223.9	32.27	-191.6	-198.0	25.76	-172.3
11.0	-292.4	35.15	-257.2	-258.0	27.74	-230.2
11.5	-379.7	37.83	-341.9	-333.7	29.41	-304.3
12.0	-397.1	33.78	-363.3	-430.4	30.70	-399.7
12.5	-509.1	34.04	-475.0	-555.2	31.54	-523.6
13.0	-806.0	42.07	-763.9	-719.5	31.95	-687.6
13.5	-1069	44.87	-1025	-914.8	32.15	-909.6
14.0	-1427	48.04	-1379	-1236	31.52	-1205

Table 4-81. Coefficient of Bulk Viscosity

Substance: Nitrogen
Radial Distribution Function: Kirkwood
Intermolecular Potential: Lennard Jones
- Temperatures: 500°K, 600°K
Remarks: ζ_s^{RG}

	T =			T =		
λ	ϕ_V	$\phi_V(R>\sigma)$	ϕ_{TOT}	ϕ_V	$\phi_V(R>\sigma)$	ϕ_{TOT}
	←×10⁶ kgm/m sec→			←×10⁶ kgm/m sec→		
0.5	.1493	.0054	.1547	.1667	.0038	.1705
1.0	.5814	.0307	.6121	.6537	.0224	.6761
1.5	1.269	.0866	1.355	1.435	.0651	1.500
2.0	2.167	.1853	2.352	2.468	.1423	2.610
2.5	3.208	.3411	3.549	3.688	.2659	3.954
3.0	4.299	.5700	4.869	5.009	.4488	5.458
3.5	5.319	.8893	6.208	6.320	.7040	7.024
4.0	6.114	1.316	7.429	7.487	1.043	8.530
4.5	6.503	1.864	8.367	8.348	1.478	9.826
5.0	6.271	2.545	8.816	8.721	2.015	10.74
5.5	5.171	3.367	8.538	8.384	2.658	11.04
6.0	2.921	4.333	7.254	7.100	3.409	10.51
6.5	-8.125	5.437	4.625	4.586	4.264	8.851
7.0	-6.398	6.671	.2731	.5313	5.213	5.745
7.5	-14.27	8.018	-6.252	-5.406	6.245	.8391
8.0	-24.91	9.454	-15.46	-13.64	7.341	-6.298
8.5	-38.91	10.95	-27.96	-24.62	8.480	-16.14
9.0	-56.96	12.47	-44.49	-38.97	9.634	-29.33
9.5	-79.94	13.98	-65.96	-57.32	10.77	-46.55
10.0	-108.9	15.42	-93.44	-80.55	11.86	-68.69
10.5	-145.1	16.75	-128.4	-109.7	12.86	-96.83
11.0	-190.6	17.89	-172.7	-146.1	13.72	-132.4
11.5	-247.5	18.79	-228.7	-191.7	14.39	-177.3
12.0	-319.2	19.34	-299.8	-248.9	14.80	-234.1
12.5	-410.2	19.46	-390.7	-321.0	14.88	-306.1
13.0	-527.0	19.04	-508.0	-412.8	14.53	-398.3
13.5	-679.3	17.96	-661.3	-531.0	13.66	-517.4
14.0	-881.3	16.19	-865.1	-681.2	11.95	-669.3
14.5	-1145	13.13	-1132			

Table 4-82. Coefficient of Bulk Viscosity

Substance: Argon
Radial Distribution Function: Percus-Yevick
Intermolecular Potential: Lennard Jones
- Temperatures: 273.15°, 328.15°K
Remarks: ζ_s^{RG}

ρ^*	ϕ_V	$\phi_V(R>\sigma)$	ϕ_{TOT}	ϕ_{OBS}
	T = 273.15°			
	←×10⁶ kgm/m sec→			
0.15	1.244	1.503	2.474	.9
0.30	4.967	4.298	9.265	11
0.45	-4.380	12.28	7.899	28
0.60	-87.81	30.31	-57.50	55
0.75	-361.9	16.00	-345.9	90
0.90	-1009	-155.5	-1164	-
1.05	-2260	-681.9	-2942	-
1.20	-4807	-2002	-6809	-
	328.15°			
0.15	1.630	1.057	2.687	
0.30	4.852	4.151	9.004	
0.45	-7.285	12.76	5.475	
0.60	-86.83	27.06	-59.77	
0.75	-333.8	17.47	-316.3	
0.90	-894.3	-98.53	-992.8	
1.05	-1956	-444.1	-2400	
1.20	-3912	-1184	-5096	

Table 4-83. Coefficient of Bulk Viscosity

Substance: Argon
Radial Distribution Function: Percus-Yevick
Intermolecular Potential: Lennard Jones
- Temperatures: 373.15°
Remarks: ζ_s^{RG}

	T = 373.15°		
ρ^*	ϕ_V	$\phi_V(R>\sigma)$	ϕ_{TOT}
	←×10^6 kgm/m sec→		
0.15	1.884	.8475	2.731
0.30	5.132	3.837	8.969
0.45	-7.415	11.97	4.559
0.60	-83.11	24.23	-58.87
0.75	-310.4	17.42	-293.0
0.90	-816.6	-69.43	-886.0
1.05	-1731	-317.2	-2048
1.20	-3292	-800.3	-4092

Table 4-84. Coefficient of Bulk Viscosity

Substance: Argon
Radial Distribution Function: CHNC
Intermolecular Potential: Lennard-Jones
- Temperatures: 273.15°K, 328.15°K
Remarks: ζ_s^{RG}

T =			T = 273.15°K			
ϕ_V	$\phi_V(R>\sigma)$	ϕ_{TOT}	ϕ_V	$\phi_V(R>\sigma)$	ϕ_{TOT}	ϕ_{OBS}
←×10⁶ kgm/m sec→			←×10⁶ kgm/m sec→			
0.15			1.146	1.638	2.783	.9
0.30			4.493	4.973	9.466	11
0.45			-4.075	12.03	7.956	28
0.60			-87.96	26.13	-61.83	55
0.75			-348.7	6.118	-342.5	90
0.90			-858.5	-108.4	-966.9	-
1.05			-1383	-274.7	-1658	-
1.20			-828.7	-228.5	-1057	-
				328.15°		
0.15			1.609	1.081	2.690	
0.30			4.607	4.369	8.976	
0.45			-8.576	12.86	4.284	
0.60			-89.17	23.61	-65.57	
0.75			-314.5	9.458	-305.1	
0.90			-710.8	-63.83	-774.6	
1.05			-1046	-161.5	-1208	
1.20			-456.0	-123.9	-579.9	

Table 4-85. Coefficient of Bulk Viscosity

Substance: Argon
Radial Distribution Function: CHNC
Intermolecular Potential: Lennard-Jones
- Temperatures: 373.15°K
Remarks: ζ_s^{RG}

T =			T = 373.15°K		
ϕ_V	$\phi_V(R>\sigma)$	ϕ_{TOT}	ϕ_V	$\phi_V(R>\sigma)$	ϕ_{TOT}
←×10⁶ kgm/m sec→			←×10⁶ kgm/m sec→		
0.15			1.862	.8612	2.723
0.30			4.867	3.991	8.858
0.45			-8.711	12.01	3.302
0.60			-84.33	21.13	-63.20
0.75			-285.1	10.77	-274.3
0.90			-622.9	-42.34	-665.3
1.05			-832.5	-107.7	-940.2
1.20			-89.76	-72.96	-162.7

Table 4-86. Coefficient of Bulk Viscosity

Substance: Argon
Radial Distribution Function: Percus-Yevick
Intermolecular Potential: Truncated Lennard-Jones
- Temperatures: 273.15°
Remarks: Comparison of ζ's

	T = 273.15°			T = 273.15°K			
ρ^*	ϕ_V	$\phi_V(R>\sigma)$	ϕ_{TOT}	ϕ_V	$\phi_V(R>\sigma)$	ϕ_{TOT}	ϕ_{OBS}
	←×10⁶ kgm/m sec→			←×10⁶ kgm/m sec→			
	Normal ζ			Sound Speed ζ			
0.15	1.120	1.417	2.537	-6.255	8.752	2.496	
0.30	1.454	4.535	5.989	-42.05	24.77	-17.27	
0.45	-30.74	15.08	-15.67	-182.9	53.38	-129.5	
0.60	-217.4	29.19	-188.2	-541.8	62.97	-478.8	
0.75	-956.9	-49.42	-1006	-1346	-67.22	-1413	

Table 4-87 Coefficient of Bulk Viscosity

Substance: Argon

Radial Distribution Function: Percus-Yevick

Intermolecular Potential: Truncated Lennard-Jones

Temperature: 273.15°K

Remarks: Comparison of ζ's

ρ^*	ϕ_V	$\phi_V(R>\sigma)$	ϕ_{TOTAL}	ϕ_{OBS}	Q^a	Q^b	Q^c
	←$\times 10^6$ kg/m sec→		← $\times 10^6$ kg/m →		← units of σ^2 →		
			Helfand ζ				
0.15	2.357	.1869	2.543		.6877	.037	-.014
0.30	9.366	.8534	10.22		.3304	-.051	-.062
0.45	14.97	3.570	18.54		.5239	.153	.196
0.60	-16.09	8.223	-7.864		1.047	.540	.571
0.75	-220.8	-15.76	-236.6		1.728	1.02	1.04
			Normal ζ; Q = 0				
0.15	3.340	.0685	3.408		0.9		
0.30	8.429	1.219	9.648		11		
0.45	6.976	2.968	9.945		29		
0.60	-11.94	-1.327	-13.27		55		
0.75	-116.8	-25.76	-142.6		90		

[a]Calculated from Integral Equations

[b]Calculated from Eq. (5-1) from Argon Viral Expansion

[c]Calculated from Eq. (5-1) from Viral Expansion fitted to pressures calculated from these g values.

Table 4-88 Coefficient of Bulk Viscosity

Substance: Argon
Radial Distribution Function: Kirkwood
Intermolecular Potential: Modified Buckingham
- Temperatures: 273°, 308°
Remarks: ζ_s^{RG}

	T = 273°				T = 308°		
λ	ϕ_V	$\phi_V(R>\sigma)$	ϕ_{TOT}	ϕ_{OBS}	ϕ_V	$\phi_V(R>\sigma)$	ϕ_{TOT}
	←×10⁶ kgm/m sec→				←×10⁶ kgm/m sec→		
0.5	.1055	.0798	.1853	-	.1250	.0604	.1854
1.0	.3536	.3950	.7486	-	.4374	.3037	.7411
1.5	.6906	.9788	1.659	0.1	.8741	.7621	1.636
2.0	1.033	1.817	2.850	1.2	1.334	1.467	2.801
2.5	1.212	2.993	4.204	3.0	1.632	2.478	4.109
3.0	.9400	4.592	5.532	5.3	1.475	3.881	5.356
3.5	-.2085	6.743	6.535	8.2	.4455	5.782	6.228
4.0	-2.814	9.584	6.770	12	-2.014	8.285	6.270
4.5	-7.629	13.24	5.608	16	-6.618	11.48	4.858
5.0	-15.60	17.79	2.188	20	-14.26	15.41	11.52
5.5	-27.93	23.29	-4.639	26	-26.06	20.11	-5.947
6.0	-46.14	29.75	-16.39	32	-43.42	25.55	-17.87
6.5	-72.33	37.21	-35.12	38	-68.25	31.72	-36.52

Table 4-89. Coefficient of Bulk Viscosity

Substance: Argon
Radial Distribution Function: Kirkwood
Intermolecular Potential: Modified Buckingham
- Temperatures: 323°, 328°
Remarks: ζ_s^{RG}

	T = 323°			T = 328°		
λ	ϕ_V	$\phi_V(R>\sigma)$	ϕ_{TOT}	ϕ_V	$\phi_V(R>\sigma)$	ϕ_{TOT}
	←×10⁶ kgm/m sec→			←×10⁶ kgm/m sec→		
0.5	.1325	.0542	.1867	.1348	.5024	.1872
1.0	.4691	.2747	.7438	.4792	.2660	.7452
1.5	.9439	.6957	1.640	.9662	.6757	1.642
2.0	1.450	1.353	2.802	1.488	1.318	2.805
2.5	1.799	2.304	4.103	1.854	2.251	4.105
3.0	1.698	3.634	5.332	1.772	3.558	5.330
3.5	.8291	5.332	6.161	1.700	4.511	6.211
4.0	-1.645	7.813	6.168	-1.519	7.665	6.150
4.5	-6.133	10.83	4.699	-5.966	10.63	4.664
5.0	-13.60	14.54	9.395	-13.38	14.27	8.937
5.5	-25.14	18.96	-6.186	-24.83	18.59	-6.232
6.0	-42.11	24.04	-18.07	-41.66	23.57	-18.09
6.5	-66.24	29.72	-36.51	-65.59	29.12	-36.47
7.0	-99.81	35.94	-63.86	-98.86	35.18	-63.68

Table 4-90. Coefficient of Bulk Viscosity

Substance: Argon
Radial Distribution Function: Kirkwood
Intermolecular Potential: Modified Buckingham
- Temperatures: 373°
Remarks: ζ_s^{RG}

	T = 373°			T =		
λ	ϕ_V	$\phi_V(R>\sigma)$	ϕ_{TOT}	ϕ_V	$\phi_V(R>\sigma)$	ϕ_{TOT}
	←×10⁶ kgm/m sec→			←×10⁶ kgm/m sec→		
0.5	.1543	.0395	.1938			
1.0	.5618	.2048	.7666			
1.5	1.150	.5330	1.683			
2.0	1.802	1.065	2.866			
2.5	2.322	1.857	4.178			
3.0	2.420	2.980	5.400			
3.5	1.700	4.511	6.211			
4.0	-.3546	6.519	6.164			
4.5	-4.392	9.055	4.662			
5.0	-11.22	12.15	.9294			
5.5	-21.81	15.79	-6.030			
6.0	-37.41	19.93	-17.48			
6.5	-59.56	24.51	-35.05			
7.0	-90.24	29.44	-60.80			

Table 4-91 Coefficient of Bulk Viscosity

Substance: Nitrogen
Radial Distribution Function: Kirkwood
Intermolecular Potential: Modified Buckingham
- Temperatures: 273°K, 308°K
Remarks: ζ_s^{RG}

	T = 273°K			T = 308°K		
λ	ϕ_V	$\phi_V(R>\sigma)$	ϕ_{TOT}	ϕ_V	$\phi_V(R>\sigma)$	ϕ_{TOT}
	←×10^6 kgm/m sec→			←×10^6 kgm/m sec→		
0.5	.1026	.0509	.1535	.1186	.0389	.1575
1.0	.3496	.2604	.6100	.4178	.2027	.6206
1.5	.6752	.6643	1.340	.8255	.5296	1.355
2.0	.9790	1.298	2.277	1.229	1.060	2.289
2.5	1.087	2.219	3.307	1.443	1.853	3.296
3.0	.7295	3.512	4.241	1.192	2.982	4.173
3.5	-.4801	5.274	4.794	.0917	4.530	4.622
4.0	-3.055	7.609	4.553	-2.359	6.578	4.219
4.5	-7.656	10.61	2.951	-6.797	9.193	2.396
5.0	-15.11	14.33	-.7733	-14.02	12.42	-1.597
5.5	-26.43	18.82	-7.612	-24.99	16.27	-8.724
6.0	-42.91	24.07	-18.85	-40.94	20.72	-20.22
6.5	-66.15	30.02	-36.12	-63.37	25.73	-37.64
7.0	-98.22	36.63	-61.59	-94.20	31.19	-63.02
7.5	-141.9	43.83	-98.07	-136.0	37.02	-98.96
8.0	-200.5	51.50	-149.0	-191.7	43.04	-148.7

Table 4-92. Coefficient of Bulk Viscosity

Substance: Nitrogen
Radial Distribution Function: Kirkwood
Intermolecular Potential: Modified Buckingham
- Temperatures: 323°
Remarks: ζ_s^{RG}

	T = 323°			T =		
λ	ϕ_V	$\phi_V(R>\sigma)$	ϕ_{TOT}	ϕ_V	$\phi_V(R>\sigma)$	ϕ_{TOT}
	←×10⁶ kgm/m sec→			←×10⁶ kgm/m sec→		
0.5	.1247	.0350	.1598			
1.0	.4439	.1842	.6282			
1.5	.8834	.4859	1.369			
2.0	1.327	.9816	2.308			
2.5	1.586	1.728	3.315			
3.0	1.385	2.797	4.182			
3.5	.3418	4.265	4.607			
4.0	-2.039	6.206	4.167			
4.5	-6.386	8.680	2.294			
5.0	-13.48	11.72	-1.753			
5.5	-24.27	15.35	-8.925			
6.0	-39.95	19.52	-20.43			
6.5	-61.99	24.19	-37.80			
7.0	-92.26	29.27	-62.99			
7.5	-133.2	34.64	-98.56			
8.0	-187.7	40.15	-147.6			

Table 4-93. Coefficient of Bulk Viscosity

Substance: Nitrogen
Radial Distribution Function: Kirkwood
Intermolecular Potential: Modified Buckingham
- Temperatures: 328°, 373°
Remarks: ζ_s^{RG}

	T = 328°			T = 373°		
λ	ϕ_V	$\phi_V(R>\sigma)$	ϕ_{TOT}	ϕ_V	$\phi_V(R>\sigma)$	ϕ_{TOT}
	←×10⁶ kgm/m sec→			←×10⁶ kgm/m sec→		
0.5	.1267	.0339	.1606	.1431	.0258	.1688
1.0	.4523	.1787	.6310	.5213	.1392	.6605
1.5	.9019	.4727	1.375	1.056	.3774	1.434
2.0	1.358	.9576	2.316	1.625	.7820	2.407
2.5	1.633	1.690	3.323	2.035	1.405	3.440
3.0	1.449	2.740	4.189	2.010	2.307	4.317
3.5	.4255	4.183	4.608	1.182	3.550	4.732
4.0	-1.931	6.090	4.159	-.9254	5.190	4.264
4.5	-6.244	8.519	2.275	-4.907	7.269	2.362
5.0	-13.29	11.51	-1.784	-11.50	9.811	-1.684
5.5	-24.02	15.06	-8.962	-21.59	12.81	-8.773
6.0	-39.61	19.15	-20.46	-36.28	16.25	-20.03
6.5	-61.51	23.71	-37.80	-56.92	20.05	-36.87
7.0	-91.59	28.67	-62.92	-85.22	24.13	-61.09
7.5	-132.3	33.91	-98.34	-123.4	28.33	-94.97
8.0	-186.4	39.26	-147.1	-173.9	32.62	-141.3

Table 4-94. Coefficient of Bulk Viscosity

Substance: Argon
Radial Distribution Function: Percus Yevick
Intermolecular Potential: Modified Buckingham
- Temperatures: 273.15°K, 328.15°K
Remarks: ζ_s^{RG}

	T = 273.15°K				T = 328.15°K		
ρ^*	ϕ_V	$\phi_V(R>\sigma)$	ϕ_{TOT}	ϕ_{OBS}	ϕ_V	$\phi_V(R>\sigma)$	ϕ_{TOT}
	←×10^6 kgm/m sec→				←×10^6 kgm/m sec→		
0.25	1.645	1.833	3.479	2	2.027	1.393	3.421
0.50	2.455	6.790	9.245	15	1.660	6.573	8.234
0.75	-44.65	23.25	-21.40	40	-47.93	21.22	-26.72
1.00	-287.1	28.58	-258.5	75	-282.0	26.78	-255.2
1.25	-1156	-137.0	-1292	-	-1046	-86.39	-1132
1.35	-1923	-350.8	-2274	-			
1.50					-2949	-590.5	-3540
1.55					-3119	-718.8	-3837
1.60					-2744	-777.4	-3522
1.65							
1.70							

Table 4-95. Coefficient of Bulk Viscosity

Substance: Argon
Radial Distribution Function: Percus Yevick
Intermolecular Potential: Modified Buckingham
- Temperatures: 373.15°K
Remarks: ζ_s^{RG}

	T = 373.15°K			T =		
ρ^*	ϕ_V	$\phi_V(R>\sigma)$	ϕ_{TOT}	ϕ_V	$\phi_V(R>\sigma)$	ϕ_{TOT}
	←×10^6 kgm/m sec→			←×10^6 kgm/m sec→		
0.25	2.324	1.148	3.473			
0.50	1.542	6.154	7.696			
0.75	-48.26	19.35	-28.92			
1.00	-269.7	24.59	-245.1			
1.25	-975.1	-60.77	-1036			
1.35	-1544	-164.9	-1709			
1.50						
1.55						
1.60						
1.65						
1.70						

Table 4-96. Coefficient of Bulk Viscosity

Substance: Argon
Radial Distribution Function: Kirkwood
Intermolecular Potential: Barker-Bobetic
- Temperatures: 273°, 308°K
Remarks: ζ_s^{RG}

	T = 272.0°K				T = 308.0°K		
λ	ϕ_V	$\phi_V(R>\sigma)$	ϕ_{TOT}	ϕ_{OBS}	ϕ_V	$\phi_V(R>\sigma)$	ϕ_{TOT}
	←×10⁶ kgm/m sec→				←×10⁶ kgm/m sec→		
0.5	.0980	.1168	.2148	-	.1209	.0869	.2078
1.0	.3075	.5857	.8933	-	.4118	.4361	.8479
1.5	.5988	1.420	2.019	.2	.8341	1.069	1.903
2.0	.9754	2.560	3.536	1.6	1.352	1.976	3.327
2.5	1.406	3.959	5.365	3.7	1.871	3.174	5.044
3.0	1.758	5.648	7.406	6.4	2.189	4.744	6.932
3.5	1.735	7.778	9.513	9.7	1.957	6.843	8.801
4.0	.8327	10.62	11.46	14	.6575	9.692	10.35
4.5	-1.680	14.55	12.87	18	-2.415	13.54	11.13
5.0	-6.758	19.95	13.19	24	-8.148	18.64	10.49
5.5	-15.56	27.16	11.60	30	-17.62	25.17	7.562
6.0	-29.44	36.40	6.962	36	-32.07	33.26	1.181
6.5	-49.98	47.77	-2.209	43	-53.03	42.90	-10.13
7.0	-79.03	61.21	-17.82	52	-82.26	54.01	-28.25
7.5	-118.9	76.58	-42.29	60	-121.9	66.43	-55.52
8.0	-172.4	93.68	-78.68	70	-174.8	79.94	-94.91
8.5	-243.4	122.4	-131.0	80	-244.6	94.33	-150.3
9.0	-337.4	132.8	-204.6	90	-336.2	109.4	-226.7

Table 4-97. Coefficient of Bulk Viscosity

Substance: Argon
Radial Distribution Function: Kirkwood
Intermolecular Potential: Barker-Bobetic
- Temperatures: 323°, 328°
Remarks: ζ_s^{RG}

	T = 323°			T = 328°		
λ	ϕ_V	$\phi_V(R>\sigma)$	ϕ_{TOT}	ϕ_V	$\phi_V(R>\sigma)$	ϕ_{TOT}
	←×10⁶ kgm/m sec→			←×10⁶ kgm/m sec→		
0.5	.1294	.0776	.2070	.1321	.0749	.2069
1.0	.4492	.3907	.8299	.4609	.3773	.8382
1.5	.9.64	.9647	1.881	.9421	.9340	1.876
2.0	1.482	1.802	3.284	1.522	1.751	3.274
2.5	2.033	2.936	4.969	2.084	2.866	4.950
3.0	2.350	4.555	6.805	2.403	4.368	6.770
3.5	2.074	6.511	8.584	2.115	6.407	8.522
4.0	.6824	9.303	9.985	.7015	9.176	9.877
4.5	-2.516	13.05	10.54	-2.528	12.89	10.26
5.0	-8.388	17.96	9.574	-8.434	17.73	9.299
5.5	-17.98	24.19	6.211	-18.05	23.86	5.807
6.0	-32.53	31.82	-.7116	-32.62	31.34	-1.272
6.5	-53.50	40.84	-12.66	-53.58	40.17	-13.41
7.0	-82.64	51.15	-31.49	-82.67	50.27	-32.43
7.5	-122.1	62.59	-59.51	-122.0	61.38	-60.65
8.0	-174.6	74.94	-99.63	-174.3	73.38	-101.0
8.5	-243.6	87.96	-155.6	-243.1	85.99	-157.1
9.0	-334.0	101.5	-232.5	-333.1	99.02	-234.1

Table 4-98. Coefficient of Bulk Viscosity

Substance: Argon
Radial Distribution Function: Kirkwood
Intermolecular Potential: Barker-Bobetic
- Temperatures: 373°
Remarks: ζ_s^{RG}

	T = 373°			T =		
λ	ϕ_V	$\phi_V(R>\sigma)$	ϕ_{TOT}	ϕ_V	$\phi_V(R>\sigma)$	ϕ_{TOT}
	←×10^6 kgm/m sec→			←×10^6 kgm/m sec→		
0.5	.1538	.0558	.2097			
1.0	.5543	.2852	.8396			
1.5	1.146	.7224	1.868			
2.0	1.847	1.396	3.243			
2.5	2.506	2.362	4.868			
3.0	2.869	3.715	6.583			
3.5	2.560	5.580	8.140			
4.0	1.065	8.108	9.173			
4.5	-2.276	11.45	9.170			
5.0	-8.274	15.72	7.446			
5.5	-17.90	20.01	3.111			
6.0	-32.32	27.35	-4.964			
6.5	-52.88	34.69	-18.19			
7.0	-81.24	42.93	-38.31			
7.5	-119.4	51.90	-67.50			
8.0	-169.8	61.37	-108.5			
8.5	-235.8	71.11	-164.7			
9.0	-321.7	80.83	-240.9			

Table 4-99. Coefficient of Bulk Viscosity

Substance: Argon
Radial Distribution Function: Percus-Yevick
Intermolecular Potential: Barker-Bobetic
- Temperatures: 273.15°K, 328.15°K
Remarks: ζ_s^{RG}

	T = 273.15°K				T = 328.15°K		
ρ^*	ϕ_V	$\phi_V(R>\sigma)$	ϕ_{TOT}	ϕ_{OBS}	ϕ_V	$\phi_V(R>\sigma)$	ϕ_{TOT}
	←×10⁶ kgm/m sec→				←×10⁶ kgm/m sec→		
0.15	.4357	1.079	1.515	-	.7531	.6831	1.436
0.30	2.113	3.304	5.417	5	2.648	2.582	5.230
0.45	3.298	6.089	9.387	14	2.242	6.331	8.573
0.60	-10.58	15.26	4.677	29	-13.85	15.14	1.290
0.75	-68.33	31.73	-36.60	47	-70.94	28.06	-42.88
0.90	-212.5	38.27	-174.1	72	-211.0	33.30	-177.7
1.05	-513.3	-3.744	-517.1	100	-499.0	3.134	-495.8
1.20	-1193	-1764	-1369	-	-1108	-119.2	-1227
1.35	-2709	-713.9	-3421	-	-2402	-474.6	-2876
1.50	-5326	-2016	-7342	-	-4742	-131.3	-6055

Table 4-100 Coefficient of Bulk Viscosity

Substance: Argon
Radial Distribution Function: Percus-Yevick
Intermolecular Potential: Barker-Bobetic
- Temperatures: 373.15°
Remarks: ζ_s^{RG}

	T = 373.15°			T =		
ρ^*	ϕ_V	$\phi_V(R>\sigma)$	ϕ_{TOT}	ϕ_V	$\phi_V(R>\sigma)$	ϕ_{TOT}
	←×10^6 kgm/m sec→			←×10^6 kgm/m sec→		
0.15	.9316	.5171	1.449			
0.30	3.021	2.205	5.227			
0.45	2.150	5.970	8.120			
0.60	-14.50	14.05	-.4471			
0.75	-70.45	25.13	-45.32			
0.90	-206.0	29.94	-176.0			
1.05	-481.4	6.695	-474.7			
1.20	-1043	-87.01	-1130			
1.35	-2186	-349.1	-2535			
1.50	-4226	-955.8	-5182			

Table 4-101 Coefficient of Thermal Conductivity

Substance: Argon
Radial Distribution Function: Kirkwood
Remarks: ζ_s^{RG}

Intermolecular Potential: Lennard-Jones
Temperature: 180°K

	T = 180°K					T =				
λ	χ_k	χ_v	$\chi_v(R>\sigma)$	χ_{CAL}	χ_{OBS}	χ_K	χ_v	$\chi_v(R>\sigma)$	χ_{CAL}	χ_{OBS}
	$\times 10^3$ watts/m °C					$\times 10^3$ watts/m °C				
1.0	.5312	.1522	15244	1.208	14.1					
2.0	.8042	.5708	1.483	2.859	17.1					
3.0	1.029	1.356	2.967	5.353	21.0					
4.0	1.241	2.791	4.331	8.363	25.9					
5.0	1.510	4.242	5.807	11.56	37.4					
6.0	1.785	5.893	7.787	15.46	41.2					
7.0	2.065	7.748	10.09	19.91	53.5					
8.0	2.347	9.828	12.87	25.04	71.2					
9.0	2.631	12.28	16.74	31.65	96.6					
10.0	2.916	15.46	23.81	42.19	133					

Table 4-102 Coefficient of Thermal Conductivity

Substance: Argon
Radial Distribution Function: Kirkwood
Remarks: ζ_s^{RG}

Intermolecular Potential: Lennard Jones
Temperatures: T = 273°; T = 308°

	T = 273°K					T = 308°K				
λ	χ_k	χ_v	$\chi_v(R>\sigma)$	χ_{CAL}	χ_{OBS}	χ_K	χ_v	$\chi_v(R>\sigma)$	χ_{CAL}	χ_{OBS}
	$\times 10^3$ watts/m °C					$\times 10^3$ watts/m °C				
0.5	.5963	.0599	.1563	.8125	17.8	.6834	.0661	.1431	.8926	19.7
1.0	.8699	.2085	.4328	1.511	19.6	.9952	.2290	.3966	1.621	21.5
1.5	1.101	.4419	.7800	2.322	21.6	1.257	.4840	.7158	2.457	23.5
2.0	1.313	.7610	1.181	3.255	23.8	1.498	.8326	1.086	3.416	25.7
2.5	1.516	1.168	1.630	4.315	26.1	1.727	1.278	1.501	4.506	28.1
3.0	1.714	1.668	2.125	5.507	28.7	1.951	1.825	1.959	5.735	30.8
3.5	1.910	2.264	2.668	6.841	31.6	2.172	2.479	2.461	7.111	33.7
4.0	2.105	2.963	3.263	8.331	34.8	2.392	3.246	3.009	8.647	36.9
4.5	2.300	3.770	3.916	9.987	38.4	2.613	4.135	3.605	10.35	40.5
5.0	2.497	4.694	4.633	11.82	42.4	2.836	5.153	4.255	12.24	44.4
5.5	2.697	5.743	5.420	13.86	46.8	3.062	6.312	4.962	14.34	48.8
6.0	2.899	6.927	6.286	16.11	51.9	3.291	7.621	5.734	16.65	53.8
6.5	3.104	8.257	7.242	18.60	57.8	3.524	9.094	6.581	19.20	59.4
7.0	3.314	9.744	8.301	21.36	64.6	3.763	10.74	7.517	22.02	65.8
7.5	3.529	11.40	9.486	24.41	72.4	4.007	12.57	8.560	25.14	73.2
8.0	3.748	13.24	10.82	27.81	81.5	4.257	14.61	9.738	28.60	81.6
8.5	3.973	15.27	12.36	31.60	92.2	4.514	16.86	11.08	32.45	91.4
9.0	4.203	17.50	14.14	35.84	104.4	4.776	19.33	12.65	36.75	103
9.5	4.439	19.94	16.26	40.63	118.4	5.045	22.03	14.51	41.58	116
10.0	4.679	22.59	18.70	45.97	135.8	5.320	24.97	16.64	46.93	131

Table 4-103 Coefficient of Thermal Conductivity

Substance: Argon
Intermolecular Potential: Lennard Jones
Radial Distribution Function: Kirkwood
Temperatures: T = 328°K; T = 373°K
Remarks: ζ_s^{RG}

	T = 328°K					T = 373°K				
λ	χ_k	χ_v	$\chi_v(R>\sigma)$	χ_{CAL}	χ_{OBS}	χ_K	χ_v	$\chi_v(R>\sigma)$	χ_{CAL}	χ_{OBS}
	$\times 10^3$ watts/m °C					$\times 10^3$ watts/m °C				
0.5	.7330	.0697	.1341	.9368	20.7	.8444	.0775	.1215	1.043	23.1
1.0	1.066	.2405	.3719	1.679	22.5	1.226	.2659	.3376	1.829	25.0
1.5	1.346	.5076	.6720	2.526	24.5	1.545	.5595	.6110	2.715	27.1
2.0	1.602	.8726	1.021	3.496	26.8	1.837	.9605	.9287	3.727	29.3
2.5	1.847	1.339	1.413	4.599	29.2	2.115	1.473	1.288	4.876	31.9
3.0	2.085	1.912	1.845	5.843	31.9	2.385	2.103	1.683	6.172	34.6
3.5	2.321	2.598	2.319	7.238	35.0	2.652	2.858	2.116	7.626	37.7
4.0	2.555	3.403	2.835	8.793	38.3	2.918	3.744	2.585	9.248	41.1
4.5	2.790	4.336	3.397	10.52	41.9	3.185	4.774	3.092	11.05	44.8
5.0	3.028	5.407	4.006	12.44	46.0	3.455	5.955	3.640	13.05	49.1
5.5	3.268	6.625	4.668	14.56	50.6	3.729	7.300	4.233	15.26	53.9
6.0	3.513	8.002	5.389	16.90	55.8	4.007	8.820	4.875	17.70	59.3
6.5	3.762	9.551	6.179	19.49	61.8	4.291	10.53	5.576	20.40	65.4
7.0	4.017	11.28	7.050	22.35	68.7	4.581	12.44	6.345	23.37	72.6
7.5	4.277	13.21	8.019	25.51	76.6	4.878	14.57	7.200	26.65	80.7
8.0	4.545	15.35	9.112	29.01	86.0	5.183	16.93	8.160	30.28	89.6
8.5	4.819	17.72	10.36	32.90	96.6	5.496	19.54	9.254	34.29	100
9.0	5.099	20.31	11.81	37.22	110	5.817	22.40	10.52	38.73	112
9.5	5.387	23.15	13.52	42.06	124	6.145	25.53	12.01	43.69	126
10.0	5.681	26.25	15.48	47.41	141	6.481	28.94	13.72	49.14	141

Table 4-104 Coefficient of Thermal Conductivity

Substance: Argon
Radial Distribution Function: Kirkwood
Remarks: ζ_s^{RG}

Intermolecular Potential: Lennard Jones
Temperatures: T = 500°K; T = 600°K

	T = 500°K					T = 600°K				
λ	χ_k	χ_v	$\chi_v(R>\sigma)$	χ_{CAL}	χ_{OBS}	χ_K	χ_v	$\chi_v(R>\sigma)$	χ_{CAL}	χ_{OBS}
	$\times 10^3$ watts/m °C					$\times 10^3$ watts/m °C				
0.5	1.157	.0988	.0926	1.348	29.2	1.401	.1150	.0612	1.577	33.8
1.0	1.672	.3342	.2585	2.264	30.4	2.018	.3855	.1726	2.577	34.0
1.5	2.099	.6984	.4702	3.267	31.9	2.529	.8017	.3165	3.647	34.5
2.0	2.488	1.194	.7183	4.400	33.6	2.993	1.366	.4873	4.847	35.2
2.5	2.857	1.827	.9980	5.683	35.5	3.432	2.086	.6818	6.201	36.2
3.0	3.216	2.605	1.306	7.128	37.7	3.859	2.970	.8981	7.727	37.4
3.5	3.571	3.536	1.642	8.749	40.0	4.280	4.027	1.135	9.441	38.9
4.0	3.924	4.632	2.004	10.56	42.7	4.698	5.269	1.390	11.36	40.6
4.5	4.278	5.902	2.392	12.57	45.7	5.119	6.708	1.665	13.49	42.6
5.0	4.636	7.361	2.807	14.80	48.9	5.544	8.358	1.957	15.86	44.9
5.5	4.999	9.020	3.253	17.27	52.6	5.974	10.23	2.268	18.48	47.6
6.0	5.369	10.90	3.732	20.00	56.5	6.414	12.35	2.601	21.36	50.6
6.5	5.746	13.00	4.249	23.00	61.1	6.859	14.72	2.958	24.54	53.9
7.0	6.132	15.35	4.814	26.30	66.1	7.316	17.37	3.344	28.03	57.8
7.5	6.527	17.97	5.435	29.93	71.6	7.783	20.30	3.767	31.85	62.1
8.0	6.932	20.86	6.128	33.92	77.8	8.262	23.55	4.235	36.04	66.8
8.5	7.347	24.04	6.910	38.30	84.7	8.752	27.11	4.762	40.63	72.1
9.0	7.773	27.54	7.809	43.12	92.2	9.254	31.02	5.363	45.64	77.8
9.5	8.209	31.35	8.858	48.42	101	9.768	35.28	6.058	51.11	83.9
10.0	8.655	35.51	10.06	54.22	110	10.29	39.92	6.849	57.06	90.5

Table 4-105 Coefficient of Thermal Conductivity

Substance: Nitrogen
Radial Distribution Function: Kirkwood
Remarks: ζ_s^{RG}

Intermolecular Potential: Lennard-Jones
Temperatures: 180°K

	T = 180°K					T =				
λ	χ_k	χ_v	$\chi_v(R>\sigma)$	χ_{CAL}	χ_{OBS}	χ_K	χ_v	$\chi_v(R>\sigma)$	χ_{CAL}	χ_{OBS}
	$\times 10^3$ watts/m °C					$\times 10^3$ watts/m °C				
1.0	.7118	.1692	.2724	1.153	23.8					
2.0	1.074	.6170	.7509	2.441	28.5					
3.0	1.401	1.352	1.204	3.958	33.9					
4.0	1.720	2.403	2.126	6.248	40.3					
5.0	2.040	3.809	3.022	8.871	48.0					
6.0	2.368	5.624	4.081	12.07	57.4					
7.0	2.708	7.915	5.343	15.97	68.7					
8.0	3.063	10.76	6.884	20.70	82.4					
9.0	3.435	14.22	8.846	26.50	98.3					
10.0	3.824	18.36	11.50	33.69	118					
11.0	4.226	23.21	15.38	42.81	140					
12.0	4.631	28.70	21.57	54.90	166					
13.0	5.022	34.66	34.58	74.26	196					

Table 4-106 Coefficient of Thermal Conductivity

Substance: Nitrogen
Radial Distribution Function: Kirkwood
Remarks: ζ_s^{RG}

Intermolecular Potential: Lennard Jones
Temperatures: T = 273°K; T = 308°K

	T = 273°K					T = 308°K				
λ	χ_k	χ_v	$\chi_v(R>\sigma)$	χ_{CAL}	χ_{OBS}	χ_K	χ_v	$\chi_v(R>\sigma)$	χ_{CAL}	χ_{OBS}
	$\times 10^3$ watts/m °C					$\times 10^3$ watts/m °C				
0.5	.7729	.0686	.0299	.8715	26.7	.8837	.0761	.0928	1.053	28.5
1.0	1.120	.2341	.0830	1.437	29.0	1.277	.2580	.2591	1.795	30.8
1.5	1.409	.4911	.1501	2.050	31.3	1.664	.5400	.4711	2.615	33.2
2.0	1.673	.8417	.2283	2.743	33.9	1.902	.9235	.7196	3.545	35.6
2.5	1.924	1.290	.3163	3.530	36.6	2.186	1.414	.9996	4.599	38.3
3.0	2.168	1.840	.4119	4.420	39.4	2.460	2.017	1.309	5.785	41.3
3.5	2.409	2.500	.5180	5.427	42.6	2.731	2.739	1.645	7.115	44.4
4.0	2.649	3.276	.6326	6.558	46.0	3.002	3.589	2.008	8.599	47.9
4.5	2.890	4.177	.7559	7.823	49.9	3.274	4.576	2.399	10.25	51.7
5.0	3.134	5.211	.8853	9.233	54.0	3.548	5.708	2.819	12.08	56.0
5.5	3.381	6.388	1.032	10.80	58.6	3.827	6.997	3.270	14.09	60.6
6.0	3.632	7.719	1.188	12.24	63.7	4.111	8.453	3.754	16.32	65.7
6.5	3.889	9.215	1.360	14.46	69.3	4.400	10.09	4.277	18.77	71.4
7.0	4.151	10.89	1.553	16.59	75.4	4.697	11.92	4.843	21.46	77.5
7.5	4.420	12.75	1.771	18.94	82.1	5.000	13.95	5.461	24.41	84.3
8.0	4.696	14.81	2.024	21.53	89.6	5.312	16.19	6.143	27.65	91.4
8.5	4.979	17.08	2.321	24.38	97.5	5.631	18.67	6.904	31.20	100
9.0	5.268	19.57	2.676	27.52	106	5.958	21.38	7.766	35.11	109
9.5	5.565	22.31	3.106	30.98	116	6.293	24.35	8.758	39.40	118

Table to be continued

Table 4-106 Coefficient of Thermal Conductivity

Substance: Nitrogen
Radial Distribution Function: Kirkwood
Remarks: ζ_s^{RG}

Intermolecular Potential: Lennard-Jones
Temperatures: 273°K, 308°K

	T = 273°K					T = 308°K				
λ	χ_k	χ_v	$\chi_v(R>\sigma)$	χ_{CAL}	χ_{OBS}	χ_K	χ_v	$\chi_v(R>\sigma)$	χ_{CAL}	χ_{OBS}
	$\times 10^3$ watts/m °C					$\times 10^3$ watts/m °C				
10.0	5.869	25.28	3.637	34.79	126	6.636	27.58	9.918	44.13	128
10.5	6.179	28.50	4.297	38.98	136	6.986	31.08	11.30	49.37	140
11.0	6.495	31.98	5.133	43.61	148	7.344	34.86	12.98	55.19	151
11.5	6.816	35.71	6.213	48.74	161	7.707	38.93	15.08	61.71	165
12.0	7.139	39.69	8.142	54.97	175	8.075	43.28	22.40	73.76	179
12.5	7.464	43.92	16.45	67.83	190	8.401	47.70	22.19	78.29	193
13.0	7.787	48.37	24.60	80.75	206	8.769	52.58	22.11	83.46	210
13.5	8.104	53.01	32.62	93.73	223	9.133	57.69	24.88	91.71	228

Table 4-107 Coefficient of Thermal Conductivity

Substance: Nitrogen
Radial Distribution Function: Kirkwood
Remarks: ζ_s^{RG}

Intermolecular Potential: Lennard Jones
Temperatures: T =

T = 323°K						T = 328°K				
λ	χ_k	χ_v	$\chi_v(R>\sigma)$	χ_{CAL}	χ_{OBS}	χ_K	χ_v	$\chi_v(R>\sigma)$	χ_{CAL}	χ_{OBS}
			$\times 10^3$ watts/m °C					$\times 10^3$ watts/m °C		
						.9350	.0797	.0745	1.089	29.6
						1.351	.2693	.2085	1.829	31.9
						1.697	.5625	.3798	2.639	34.2
						2.012	.9613	.5811	3.554	36.7
						2.311	1.470	.8089	4.590	39.4
						2.601	2.095	1.061	5.757	42.4
						2.887	2.843	1.336	7.067	45.5
						3.172	3.723	1.634	8.530	49.1
						3.459	4.743	1.956	10.16	52.9
						3.748	5.914	2.302	11.96	57.2
						4.041	7.245	2.673	13.96	61.9
						4.339	8.750	3.072	16.16	67.0
						4.644	10.44	3.503	18.59	72.7
						4.955	12.33	3.970	21.25	78.9
						5.273	14.42	4.482	24.18	85.7
						5.600	16.75	5.048	27.39	93.1
						5.934	19.30	5.683	30.92	101.
						6.277	22.11	6.406	34.79	111
						6.628	25.17	7.244	39.05	120

to be continued

Table 4-107 Coefficient of Thermal Conductivity

Substance: Nitrogen
Radial Distribution Function: Kirkwood
Remarks: ζ_s^{RG}

Intermolecular Potential: Lennard-Jones
Temperatures: 328°K

T = 323°K						T = 328°K				
λ	χ_k	χ_v	$\chi_v(R>\sigma)$	χ_{CAL}	χ_{OBS}	χ_K	χ_v	$\chi_v(R>\sigma)$	χ_{CAL}	χ_{OBS}
			$\times 10^3$ watts/m °C					$\times 10^3$ watts/m °C		
						6.988	28.51	8.232	43.73	131
						7.354	32.13	9.431	48.90	142
						7.728	36.03	10.88	54.63	154
						8.108	40.23	12.69	61.03	167
						8.492	44.71	10.95	64.15	181
						8.826	49.71	12.40	71.04	196
						9.318	54.81	19.94	84.07	212
						9.708	60.18	23.44	93.32	230

Table 4-108 Coefficient of Thermal Conductivity

Substance: Nitrogen
Radial Distribution Function: Kirkwood
Remarks: ζ_s^{RG}

Intermolecular Potential: Lennard Jones
Temperatures: T = 373°K; T = 500°K

	T = 373°K					T = 500°K				
λ	χ_k	χ_v	$\chi_v(R>\sigma)$	χ_{CAL}	χ_{OBS}	χ_K	χ_v	$\chi_v(R>\sigma)$	χ_{CAL}	χ_{OBS}
	$\times 10^3$ watts/m °C					$\times 10^3$ watts/m °C				
0.5	1.076	.0890	.0895	1.254	32.1	1.456	.1136	.0473	1.617	38.8
1.0	1.551	.2987	.2504	2.100	34.5	2.090	.3760	.1334	2.600	41.2
1.5	1.944	.6218	.4563	3.022	36.8	2.612	.7762	.2445	3.632	43.7
2.0	2.301	1.061	.6982	4.060	39.4	3.083	1.317	.3755	4.775	46.4
2.5	2.640	1.620	.9712	5.231	42.2	3.529	2.003	.5233	6.055	49.3
3.0	2.969	2.307	1.272	6.548	45.2	3.961	2.843	.6846	7.488	52.3
3.5	3.293	3.129	1.599	8.021	48.5	4.386	3.846	.8605	9.092	55.7
4.0	3.616	4.095	1.953	9.664	52.0	4.809	5.020	1.050	10.88	59.4
4.5	3.940	5.214	2.334	11.49	56.0	5.233	6.379	12.53	12.87	63.5
5.0	4.268	6.498	2.742	13.51	60.2	5.661	7.933	1.470	15.06	68.0
5.5	4.600	7.958	3.179	15.73	65.0	6.095	9.695	1.700	17.49	72.9
6.0	4.938	9.605	3.648	18.19	70.2	6.535	11.68	1.944	20.16	78.4
6.5	5.283	11.45	4.152	20.89	76.1	6.983	13.89	2.204	23.08	84.4
7.0	5.635	13.51	4.695	23.84	82.3	7.441	16.36	2.481	26.28	91.4
7.5	5.995	15.80	5.286	27.08	89.6	7.909	19.09	2.780	29.78	98.3
8.0	6.365	18.33	5.933	30.63	96.6	8.387	22.09	3.104	33.59	106
8.5	6.743	21.11	6.652	34.51	105	8.875	25.39	3.460	37.73	115
9.0	7.131	24.16	7.460	38.75	114	9.375	28.99	3.857	42.23	124
9.5	7.528	27.48	8.304	43.40	124	9.886	32.92	4.307	47.11	134

Table to be continued

Table 4-108 Coefficient of Thermal Conductivity

Substance: Nitrogen
Radial Distribution Function: Kirkwood
Remarks: ζ_s^{RG}

Intermolecular Potential: Lennard-Jones
Temperatures: 373°K, 500°K

	T = 373°K					T = 500°K				
λ	χ_k	χ_v	$\chi_v(R>\sigma)$	χ_{CAL}	χ_{OBS}	χ_K	χ_v	$\chi_v(R>\sigma)$	χ_{CAL}	χ_{OBS}
	$\times 10^3$ watts/m °C					$\times 10^3$ watts/m °C				
10.0	7.934	31.10	9.459	48.50	134	10.41	37.17	4.828	52.41	145
10.5	8.348	35.02	10.73	54.10	146	10.94	41.78	5.440	58.16	158
11.0	8.771	39.26	12.27	60.30	158	11.48	46.75	6.172	64.40	170
11.5	9.201	43.81	14.16	67.17	171	12.04	52.09	7.064	71.20	184
12.0	9.638	48.70	15.86	74.19	185	12.60	57.83	8.169	78.60	198
12.5	10.08	53.91	16.43	80.42	201	13.17	63.97	9.563	86.70	215
13.0	10.52	59.46	17.20	87.18	218	13.75	70.52	11.35	95.62	231
13.5	10.97	65.33	19.16	95.46	235	14.33	77.50	13.30	105.1	250

Table 4-109 Coefficient of Thermal Conductivity

Substance: Nitrogen Intermolecular Potential: Lennard Jones
Radial Distribution Function: Kirkwood
Remarks: ζ_s^{RG} Temperature: 600°K

			T = 600°K		
λ	χ_k	χ_v	$\chi_v(R>\sigma)$	χ_{CAL}	χ_{OBS}
			$\times 10^3$ watts/m °C		
0.5	1.753	.1324	.0320	1.917	41.1
1.0	2.510	.4341	.0910	3.035	46.6
1.5	3.129	.8913	.1678	4.188	49.2
2.0	3.688	1.506	.2592	5.454	52.0
2.5	4.216	2.284	.3628	6.863	54.9
3.0	4.726	3.235	.4821	8.442	58.1
3.5	5.227	4.366	.6012	10.19	61.6
4.0	5.726	5.690	.7272	12.14	65.4
4.5	6.225	7.217	.8594	14.30	69.6
5.0	6.728	8.960	.9976	16.69	74.2
5.5	7.237	10.93	1.141	19.31	79.4
6.0	7.754	13.15	1.291	22.19	84.9
6.5	8.279	15.62	1.447	25.34	91.4
7.0	8.815	18.36	1.612	28.79	98.3
7.5	9.361	21.39	1.788	32.53	105
8.0	9.918	24.71	1.978	36.61	113
8.5	10.49	28.36	2.189	41.03	123
9.0	11.07	32.33	2.429	45.83	132
9.5	11.66	36.65	2.707	51.02	143
10.0	12.27	41.32	3.039	56.63	154
10.5	12.89	46.38	3.441	62.70	166
11.0	13.52	51.82	3.938	69.27	179
11.5	14.16	57.67	4.562	76.39	193
12.0	14.81	63.94	5.358	84.11	209
12.5	15.47	70.66	6.388	92.51	225
13.0	16.14	77.83	7.744	101.7	243
13.5	16.82	85.48	8.602	110.9	261

Table 4-110 Coefficient of Thermal Conductivity

Substance: Argon
Intermolecular Potential: Lennard-Jones
Radial Distribution Function: Percus-Yevick
Remarks: ζ_s^{RG}
Temperatures: 273.15°K, 328.15°K

	T = 273.15°K					T = 328.15°K				
ρ^*	χ_k	χ_v	$\chi_v(R>\sigma)$	χ_{CAL}	χ_{OBS}	χ_K	χ_v	$\chi_v(R>\sigma)$	χ_{CAL}	χ_{OBS}
	$\times 10^3$ watts/m °C					$\times 10^3$ watts/m °C				
0.15	1.267	.6823	1.044	2.993	23.2	1.546	.7827	.9542	3.283	26.3
0.30	2.014	2.680	2.617	7.311	33.3	2.443	3.073	2.411	7.928	36.7
0.45	2.763	6.456	4.418	13.64	48.3	3.345	7.402	4.047	14.79	52.1
0.60	3.602	13.01	6.331	22.94	73.0	4.353	14.82	5.662	24.84	77.4
0.75	4.619	23.98	8.161	36.76	117	5.561	27.00	6.961	39.52	122
0.90	5.904	41.82	9.425	57.15	193	7.059	46.33	7.372	60.76	200
1.05	7.547	69.86	9.652	87.06	325	8.938	76.08	6.078	91.09	336
1.20	9.659	113.0	8.185	130.8	543	11.28	119.9	3.380	134.6	559

Table 4-111 Coefficient of Thermal Conductivity

Substance: Argon
Radial Distribution Function: Percus-Yevick
Remarks: ζ_s^{RG}

Intermolecular Potential: Lennard-Jones
Temperature: 373°K

ρ^*	χ_k	χ_v	$\chi_v(R>\sigma)$	χ_{CAL}	χ_{OBS}	χ_K	χ_v	$\chi_v(R>\sigma)$	χ_{CAL}	χ_{OBS}
	T = 373°K					T =				
	$\times 10^3$ watts/m °C					$\times 10^3$ watts/m °C				
0.15	1.771	.8616	.7669	3.400	28.8					
0.30	2.790	3.377	1.980	8.147	39.5					
0.45	3.813	8.116	3.281	15.21	55.4					
0.60	4.955	16.17	4.428	25.55	81.4					
0.75	6.310	29.20	4.989	40.50	124					
0.90	7.969	49.55	4.311	61.83	207					
1.05	10.02	80.25	.4747	90.73	346					
1.20	12.54	124.9	-4.319	133.1	574					

Table 4-112 Coefficient of Thermal Conductivity

Substance: Argon
Radial Distribution Function: CHNC
Remarks: ζ_s^{RG}

Intermolecular Potential: Lennard-Jones
Temperatures: 273.15°K, 328.15°K

	T = 273.15°K					T = 328.15°K				
ρ^*	χ_k	χ_v	$\chi_v(R>\sigma)$	χ_{CAL}	χ_{OBS}	χ_K	χ_v	$\chi_v(R>\sigma)$	χ_{CAL}	χ_{OBS}
	$\times 10^3$ watts/m °C					$\times 10^3$ watts/m °C				
0.15	1.266	.6829	1.024	2.974	23.2	1.545	.7835	.9496	3.278	26.3
0.30	2.016	2.693	2.318	7.027	33.3	2.444	3.093	2.175	7.712	36.7
0.45	2.776	6.584	3.376	12.74	48.3	3.359	7.565	3.195	14.12	52.1
0.60	3.666	13.62	4.105	21.40	73.0	4.425	15.52	3.762	23.70	77.4
0.75	4.810	25.83	3.841	34.49	117	5.765	28.83	3.300	37.89	122
0.90	6.301	45.32	1.552	53.18	193	7.453	49.24	.4966	57.19	200
1.05	8.132	72.36	-4.629	75.87	325	9.468	76.51	-6.438	79.54	336
1.20	10.15	102.3	-19.55	92.93	543	11.63	105.5	-20.74	96.43	559

Table 4-113 Coefficient of Thermal Conductivity

Substance: Argon
Radial Distribution Function: Percus-Yevick
Remarks: ζ_s^{RG}

Intermolecular Potential:
Temperature: 373°K

	T = 373°K					T =				
ρ^*	χ_k	χ_v	$\chi_v(R>\sigma)$	χ_{CAL}	χ_{OBS}	χ_K	χ_v	$\chi_v(R>\sigma)$	χ_{CAL}	χ_{OBS}
	$\times 10^3$ watts/m °C					$\times 10^3$ watts/m °C				
0.15	1.771	.8626	.7792	3.413	28.8					
0.30	2.790	3.400	1.822	8.013	39.5					
0.45	3.828	8.298	2.572	14.70	55.4					
0.60	5.032	16.89	2.809	24.73	81.4					
0.75	6.521	30.98	1.812	39.31	124					
0.90	8.360	52.02	-1.393	58.99	207					
1.05	10.51	79.38	-9.609	80.28	346					
1.20	12.80	108.0	-23.70	97.10	574					

Table 4-114 Coefficient of Thermal Conductivity

Substance: Argon
Radial Distribution Function: Percus-Yevick
Remarks: Normal ζ_s^{RG}

Intermolecular Potential: Lennard-Jones, Truncated
Temperatures: 273.15°K, 328.15°K, 373.15°K

	T = 273.15°K					T = 328.15°K				
ρ^*	χ_k	χ_v	$\chi_v(R>\sigma)$	χ_{CAL}	χ_{OBS}	χ_K	χ_v	$\chi_v(R>\sigma)$	χ_{CAL}	χ_{OBS}
	$\times 10^3$ watts/m °C					$\times 10^3$ watts/m °C				
0.15	1.260	.6858	1.062	3.009	23.2	1.535	.7881	.9728	3.295	26.3
0.30	1.994	2.725	2.735	7.454	33.3	2.412	3.140	2.518	8.070	36.7
0.45	2.727	6.677	4.719	14.12	46.3	3.292	7.724	4.326	15.34	52.1
0.60	3.552	13.75	6.891	24.20	73.0	4.285	15.90	6.220	26.40	77.4
0.75	4.562	26.09	9.662	40.31	117	5.492	30.01	8.605	44.10	122
			373.15°K							
0.15	1.756	.8686	.7859	3.411	28.8					
0.30	2.749	3.463	2.081	8.292	39.5					
0.45	3.746	8.528	3.582	15.86	55.4					
0.60	4.871	17.53	5.075	27.48	81.4					
0.75	6.233	32.97	6.908	46.11	124					

Table 4-115 Coefficient of Thermal Conductivity

Substance: Argon
Radial Distribution Function: Percus-Yevick
Remarks: ζ_s^{ss}

Intermolecular Potential: Lennard-Jones, Truncated
Temperatures: 273.15°K
328.15°K
373.15°K

	T = 273.15°K					T = 373.15°K				
ρ^*	χ_k	χ_v	$\chi_v(R>\sigma)$	χ_{CAL}	χ_{OBS}	χ_K	χ_v	$\chi_v(R>\sigma)$	χ_{CAL}	χ_{OBS}
	$\times 10^3$ watts/m °C					$\times 10^3$ watts/m °C				
0.15	.2148	.4887	.1720	.8755	23.2					
0.30	.3928	2.121	.5007	3.015	33.3					
0.45	.8376	5.609	1.333	7.780	46.3					
0.60	1.780	12.42	3.195	17.39	73.0					
0.75	3.514	25.10	7.104	35.72	117					
	328.15°K									
0.15	.3652	.5677	.2194	1.152	26.3	.5232	.6362	.2219	1.381	28.8
0.30	.6456	2.474	.6244	3.744	36.7	.9057	2.768	.6351	4.309	39.5
0.45	1.341	6.622	1.624	9.587	52.1	1.849	7.456	1.638	10.94	55.4
0.60	2.787	14.77	3.800	21.36	77.4	3.773	16.71	3.759	24.24	81.4
0.75	5.346	29.87	8.322	43.54	122	7.059	33.75	8.100	48.91	124

Table 4-116 Coefficient of Thermal Conductivity

Substance: Argon
Radial Distribution Function: Percus-Yevick
Remarks: Helfand ζ

Intermolecular Potential: Lennard-Jones, Truncated
Temperatures: 273.15°K
328.15°K
373.15°K

	T = 273.15°K					T = 328.15°K				
ρ^*	χ_k	χ_v	$\chi_v(R>\sigma)$	χ_{CAL}	χ_{OBS}	χ_K	χ_v	$\chi_v(R>\sigma)$	χ_{CAL}	χ_{OBS}
	$\times 10^3$ watts/m °C					$\times 10^3$ watts/m °C				
0.15	6.858	1.741	8.056	16.66	23.2	8.887	2.174	8.608	19.67	26.3
0.30	7.711	4.880	14.53	27.13	33.3	9.804	5.927	15.33	31.06	36.7
0.45	8.461	9.920	19.93	38.31	48.3	10.64	11.88	20.66	43.18	52.1
0.60	9.296	18.09	24.46	51.84	73.0	11.63	21.44	24.79	57.87	77.4
0.75	10.47	31.66	30.31	72.43	117	13.03	37.11	30.17	80.31	122
	373.15°K									
0.15	10.49	2.515	7.705	20.71	28.8					
0.30	11.45	6.743	13.87	32.06	39.5					
0.45	12.36	13.40	18.59	44.36	55.4					
0.60	13.47	24.02	21.89	59.38	81.4					
0.75	15.03	41.26	26.16	82.44	124					

Table 4-17 Comparison of Drag Coefficients

Substance: Argon
Intermolecular Potential: Lennard-Jones, Truncated
Radial Distribution Function: Percus Yevick
Remarks: ζ_s^{ss}

	T = 55°C				T = 100°C			
ρ^*	P_{CAL} bars	P_{OBS} bars	ζ_s^{ss}	ζ_s^H	P_{CAL} bars	P_{OBS} bars	ζ_s^{ss}	ζ_s^H
			← $\times 10^{13}$ kg/sec →				← $\times 10^{13}$ kg/sec →	
0.15	178.6	166.5	6.347	.1618	204.9	196.4	5.017	.1445
0.30	395.3	360.6	8.588	.3499	484.0	437.5	6.941	.3178
0.45	787.8	667.0	9.457	.5862	971.6	817.6	6.114	.5385
0.60	1583	1261	5.776	.8852	1923	1523	4.764	.8179
0.75	3194	2487	4.504	1.242	3782	2914	3.716	1.151

Table 4-118 Coefficient of Thermal Conductivity

Substance: Argon
Radial Distribution Function: Kirkwood
Remarks: RG
S

Intermolecular Potential: Modified Buckingham
Temperatures: 273°K, 308°K

	T = 273°					T = 308°				
λ	χ_k	χ_v	$\chi_v(R>\sigma)$	χ_{CAL}	χ_{OBS}	χ_K	χ_v	$\chi_v(R>\sigma)$	χ_{CAL}	χ_{OBS}
	$\times 10^3$ watts/m °C					$\times 10^3$ watts/m °C				
0.5	.6018	.0601	.1555	.8174	17.8	.6896	.0664	.1419	.8978	19.7
1.0	.8745	.2100	.4275	1.512	19.5	1.000	.2307	.3904	1.621	21.4
1.5	1.103	.4476	.7671	2.317	21.4	1.259	.4903	.7005	2.450	23.4
2.0	1.311	.7769	1.159	3.247	23.6	1.495	.8497	1.058	3.403	25.6
2.5	1.511	1.204	1.598	4.313	25.9	1.721	1.316	1.456	4.493	27.9
3.0	1.705	1.736	2.085	5.526	28.5	1.941	1.896	1.896	5.732	30.5
3.5	1.898	2.382	2.625	6.905	31.2	2.159	2.601	2.379	7.139	33.3
4.0	2.091	3.151	3.227	8.470	34.4	2.378	3.441	2.912	8.731	36.5
4.5	2.287	4.056	3.905	10.25	37.8	2.600	4.428	3.507	10.54	39.9
5.0	2.486	5.107	4.678	12.27	41.6	2.825	5.575	4.180	12.58	43.7
5.5	2.689	6.316	5.575	14.58	46.0	3.055	6.895	4.952	14.90	48.0
6.0	2.897	7.696	6.633	17.23	50.8	3.291	8.400	5.856	17.55	52.7
6.5	3.110	9.257	7.065	20.23	56.5	3.534	10.10	6.902	20.54	58.1

Table 4-119 Coefficient of Thermal Conductivity

Substance: Argon
Radial Distribution Function: Kirkwood
Remarks: ζ_s^{RG}

Intermolecular Potential: Modified Buckingham
Temperatures: 323°K, 328°K

	T = 323°					T = 328°				
λ	χ_k	χ_v	$\chi_v(R>\sigma)$	χ_{CAL}	χ_{OBS}	χ_K	χ_v	$\chi_v(R>\sigma)$	χ_{CAL}	χ_{OBS}
	$\times 10^3$ watts/m °C					$\times 10^3$ watts/m °C				
0.5	.7271	.0691	.1342	.9304	20.5	.7396	.0696	.1323	.9419	20.7
1.0	1.054	.2394	.3696	1.663	22.2	1.072	.2423	.3644	1.678	22.5
1.5	1.326	.5082	.6638	2.498	24.2	1.348	.5142	.6545	2.517	24.5
2.0	1.574	.8802	1.003	3.457	26.4	1.600	.8902	.9886	3.479	26.6
2.5	1.810	1.362	1.380	4.553	28.8	1.840	1.377	1.361	4.579	29.1
3.0	2.041	1.963	1.795	5.799	31.4	2.075	1.984	1.770	5.829	31.7
3.5	2.271	2.692	2.251	7.213	34.3	2.308	2.721	2.218	7.247	34.6
4.0	2.500	3.560	2.752	8.812	37.5	2.541	3.600	2.710	8.851	37.7
4.5	2.733	4.581	3.308	10.62	41.0	2.777	4.362	3.256	10.66	41.3
5.0	2.969	5.767	3.934	12.67	44.8	3.017	5.830	3.871	12.72	45.3
5.5	3.211	7.131	4.652	14.99	49.2	3.263	7.209	4.573	15.04	49.7
6.0	3.459	8.688	5.489	17.64	54.1	3.515	8.782	5.392	17.79	54.7
6.5	3.714	10.45	6.455	20.62	59.7	3.773	10.56	6.337	20.67	60.4

Table 4-120 Coefficient of Thermal Conductivity

Substance: Argon
Intermolecular Potential: Modified Buckingham
Radial Distribution Function: Kirkwood
Temperatures: 373°K
Remarks: ζ_s^{RG}

	T = 373°					T =				
λ	χ_k	χ_v	$\chi_v(R>\sigma)$	χ_{CAL}	χ_{OBS}	χ_K	χ_v	$\chi_v(R>\sigma)$	χ_{CAL}	χ_{OBS}
	$\times 10^3$ watts/m °C					$\times 10^3$ watts/m °C				
0.5	.8521	.0778	.1125	1.042	23.1					
1.0	1.232	.2677	.3107	1.810	24.9					
1.5	1.547	.5663	.5592	2.673	27.0					
2.0	1.835	.9786	.8453	3.658	29.2					
2.5	2.108	1.512	1.163	4.783	31.6					
3.0	2.375	2.176	1.509	6.060	34.4					
3.5	2.639	2.982	1.886	7.507	37.3					
4.0	2.905	3.942	2.295	9.142	40.6					
4.5	3.173	5.068	2.746	10.99	44.2					
5.0	3.447	6.376	3.248	13.07	48.3					
5.5	3.726	7.879	3.817	15.42	52.9					
6.0	4.013	9.594	4.477	18.08	58.1					
6.5	4.307	11.53	5.233	21.07	64.1					

Table 4-121 Coefficient of Thermal Conductivity

Substance: Nitrogen
Radial Distribution Function: Kirkwood
Remarks: ζ_s^{RG}

Intermolecular Potential: Modified Buckingham
Temperatures: 273°K, 308°K

	T = 273°K					T = 308°				
λ	χ_k	χ_v	$\chi_v(R>\sigma)$	χ_{CAL}	χ_{OBS}	χ_K	χ_v	$\chi_v(R>\sigma)$	χ_{CAL}	χ_{OBS}
	$\times 10^3$ watts/m °C					$\times 10^3$ watts/m °C				
0.5	.7423	.0692	.1266	.9381	27.0	.8487	.0766	.1154	1.041	28.7
1.0	1.075	.2387	.3520	1.666	29.4	1.227	.2626	.3208	1.810	31.2
1.5	1.353	.5052	.6379	2.496	32.1	1.541	.5541	.5813	2.676	33.9
2.0	1.605	.8726	.9720	3.450	34.9	1.827	.9554	.8849	3.667	36.6
2.5	1.846	1.347	1.349	4.542	37.9	2.098	1.473	1.226	4.798	39.7
3.0	2.080	1.937	1.767	5.784	41.3	2.363	2.117	1.602	6.082	43.0
3.5	2.312	2.651	2.226	7.189	44.9	2.624	2.896	2.014	7.535	46.7
4.0	2.545	3.500	2.732	8.776	49.0	2.886	3.823	2.464	9.173	50.8
4.5	2.779	4.495	3.290	10.56	53.5	3.151	4.910	2.958	11.02	55.3
5.0	3.017	5.650	3.913	12.58	58.6	3.419	6.170	3.506	13.10	60.6
5.5	3.259	6.977	4.617	14.85	64.1	3.693	7.618	4.122	15.43	66.1
6.0	3.507	8.490	5.427	17.42	70.3	3.974	9.269	4.825	18.07	72.4
6.5	3.762	10.20	6.374	20.34	77.2	4.262	11.14	5.645	21.04	79.4
7.0	4.023	12.12	7.466	23.61	84.8	4.557	13.24	6.586	24.38	87

Table 4-122 Coefficient of Thermal Conductivity

Substance: Nitrogen
Radial Distribution Function: Kirkwood
Remarks: ζ_s^{RG}

Intermolecular Potential: Modified Buckingham
Temperatures: 323°K, 328°K

	T = 323°K					T = 328°K				
λ	χ_k	χ_v	$\chi_v(R>\sigma)$	χ_{CAL}	χ_{OBS}	χ_K	χ_v	$\chi_v(R>\sigma)$	χ_{CAL}	χ_{OBS}
	$\times 10^3$ watts/m °C					$\times 10^3$ watts/m °C				
0.5	.8943	.0797	.1091	1.083	29.5	.9094	.0807	.1075	1.098	29.8
1.0	1.292	.2726	.3036	1.868	32.0	1.313	.2759	.2993	1.889	32.3
1.5	1.621	.5746	.5502	2.746	34.6	1.647	.5813	.5425	2.772	35.0
2.0	1.921	.9900	.8378	3.749	37.5	1.952	1.001	.8259	3.780	37.8
2.5	2.206	1.526	1.160	4.892	40.6	2.241	1.543	1.144	4.929	40.8
3.0	2.483	2.192	1.516	6.191	43.9	2.523	2.217	1.494	6.233	44.2
3.5	2.757	2.998	1.904	7.659	47.7	2.801	3.032	1.876	7.709	48.0
4.0	3.032	3.957	2.327	9.316	51.8	3.080	4.001	2.292	9.372	52.0
4.5	3.309	5.081	2.791	11.18	56.4	3.361	5.137	2.747	11.25	56.7
5.0	3.590	6.384	3.304	13.28	61.5	3.647	6.454	3.250	13.35	61.8
5.5	3.878	7.881	3.879	15.64	67.1	3.939	7.968	3.814	15.72	67.4
6.0	4.172	9.588	4.534	18.29	73.5	4.238	9.693	4.456	18.39	73.8
6.5	4.473	11.52	5.297	21.29	80.5	4.544	11.64	5.203	21.39	80.7
7.0	4.783	13.69	6.171	24.64	87.9	4.858	13.84	6.061	24.75	88.8

Table 4-123 Coefficient of Thermal Conductivity

Substance: Nitrogen
Radial Distribution Function: Kirkwood
Remarks: ζ_s^{RG}

Intermolecular Potential: Modified Buckingham
Temperatures: 373°K

	T = 373°K					T =				
λ	χ_k	χ_v	$\chi_v(R>\sigma)$	χ_{CAL}	χ_{OBS}	χ_K	χ_v	$\chi_v(R>\sigma)$	χ_{CAL}	χ_{OBS}
	$\times 10^3$ watts/m °C					$\times 10^3$ watts/m °C				
0.5	1.046	.0899	.0914	1.227	32.3					
1.0	1.507	.3054	.2548	2.067	34.9					
1.5	1.888	.6412	.4623	2.991	37.6					
2.0	2.233	1.102	.7039	4.039	40.5					
2.5	2.561	1.696	.9742	5.232	43.6					
3.0	2.881	2.433	1.270	6.584	47.8					
3.5	3.196	3.325	1.592	8.113	50.9					
4.0	3.512	4.385	1.940	9.837	55.1					
4.5	3.831	5.626	2.318	11.78	59.7					
5.0	4.155	7.065	2.732	13.95	64.9					
5.5	4.486	8.716	3.194	16.40	70.7					
6.0	4.824	10.60	3.719	19.14	77.1					
6.5	5.171	12.72	4.326	22.22	84.2					
7.0	5.527	15.11	5.021	25.66	92.2					

Table 4-124 Coefficient of Thermal Conductivity

Substance: Argon
Radial Distribution Function: Percus Yevick
Remarks: ζ_s^{RG}

Intermolecular Potential: Modified Buckingham
Temperatures: 273.15°K, 328.15°K

	T = 273.15°					T = 328.15°				
ρ^*	χ_k	χ_v	$\chi_v(R>\sigma)$	χ_{CAL}	χ_{OBS}	χ_K	χ_v	$\chi_v(R>\sigma)$	χ_{CAL}	χ_{OBS}
	$\times 10^3$ watts/m °C					$\times 10^3$ watts/m °C				
0.25	1.385	.7895	1.145	3.319	24.5	1.684	.9067	1.057	3.647	27.7
0.50	2.225	3.126	2.703	8.053	37.2	2.687	3.584	2.492	8.762	40.7
0.75	3.094	7.725	4.431	15.25	58.0	3.725	8.815	3.972	16.51	62.0
1.00	4.116	16.11	6.128	26.35	96.6	4.936	18.15	5.201	28.29	101
1.25	5.410	30.75	8.270	44.43	171	6.437	34.00	6.479	46.91	178

Table 4-125 Coefficient of Thermal Conductivity

Substance: Argon
Radial Distribution Function: Percus Yevick
Remarks: ζ_s^{RG}

Intermolecular Potential: Modified Buckingham
Temperature: 373.15°K

	T = 373.15°K					T =				
ρ^*	χ_k	χ_v	$\chi_v(R>\sigma)$	χ_{CAL}	χ_{OBS}	χ_K	χ_v	$\chi_v(R>\sigma)$	χ_{CAL}	χ_{OBS}
	$\times 10^3$ watts/m °C					$\times 10^3$ watts/m °C				
0.25	1.926	.9991	.8402	3.765	30.2					
0.50	3.060	3.936	1.979	8.974	43.6					
0.75	4.233	9.636	2.987	16.86	65.6					
1.00	5.590	19.66	3.468	28.72	104					
1.25	7.249	36.35	3.382	46.98	173					

Table 4-126 Coefficient of Thermal Conductivity

Substance: Argon
Radial Distribution Function: Kirkwood
Remarks: ζ_s^{RG}

Intermolecular Potential: Barker-Bobetic
Temperatures: 273°K, 308°K

	T = 273°					T = 308°				
λ	χ_k	χ_v	$\chi_v(R>\sigma)$	χ_{CAL}	χ_{OBS}	χ_K	χ_v	$\chi_v(R>\sigma)$	χ_{CAL}	χ_{OBS}
	$\times 10^3$ watts/m °C					$\times 10^3$ watts/m °C				
0.5	.5199	.0570	.1721	.7489	17.9	.5960	.0628	.1568	.8156	19.8
1.0	.7597	.2014	.4733	1.434	19.8	.8693	.2207	.4314	1.521	21.7
1.5	.9622	.4303	.8477	2.240	21.8	1.099	.4707	.7729	2.343	23.8
2.0	1.149	.7456	1.276	3.171	24.1	1.311	.8150	1.164	3.290	26.1
2.5	1.327	1.151	1.751	4.229	26.7	1.513	1.258	1.597	4.368	28.7
3.0	1.501	1.651	2.271	5.423	29.5	1.710	1.806	2.070	5.586	31.6
3.5	1.674	2.252	2.837	6.762	32.6	1.905	2.465	2.583	6.953	34.7
4.0	1.846	2.290	3.455	8.261	36.1	2.099	3.244	3.140	8.484	38.2
4.5	2.018	3.785	4.130	9.934	39.9	2.295	4.153	3.744	10.19	42.0
5.0	2.193	4.737	4.872	11.80	44.4	2.494	5.203	4.403	12.10	46.4
5.5	2.370	5.825	5.692	13.89	49.3	2.695	6.404	5.127	14.23	51.3
6.0	2.551	7.063	6.607	16.22	50.1	2.901	7.772	5.929	16.60	56.8
6.5	2.735	8.462	7.636	18.83	61.8	3.111	9.318	6.829	19.26	63.2
7.0	2.924	10.04	8.811	21.77	69.5	3.327	11.06	7.853	22.24	70.5
7.5	3.118	11.80	10.17	25.09	78.6	3.548	13.00	9.038	25.59	78.9
8.0	3.317	13.37	11.78	28.86	88.8	3.776	15.17	10.44	29.38	88.8
8.5	3.521	15.93	13.73	33.17	102	4.010	17.57	12.12	33.70	100
9.0	3.729	18.31	16.00	38.04	117	4.249	20.20	14.09	38.54	114

Table 4-127 Coefficient of Thermal Conductivity

Substance: Argon
Radial Distribution Function: Kirkwood
Remarks: ζ_s^{RG}

Intermolecular Potential: Barker-Bobetic
Temperatures: 323°K, 328°K

	T = 323°					T = 328°				
λ	χ_k	χ_v	$\chi_v(R>\sigma)$	χ_{CAL}	χ_{OBS}	χ_K	χ_v	$\chi_v(R>\sigma)$	χ_{CAL}	χ_{OBS}
	$\times 10^3$ watts/m °C					$\times 10^3$ watts/m °C				
0.5	.6286	.0652	.1482	.8420	20.5	.6394	.0660	.1461	.8515	20.8
1.0	.9161	.2289	.4081	1.553	22.4	.9317	.2315	.4023	1.566	22.7
1.5	1.158	.4876	.7317	2.377	24.6	1.177	.4932	.7215	2.392	24.9
2.0	1.380	.8441	1.103	3.327	27.0	1.403	.8537	1.085	3.344	27.2
2.5	1.592	1.303	1.514	4.409	29.6	1.618	1.318	1.493	4.429	29.9
3.0	1.799	1.871	1.964	5.633	32.5	1.828	1.892	1.936	5.656	32.8
3.5	2.003	2.554	2.450	7.008	35.7	2.036	2.583	2.416	7.035	36.0
4.0	2.208	3.362	2.977	8.547	39.3	2.244	3.401	2.935	8.579	39.6
4.5	2.413	4.305	3.548	10.27	43.2	2.453	4.355	3.497	10.30	43.5
5.0	2.622	5.395	4.169	12.19	47.6	2.664	5.458	4.108	12.23	48.0
5.5	2.833	6.642	4.850	14.33	52.7	2.879	6.720	4.777	14.38	53.2
6.0	3.050	8.062	5.605	16.72	58.4	3.089	8.157	5.516	16.77	59.0
6.5	3.271	9.667	6.450	19.39	65.0	3.324	9.782	6.344	19.45	65.8
7.0	3.498	11.47	7.410	22.38	72.7	3.555	11.61	7.285	22.45	73.7
7.5	3.731	13.49	8.519	25.74	81.7	3.792	13.65	8.373	25.82	82.9
8.0	3.971	15.74	9.825	29.54	9.2	4.036	15.93	9.655	29.62	94.0
8.5	4.217	18.23	11.40	33.84	104	4.286	8.44	11.20	33.93	106
9.0	4.470	20.96	13.24	38.67	119	4.543	21.21	13.00	38.75	122

Table 4-128 Coefficient of Thermal Conductivity

Substance: Argon
Radial Distribution Function: Kirkwood
Remarks: ζ_s^{RG}

Intermolecular Potential: Barker-Bobetic
Temperatures: 373°K

	T = 373					T =				
λ	χ_k	χ_v	$\chi_v(R>\sigma)$	χ_{CAL}	χ_{OBS}	χ_K	χ_v	$\chi_v(R>\sigma)$	χ_{CAL}	χ_{OBS}
	$\times 10^3$ watts/m °C					$\times 10^3$ watts/m °C				
0.5	.7369	.0733	.1240	.9342	23.2					
1.0	1.072	.2554	.3423	1.669	25.2					
1.5	1.352	.5426	.6156	2.510	27.4					
2.0	1.609	.9382	.9298	3.477	29.9					
2.5	1.854	1.448	1.279	4.581	32.5					
3.0	2.093	2.078	1.660	5.831	35.5					
3.5	2.329	2.839	2.070	7.238	38.7					
4.0	2.566	3.739	2.511	8.816	42.5					
4.5	2.804	4.790	2.988	10.58	46.6					
5.0	3.045	6.004	3.503	12.55	51.2					
5.5	3.291	7.396	4.065	14.75	56.6					
6.0	3.542	8.978	4.684	17.20	62.7					
6.5	3.799	10.77	5.376	19.94	69.6					
7.0	4.063	12.78	6.156	23.00	77.7					
7.5	4.335	15.03	7.058	26.42	86.9					
8.0	4.614	17.53	8.116	30.26	97.5					
8.5	4.901	20.29	9.387	34.58	110					
9.0	5.195	23.34	10.87	39.40	124					

Table 4-129 Coefficient of Thermal Conductivity

Substance: Argon
Radial Distribution Function: Percus Yevick
Remarks: ζ_s^{RG}

Intermolecular Potential: Barker Bobetic
Temperatures 273.15°K, 328.15°K

	T = 273.15°K					T = 328.15°K				
ρ^*	χ_k	χ_v	$\chi_v(R>\sigma)$	χ_{CAL}	χ_{OBS}	χ_K	χ_v	$\chi_v(R>\sigma)$	χ_{CAL}	χ_{OBS}
			$\times 10^3$ watts/m °C					$\times 10^3$ watts/m °C		
0.15	1.466	.4704	.5205	2.457	21.2	1.804	.5253	.4896	2.819	24.2
0.30	2.299	1.734	1.343	5.376	27.8	2.787	1.916	1.302	6.005	31.1
0.45	3.094	3.860	2.384	9.338	36.5	3.712	4.252	2.309	10.27	39.9
0.60	3.898	7.029	3.566	14.49	48.3	4.642	7.728	3.388	15.76	52.0
0.75	4.739	11.54	4.640	20.92	65.4	5.611	12.64	4.378	22.63	69.6
0.90	5.648	17.80	5.504	28.96	91.4	6.650	19.37	5.188	31.20	96.6
1.05	6.650	26.29	6.169	39.11	131	7.786	28.34	5.776	41.90	138
1.20	7.771	37.49	6.619	51.88	192	9.043	39.99	6.058	55.09	200
1.35	9.032	51.84	6.751	67.62	285	10.44	54.67	5.914	71.08	294
1.50	10.46	69.57	6.794	86.81	419	11.99	72.47	5.316	89.79	432

Table 4-130 Coefficient of Thermal Conductivity

Substance: Argon
Radial Distribution Function: Percus Yevick
Remarks: ζ_S^{RG}

Intermolecular Potential: Barker Bobetic
Temperature: 373.15°K

	T = 373.15°K					T =				
ρ^*	χ_k	χ_v	$\chi_v(R>\sigma)$	χ_{CAL}	χ_{OBS}	χ_K	χ_v	$\chi_v(R>\sigma)$	χ_{CAL}	χ_{OBS}
	$\times 10^3$ watts/m °C					$\times 10^3$ watts/m °C				
0.15	2.078	.5708	.3872	3.036	26.7					
0.30	3.181	2.065	1.054	6.300	33.7					
0.45	4.210	4.567	1.964	10.72	42.8					
0.60	5.239	8.275	2.934	16.44	55.4					
0.75	6.308	13.48	3.829	23.62	73.5					
0.90	7.449	20.56	4.517	32.52	100					
1.05	8.689	29.90	4.954	43.54	138					
1.20	10.05	41.91	4.983	56.94	192					
1.35	11.55	56.85	4.529	72.93	267					
1.50	13.22	74.78	3.331	91.33	367					